Universidad Autónoma de Madrid

Facultad de Ciencias

Departamento de Biología Molecular

The Sonic Hedgehog Binding Protein Cdon is Required for Patterning and Morphogenesis of the Vertebrate Eye

Trabajo de Investigación que presenta

Marcos Julián Cardozo Ruiz

Para optar al grado de Doctor en Ciencias

Por la Universidad Autónoma de Madrid.

Marzo, 2013

Fdo. Lic. Marcos Julián Cardozo Ruiz

Dirigido por la Doctora

Paola Bovolenta

Profesor de Investigación del CSIC

Centro de Biología Molecular “Severo Ochoa”

Fdo. Dra. Paola Bovolenta

Paola Bovolenta, Doctor en Biología, Profesor de Investigación del CSIC en el Centro de Biología Molecular Severo Ochoa:

CERTIFICA:

Que Marcos Julián Cardozo Ruiz ha realizado bajo su dirección el trabajo de Tesis Doctoral titulado "The Sonic Hedgehog Binding Protein Cdon is Required for Patterning and Morphogenesis of the Vertebrate Eye". Los datos que se presentan en esta Tesis son originales y resultado de trabajo realizado en el Instituto Cajal, CSIC durante los años 2008-2010, en el Centro de Biología Molecular "Severo Ochoa" durante los años 2011-2012 y en el laboratorio de Steve Wilson en "University College London, London, UK", donde Marcos Julián Cardozo Ruiz realizó una estancia de tres meses. Considero que el trabajo es novedoso, bien realizado y de relevancia en el área de la Neurobiología del Desarrollo y que, por lo tanto, tiene la debida calidad para su defensa y calificación en la Facultad de Ciencias Biológicas de la Universidad Autónoma de Madrid, para la obtención del Título de Doctor en Biología.

Dra. Paola Bovolenta

Madrid. Marzo, 2013.

ACKNOWLEDGEMENTS

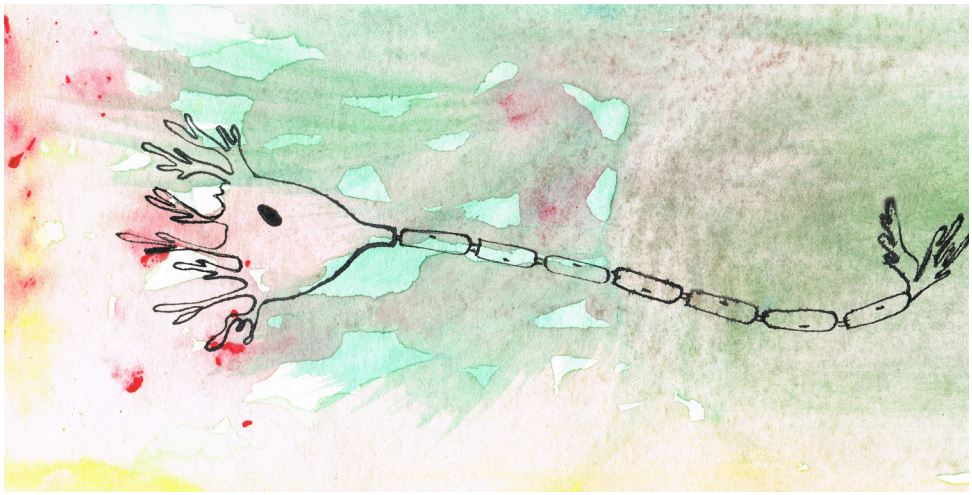

Quiero agradecer a toda la gente que me ha ayudado y apoyado durante todo este período de Tesis.

En primer lugar quiero agradecer profundamente a Paola. Por confiar en mí desde la primera conversación telefónica, por todo su apoyo en todo momento a lo largo de estos años, por nunca decir "ahora no puedo", por su comprensión en distintas situaciones, por ser una excelente profesional y sobretodo buena persona. Por darme la libertad para pensar, trabajar y cometer errores. Un muchas gracias me queda corto!!!

A Luisa porque sin ella el trabajo hubiese sido otro. Agradezco desde que la conozco su pensamiento crítico. Por su ayuda infinita con los pollos, por las charlas dentro y fuera del lab, por ser una excelente compañera de trabajo. Gracias!!!

A Raquel por haberme ayudado todos los días un poquito con una infinidad de cosas. Por su ayuda para entrar y sobrevivir al fantástico mundo de los peces. Por todas las incursiones con los peces, por mantener peces en tres institutos al mismo tiempo (con Leo y Noe claro)... En fin, gracias!!! Y hablando de Noe, obviamente muchísimas gracias por la ayuda con los peces, papeles y por centrarnos un poquito cada día.

A Leo por su fascinación por la ciencia y asuntos informáticos (aunque ama Apple... (chiste Leo)). Por haberme ayudado con la parte informática, clonajes y tantas otras cosas. Por las charlas que a veces se nos iban al mismísimo delirio. Gracias!!!

A Seve por las venturas con la guía axonal, por enseñarme varias técnicas en el laboratorio y por los increíbles *Time-Lapse*. Por reírnos tanto y por la pasión que le pone a lo que hace. Gracias!!!

A África por haberme ayudado siempre en el lab con distintas cosas. Por haber pasado muy buenos momentos tanto dentro como fuera del lab. Por la alegría y fuerza que me contagia. Gracias!!!

A Pilar por aquellas épocas de ratones y Uncs en la que realicé el trabajo de Master y fui aprendiendo las primeras cosas en el lab. Por las risas y demás. Gracias!!!

A Flor por la ayuda para realizar los trasplantes en Londres, por las sondas para ISH y por todo el esfuerzo para establecer los peces en el CBM. Gracias!!!

A Curro por el vector para realizar la sobre-expresión de Cdon. Gracias!!!

A todos los demás integrantes del lab que siempre me han ayudado en distintas situaciones y que tan buena energía le ponen a todos los días. Isidro, Elsa, Cristina, Maku, Lara, Javier, Sergio, Raquel T., Bea, María y Chus. Gracias!!!

A Gaia Gestri por su ayuda fundamental para el trabajo durante mi estancia en Londres. Por ser crítica y ayudarme todos los días que estuve en su lab.

A Paty, Ale, Inma, Ainhoa, Ruth y Aixa por su ayuda y por la buena convivencia en el MAO (Instituto Cajal).

A Steve Wilson y José Luis Gomez-Skarmeta por haberme acogido en sus laboratorios brindándome su apoyo.

A Cristina Puyades por permitirme hacer algunos ensayos en su laboratorio, aunque no figuran en este manuscrito

A Álvaro Sebastián y Marta Nieto por permitirme colaborar en su trabajo.

A Ana Guarner por su ayuda para maquetar la tesis

A mi familia por siempre estar ahí a pesar de la distancia física. Por darme siempre fuerzas y alegría, por extrañarlos un montón todo el tiempo, por la felicidad que me dan. (Le agradezco a mi hermana en particular las fantásticas ilustraciones que hizo!)

A mis amigos Javier y Guido que son de hierro. Así como a Patro, Diego, Guille, Alfredo y el Mercha con los cuales he tenido algunas movidas europeas. Ellos son parte mía y yo un poquito parte de ellos. A Marina por haber vivido tantos momentos felices.

A mi familia y amigos

CONTENTS

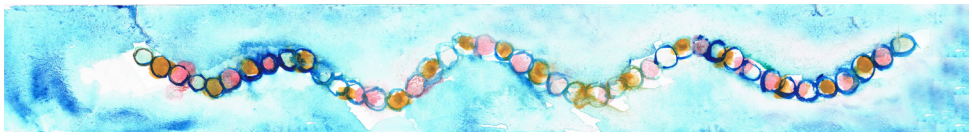

ABBREVIATIONS

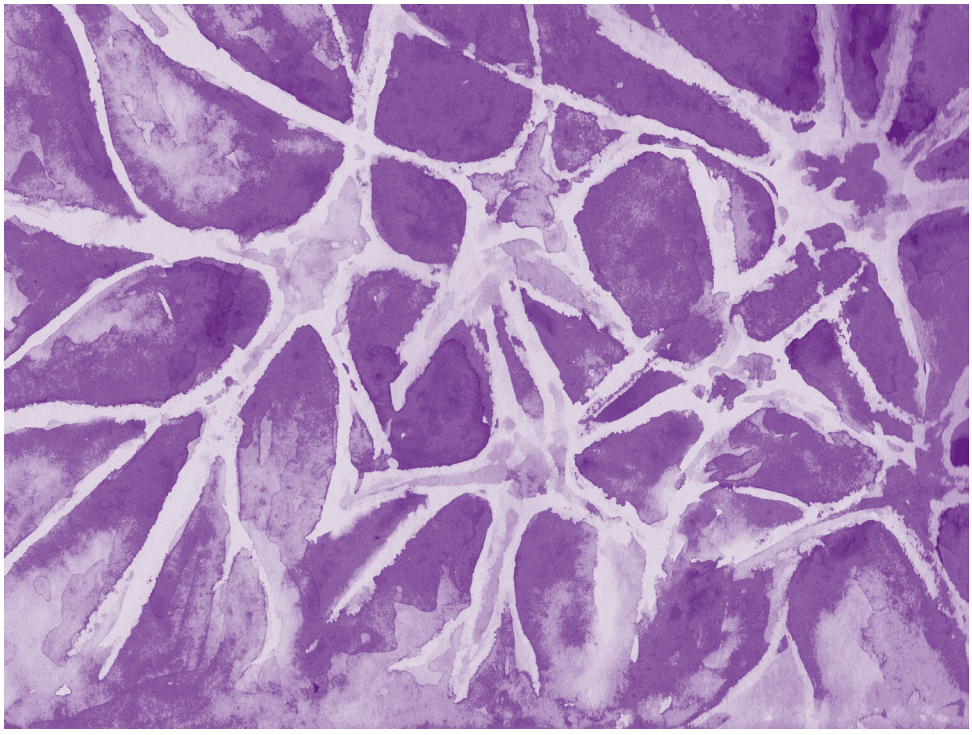

D, distal

d, dorsal

di, diencephalon

dOS, dorsal optic stalk

e, eye

FB, forebrain

FP, floor plate

HB, hindbrain

HPE, holoprosencephaly

hyp, hypothalamus

l, lens

lp, lens placode

lv, lens vesicle

MB, midbrain

mes, mesencephalon

MHB, midbrain hindbrain boundary

N, nasal

Nc, notochord

nr, neural retina

OC, optic chiasm

oc, optic cup

OD, optic disc

ON, optic nerve

os, optic stalk

ot, optic tectum

ov, optic vesicle

P, proximal

r, retina

RGC, retinal ganglion cells

rh, rhombencephalon

RPE, retina pigmented epithelium

SE, surface ectoderm

T, temporal

tel, telencephalon

v, ventral

vF, ventral forebrain

vOS, ventral optic stalk

RESUMEN EN CASTELLANO

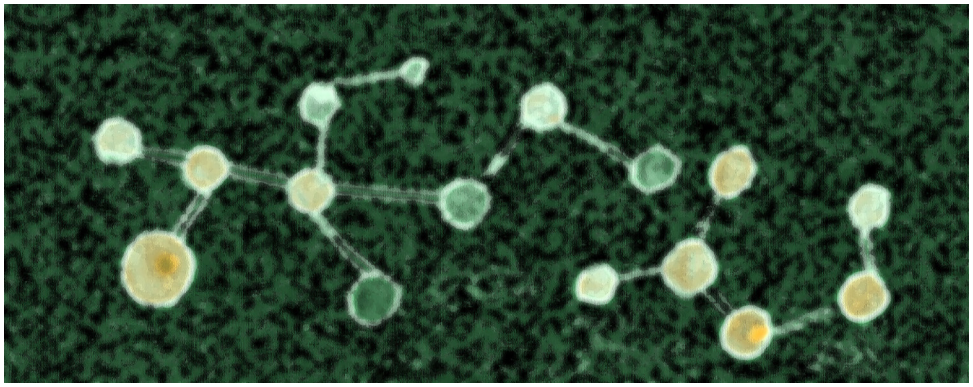

Resumen

Los miembros de la familia Hedgehog (Hh) activan una vía de señalización conservada evolutivamente que es crucial para el desarrollo embrionario y para la homeostasis de tejidos adultos. La activación de la via es iniciada por la unión del ligando Hh a la proteína de transmembrana Patched (Ptch). Sin embargo estudios recientes han demostrado que otras proteínas asociadas a membrana, como Cdon (cell-adhesion-molecule-related/down-regulated by oncogenes), pueden unir proteínas Hh y cooperar en la activación de su vía. La inactivación génica de *Cdon* en ratones provoca holoprosencefalia (HPE), una anomalía congénita que se caracteriza por defectos en la línea media del cerebro anterior asociada frecuentemente a mutaciones en genes de la via de Hh y por lo tanto a una reducción de su señalización. Este fenotipo es consistente con la función propuesta de Cdon como co-receptor de Hh. La HPE se asocia de manera frecuente a defectos oculares, pero la relevancia de *Cdon* en el desarrollo del ojo de los vertebrados ha sido poco analizada.

En este estudio hemos investigado la expresión y funcion de *Cdon* durante la formación temprana del ojo. Los fenotipos obtenidos después de la pérdida de función de Cdon fueron analizados con marcadores específicos de tejido usando técnicas de inmunohistoquimica o de hibridación *in situ* (ISH). Tanto en embriones de pollo como de pez cebra, *Cdon* se expresa de manera temprana en el mesodermo axial, en la retina neural presuntiva y en áreas dorsales del cerebro anterior entre otras regiones. Estudios previos han demostrado que la pérdida de la función de Hh provoca un fenotipo de ciclopia con una reducción del tallo óptico. La reducción de la actividad de *Cdon* produjo en cambio una marcada expansión del tallo óptico interfiriendo con el cierre de la fisura óptica (defecto conocido como coloboma). La expansion del tallo óptico observada en los morfantes de Cdon fue rescatada al tratar los embriones con un inhibidor de la vía de Hh, indicando que la función de Cdon es dependiente de Hh. Estudios recientes en *Drosophila* han sugerido que los homólogos de Cdon (Ihog/Boi), además de actuar como co-receptores de Hh, pueden también limitar la difusión de Hh y por lo tanto interferir con la expresión de genes diana de Hh.

Estas evidencias dan lugar a considerar que Cdon pueda actuar de una manera similar durante la regionalización del ojo. Para evaluar esta posibilidad, hemos diseñado MO específicos para interferir el procesamiento normal del pre-ARNm de *Cdon*. De esta manera removimos de manera eficiente los exones que codifican para los dominios de unión a Shh o Ptch en Cdon. Estos estudios demuestran que la interacción entre Cdon-Ptch no parece tener relevancia en el fenotipo de los embriones mientras que la interacción entre Cdon-Shh produjo coloboma y aumento del tallo óptico. Adicionalmente, la expresión ectópica de Cdon en el tubo neural de pollo induce una acumulación de Shh en las células que expresan Cdon en

regiones cercanas a la placa del suelo (células productoras de Shh). Por lo tanto proponemos que Cdon expresado en la retina protege a la copa óptica de la actividad de Shh mediante su unión previniendo de esta forma su difusión. Esto conlleva a considerar que Cdon puede actuar como un modulador negativo de la vía de Hh en vertebrados.

De manera complementaria estudiamos otras moléculas que podrían estar actuando durante el desarrollo en respuesta a la función de Cdon. La expresión de *Fgf8* se encuentra expandida en morfantes de Cdon y se conoce que la vía de FGF es necesaria para la especificación de la retina (Pittack et al., 1997; Hyer et al., 1998) así como también de determinar el eje naso-temporal de la retina (Picker and Brand, 2005). La señalización de FGF también controla el cierre de la fisura óptica (Chen et al., 2012). Acorde a estas evidencias, rescatamos el fenotipo de los morfantes de Cdon mediante el bloqueo farmacológico de la vía de FGF o usando un fondo mutante para *Fgf8* en pez cebra (*ace*). Esto sugiere que la vía de señalización de FGF media la función de Cdon.

El conocimiento sobre cómo se regula la expresión de *Cdon* durante el desarrollo es limitado. Por esa razón comenzamos un análisis de secuencias con posible actividad reguladora en el *locus* de *Cdon*. Aislamos nueve secuencias que se encuentran conservadas en la evolución y comprobamos su actividad *enhancer*. Algunas de las secuencias parecen funcionar como *enhancer*. En particular, una de las secuencias (chr18:42,516,402-42,517,273) dirige la expresión de GFP de manera específica en el telencéfalo de embriones de pez cebra.

Introducción

Durante el desarrollo embrionario es fundamental la acción de vías específicas de señalización. Estas vías se activan mediante la unión de morfogenos a sus receptores en células receptoras, lo que desencadena una cascada intracelular específicas de transducción. Diferentes moléculas de señalización han sido identificadas, las cuales se pueden agrupar en diferentes familias génicas. Entre las más relevantes y mejores estudiadas se encuentran: *wingless* (Wnt), *transforming growth factor*-β (TGF-β), *fibroblast growth factor* (FGF) y *Hedgehog* (Hh).

Los receptores de la vía de señalización de Hh son *Patched* (Pcth) (Hooper and Scott, 1989; Nakano et al., 1989; Stone et al., 1996; Fuse et al., 1999) y la proteína asociada *Smoothened* (Smo) (Alcedo et al., 1996; van den Heuvel and Ingham, 1996). Además en los últimos años se han identificado otras proteínas capaces de unirse a los ligandos Hh. Una de estas moléculas es Cdon (*cell adhesion molecule-related, down-regulated by oncogenes* (también referido como Cdo)) (Kang et al., 1997; Cole and Krauss, 2003).

Cdon ha sido caracterizada como una glicoproteína de superficie celular que pertenece al subgrupo de la superfamilia de inmunoglobulinas (Ig) de moléculas de adhesión celular (CAMs). Cdon es capaz de unir de manera directa los ligandos Hh (Okada et al., 2006; Tenzen et al., 2006; Yao et al., 2006; McLellan et al., 2008) y de interaccionar con Ptch1 (Bae et al., 2011). Ratones deficientes en *Cdon* presentan HPE, una malformación congénita caracterizada por defectos faciales y malformaciones en el cerebro y en los ojos (Cole and Krauss, 2003; Zhang et al., 2006; Zhang et al., 2009; Hong and Krauss, 2012).

El paso inicial en la formación de los ojos es la especificación de un dominio coherente de células en la placa neural anterior durante la gastrulación (Chuang and Raymond, 2002). El campo de ojo es definido por la expresión de una serie de factores de transcripción altamente conservados. Una vez definido el campo de ojo, sus células neuroepiteliales evaginan para formar las vesículas ópticas. Estás vesículas se regionalizan a lo largo de eje nasotemporal en dos dominios laterales (retina) y dos mediales (tallo óptico). El establecimiento de esta regionalización es definida por la expresión de los factores de transcripción Pax2 y Pax6 (Schwarz et al., 2000).

Después de la evaginación de las vesículas ópticas, comienza la formación de la copa óptica. Durante este proceso, se vuelve evidente una estructura ventral que es la fisura óptica. Esta estructura es transitoria y es necesario que se cierre durante una ventana de tiempo específica para que el ojo se desarrolle y funcione de manera normal.

La vía de señalización de Hh actúa en diferentes pasos del desarrollo ocular. Estos

incluyen la separación de las vesículas ópticas, el establecimiento del eje próximo distal (Ekker et al., 1995; Macdonald et al., 1995; Chiang et al., 1996), el desarrollo de la fisura óptica (Dakubo et al., 2003; Morcillo et al., 2006), la neurogénesis de la retina (Neumann and Nuesslein-Volhard, 2000), la diferenciación del epitelio pigmentario de la retina (RPE) (Perron et al., 2003), la proliferación y supervivencia celular (Neumann and Nuesslein-Volhard, 2000; Zhang and Yang, 2001), la organización laminar de la retina (Wang et al., 2002) y la guía de los axones de las células ganglionares de la retina (RGC) (Trousse et al., 2001; Sanchez-Camacho and Bovolenta, 2008).

A pesar de estas observaciones, se conoce poco sobre los mecanismos moleculares a través de los cuales *Cdon* participa en el desarrollo del ojo y si su función está relacionada a la vía de señalización de Hh. Por esto decidimos explorar el papel de *Cdon* durante el desarrollo del ojo con el objetivo de entender su función y relación con la vía de señalización de Hh.

Objetivos

La función de Cdon durante el desarrollo ha sido determinada a partir de estudios con ratones mutantes de *Cdon*. En estos estudios sin embargo la función específica de Cdon en el ojo ha sido pobremente explorada. Para completar esta falta de conocimiento abordamos los siguientes objetivos específicos en embriones de pez cebra y de pollo como sistemas modelo.

El objetivo principal de este estudio fue explorar el rol de Cdon durante el desarrollo del ojo a través de los siguientes objetivos específicos.

- Determinar si el patrón de expresión embrionaria de *Cdon* esta conservado en vertebrados.
- Analizar si Cdon tiene un papel en el desarrollo del ojo de los vertebrados.
- Determinar si la función de Cdon en el ojo es dependiente de Hh.
- Caracterizar los elementos regulatorios que dirigen la expresión de *Cdon* durante el desarrollo del cerebro anterior.

Resultados

En embriones de pez cebra *Cdon* se expresa en la vesícula de *Kuppfer* y en la línea media en estadios de gastrulación. Posteriormente *Cdon* se expresó abundantemente en la vesícula y la copa óptica y en otras regiones del embrión como por ejemplo el tubo neural dorsal. La expresión de *Cdon* en pollo es similar. Un análisis más detallado de la expresión de *Cdon* en estadios tempranos del desarrollo del ojo develó que el patrón de expresión es similar en pez cebra, pollo y ratón.

Para entender el papel funcional de *Cdon* en el desarrollo, interferimos con su expresión inyectando (pez cebra) o electroporando (pollo) oligonucleótidos anti-sentido (morfolinos, MO). En pez cebra observamos que los embriones deficientes en Cdon poseen defectos oculares en la región ventral de la retina. Los embriones morfantes para Cdon presentaron un fallo en el cierre de la fisura óptica como también una expansión del tallo óptico y de la retina ventral. Mediante trasplante de células en pez cebra y electroporación de un MO específico en embriones de pollo, determinamos que la expresión de *Cdon* en la retina es la responsable de mantener bajos los niveles de *Pax2* en esta región.

El fenotipo observado en los morfantes de *Cdon* es consistente con una ganancia de la vía de señalización de Hh. Para comprobar si la vía de Hh se encuentra expandida en los embriones con bajos niveles de Cdon, bloqueamos la vía mediante la administración de ciclopamina. Este tratamiento produjo un rescate del fenotipo de tallo óptico en los morfantes de Cdon. Además, mediante el uso de MO que interfieren el procesamiento del pre-mARN de *Cdon* fuimos capaces de observar que el dominio de unión a Shh en Cdon es importante para su función durante el desarrollo del ojo. La electroporación de Cdon en el tubo neural de pollo sugirió que Cdon es capaz de unirse a Shh de manera eficiente.

Como FGF es una vía que participa en la ventralización de la retina, hipotetizamos que la vía de FGF media la actividad de *Cdon*. Para comprobar este hipótesis bloqueamos la vía de FGF mediante la administración de SU5402. Este tratamiento produjo un rescate del fenotipo de tallo óptico en los morfantes de Cdon. Debido a que FGF es necesario para una correcta regionalización de los dominios nasal y temporal de la retina, decidimos analizar este proceso en los morfantes de Cdon. Como era de esperar, el dominio nasal de la retina se presentó expandido respecto al dominio temporal en morfantes de Cdon. Inyectando el MO de Cdon en mutantes para *Fgf8* (*ace*) pudimos observar un rescate del fenotipo.

Existe poca información sobre cómo se regula la expresión de *Cdon* durante el desarrollo. Por lo tanto, decidimos intentar identificar las regiones reguladoras del gen que pudiesen funcionar como *enhancer* durante el desarrollo. La comparación de secuencias y marcas

epigenéticas (H3K27AC) permitieron identificar varios posibles enhancers. Determinamos nueve secuencias no-codificantes del *locus* de Cdon que se encuentran evolutivamente conservadas. Clonamos estas secuencias en un vector reportero e inyectamos embriones de pez cebra. Hasta el momento logramos determinar una secuencia de 872pb (chr18:42,516,402-42,517,273) que dirige la expresión de una proteína reportera al telencéfalo de los embriones de pez cebra.

Conclusiones

1. El patrón de expresión embrionario de *Cdon* en el ojo se encuentra conservado desde teleósteos hasta mamíferos.

2. Una reducción de los niveles de expresión de *Cdon* produce defectos oculares ventrales y una expansión del tallo óptico en pez cebra.

3. La expresión de *Cdon* en la retina presuntiva previene la expansión del tallo óptico.

4. La vía de señalización de Hh media el aumento del tallo óptico observado en los morfantes de Cdon.

5. La interacción de Cdon con Shh (pero no con Ptc) es crítica para establecer el límite entre tallo óptico y retina neural.

6. Células neuroepiteliales que expresan Cdon de manera ectópica, pueden acumular la proteína Shh secretada desde la placa del suelo.

7. Cdon actúa como un modulador negativo de la vía de señalización de Hh durante la formación del ojo.

8. La vía de señalización de FGF media el aumento del dominio de tallo óptico en los morfantes de Cdon.

9. Cdon es requerido para un correcto establecimiento de los dominios nasal y temporal de la retina.

10. Fgf8 media la actividad de Cdon durante el establecimiento de los dominios nasal y temporal de la retina.

Discusión

Shh liberado desde la línea media es crítico para establecer y mantener la regionalización próximo-distal del ojo, controlando el balance de la expresión de Pax2/Pax6 en el tallo óptico y en la retina respectivamente (Macdonald et al., 1995; Take-uchi et al., 2003). En este trabajo, proponemos que Cdon, una molécula capaz de unir Shh, puede actuar como un modulador negativo de la vía de señalización de Hh en vertebrados. Cdon expresado en la retina protege a la copa óptica de la actividad de Shh mediante la unión directa de Shh, controlando así su difusión. Esta función es necesaria para establecer una correcta regionalización próximo-distal del ojo. En ausencia de Cdon, el gradiente de Shh se expandiría a regiones más distales generando un aumento del dominio de tallo óptico a expensas de la retina.

Trabajos previos han propuesto que Cdon funciona como un modulador positivo de la vía de señalización de Hh (Tenzen et al., 2006; Zhang et al., 2006). Sin embargo, de manera inesperada, el fenotipo de ojo que presentan los morfantes de Cdon es compatible con una ganancia de función de la vía de señalización de Hh. Los morfantes de Cdon se caracterizan principalmente por un aumento de dominios proximales como es el tallo óptico, evidenciado por el aumento de expresión del marcador *Pax2.1* y defectos ventrales en el ojo. Este mismo fenotipo se ha observado en el pez teleósteo *Astyanax mexicanus* (Yamamoto et al., 2004), en morfantes de Zic2a (Sanek et al., 2009) y en el mutante de *Ptc1* Blowout (Lee et al., 2008). En todos estos modelos, la vía de señalización de Hh se encuentra claramente aumentada. En nuestro modelo, pudimos revertir la expansión del dominio de tallo óptico mediante el bloqueo de la vía de Hh. Así como también pudimos obtener un fenotipo similar al de los morfantes de Cdon removiendo el dominio de unión a Shh en Cdon. Los resultados obtenidos sugieren que la vía de señalización de Hh se encuentra sobreactivada en los morfantes de Cdon.

A pesar de la posible implicación de la vía de Hh en el fenotipo de los morfantes de Cdon, no fuimos capaces de observar una modificación en los patrones de expresión de distintos genes cuya expresión varía en respuesta a la actividad de la via de Hh como es *Ptc1*. Creemos que esto podría deberse a la baja sensibilidad de la técnica empleada (ISH) así como a la capacidad que tiene la vía para amortiguar cambios en alguno de sus componentes.

Los morfantes de Cdon poseen un fenotipo ocular similar a los mutantes de *Cdon* en ratón (Zhang et al., 2009), sin embargo la expresión de marcadores moleculares se encuentra modificada de manera distinta en ambos modelos. Creemos que esta diferencia se debe a que los defectos observados en mutantes de *Cdon* dependen de defectos de línea media, que en cambio no parecen estar presentes en los morfantes de Cdon. De esta manera, con

las evidencias obtenidas mediante la reducción de los niveles de *Cdon* específicamente en el ojo, creemos que el fenotipo que presentan los morfantes de Cdon se debe a la ausencia de expresión de Cdon en el ojo.

La ausencia de Cdon interfiere con la vía de señalización de Hh, pero parece afectar también a la vía de señalización de FGF. Las vías de señalización de FGF y de Hh actúan en un ciclo de retroalimentación positiva en diferentes contextos durante el desarrollo (Brewster et al., 2000), incluyendo el desarrollo del cerebro anterior (Bertrand and Dahmane, 2006). Una posible explicación al aumento de señalización de ambas vías en los morfantes de Cdon es que exista una heterocronía entre el comienzo de la expresión de *Shh* y *Fgf8* en los morfantes. Este efecto ha sido observado en el pez teleósteo *Astyanax mexicanus* (Pottin et al., 2011). Es importante para futuros estudios analizar la posible implicación de Cdon en la vía de señalización de FGF como así también en otras vías de señalización como puede ser la de Wnt.

En la actualidad, existe poca información sobre cómo funciona la regulación del gen *Cdon*. Se sabe que *Cdon* y *Boc* parecen estar regulados de manera negativa por la vía de señalización de Hh en estadios tempranos del desarrollo embrionario (Tenzen et al., 2006; Bergeron et al., 2011). Hemos podido identificar una secuencia no codificante, localizada dentro del primer intrón de Cdon que tiene actividad *enhancer*. Sin embargo, mediante la observación de secuencias conservadas y del perfil correspondiente a distintas modificaciones de histonas, creemos que el primer intrón de *Cdon* contiene varias secuencias que podrían dirigir la expresión del gen durante el desarrollo.

En conclusión, en este trabajo proponemos que Cdon es capaz de actuar como un modulador negativo de la vía de señalización de Hh en vertebrados, al menos en el contexto del desarrollo del ojo. La descripción de esta nueva función, ayudará a entender mejor la complejidad y dinámica de la vía de señalización de Hh.

ABSTRACT

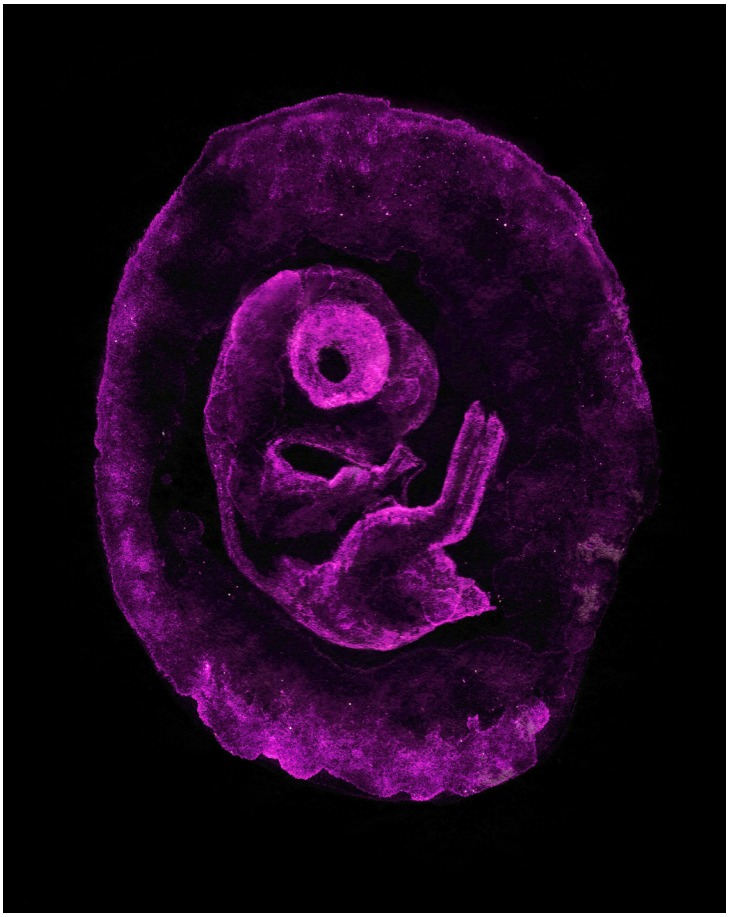

Hedgehog (Hh) family members activate an evolutionarily conserved signal transduction pathway crucial for embryonic development and adult tissue homeostasis. Pathway activation is initiated by binding of the ligand to the seven-pass transmembrane protein Patched (Ptch). Recent studies have however demonstrated that other membrane-associated proteins, including Cdon (cell-adhesion-molecule-related/down-regulated by oncogenes), can bind Hh proteins and cooperate in Hh mediated signaling. Consistent with the proposed function as a Hh co-receptor, genetic inactivation of *Cdon* in mice causes holoprocencephaly (HPE), a human congenital anomaly defined by forebrain midline defects that is often caused by mutations in genes of the Hh pathway. HPE is also frequently associated to multiple eye defects but whether Cdon is relevant to vertebrate eye development is still poorly explored.

To address this issue, we investigated *Cdon* distribution during zebrafish and chick early eye formation and analyzed the consequences of interfering with its expression. In both chick and zebrafish embryos, *Cdon* was expressed in the early axial mesoderm and then in the presumptive neural retina and dorsal forebrain, among other regions. Previous studies have demonstrated that loss of Hh function causes a cyclopic phenotype with reduction of the optic stalks. In contrast, knock-down of Cdon activity caused a marked expansion of the expression of optic stalk markers, such as *Pax2* and *Fgf8* and interfered with optic fissure closure (a defect known as coloboma). The expansion of the optic stalk observed in Cdon morphants was counteracted by treating the embryos with a drug that block Hh signaling, indicating that Cdon function is Hh dependent. Recent studies in *Drosophila* have suggested that Cdon homologs (Ihog/Boi), besides acting as Hh co-receptors, can limit Hh diffusion thereby interfering with the expression of Hh target genes. This raises the possibility that Cdon may act in a similar way during optic vesicle patterning. To address this possibility, we have designed splice-site specific MO, which efficiently removed Shh or Ptch interacting domains in the Cdon protein. Notably, abrogation of Cdon-Ptch interaction seemed to have no effect whereas lack of Cdon–Shh binding caused coloboma and *Pax2* up-regulation. In agreement with this result, the ectopic expression of Cdon in the chick ventral neural tube induces a detectable Shh accumulation in the Cdon expressing cells closer to the floor plate (the Shh producing cells). We thus propose that Cdon expressed in the retina acts to protect the optic cup from Shh activity by binding and preventing Shh diffusion. This implies that Cdon can act as a negative modulator of Hh signaling in vertebrates.

Looking for molecules that downstream of Cdon might be implicated in the Cdon morphant phenotype, we focused on Fgf8, the expression of which is highly expanded in the morphants. FGF signaling controls the specification of the neural retina (Pittack et al., 1997; Hyer et al., 1998) and determinates the naso-temporal axis of the eye vesicle (Picker and Brand, 2005). FGF signaling also controls the closure of the optic fissure (Chen et al., 2012). In agreement with these evidences, we rescued the Cdon morphant phenotype with pharmacological blockade of FGF pathways or in an *Fgf8* mutant background (*ace*). This suggests that FGF signaling operates downstream of Cdon function.

At the moment there is little information about the precise regulation of *Cdon*. To understand how *Cdon* expression is regulated during forebrain development we have undertaken an analysis of its regulatory elements. We isolated nine evolutionary conserved sequences on the *Cdon locus* and tested their enhancer activity. Some of the isolated sequences appear to have enhancer activity. One of the sequences (chr18:42,516,402-42,517,273) drives the expression of a reporter gene (GFP) specifically in the telencephalon of zebrafish embryos.

INTRODUCTION

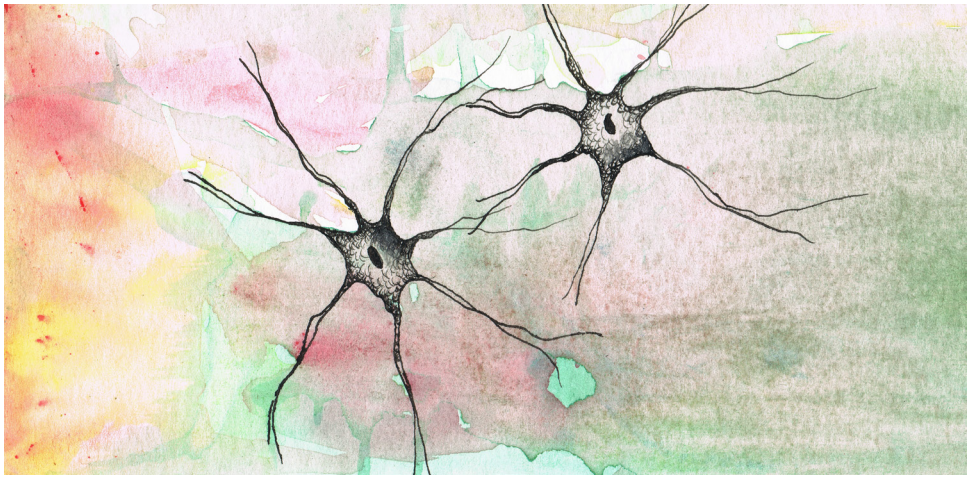

Developmental biology and secreted signaling molecules

Developmental biology seeks to explain how the structure of organisms changes with time. During the course of embryonic development as the fertilized egg develops into a complete organism, multiple developmental processes take place. The formation of the body plan and the organization of the different tissues and organs in multicellular organisms are central areas of research in developmental biology. This level of organization highly depends on an efficient communication among cells.

The capacity of a cell to secrete a product, which preceded multicellularity in the history of life, acquired a new meaning once multicellularity arose: it provided a mean for establishing differences across an otherwise undifferentiated population of cells (Fig.1) (Newman and Müller, 2006). Signaling between cells is an essential condition for the development of multicellular organisms and to control regional specification, proliferation, differentiation, morphogenesis as well as growth. These processes and the action of specific signaling pathways are triggered by the secretion of molecules that interact with receptor proteins in the receiving cells activating specific intracellular transduction cascades. These specific cascades finally control the activity of sets of transcription factors, which then dictate the fate of the responding cells by orchestrating the genomic response to extracellular information.

Different secreted signaling molecules that modulate intracellular signaling cascades and transcription control have been identified during the last decades. These molecules can be grouped in distinct gene families. The wingless (Wnt), transforming growth factor-β (TGF-β), fibroblast growth factor (FGF) and Hedgehog (Hh) families are among the largest and best studied molecular systems.

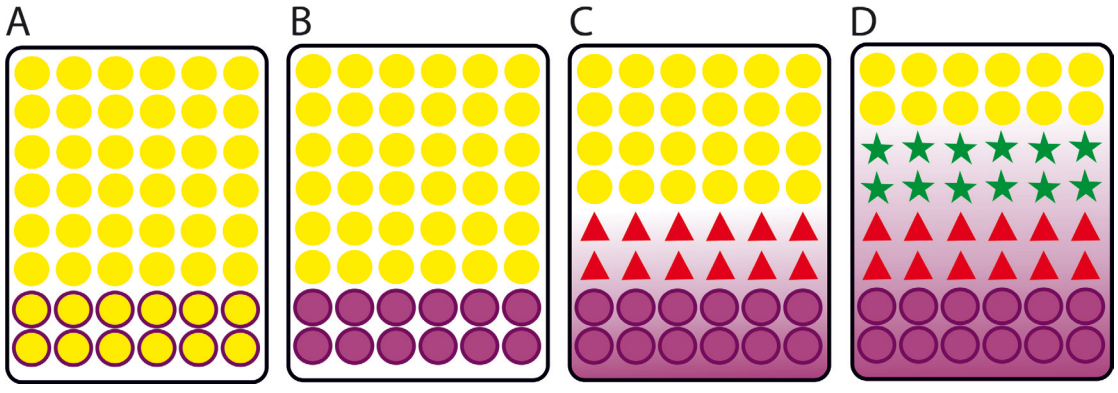

Fig. 1. Schematic model of pattern formation. The yellow circles depict an undifferentiated epithelium. **A)** The cells at the bottom begin to differentiate (purple perimeter). **B)** Terminally differentiated cells (purple circles**)** start secreting a morphogen (purple gradient in **C**). **C)** The concentration of the morphogen is higher near the source and decreases with the distance. If cells can respond to threshold concentration of this molecule, for instance, above a particular concentration, they adopt a specific fate (red triangles). **D)** Responding cells that are exposed to lower concentrations of the morphogen can adopt a different fate (green stars). Thus, the gradient confers positional information to the cells.

Members of the Wnt family are secreted ligands that regulate numerous developmental pathways (Cadigan and Peifer, 2009; van Amerongen and Nusse, 2009). Wnts bind to members of the family of Frizzled receptors, activating a canonical signaling pathway that targets members of the LEF/TCF transcription factor family. These transcription factors control gene expression programs that regulate cell fate and morphogenesis (van Amerongen and Nusse, 2009). Wnts also activate the so-called non-canonical pathways, which regulate planar cell polarity by stimulating cytoskeletal reorganization (Veeman et al., 2003).

TGFβ superfamily ligands bind to a type II receptor, which recruits and phosphorylates a type I receptor. The type I receptor then phosphorylates receptor-regulated SMADs (R-SMADs), which thereafter bind the coSMAD SMAD4. R-SMAD/coSMAD complexes accumulate in the nucleus, where they act as transcription factors and participate in the regulation of target gene expression (Shi and Massague, 2003). Bone morphogenetic proteins (BMPs) and nodal belong to this family.

FGF ligands, with the exception of the intracellular FGFs (iFGFs, FGF11-14), signal through a family of tyrosine kinase receptors, the FGF receptors (FGFRs). FGF ligands bind the extracellular domain of the FGFRs in combination with heparan sulphate to form a 2:2:2 FGF:FGFR:heparan complex. The dimerization of the receptor results in the transphosphorylation of specific intracellular tyrosine residues. This triggers the activation of different cytoplasmic signal transduction pathways: the Ras/ERK pathway, which is associated with proliferation and differentiation; the Akt pathway, associated with cell survival and the protein kinase C (PKC) pathway, involved in cell morphology and migration (Schlessinger, 2000; Dailey et al., 2005; Mohammadi et al., 2005).

Although the members of these families activate particular intracellular cascades, there are many cross-regulations among the different components and integration among these and other signaling pathways, forming a complex network. This super organization adds complexity to the system and makes it harder to understand specific functional mechanisms. Nevertheless, the fact that signaling pathways are used repeatedly during development and in the maintenance, regeneration and pathology of the adult organism makes the research of their function, mechanisms and interactions interesting and useful.

Hedgehog signaling

The Hedgehog family is one of the most studied families of signaling molecules. This family was identified over thirty years ago in a *Drosophila* screen aimed at identifying larval patterning genes (Nusslein-Volhard and Wieschaus, 1980). From this discovery, many studies have elucidated that Hh signaling plays a central role in the development of most metazoans. This signaling pathway is redeployed multiple times in the life of an organism with a myriad of specific effects, and is involved in several human pathologies, including many types of cancers. A schema of the main molecular players of this family is depicted in figure 2.

Hh proteins are secreted signaling molecules that mediate essential tissue-patterning events during embryonic development and regulate homeostasis and regeneration of adult tissues. There are three Hh homologs in amniote vertebrates: Sonic (Shh), Desert (Dhh) and Indian hedgehog (Ihh) (Fietz et al., 1994) and there are five members in teleost: Shh, Dhh,

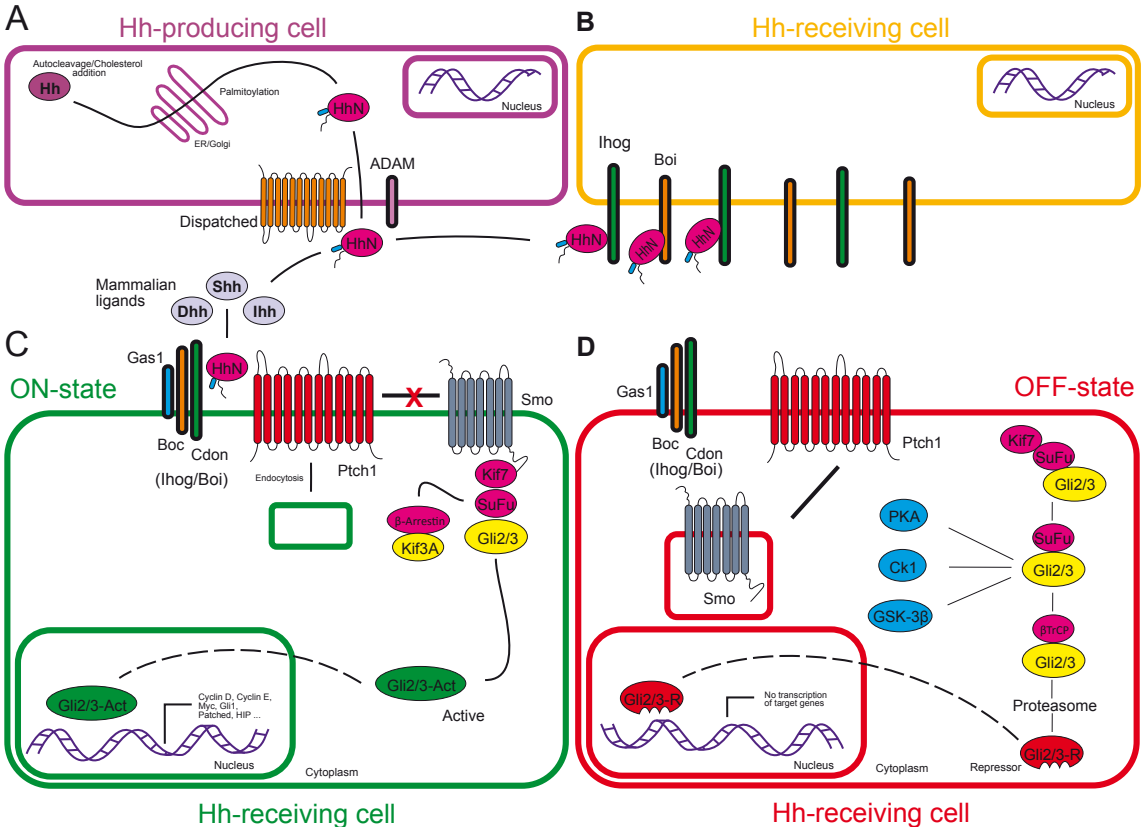

Fig. 2. Schematic representation of the Hedgehog signaling pathway. Components identified in vertebrates and *Drosophila* are shown. A Hh producing cell is depicted in **A** and Hh receiving cells are represented in **B-D**. **A)** The Hh precursor is processed and released into the extracellular space. **B)** HhN is titrated by Ihog and Boi at the cell membrane. **C)** HhN is received at the cell membrane of a responding cell. HhN binding to Patched releases Smoothened (Smo) inhibition activating the Gli2/3 transcription factors (ON-state). **D)** If HhN does not reach the surface of the receiving cell, Smo remains inactive (OFF-state). The Hh pathway components and their relationships are detailed in the text. (Modified from Ingham, 2012.).

Tiggy winkle hedgehog (Twhh), Echidna hedgehog (Ehh), and Qiqihar hedgehog (Qhh). These proteins differ primarily in their tissue distribution (Ingham and McMahon, 2001; Ingham et al., 2011). Shh is the only member expressed in the vertebrate central nervous system (CNS), mostly in ventral structures such as the floor plate or the ventral forebrain. Shh catched the attention of many researchers because it acts as a morphogenetic factor in many organizing centers also outside the CNS, including the zone of polarizing activity in the limb bud, the notochord and prechordal plate within the axial mesoderm (Echelard et al., 1993; Krauss et al., 1993; Riddle et al., 1993; Chang et al., 1994; Roelink et al., 1994).

The release and reception of Hh ligands have been extensively studied in flies and mice, and have revealed that nearly all core components of the pathways are highly conserved (Goodrich et al., 1996; Ryan and Chiang, 2012). In Hh producing cells, Hh is autocleaved (HhN) and covalently modified by the attachment of cholesterol to its C terminus, which confers Hh high affinity for the plasma membrane (Beachy et al., 1997). Hh is also palmitoylated at its N terminus. Once Hh undergoes the intracellular processes described above (HhN-p), Dispatched (Disp), a 12-pass transmembrane protein belonging to the RND family of bacterial transporters, contributes to the final release of HhN-p (Burke et al., 1999; Kawakami et al., 2002; Ma et al., 2002; Tukachinsky et al., 2012). In vertebrates, the release of ShhN-p is also mediated by metalloprotease ectodomain shedding, resulting in a soluble and biologically active morphogen (Dierker et al., 2009). Multiple sheddases (ADAM10, ADAM12 and ADAM17) can contribute to ShhN-p release (Ohlig et al., 2011).

In the receiving cells, the core components that mediate Hh signal response are Patched (Ptch), a 12-pass integral membrane protein (Hooper and Scott, 1989; Nakano et al., 1989; Stone et al., 1996; Fuse et al., 1999), and Smoothened (Smo), a seven-pass integral membrane protein with homology with G-protein-coupled receptors (Alcedo et al., 1996; van den Heuvel and Ingham, 1996). Ptch inhibits the activity of Smo, a positive regulator of Hedgehog pathway activation (Denef et al., 2000; Taipale et al., 2002). Binding of Hh ligands to Ptch relieve this inhibition (Ingham et al., 1991; Chen and Struhl, 1996; Marigo et al., 1996), triggering a cascade of intracellular events that lead to the accumulation of the gene-activating form of the Gli transcription factors (Gli1-Gli3).

Gli2 and Gli3 (but not Gli1) are bifunctional transcription factors: their full-length forms act as transcriptional activators, but they can be converted into lower-molecular-weight transcriptional repressors. This conversion is achieved by the phosphorylation of a series of motifs within the carboxy-terminal domain of the protein. These motifs are sequentially phosphorylated by the protein kinase A (PKA), the glycogen synthase kinase 3 β (GSK3 β), and the casein kinase I (CKI) to generate recognition signals for the F-box protein β-transducin repeat-containing protein (β-TrCP). This phosphorilation catalyzes the ubiquitylation of the

carboxyl terminus, targeting it for degradation by the proteasome to yield the truncated amino-terminal repressor forms, Gli2/3R (Ingham et al., 2011). Gli2/3R bind to Hh target genes to repress their transcription. A notable difference between the vertebrate and non-vertebrate Hh signaling is that in vertebrates the primary cilium is involved in the signal transduction. Primary cilia are microtubule-based, non-motile structures that project from the surface of nearly all vertebrate cells but that are conspicuously absent in most *Drosophila* and invertebrate cell types (Goetz and Anderson, 2010). Gli2/3 proteins appear to shuttle up and down the primary cilium in association with the Cos/Kif7 and SuFu proteins; in the absence of Smo activity, this association seems to promote their processing at the base of the primary cilium. Binding of HhN to Ptch promotes Smo release which is then transported to the tip of the primary cilium. The process requires Kif3a and β-arrestin activity. At the tip of the cilium, Smo promotes the dissociation of the Gli2/3-Cos-SuFu complex (Tukachinsky et al., 2010), releasing the full-length highly labile forms of the Gli proteins. These translocate to the nucleus and activate transcription of target genes, such as Ptch1, which attenuates the signal, Gli1, which amplifies the signal, and genes encoding the cell cycle regulators, Myc, cyclin D, and E.

After being released, Hh ligands diffuse in the extracellular space with a complex mechanism. Heparan sulfate proteoglycans (HSPG) play a crucial role shaping the gradient of the HhN-P form of Hh in the extracellular space, modulating its long-range diffusion (The et al., 1999; Bornemann et al., 2004; Ayers et al., 2010; Ayers et al., 2012). Furthermore, membrane extensions resembling filopodia (cytonemes) appears to mediated the delivery of Hh (Rojas-Rios et al., 2012).

The dynamics of the establishment of Hh gradient is very complex. As with other morphogenes, the temporal adaptation of cells to a Shh gradient integrates the concentration and duration of the signal to control differential gene expression (Pages and Kerridge, 2000; Dessaud et al., 2007). Additionally different cells may harbor different sets of Hh pathway components thereby responding to Hh ligands in different manners. Therefore Hh signaling seems to implicate the function of a variety of distinct molecular modules which are context-dependent. In addition to canonical pathway components, in the last few years a number of transmembrane or peripheral membrane proteins have been identified, which bind to Hh, playing a key role in shaping the extracellular gradient and thus finally modulating its signaling. In vertebrates, these Hh-binding proteins are: Cdon (cell adhesion molecule-related, down-regulated by oncogenes, (also noted as Cdo) (Kang et al., 1997; Cole and Krauss, 2003), Boc (Brother of Cdo) (Kang et al., 2002), Gas1 (Allen et al., 2007; Martinelli and Fan, 2007), Hh interacting protein (Hhip) (Chuang and McMahon, 1999) , LRP2 (McCarthy et al., 2002; Christ et al., 2012) and Scube2 (Hollway et al., 2006; Creanga et al., 2012).

Cdon and Boc transmembrane proteins

Cdon and Boc proteins have been characterized as cell surface glycoproteins belonging to a subgroup of the Immunoglobulin (Ig) superfamily of cell adhesion molecules (CAMs), that also includes L1 and the Robo axon-guidance receptors (Kamiguchi and Lemmon, 2000). Their ectodomain respectively contains five and four Ig-like domains, followed by three fibronectin III (FNIII) repeats (Fn1-3), a single trans-membrane domain and a divergent intracellular region of variable length (Fig. 3A), which may account for some of their functional differences (Kang et al., 2002; Mulieri et al., 2002). The *Drosophila* homologues Ihog and Boi present four Ig domains and only two FNIII repeats (Fn1, 2) (Kang et al., 2002; Yao et al., 2006). Sequence analysis reveals that Cdon/Boc Fn2 and Fn3 are respectively homologous to the Fn1 and Fn2 of Ihog/Boi (Kang et al., 2002). Notably, *Cdon* homologs have been found in the genomes of the sponge *Amphimedon queenslandica* and the placazoan *Trichoplax adhaerens*, where no other Hh signaling homologs components have been found. Thus Cdon predates the origins of the Hh pathway (Srivastava et al., 2010; Ingham et al., 2011).

Cdon and Boc form homophilic and heterophilic complexes in cis by interaction of the ecto- and intracellular domains (Kang et al., 2002) (Fig. 3B–D). Cdon has been shown to interact also with Neogenin (Kang et al., 2004), an Ig/FnIII CAM family member that acts as receptor for the axon guidance cue Netrin. Furthermore, during myoblast and neuronal differentiation, cis-interaction of N-Cadherin with Fn1 (Kang et al., 2003; Lu and Krauss, 2010) promotes binding of the Cdon intracellular domain to Bnip-2 and JLP, two proteins that func-

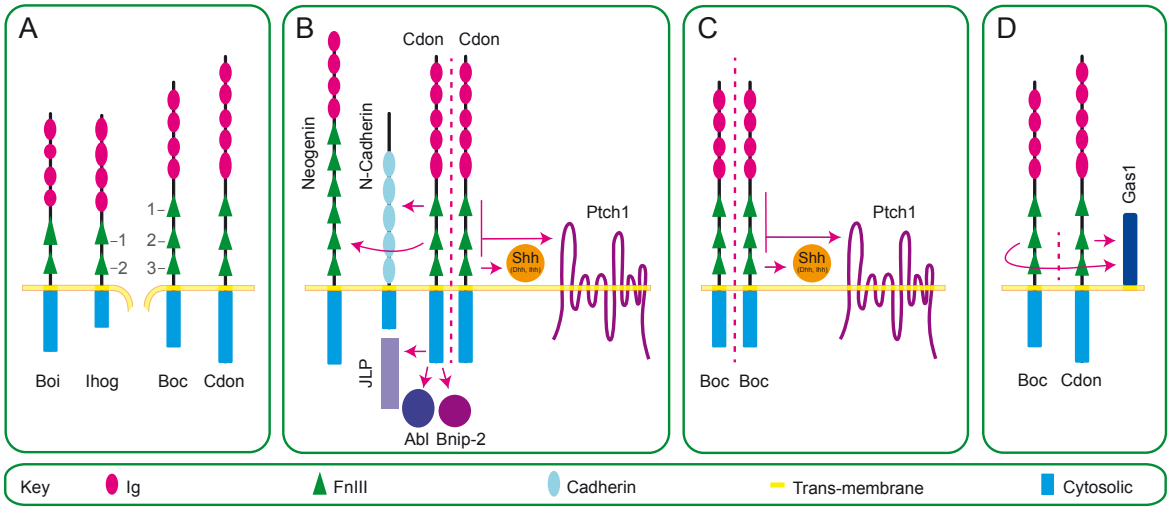

Fig. 3. Schematic diagram representing the structure and the interactions of Cdon and Boc. A) Comparison of the domain organization of Boc and Cdon with that of their *Drosophila* homologs, Boi and Ihog. Numbers indicate the position of each Fibronectin type III (FnIII) domain. **B)** Cdon forms homo- and heteromeric complexes binding to Neogenin and N-cadherin and interacts with the cytosolic proteins JLP, Abl, Bnip-2. Within the Shh signaling pathways Cdon **(B)** and Boc **(C)** associate with Shh, Dhh, Ihh and Ptch1. **(D)** Boc and Cdon can interact in *cis* and bind Gas1. Arrows and dotted lines depict protein interactions. Ig, Immunoglobulin domain. FnIII, Fibronectin type III domain.

tion as scaffolds for small GTPases and p38 pathway components, respectively (Takaesu et al., 2006; Kang et al., 2008; Oh et al., 2009).

Notably Cdon/Boc and Ihog/Boi bind members of the Hh family with high-affinity, but, notably, with different and evolutionary non-conserved modes (Okada et al., 2006; Tenzen et al., 2006; Yao et al., 2006; McLellan et al., 2008). Biochemical, biophysical, and X-ray structural studies demonstrated that Shh-Cdon interaction is calcium dependent and involves a previously unappreciated binuclear calcium-binding site on ShhN (McLellan et al., 2008) and the Cdon/Boc Fn3 domain (Tenzen et al., 2006; Yao et al., 2006; McLellan et al., 2008) This interaction mode is conserved for all vertebrate Hh proteins (Kavran et al., 2010). In addition, CDON also binds PTCH1 through Fn1-2 domains (Bae et al., 2011).

Cdon deficient mice display different forms of holoprosencephaly (HPE) with strain-specific severity. HPE has been defined as the failure of the most anterior portion of the CNS (forebrain) to divide into two distinct cerebral hemispheres during development [see (Gongal et al., 2011)]. In *Cdon* mutants, HPE goes from mild facial defects to brain and eye malformations (Cole and Krauss, 2003; Zhang et al., 2006; Zhang et al., 2009; Hong and Krauss, 2012) suggesting that Cdon has some spatio-temporal unique function during embryonic development. Nevertheless, defects of $Cdon^{-/-}$ embryos aggravate in absence of *Boc*. Indeed, $Cdon^{-/-}$;$Boc^{-/-}$ animals display severe brain defects and strong craniofacial anomalies, associated to reduced expression of Shh and its target genes (Zhang et al., 2011).

In *Drosophila*, loss of either Boi or Ihog function has no consequences in the development of the imaginal discs that are normally strongly dependent on Hh signaling. Their combined inactivation however recapitulates hh loss of function, suggesting that Boi and Ihog play a redundant function in Hh pathway activation (Camp et al., 2010; Zheng et al., 2010). Notably, Ihog and Boi have been also related to the formation of the Hh gradient, as both proteins can sequester and titrate the amount of ligand available for Ptch binding, thus limiting long-range signaling (Hartman et al., 2010; Yan et al., 2010; Zheng et al., 2010; Bilioni et al., 2012). One proposed model is that Ihog has biphasic activity, so that low Ihog expression favors Hh–Ptch interaction and hence enhanced signal transduction to the nucleus, whereas increased Ihog expression partially titrates Hh from binding to Ptch, reducing the level of signaling. The corollary is that Ihog expression is downregulated in target cells, transducing the highest level of Hh signaling (Yan et al., 2010). Whether Cdon and/or Boc work in a similar manner in vertebrates is still unknown.

In vertebrates, Boc, Gas1 as well as Cdon play overlapping and essential roles during early Hh-dependent patterning of the mammalian ventral neural tube and further contribute the specification of different neural progenitors (Allen et al., 2011). Only embryos deficient

in the three genes die before birth and are characterized by a phenotype similar to that in Shh null embryos, with severe HPE (Allen et al., 2011; Izzi et al., 2011). This overlapping activity does not seem to be entirely conserved in zebrafish, where loss of Boc function, that characterizes the umleitung (uml) mutant, is sufficient to cause defects in patterning of the ventral neural tube, somites and upper jaw. Mechanistically, Boc seems to be required to maximize the response of cells exposed to high Hh concentrations; in its absence, cells no longer express genes that are normally activated by high Hh levels (Bergeron et al., 2011).

In addition, Boc, but not Cdon, has been implicated in Shh-induced axon guidance. Inactivation of either Smo or Boc in mouse commissural neurons disrupts the trajectory of the axons at the ipsilateral edge of the floor plate, indicating that signaling through both of these molecules is necessary to attract pre-crossing axons to the midline (Charron et al., 2003; Okada et al., 2006).

Mutations in CDON, as in mouse, have been associated with human HPE (Bae et al., 2011). However, besides HPE, alterations in Shh signaling cause other severe pathological conditions including Carpenter, Ellis-van Creveld, Smith-Lemli-Opitzl and Pallister-Hall Diseases, Greig Cephalopolysyndactyly or the Gorlin syndrome (Cohen, 2010). Cdon does not seem to be involved, at least so far, in those anomalies.

Search for possible implications of Cdon and Boc in these conditions is thus a necessary step toward the understanding of the possible medical implication of these molecules. The development of the ventral forebrain and the retina is controlled by similar molecular mechanisms. This suggests that *Cdon* and *Boc* genes may be possible candidates for inborn ocular malformations.

Eye Development

The vertebrate embryonic brain is composed by three main structures arranged along the anterior-posterior axis: the forebrain, the midbrain and the hindbrain. The forebrain arises from the anterior-most neuroectoderm during gastrulation, and by the end of somitogenesis it comprises the dorsally positioned telencephalon, the eyes, the ventrally positioned hypothalamus, and the more caudally located diencephalon (Fig. 4). This general organization of the forebrain is conserved in all vertebrates (Wilson and Houart, 2004). Eye formation begins during gastrulation, with the emergence of a group of cells, the eye field, located centrally in the developing forebrain (Adelmann, 1929).

The eye undergoes many complex morphological changes that are somewhat difficult to visualize in three dimensions. The main axes used to refer to the morphology of the eye are

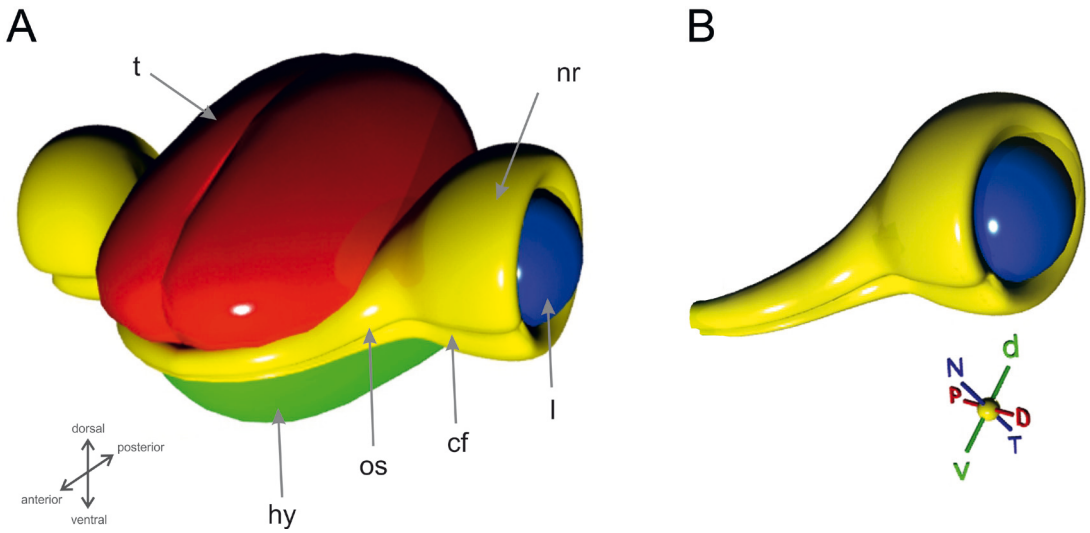

Fig. 4. Organization of the forebrain in embryonic zebrafish. A) The cartoon depicts a frontal view of the forebrain and the relationship between the eyes and the brain. Abbreviations: cf, choroid fissure; hy, hypothalamus; l, lens; nr, neural retina; os, optic stalk; t, telencephalon. Adapted from Wilson and Houart, 2004. **B)** The picture represents an eye at the optic cup stage connected by the optic stalk. The axes are depicted below the eye. Abbreviations: d, dorsal; D, distal; N, nasal (anterior); P, proximal (medial); T, temporal (posterior); v, ventral.

depicted in Figure 4b.

The initial step in eye formation is the specification of a coherent domain of cells in the anterior neural plate during gastrulation (Chuang and Raymond, 2002). The eye field is defined by the overlapping expression of highly conserved transcription factors. Once the eye field is established, its neuroepithelial cells evaginate to form the optic vesicles (Fig.5A). The optic vesicles become then patterned along the proximo-distal (P-D) axis in two lateral (retina) and two medial domains (optic stalk). The optic stalk connects the optic vesicle to the forebrain and finally differentiates generating the glial cells of the optic nerve. The establishment of the early P-D patterning of the optic vesicles is defined by the expression of the homeobox transcription factors Pax2 and Pax6 (Schwarz et al., 2000). Normally, Pax6 expression is restricted to the developing retina and retina pigmented epithelium (RPE), whereas Pax2 expression is localized to the optic stalk.

At the optic vesicle stage, the presumptive retinal cells come in close contact with the surface ectoderm. This event is followed by a complex series of reciprocal inductive interactions that result in the formation of the lens placode from the surface ectoderm and the invagination of the underlying optic vesicle to form a bilayered optic cup (Fig. 5B) (Graw, 2010). Studies using embryonic stem cell aggregates have recently suggested that optic cup morphogenesis depends on intrinsic self-organizing programs, involving stepwise and domain-specific regulation of local epithelial properties (Eiraku et al., 2011; Nakano et al., 2012). Optic cup formation occurs approximately between 14 and 24 hpf in the zebrafish (Schmitt and Dowl-

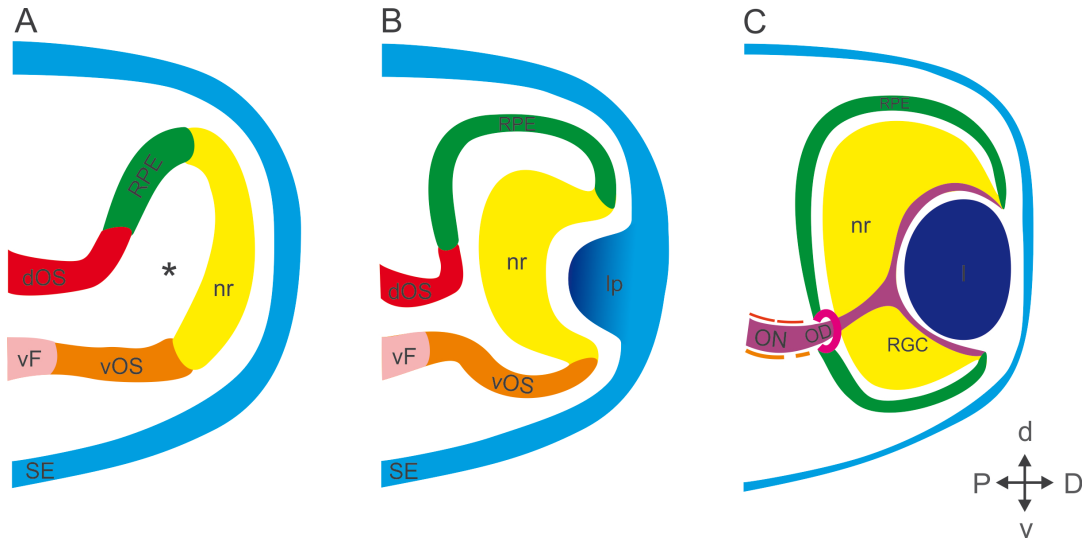

Fig. 5. Summary of early eye development in vertebrates. In panels **A–C**, presumptive or differentiated eye tissues are color-coded: blue, lens; yellow, neural retina; light blue, non-neural surface ectoderm, orange, ventral optic stalk; red, dorsal optic stalk; pink, ventral forebrain; green, retinal pigmented epithelium (RPE), violet; retinal ganglion cell projections. Dotted line depicts the optic stalk regression. **A)** Formation of the optic vesicle is initiated by an evagination (indicated by asterisk) of the presumptive forebrain region. The optic vesicle region is divided into ventral optic stalk (VOS), neural retina (NR), retinal pigmented epithelium (RPE) and dorsal optic stalk (DOS). Growth of the optic vesicle culminates with the close contact between the lens placode (LP) and the presumptive neural retina (NR). **B)** During optic cup formation, the optic vesicle invaginates and the lens vesicle (LV) and neural retina (NR) are established. **C)** Later on, the axons from the ganglion cells of the retina (RGC) meet at the posterior pole of the eye, exit through the optic disc (OD) and travel along to the optic nerve. Abbreviations: dOS, dorsal optic stalk; l, lens; lp, lens placode; NR, neural retina; OD, optic disc; ON, optic nerve; RGC, retinal ganglion cells; RPE, retina pigmented epithelium; SE, surface ectoderm; vF, ventral forebrain; vOS, ventral optic stalk.

ing, 1994). During this process a transient structure becomes evident in the ventral region, this is the optic fissure (or choroid fissure). The fissure forms as the walls of the invaginating optic vesicle deepen. The optic fissure extends from the most distal point of the optic cup to the proximal end of the optic stalk (Fig. 4A).

Eye morphogenesis in zebrafish is similar to that observed in other vertebrates (Li et al., 2000). However, during evagination in most vertebrates, the optic vesicle form a hollow structure, whereas in zebrafish the developing optic vesicles are solid masses with the optic stalk positioned anteriorly (Kimmel et al., 1995). Subsequent rotation of the optic vesicle brings the optic stalk into a ventral position (Schmitt and Dowling, 1994). Despite these differences, the regulatory components required for eye field specification and morphogenesis are conserved among species (Chuang and Raymond, 2002).

Once the optic cup is formed around 25hpf, a wave of differentiation begins in the ventronasal retina, adjacent to the choroid fissure, and spread with a fan-shape to the dorsal and temporal retina (Masai et al., 2000; Neumann and Nuesslein-Volhard, 2000). The pool of

retinal progenitor cells expands by proliferation and will subsequently generate six types of neurons: the retinal ganglion cells (RGCs), amacrine cells, horizontal cells, bipolar cells, and the light-sensitive photoreceptor cells (rods and cones) and other type of glial cells, the Müller cells

RGCs are the first cells to differentiate cells in the retina, (Schmitt and Dowling, 1996). Following their differentiation, RGCs extend their axons into the optic fiber layer at the inner surface of the retina, where they grow in a highly direct, radial fashion towards their exit point, the optic disc (Fig. 5C). The optic disc is a structure that constitutes the interface between the optic stalk and the retina, and develops from the edges of the optic fissure. The axons enter the optic nerves and extend towards the ventral midline of the diencephalon, where the two nerves meet and form the optic chiasm, a major brain commissure. In species with eyes located laterally, all axons cross the midline at the chiasm, whereas in animals with binocular vision a proportion of axons originating in the temporal region of the retina do not cross but instead project ipsilaterally. Irrespective of their behaviour at the chiasm, RGC axons then project dorsally within the optic tracts towards their targets in the midbrain and thalamus (see Erskine and Herrera, 2007).

Mesodermal and neural crest cells also contribute to eye development. Periocular mesenchyme cells (POMs) enter the eye through the optic fissure beginning around 24 hpf in zebrafish (Soules and Link, 2005). These cells will ultimately contribute to specialize anterior structures, including the corneal endothelium and the hyaloid vasculature (Soules and Link, 2005; Langenberg et al., 2008). As the POM that give rise to the retinal vasculature enter and the RGC axons leave the eye, the fissure lips fuse to close permanently. A timely closure of the optic fissure is critical for normal eye development and function. Failure of the choroid fissure to close leads to the formation of a permanent opening of the ventral retina, a condition known as coloboma (Fig. 6 A-C). The term coloboma refers to a family of common ocular pathologies that can cause severe visual impairment (Chang et al., 2006). The closure of the optic fissure requieres two events: the edges of the optic fissure need to become closely apposed, and the apposed edges need to express at the right time a number of molecular components appropriate to bring about the fusion. Disruption of either one or both of these processes may result in the formation of a coloboma. Colobomata can have variable appearances, since any of the structures traversed by the optic fissure, from the iris to the optic nerve, in the infero-nasal quadrant of the eye can be involved: iris, ciliary body, zonules, choroid, retina, and optic nerve.

Besides coloboma, other congenital eye disorders, including anophthalmia, microphthalmia, aniridia, and retinal dysplasia arise from an abnormal eye development. Thus, understanding the mechanisms that lead to initial specification and differentiation of ocular tissues

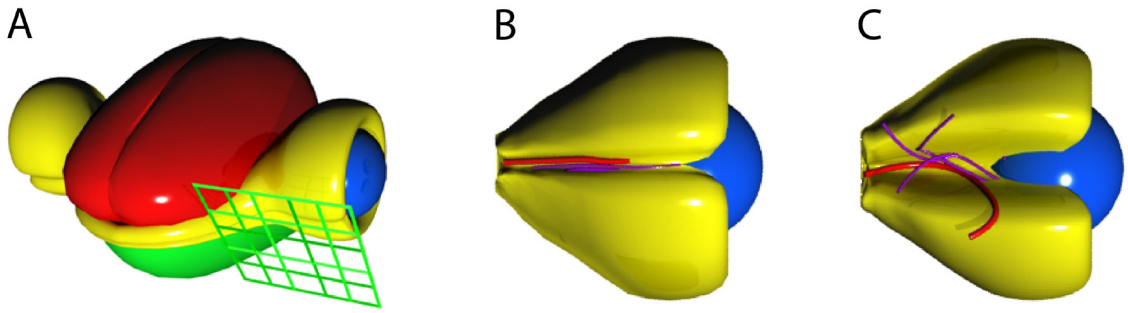

Fig. 6. Developmental defects associated to the failure of the optic fissure closure. A) View of the forebrain structures; the grid indicate the plane of view of the cartoons in B and C. **B)** In a normal eye the optic fissure allows for passage of the hyaloid artery (red) into the eye and of the retinal axons (violet) out of the eye into the optic nerve. **C)** In a colobomatous eye, the temporal and nasal borders of the fissure fail to fuse, and at least in teleosts, the axons of the RGC project aberrantly around the eye or leave the retina from ectopic locations. Additionally, the hyaloid artery does not form properly.

is critical to identify the causes of these defects.

Hedgehog signaling in eye development

Ingham and McMahon reported in a review in 2001 that Hh signaling plays a role in more than 20 different tissues, organs and/or cell types. Since then the number of the described Hh functions has still considerably increased.

Hh signaling acts at different steps of eye development. These include, the separation of the optic vesicles, the establishment of the P-D axis (Ekker et al., 1995; Macdonald et al., 1995; Chiang et al., 1996), the development of the optic fissure (Dakubo et al., 2003; Morcillo et al., 2006), retinal neurogenesis (Neumann and Nuesslein-Volhard, 2000), RPE differentiation (Perron et al., 2003), cell proliferation and survival (Neumann and Nuesslein-Volhard, 2000; Zhang and Yang, 2001), the laminar organization of the retina (Wang et al., 2002), and the guidance of the RGCs axons (Trousse et al., 2001; Sanchez-Camacho and Bovolenta, 2008).

During early eye development Shh secreted from the midline in the ventral forebrain, plays a primary role in the splitting of the eye field in two individual optic vesicles and in establishing the P-D axis of the optic vesicle. Gain of function experiments led to the conclusion that Shh promotes the expression of Pax2, a marker of the optic stalk, and represses the expression of Pax6, a retinal marker, forming a precise boundary between the retina and the optic stalk. Basically, Shh signaling induces the specification of optic stalk tissue at the expense of the neural retina (Macdonald et al., 1995; Schwarz et al., 2000). Hh signaling maintains the optic stalk-retina interface also by regulating *Vax* gene activity (Take-uchi et

al., 2003).

Hh signaling interacts with various signaling pathways to produce distinct temporal and spatial outcomes. Particularly, the interaction between the Hh and FGF pathways is essential for correct forebrain patterning (Bertrand and Dahmane, 2006). The specific mechanism of this interaction however is still unclear. Similar to Hh signaling, FGF pathway reiterative contributes to eye development. Studies in zebrafish, frog and chicken have suggested that FGF signaling regulates the initial formation of the eye field (Moore et al., 2004), the specification of the neural retina (Pittack et al., 1997; Hyer et al., 1998), the determination of the naso-temporal axis of the eye vesicle (Picker and Brand, 2005), and the differentiation of retinal neurons (Guillemot and Cepko, 1992; Martinez-Morales et al., 2005). FGF signaling also controls the closure of the optic fissure by modulating retinal progenitor proliferation. Inactivation of *Fgfr1* and *Fgfr2* in the developing optic cup results in coloboma in mice (Chen et al., 2012).

Following the formation of the optic cup, retinal neurogenesis is initiated and RGCs begin to express Shh which spreads the wave of RGC differentiation throughout the retina (Neumann and Nuesslein-Volhard, 2000).

So far it has been difficult to develop a picture of the precise interactions between Hh proteins and their cell surface partners, of their molecular consequences and of how these interactions control eye development in vertebrates.

A few observations highlight the importance of the different Hh surface components in eye development. Loss of Xhip (Hhip *Xenopus* homolog) results in the suppression of lens placode formation (Cornesse et al., 2005). In LRP2/megalin mutant mice the eyes are small or absent although with little penetrance (Willnow et al., 1996). Gas1 mutant mice display microphthalmia and present an ectopic overgrowth of neural retina in the ventral region of the RPE (Lee et al., 2001). Scube2 is expressed in the neuroepithelium of the optic cup in mice but its function there is unknown (Xavier and Cobourne, 2011). *Boc* mutant mice present defects at later stages of eye development. After optic cup formation, RGC axons are guided by Shh (Trousse et al., 2001; Sanchez-Camacho and Bovolenta, 2008) and Boc contributes to the specification of the RGCs that project ipsilaterally (Sanchez-Arrones et al., 2013, submitted) and possible contributes also to the segregation of ipsilateral axons at the optic chiasm (Fabre et al., 2010). Despite these observations, little is known about the molecular mechanisms with which these Hh interacting proteins contribute to eye development and whether their function is related to Hh signaling transduction.

Cdon mutant mice present eye defects which have been analyzed only superficially (Zhang et al., 2009). We therefore decided to explore Cdon function during eye development

using the zebrafish and chick as model systems. We also investigated Cdon relationship with Hh signalling.

OBJECTIVES

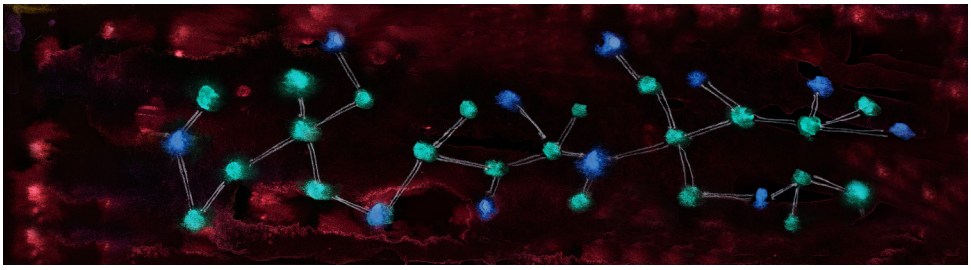

The function of Cdon during development has been determined in studies that have used Cdon mutant mice. However, the specific function of Cdon in eye development has been poorly explored. To fill this gap we addressed its function using the zebrafish and chick embryos as model systems addressing the following specific aims.

- To determine if the embryonic expression pattern of *Cdon* is conserved in vertebrates.

- To investigate if Cdon is important for vertebrate eye development.

- To understand if Cdon function in the eye is Hh dependent.

- To characterize the regulatory elements that drive *Cdon* expression in the developing forebrain.

MATERIALS & METHODS

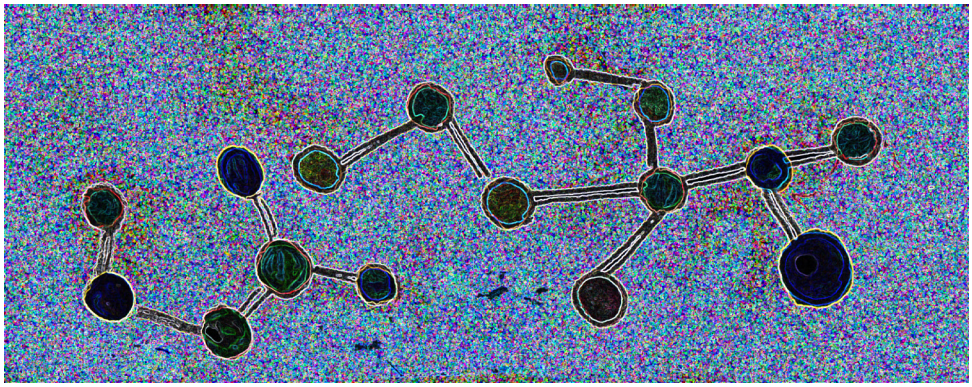

Maintenance of fishes and fish lines.

Adult zebrafish (*Danio Rerio*) were maintained at 28.5°C on a 14-hour light/10-hour dark cycle. Embryos (AB/Tu or WIK strains) were raised at 28°C and staged according to hours post-fertilization (hpf) and morphology (Kimmel et al., 1995). The following transgenic lines were used: Tg(*βactin*:HRAS-EGFP) vu119, *ath5::gap-gfp* and Tg(-8.0 *cldnb*:lynGFP) zf106 (Cooper et al., 2005; Haas and Gilmour, 2006; Zolessi et al., 2006). For convenience, these transgenic lines are referred to in the remainder of the text as *βactin*::mGFP, *ath5*::GFP and *cldnb*::GFP. The *Fgf8a* mutant *acerebellar* (*ace*) line was also used (Reifers et al., 1998). Zebrafish developmental stages from 1 cell stage to 72hpf are illustrated in figure 7 according to the classification of Kimmel et al., 1995. The morphogenetic steps of zebrafish eye formation are summarized in Table I. Embryos were growth in E3 medium (NaCl, 5mM; KCl, 0.17mM; CaCl, 0.33mM; MgSO4, 0.33mM, 10^{-5}% Methylene Blue (Nuesslein-Volhard and Dahm, 2002)).

Table I. Summary of the features that characterize the morphogenesis of the eye and other zebrafish forebrain structures.

	Optic primordium	**Other features**
6-7 somites	Solid mass of cells continuous with neural keel	Ventricle in neural keel appears. Mesenchyme migration ventral to optic primordia.
8-9 somites	Anterior border flattened. Posterior border rounded. Separation from neural keel commences along posterlor edge.	Constriction arises within forebrain.
10-12 somites	Ventral bending. Early eye rotation. Optic lumen and optic stalk formation	Initial flexure of forebrain. Mesenchyme migration dorsal and ventral to optic primordia.
14-30 somites	(14-15 somites) Invagination from center. Posterior groove formation. Pseudostratified retina. Stretching of cubodial layer of pigmented epithelium	Lens placode formation. Aggregation of mesenchyme on proximal surface of eye.
	(18-20 somites) Choroid flssure formation. Pigmented epithelium reduced to flat elongated layer with little proliferation.	Radial arrangement of lens cells.
>30 somites (24hpf)	Increase in retinal cell density optic stalk atrophy. Pigmented epithelium pigmentation begins. Late eye rotation begins	Mayor eye vasculature formed (e.g. hyaloid artery). Lens detached from ectoderm.
36hpf	Eye rotation completed. Choroid fissure at ventral pole. Posterior groove at dorsal pole. Optic axons exit eye. Choroid fissure closing.	Nasal placode anterior to eye.

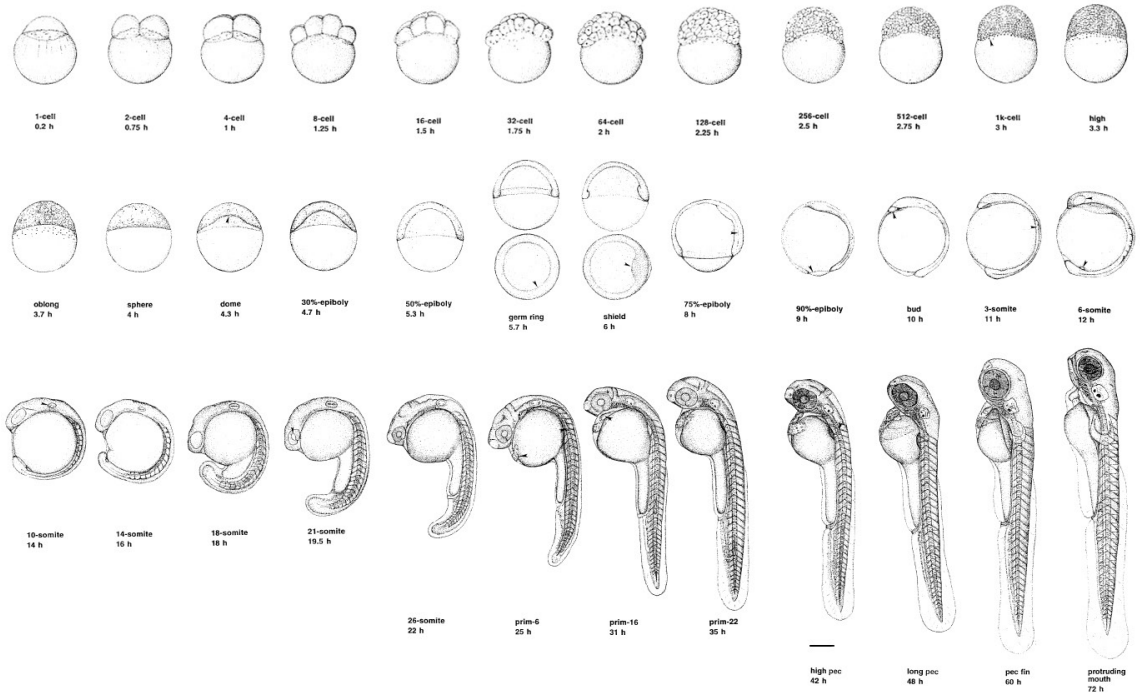

Fig7. A series of stages of the development of the zebrafish embryo, *Danio (Brachydanio) rerio:* from 1 cell stage to 72 hpf. Adapted from (Kimmel et al., 1995).

Chicken embryos.

For this study we used chicken embryos (*Gallus gallus domestica*) of the White Leghorn breed raised in the Santa Isabel farm (Córdoba, Spain). The embryonic stages used in this study according to Hamburguer and Hamilton, 1951 are represented in figure 8 and listed in Table II.

Table II. List of the main characteristics of chicken embryo development at 38ºC from stage HH4 to HH14. Adapted from (Hamburger and Hamilton, 1992).

Stage	Incubation time	Main Feature	Other features
4	18-19 hs	Definitive Streak	Maximal length of the primitive streak
5	19-22 hs	Head-Process	Notochord becomes visible
6	23-25 hs	Head-Fold	A definitive fold of the blastoderm anterior to the notochord
7	23-26 hs	One somite	Neural folds in the region of the head
8	26-29 hs	Four somites	Neural folds at the level of the midbrain
9	29-33 hs	Seven somites	Primitive optic vesicles are present
10	33-38 hs	Ten somites	Optic vesicles not constricted at base

11	40-45 hs	Thirteen somites	Optic vesicles are constricted at the base
12	45-49 hs	Sixteen somites	Primary optic vesicles and optic stalk well established
13	48-52 hs	Nineteen somites	Distinct enlargement of the telencephalon
14	50-53 hs	Twenty-two somites	Primary optic vesicles begins to invaginate and lens placode is formed

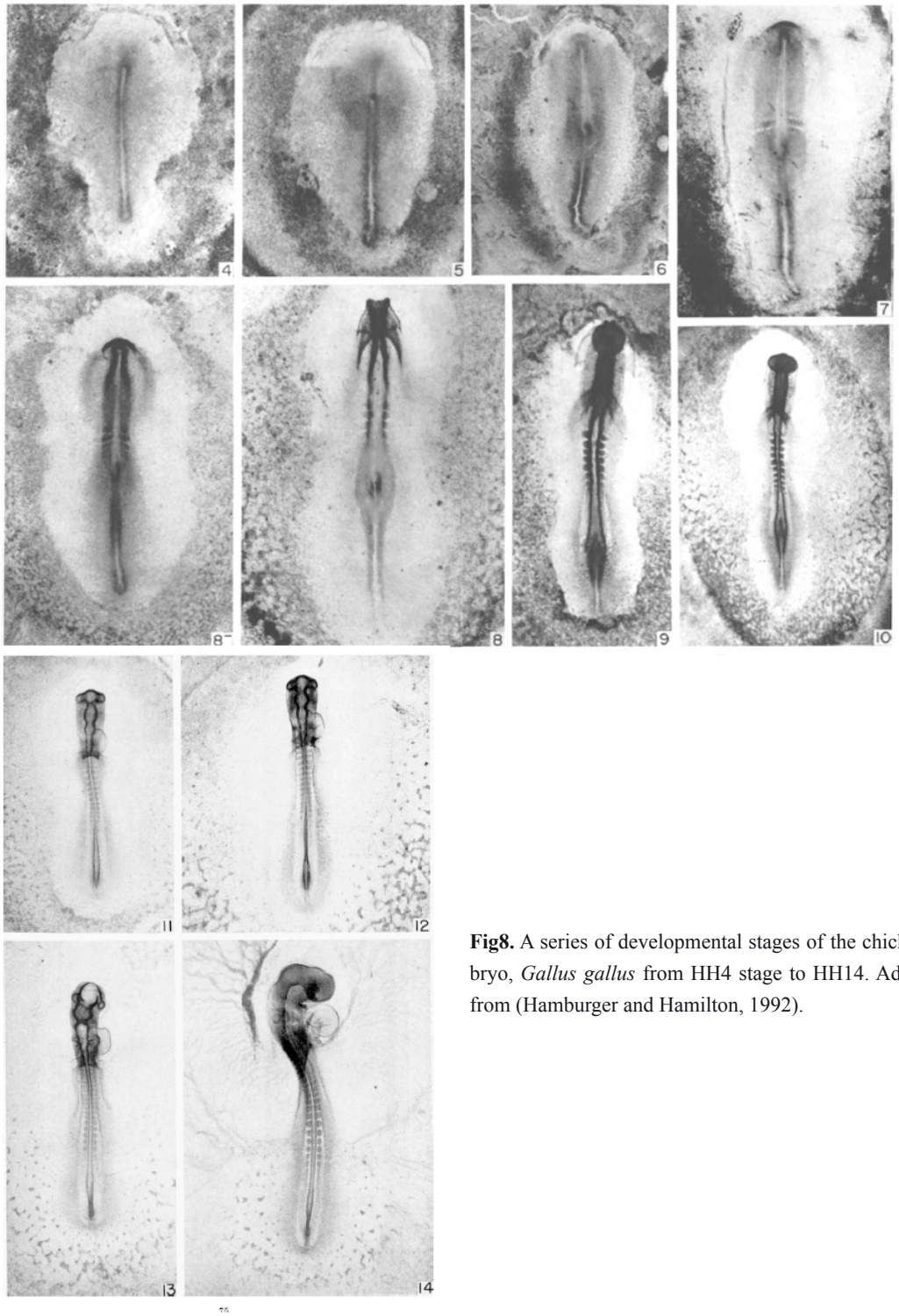

Fig8. A series of developmental stages of the chick embryo, *Gallus gallus* from HH4 stage to HH14. Adapted from (Hamburger and Hamilton, 1992).

Morpholinos.

In table III are listed the morpholinos used in this study. CdonMO and cCdonMO are translation-blocking MOs and spl8MO, spl11MO and spl14MO are splice-blocking MO. The ctlMO and cctlMO are standard control MO from Gene Tools.

Table III. List of morpholinos used in this study.

Name	Sequence	Modification	Specificity
ctlMO	CCTCTTACCTCAGTTACAATTTATA	3´- Lissamine	-
CdonMO	ATAATCTCAGGCCACCGTCCTCCAT	3´- Lissamine	*Danio Rerio*
spl8MO	ACTGTATGAACTCTTCTCACCTTGC	-	*Danio Rerio*
spl11MO	GCAGTAACCTCACCTGGCTCAAGGT	-	*Danio Rerio*
spl14MO	GACGGTACTTCAGACTCTCACCTTT	-	*Danio Rerio*
cctlMO	CCTCTTACCTCAGTTACAATTTATA	3´-Carboxyfluorescein	-
cCdonMO	CCGACTGCATAGCGCCCGGACAGCA	3´-Carboxyfluorescein	*Gallus gallus*

-Injections.

In pilot experiments, morpholino oligonucleotides were injected at concentrations ranging from 50 to 300 uM in water by using a microinjector (FemtoJet, Eppendorf). Injection/electroporation with the concentrations shown in table IV gave the strongest phenotype without evidence of apoptosis. The results presented in this work were obtained using the amounts reported in table IV.

Table IV. MO working concentrations.

Name	Working concentration
MO-Ctl	160uM-200uM
MO-Cdon	160uM
MO-Spl8	200uM
MO-Spl11	600uM
MO-Spl14	400uM
MO-cCtl	2mM
MO-cCdon	2mM

-Test.

To confirm sequence specificity, the CdonMO or ctlMO were co-injected into medaka fish embryos at one-cell stage with the cRNA (50ng/ul) of a reporter construct (5´*cdon*-GFP) carrying the *Cdon* 5´ sequence upstream of the GFP sequence. As a control, CdonMO and ctlMO were coinjected also with GFP alone. To corroborate the exon removal capacity of spl8MO, spl11MO and spl14MO we performed RT-PCR from cDNA of injected embryos with the respective MO. The primers used are listed in table V.

Table V. Primers to verify splicing products in spl8MO, spl11MO and spl14MO injected embryos.

Name	Sequence
Ex7F	TATCCATCCTGCGAGGTTTG
Ex9R	GACCTCATACAGGCTGGACG
Ex10F	CCAATAAGAATCCCTCCAAAG
Ex12R	CCAGCGTAACAGAATCTGAG
Ex13F	ACACTCCATCCAGCAATAAC
Ex15R	TCCTCCATAAGCACATGACG

Cryostat sections.

Fish, chicken and mouse embryos were fixed by immersion in 4% paraformaldehyde (PFA)-phosphate buffer (wt/vol) overnight at 4ºC. Embryos were then washed in phosphate buffer saline (PBS), incubated in a 30% sucrose-PBS solution (wt/vol), embedded and frozen in a 7.5% gelatin in 15% sucrose solution (wt/vol). Cryostat sections were processed for immunohistochemistry (IHC) or for *in situ* hybridization (ISH).

Immunohistochemistry (IHC).

Cryostat sections or whole embryos were stained by a standard protocol using antibodies against the following antigens: Cdon (1:100, R&D system), Pax6 (1:500, Covance), Pax2 (1:500, Zymed) and Fluorescein (1:500, Roche). Nuclei were counterstained with Hoecht.

In situ hybridization (ISH).

Chicken embryos were hybridized following the protocol described by Stern (Stern, 1998). Digoxigenin- or fluorescein-UTP-labelled antisense chicken riboprobes were used to detect *Pax2* and *Cdon*. Probes were visualized with NBT/BCIP (dark blue). *Cdon* chicken

probe was kindly provided by Ruth Diez del Corral (NotI/T3 pBSII KS+ probe 1.3Kb).

Zebrafish embryos were hybridized following Standard methods for whole-mount *in situ* hybridization. Digoxigenin-UTP-labelled antisense riboprobes were used to detect the markers listed in table VI. The *Boc* and *Cdon* coding sequences were obtained by RT-PCR from cDNA of embryos collected at different developmental stages using specific primers (Table VII).

Table VI. Probes used in zebrafish

Gene	Enzyme	Polymerase
Tbx5.1	NotI	T3
Vax1	NotI	SP6
Fgf8	EcoRV	SP6
Gli2	BamHI	T7
Gli2b	NcoI	SP6
Gli3	SpeI	T7
Pax2.1 (pax2a)	BamH1	T7
Ptc1	BamH1, (o XbaI)	T3
Shh	HindIII	T7
Nkx2.1a	KpnI	SP6
Nkx2.1b	SacII	T3
Nkx2.2	BamH1	T7
Foxg1	BamH1	T7
NLZ	SalI	SP6
Boc	BspH1	SP6
Cdon	KpnI	SP6
FoxD1	speI	T7
EfnA5a (347)	XbaI	T7
VSP	SalI	T7

Table VII. *Boc* and *Cdon* zebrafish probes.

Gene name	Primer forward	Primer reverse	Vector	Polymerase	Restriction Enzyme
Boc	CATCGATCCTTTCAATG-CAAG	GGGAGTATTCTT-GTTTCATCCA	pDrive (Qia-gen)	SP6	BspH1
Cdon	CATCGGGAGAATGT-GTTTCG	TCCAC-CAATATCTTCATTCG	pDrive (Qia-gen)	SP6	KpnI

mRNA and cDNA synthesis and cloning.

Embryos were injected with different splicing MO´s at 1-2 cells stage and at 24hpf were frozen in dry ice. RNA purification was performed with PureLink miniKit (Invitrogen) and cDNA was synthesized with iScript cDNA synthesis Kit (Bio-Rad). PCR products were run in agarose geles (1%-2%) and visualized with FastRed (Biotium).

5´*Cdon*-GFP construct was obtained by cloning the Cdon 5´ sequence, including its initial ATG. 5´*Cdon* was amplified by PCR with the following primers: zCdon_ClaI_ F: ATAATCGATCATCGGGAGAATGTGTTTCG and zCdon_NcoI_R: ATACCATGGCACG-GAAAGAGAAAGAAAG. The amplified product was cloned upstream of the GFP sequence lacking the ATG in a pCS2 vector (pCS2-5´*cdon*-GFP). Capped RNA (cRNA) was synthesized using pCS2-5´*Cdon*-GFP template and the mMessage mMachine® SP6 Kit (Ambion). The resulting mRNA was purified using RNeasy Mini Kit (Qiagen).

Deletion of the fibronectin domains of Boc. Boc-GFP expression vector was kindly provided by Ami Okada lab. PCR using Boc-GFP DNA as a template was performed with a PfuUltra DNA polymerase (Agilent) and the primers listed in table VIII. Primers were phosphorylated at the 5´ end to promote an efficient ligation reaction. The amplified products were ligated (Ligase, Roche) overnight at 16ºC and later digested with DpnI enzyme to remove the non-amplified DNA. The reaction product was used to transform *Escherichia coli* competent cells and individual colonies were selected to obtain the corresponding truncated construct.

Table VIII. Primers used to perform deletion in Boc-GFP plasmid.

Construct	Primer Forward	Primer Reverse
BocΔFn1	CCCAAACCTGAGATCGTG	GGCTACCTGCTCTTCTCC
BocΔFn2	GTGTCAGGCTACAGTGGC	ATGGTCAGGCTGGCTGCT
BocΔFn3	TTTTCTGGTCAGCCTGGA	CCTCTCATATACACGGCC

Chicken electroporation.

Fertilized chicken eggs were incubated at 38°C to reach the desired stage. pCAG vector carrying the coding sequence of mouse *Cdon* (pCAG-Cdon), was cloned by Francisco Lopez Nieto. For *ex ovo* electroporation, pCAG-GFP and pCAG-Cdon were co-electroporated at 1ug/ul in HH5 chick embryos, then transferred to New culture (Voiculescu et al., 2008). The electroporation was performed at 5-6V with 3 pulses of 50ms at an interval of 500ms.

The electroporated embryos were selected and then fixed in PFA 4% or ethanol at HH11 for further processing.

For *in ovo* chicken electroporations, embryos were injected in the optic vesicle with the following electroporation mixture: MO-control or MO-Cdon at 2mM, GFP DNA, 0.2% Fast Green and 15% sucrose The electrodes were place to both sides of the head. Electroporation conditions were: voltage, 14V; pulses, 5; interval, 300ms and pulse length, 50ms. After the procedure, the embryos were incubated again at 38°C to reach HH14 stage and then fixed in PFA 4%.

Cell transfection.

Subconfluent Human Embryonic Kidney 293T (HEK293) cells were transiently co-transfected with a construct encoding mouse Boc-GFP or pCAG-Cdon using the FuGENE HD Transfection Reagent (Roche). After 48 h, cells were visualized by fluorescence in a microscope or scraped in lysis buffer for Western Blot analysis.

Western Blotting.

HEK293 cell or tissue samples (fishes, electroporated chicken eyes, mouse telencephalon) were collected or dissected under a microscope, treated with lysis buffer (150 mM NaCl , 1% NP40 , 50 mM Tris pH8) and denaturalized in protein loading buffer (50 mM Tris-HCl pH 6.8, 2% SDS, 10% glycerol, 1% β-mercaptoethanol, 12.5 mM EDTA and 0.02 % bromophenol blue). Proteins were resolved by 6% SDSP-gels, blotted onto a PVDF membrane, blocked for 1 h in 5% milk in PBST, incubated over night at 4ºC with Cdon polyclonal antibody (R&D system) in blocking buffer, washed 4 times with PBST, and incubated for 1 h with peroxidase-conjugated secondary antibody. Labeled proteins were detected with the chemiluminescence reagent ECL (Amersham Biosciences).

Treatment with Hedgehog and FGF inhibitors.

Cyclopamine (Calbiochem) was used to antagonize Hh signaling. Embryos at 90% epiboly were incubated in E3 medium containing 1-120 uM Cya (dissolved in DMSO) at 28ºC. Embryos were fixed in 4% PFA at 28 hpf. Embryos were treated with the drug SU5204 (Calbiochem) to block FgfR activity (Mohammadi et al., 1997). Embryos at 90% epiboly were incubated in E3 medium containing 0.1-5 uM SU5204 (dissolved in DMSO) at 28ºC. Embryos were fixed in 4% PFA at 28 hpf.

Cell Transplantation Experiments.

Cell transplantation was performed essentially as described (Cavodeassi et al., 2005). Embryos injected with CdonMO were used as donors at the midblastula stage and cells were transplanted to early gastrula stage hosts (55%–65% epiboly) in the region fated to become the eye field (Woo and Fraser, 1995). Manipulated embryos were let develop until 28hp, and then either fixed and prepared for ISH or mounted for live imaging.

Imaging.

Sections were analyzed with a DM microscope, whereas whole embryos were observed with a stereomicroscope (Leica Microsystems). Digital images were obtained using a Leica DFC500 and the Leica DFC350 FX camera. Some images were acquired with a confocal microscope (Zeiss). Images were processed with Photoshop® CS5 or ImageJ (Fiji) software.

Statistical analysis.

Data analyses were performed in the IBM SPSS statistic software. The analysis of the collected data was conducted by t-test for two groups and ANOVA for three or more groups. Pearson's chi-squared test ($\chi 2$) was performed to test statistically differences between treated (MO, drugs, electroporations) and not treated embryos.

RESULTS

Embryonic expression pattern of *Cdon* in zebrafish and chicken.

The *Cdon* gene in *Danio rerio* has been poorly studied. There is only one *Cdon* copy in the zebrafish genome (NM_001081628), despite of the whole-genome duplication that occurred in the teleost lineage, subsequent to its divergence from mammals (Amores et al., 1998; Jaillon et al., 2004). Amino-acid sequence alignments indicate that the zebrafish *Cdon* is closely related to the mammalian *Cdon* and shares similarities with the closely related Boc protein (Bergeron et al., 2011).

Partial information about *Cdon* expression in zebrafish is available at www.zfin.org. This information derives from ISH screening approaches (Thisse, 2001; Thisse, 2004). Partial *Cdon* expression data have been also presented in a study of a zebrafish *Boc* mutant (Bergeron et al., 2011). Lack of a detailed description prompted us to clone the zebrafish *Cdon* and to analyze its expression pattern at different embryonic stages. We also cloned the *Boc* zebrafish homolog to compare their distribution.

C*don* full length was cloned by PCR amplification from a zebrafish cDNA library (see Material and Methods). Its expression profile was studied by ISH. Zebrafish embryos were fixed at different stages of development and hybridized *in situ* with the *Cdon* probe. *Cdon* was first expressed at the onset of gastrulation in the dorsal shield of the embryo (Kupffer´s vesicle or Spemann organizer) (Fig. 9A, A´). During gastrulation, *Cdon* was expressed in the ventral axial midline (Fig. 9B, B´), and by the end of gastrulation it localized to the presumptive neural crest (Fig. 9C, C´). Notably *Cdon* and *Shh* expression overlaped in the axial midline (Fig. 9O-P´). By 1 somite stage, Cdon expression disappeared from the anterior ventral midline (Fig. 9D, D´) and became localized to more caudal domains of the dorsal neural tube. At 10 somite stage *Cdon* was still localized to the notochord and the floorplate of the spinal cord, in the ventral mesoderm, Kupffer´s vesicle and dorsal neural tube (data not shown). In the developing eye, *Cdon* expression was first detected after the evagination of the optic vesicles (Fig. 9E, E´). At 17 somite stage *Cdon* was highly expressed in the telencephalon and optic cups (Fig. 9F, F´). During pharyngula stage (24 hpf), *Cdon* was detected in the eyes and in more dorsal restricted areas of the telencephalon, diencephalon, midbrain, hindbrain and spinal cord (Fig. 9G, G´). In addition *Cdon* was expressed in the otic vesicles, pronephros, somites, pectoral fins, surface ectoderm, optic lens among others (data not shown).

Comparative studies using chick embryos revealed a similar distribution of *Cdon* mRNA. *Cdon* expression was first detected in the Hensen´s node region during primitive streak grooving at HH4 (Fig. 9H). Later on the expression became evident in the presumptive neural crest cell at HH5, 6 (Fig. 9I, J) and in somites at HH7 (Fig. 9K). Notably, the expression in the ventral midline at these stages was very faint in comparison to the signal detected

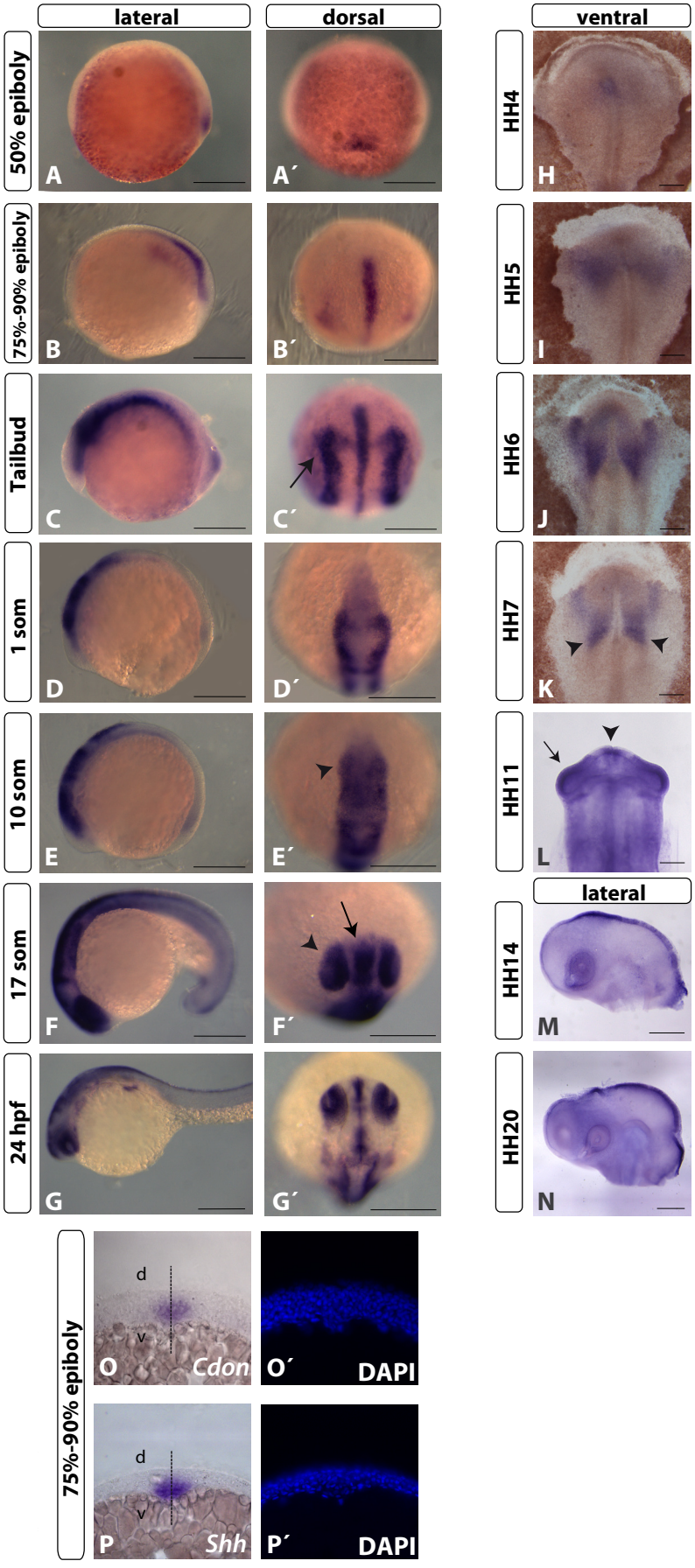

Fig. 9. *Cdon* expression in zebrafish and chicken embryos. Lateral **(A-G) and** dorsal **(A´-G´)** views of zebrafish embryos and ventral **(H-L) and** lateral **(M, N)** views of chicken embryos hybridized *in toto* with specific probes for *Cdon* at different stages of development. Coronal **(O-P´)** cryostat sections of zebrafish embryos hybridized *in toto*. In zebrafish, *Cdon* expression starts at 50% epiboly in the shield **(A, A´)** and by 75-90% epiboly *Cdon* transcripts are detected in the ventral midline **(B, B´)** overlapping with *Shh* expression (O-P´). At tailbud stage Cdon expression is also observed in the presumptive neural crest **(C, C´** arrow**)**. At 1 somite stage *Cdon* mRNA localizes to the presumptive neural crest, the ventral midline and becomes evident in the dorsal neural tube **(D, D´)**. Later on, at 10-17 somite stages, expression is detected in the optic vesicles **(E´, F´** arrowhead**)**, prechordal plate and telencephalon **(E-F´** arrow**)**. At 24 hpf the expression becomes restricted to the retina and to the dorsal midline of the entire neural tube **(G, G´)**. In chicken embryos, *Cdon* expression is first detected in the Hensen´s node at HH4 **(H)**, and later on in the presumptive neural crests **(I, J)** and in the somites **(K** arrowheads**)**. At HH11 *Cdon* mRNA localizes to the optic vesicles and dorsal CNS **(L,** arrow and arrowhead respectively**)**. At HH14-HH20 *Cdon* expression is restricted to regions of the telencephalon, dorsal neural tube and retina **(M-N´)**. Scale bars: 200 µm. In O-P´: d, dorsal; v, ventral and the dashed line indicates the midline.

in zebrafish. At HH11 Cdon mRNA localized to the optic vesicles and the dorsal CNS (Fig. 9L). At HH14 its expression was also found in the telencephalon (Fig. 9M) and, as in zebrafish, the expression pattern became restricted to specific areas of the eyes and brain among others (Fig. 9N and data not shown).

Because of our interest in visual system development, C*don* expression in the eye was explored in detail in zebrafish, chicken and mouse embryos. At 10 somite stage, *Cdon* expression in zebrafish was restricted to the presumptive neural retina (Fig. 10A). Later on at 24-48 hpf the expression became progresively restricted to the ciliary marginal zone (CMZ) of the retina (Fig. 10B, C). In chicken, C*don* expression was observed also in the retina at HH14. *Cdon* was expressed in the prospective lens, surface ectoderm and possibly in part of the RPE (Fig. 10D). *Cdon* expression profile in the eyes was evolutionary conserved in mice. At E9, *Cdon* immunostaining localized to the neural retina (Fig. 10E) and later on also to the

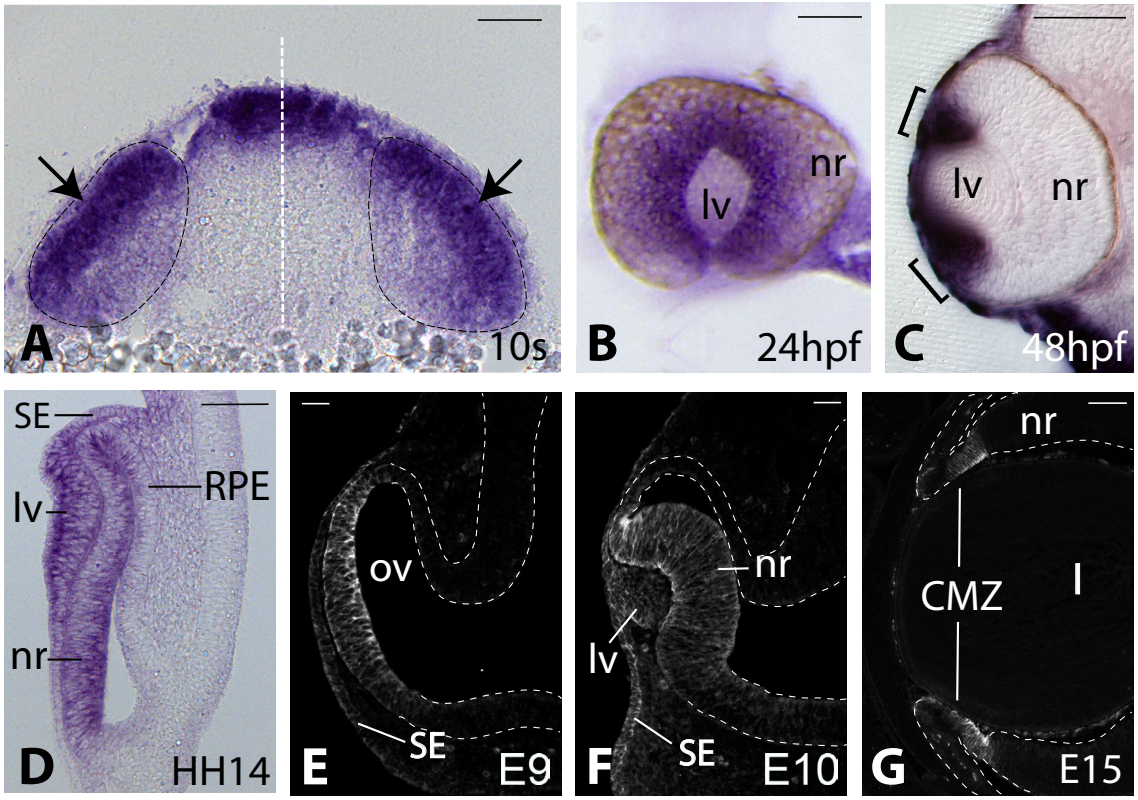

Fig. 10. *Cdon* expression in the presumptive retina is conserved among vertebrates. Coronal sections **(A, C)** and lateral view **(B)** of zebrafish and chicken **(D)** embryos hybridized with probes specific for *Cdon* and immunostaining of mouse coronal sections with a Cdon specific antibody **(E-G)**. *Cdon* is expressed in the presumptive retinal domain of the optic vesicle in zebrafish at 10 somite stage **(A, arrow)**, Later in development, the expression becomes restricted to the ciliary margin zone (CMZ) **(B, C).** *Cdon* is expressed in a similar manner in chicken HH14 **(D)** and in mice at E9 and E10 **(E, F)**. Later on, the expression becomes restricted to the CMZ at E15 **(G)**. The black dashed lines in **A** indicate the midline and the optic vesicles. The white dashed line in **E-G** delineates the neural epithelium. Scale bars: 50 µm. l, lens; lv, lens vesicle; nr, neural retina; ov, optic vesicle; RPE, retinal pigmented epithelium; SE, surface ectoderm.

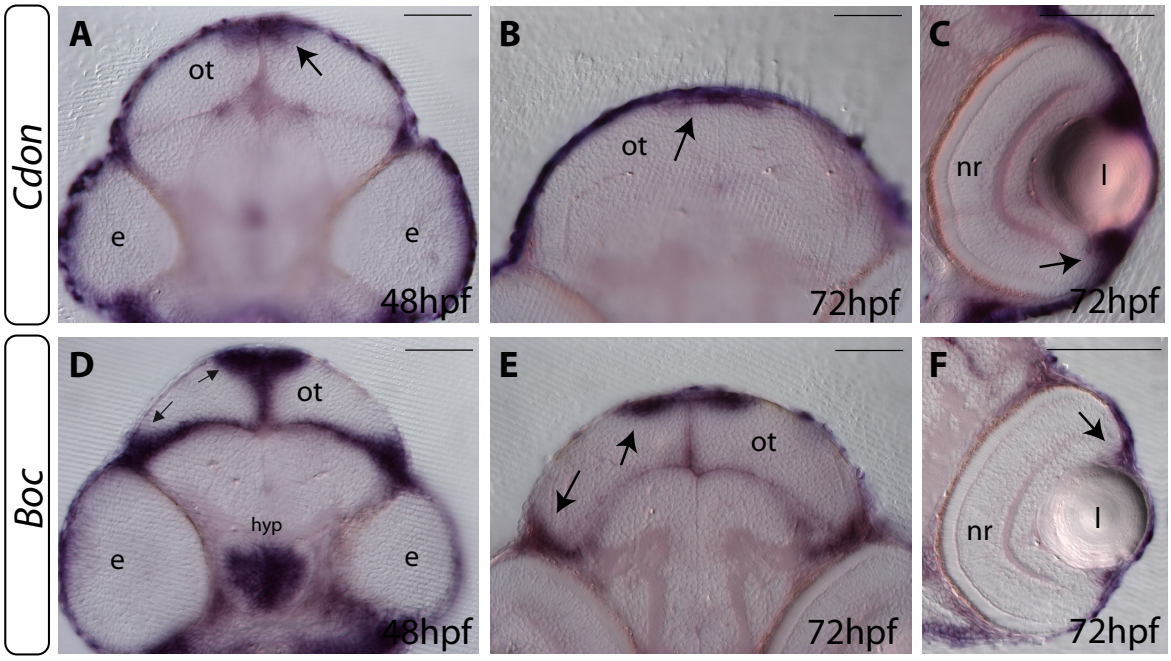

Fig. 11. Distribution of *Cdon* and *Boc* in the visual system. Coronal sections of zebrafish embryos at 48 hpf and 72 hpf hybridized with probes specific for *Cdon* and *Boc*. In the brain, *Cdon* and *Boc* mRNAs localized to the dorsal and lateral tectal marginal zones **(A, D)** at 48 hpf. *Boc* is also expressed in hypothalamus **(D)**. At 72 hpf the expression of *Cdon* and *Boc* become more restricted but are still present in the tectal **(B, E)** and ciliary marginal zones **(C, F)**. Arrows indicate gene expression in proliferative regions. Scale bars: 50 µm. e, eye; hyp, hypothalamus; l, lens; nr, neural retina; ot, optic tectum.

lens and surface ectoderm (Fig. 10F), to become finally restricted to the CMZ at E15 (Fig. 10G). Notably, *Cdon* was accumulated at the basolateral plasma membrane at E10 and E15, as described for the *Drosophila* homolog Ihog (Fig. 10F, G) (Callejo et al., 2011).

Cdon was expressed also in the optic tectum restricted to its proliferative area: the dorsal tectal marginal zone (TMZ) between 48-72 hpf (Fig. 11A, B). It homolog, *Boc* was expressed in the hypothalamus at 48 hpf (Fig. 11D). *Boc* was not expressed in the eye at early stages (Bergeron et al., 2011 and data not shown), but localized to the dorsal and lateral TMZ between 48-72 hpf (Fig. 11D, F). *Boc* expression overlapped also with *Cdon* in the CMZ at 72 hpf (Fig. 11C, F).

Knock-down of *Cdon* function causes alteration in the proximo-distal patterning of the vertebrate eye.

The conserved localization of *Cdon* expression in the prospective neural retina at early stages of ocular development suggests a possible important developmental role.

To explore this possibility, *Cdon* expression was knocked down in zebrafish using an antisense morpholino oligonucleotide (MO) complementary to the translation start site region of the *Cdon* mRNA (CdonMO). The CdonMO was designed and tested for its capability to block *Cdon* translation in a sequence specific manner (CdonMO injected embryos will be referred to as Cdon morphants).

To verify that the selected MO was efficiently interfering with *Cdon* expression, we initially attempted to perform Western Blot and immunostaining of injected embryos using a specific antibody generated against mouse Cdon (R&D systems). Unfortunately, the antibody did not seem to cross-react with the fish protein (data not shown). Therefore, we used an alternative strategy. The CdonMO or a standard control MO (Gene Tools) were co-injected into medaka fish embryos with the cRNA of a reporter construct (5′*cdon*-GFP) carrying the zebrafish *Cdon* 5′ sequence upstream of the GFP sequence (Fig. 12A). Translation of this construct was efficiently knocked down by the *Cdon* specific MO (Fig. 12C) but not by the control MO (Fig. 12B). None of the two MOs interfered with the translation of GFP alone (Fig. 12D, E).

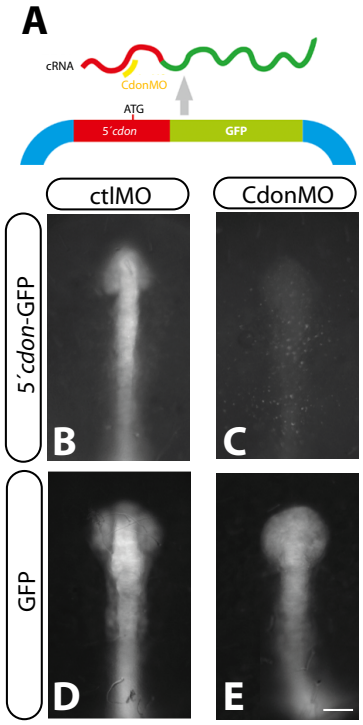

Fig. 12. Cdon morpholino efficently blocks *Cdon* translation in a sequence specific manner. An antisense morpholino (MO) complementary to the translation start site region of the *Cdon* gene (CdonMO) was designed. To confirm its specificity, the CdonMO or a standard control MO (Gene Tools) were co-injected into medaka fish embryos with the cRNA of a reporter construct (5′*cdon*-GFP) carrying the *Cdon* 5′ sequence upstream of the *gfp* sequence **(A)**. Translation of this construct (evident by expression of GFP) was efficiently knocked down by the *Cdon* specific MO **(C)** (25/25 embryos) but not by the control MO **(B)** (20/20 embryos). None of the two MO interfered with the translation of the GFP alone **(D, E)** (23/23 embryos). Scale bars: 40 µm.

These experiments demonstrated that the designed MO can efficiently interfere with Cdon expression. Next CdonMO or a control MO were injected in zebrafish embryos at 1-2 cells stage and their phenotypes were visualized in bright field at different developmental stages. The Cdon morphants displayed a clear defect in the ventral region of the retina (Fig. 13B-C´) when compared to ctlMO injected embryos (Fig. 13A, A´). The ventro-nasal quadrant of the retina seemed abnormally folded (Fig. 13B´, C´) and the eyes were characterized by the presence of coloboma: the nasal and temporal regions of the retina were not properly fused (Fig. 13D, E). About 70% of the CdonMO injected embryos displayed eye anomalies (Fig. 13F).

Because previous studies have shown that MOs can have off-target effects mediated by the activation of p53, that leads to unspecific apoptosis (Robu et al., 2007), a p53MO was coinjected with CdonMO at 1-2 cell stage in zebrafish embryos. This MO did not prevent the eye abnormalities observed with CdonMO, indicating that the defects were specific (70% of

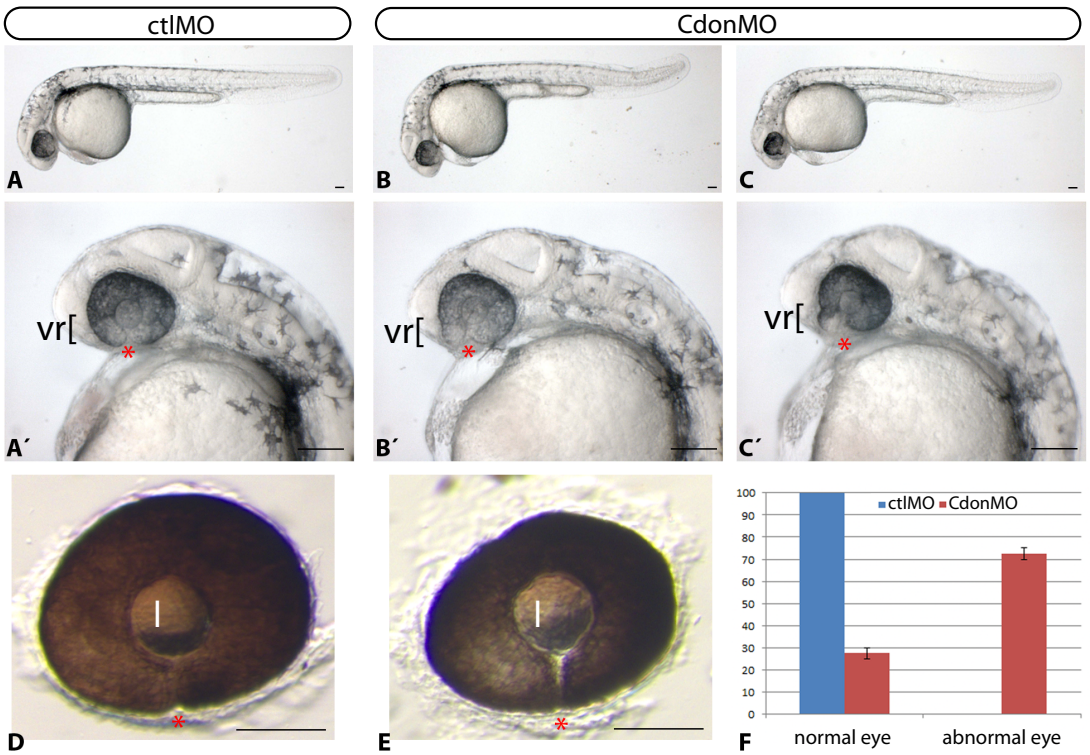

Fig. 13. *Cdon* morphants are characterized by defects in the ventral region of the eye. Bright field and lateral view of embryos injected with control **(A, A´)** or CdonMO **(B-C´)**. CdonMO **(B-C´)** but not control MO **(A, A´)** injected embryos are characterized by alteration of the ventral retina (vr) at 28 hpf. The red asterisks indicate the position of the choroid fissure in the ventral retina, which is still open at 36 hpf in Cdon morphants **(B´, C´)** originating a coloboma **(E)** not observed in controls **(A´, D)**. Quantification of the percentage of injected embryos with a control MO or CdonMO displaying normal or abnormal eye phenotypes **(F)**. T-tests: control MO versus CdonMO normal phenotype, $p < 0.05$; control MO versus CdonMO abnormal phenotype, $p < 0.05$. Control MO (n=144), CdonMO (n= 292). l, lens. Scale bars: 100 µm.

the co-injected embryos at 28 hpf, n=52) (data not shown).

To confirm the presence of a coloboma in Cdon morphants, a transgenic membrane-GFP *βactin*::mGFP zebrafish line (Cooper et al., 2005) was injected with CdonMO. Indeed, in CdonMO injected embryos the choroid fissure was still open at 36 hpf in contrast to what observed in controls (Fig. 14A, B). Despite the eye in figure B is smaller than control eye (Fig 14B), it is important to note that Cdon morphants could display microphtalmia. The choroid fissure in the ventral side of the optic cup provides an entry point for newly forming blood vessels and the site of exit for the efferent retinal ganglion cell axons. A failure in choroid fissure formation usually affects both processes (See Introduction Fig.6 and Lupo et al., 2011). To determine whether the defects caused by Cdon knock-down interfered with the proper formation of the ventral retina, we injected control and CdonMO in different reporter lines. The

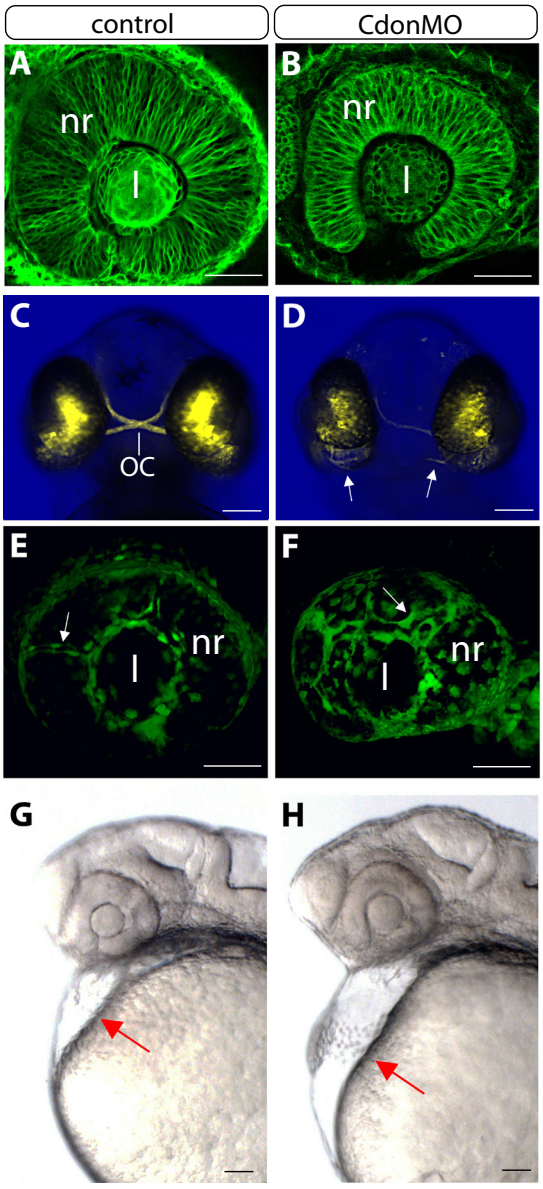

Fig. 14. Failure of choroid fissure closure in *Cdon* morphants is associated with navigation defects of the RGC axons and with abnormal vascularization. Zebrafish transgenic reporter lines were injected with control MO or CdonMO, fixed at 36 hpf or 48 hpf and visualized by fluorescence **(A-F)** or in bright field **(G, H)**. Lateral views of the eye of transgenic *βactin*::mGFP embryos injected with control and CdonMO **(A, B)**. The ventral retina remains open in Cdon morphants (32/50 embryos) **(B)**. Frontal views of the *ath5*::GFP reporter line injected with control MO **(C)** or CdonMO **(D)**. Cdon morphants show defects in the outgrowth of the GFP positive RGCs axons that leave the eye cup in ectopic locations (54/80) **(D** white arrow**)**. Lateral views of the eye of the endothelial reporter *fli1a*:EGFP embryos injected with control **(E)** or CdonMO **(F)**. *Cdon* morphants exhibit a thickening of the vasculature in the eye (27/30 embryos) **(F** white arrow**)** in comparison to controls **(E** white arrow**)**. The pericardial cavity is also expanded in *Cdon* morphants **(G, H** red arrows**)**. Scale bars: 100 µm. l, lens; nr, neural retina; OC, optic chiasm.

reporter transgenic line *ath5::gap-gfp* drives GFP under the control of an enhancer-promoter from the *Ath5* gene specifically in the RGCs (Zolessi et al., 2006). This strain was injected with CdonMO or control MO and visualized at 48 hpf. In control eyes, retinal axons form a compact bundle at the optic nerve head and project contralaterally at the midline, where the two optic nerves meet to form the optic chiasm (Fig. 14C). In Cdon morphants the axons projected aberrantly and exited the eye in ectopic locations (Fig. 14D). Note that differentiation of the RGCs could be affected in Cdon morphants (Fig14D). In order to visualize the vasculature of the retina, the endothelial cell reporter *fli1a*::EGFP (Lawson and Weinstein, 2002) was injected with CdonMO or control MO. The blood vessels in the eye of Cdon morphants were thicker than those of control embryos (Fig. 14E, F). The pericardial membrane was also expanded. The enlarged pericardial cavity in Cdon morphants could be caused by a poorly developed vascular system, which could result in an accumulation of fluid in the pericardial cavity (Fig. 14G, H).

Cdon was expressed also in neural crest cells. Developmental abnormalities in neural crest cells may result in ventro-ocular malformations (Ozeki et al., 1999; Lupo et al., 2011). To determine whether the neural crest cells presented abnormal characteristics or distribution after interference with *Cdon* expression, we injected the MOs in a *sox10*::EGFP reporter line that label neural crest–derived cells (Hoffman et al., 2007). The results of these experiments suggest that the eye phenotype is not associated with neural crest defects (data not shown).

The abnormal eye development displayed by Cdon morphants suggested that the expression pattern of region specific eye molecular markers could be affected. To addresss this issue we analyzed the expression pattern of different genes by ISH. *Vax1, Fgf8a and Pax2.1* are expressed in the optic stalk and contribute to its development (Macdonald et al., 1995; Take-uchi et al., 2003; Lupo et al., 2005). *Vax1* expression did not seem to be affected in Cdon morphants (data not shown). *Fgf8a* expression in the brain was mainly detected at the midbrain-hindbrain boundary (MHB), dorsal diencephalon, telencephalon and optic stalks (Fig. 15A-A´´, E). In Cdon morphant, *Fgf8a* expression was highly expanded caudally in the optic stalk and dorsal telencephalon (Fig. 15B-B´´, E). The boundary between the hypothalamus and telencephalon, which was negative for *Fgf8* expression, was reduced or absent in Cdon morphants (Fig. 15B). *Pax2.1* was mainly expressed in the optic stalk, MHB and along the hindbrain (Fig. 15C-C´´, F). In Cdon morphants *Pax2.1* was also abnormally expanded in the optic stalk region (Fig. 15D-D´´, F). In contrast to its expansion in the optic stalk, *Pax2.1* was strikingly reduced in the hindbrain region of many CdonMO injected embryos (Fig. 15D). In conclusion, *Pax2.1* and *Fgf8a* expression were clearly increased in the optic stalk of Cdon morphants, whereas *Vax1* expression was unaltered.

In order to rule out the possibility that the phenotype of Cdon morphants could be

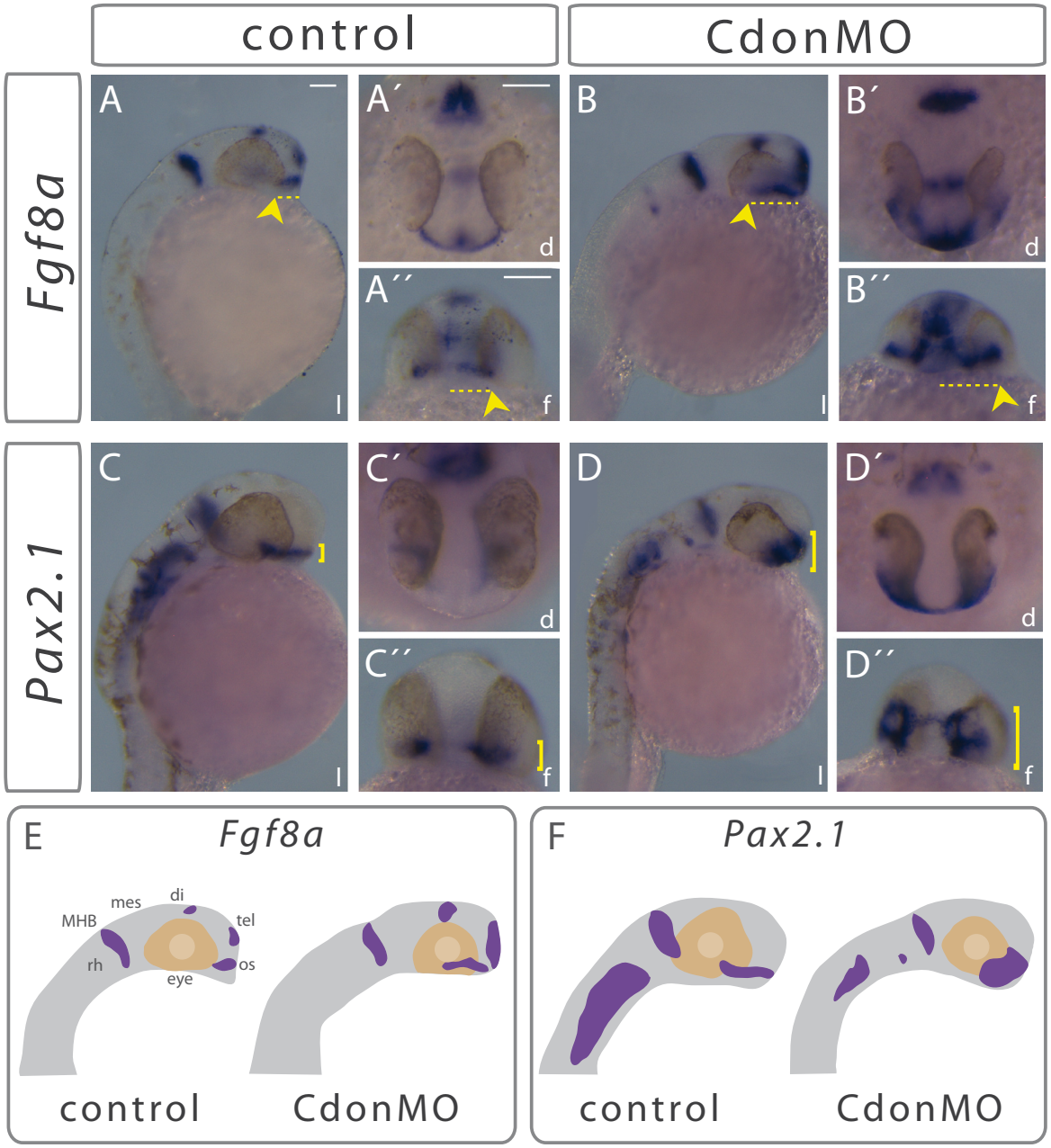

Fig. 15. *Fgf8a* and *Pax2.1* expression patterns are altered in Cdon morphants. *In situ* hybridization analysis of the expression pattern of two optic stalk markers, *Fgf8a* **(A-B´´)** and *Pax2.1* **(C-D´´)** at 24 hpf and 28 hpf respectively. Embryos are shown in lateral (l), dorsal (d) and frontal (f) views. The expression pattern of both genes is schematically represented in **E** and **F**. In *Cdon* morphants, *Fgf8a* expression is expanded caudally and laterally in the optic stalk **(B, B´´** arrowhead and dotted lines**)** as well as in the telencephalon **(B-B´´)** when compared to control embryos **(A, A´´** arrowhead and dotted lines**)** (93/112). *Pax2.1* expression is also dorsally expanded in the optic stalk of *Cdon* morphants **(D, D´´** brackets**)** in comparison to controls **(A-A´´)** (124/140). Scale bars: 100 µm. di, diencephalon; mes, mesencephalon; MHB, midbrain-hindbrain boundary; os, optic stalk; rh, rhombencephalon; tel, telencephalon.

an outcome of unspecific effects produced by the CdonMO, *Cdon* translation was blocked with a different MO. MOs can block translation of a mRNA, by modifying the pre-mRNA splicing. We designed a MO (spl8MO) that targeted the intron splice junction of exon 8 of the *Cdon* pre-mRNA, thus inducing a frameshift of the corresponding mRNA and leading to a truncated translation product. Zebrafish embryos were injected at 1-2 cells stage with spl8MO and analyzed at 28 hpf by RT-PCR or ISH (Fig. 16). Spl8MO induced exon 8 skipping in *Cdon* mRNA as determined by RT-PCR with primers targeting exons 7 and 9 (Fig. 16A). Note that spl8MO altered just a fraction of Cdon mRNA. ISH showed that *Pax2.1* expression was expanded in spl8MO injected embryos (Fig. 16B-E) as observed with the initial CdonMO.

As CdonMO, spl8MO morphants presented coloboma (Fig. 16F, G). Curiously, many CdonMO and spl8MO injected embryos showed an ectopic spot of *Pax2.1* expression located in the dorsal midline (Fig. 16H-J). The position of the spots was variable along the ven-

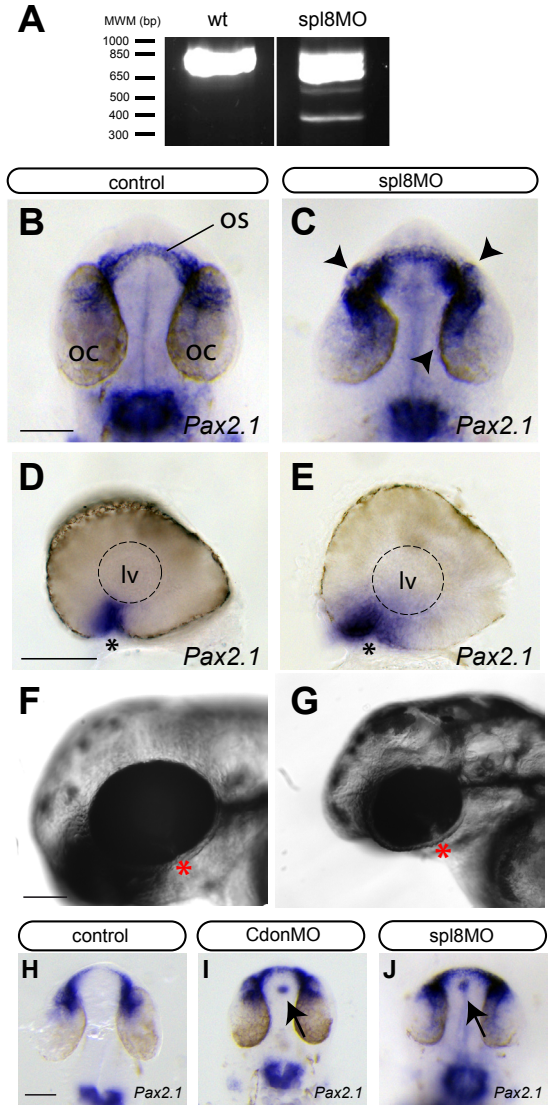

Fig. 16. The *Cdon* splicing spl8MO reproduces the phenotype of *Cdon* morphants. Validation of the splice blocking activity of the spl8MO by PCR **(A)** and *Pax2.1 in situ* hybridization of the expression pattern of *Pax2.1* analysis in spl8MO injected embryos or controls **(B-E, H-J).** Bright field images are used to show the presence of coloboma in spl8MO morphants **(F, G)**. PCR using two primers complementary to regions of exon 7 and 9 of *Cdon*, amplified a region of ~700pb in wild type cDNA. An additional band of ~400pb was observed in the cDNA of spl8MO morphants. The band corresponds to the expected product if exon 8 is removed **(A)**. In spl8MO injected embryos *Pax2.1* expression is expanded in the optic stalk and in the retina (35/64) **(C, E** arrowheads**)** in comparison to controls **(B, D)**. At 48 hpf the choroid fissure is closed in control embryos **(F)** and remains open in embryos injected with spl8MO (17/40 embryos) **(G)**. Dorsal view of control and CdonMO or spl8MO injected embryos hybridized with *Pax2.1* probe **(H-J).** Morphants display similar phenotypes. Note the presence of an ectopic spot of *Pax2.1* in the dorsal midline of some Cdon morphants **(I, J** arrows**)** in comparison to control **(H)**. The asterisks in D-G indicate the position of the optic fissure. Scale bars: 100 µm. lv, lens vesicle; oc, optic cup; os, optic stalk.

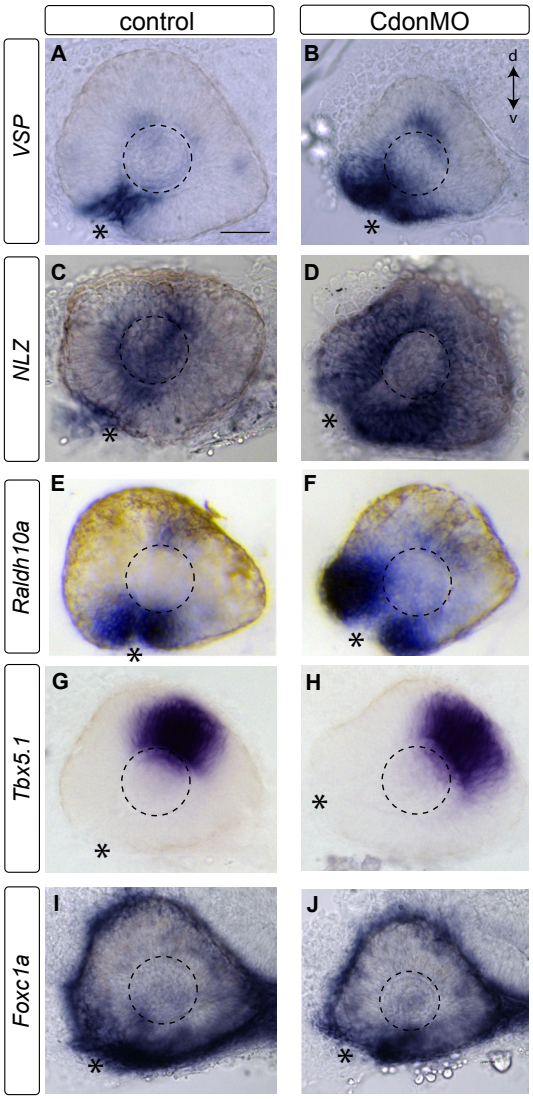

Fig. 17. Cdon knock down increases the expression of ventral ocular markers in the retina. ISH analysis of specific ventral retina markers, *VSP*, *NLZ* and *Raldh10a* **(A-F)** of the dorsal retina marker *Tbx5.1* **(G-H)** and of the periocular cell marker *Foxc1a* **(I-J)**. Ventral retina markers *VSP* **(B)** (28/54 embryos), *NLZ* **(D)** (39/60 embryos) and *Raldh10a* **(F)** (32/44 embryos) are expanded in CdonMO injected embryos in comparison to controls **(A, C, E)**. The dorsal retina **(H)** (62 embryos) and periocular cells derived from neural crest **(J)** (24 embryos) do not show evident alterations in CdonMO injected embryos in comparison to controls **(G, I)**. The dashed line marks the retina and the asterisk the position of the optic fissure. Scale bar: 100 µm.

tro-dorsal or anterior-posterior axis (data not shown). The coincidence of these phenotypes indicates that the defects are specially caused by the knock-down of Cdon.

Coloboma phenotypes can arise because of impaired dorso-ventral patterning of the eye (Chang et al., 2006). We thus examined the expression of eye polarity markers in Cdon knocked down embryos at 28 hpf. The expression of the ventral retina markers *VSP* (gift of Gaia Gestri), the zinc finger protein *NLZ* that has been associated to coloboma (Brown et al., 2009) and *Rdh10a* (retinol dehydrogenase 10a) a retinoic acid pathway gene, were enlarged in the eyes of CdonMO injected embryos (Fig. 17B, D, F) in comparison to that of control embryos (Fig. 17A, C, E). In contrast, Cdon morphants showed no appreciable defects in the expression of the dorsal retinal marker *Tbx5.1* (Fig. 17G, H). These results suggest that *Cdon* is necesary for ventral patterning of the eye.

Defects in neural crest–derived periocular mesenchymal cells are also associated with the failure of the choroid fissure closure or in some cases with more severe morphogenetic alterations of the ventral optic cup (McMahon et al., 2009). Because *Cdon* was also expressed in the presumptive neural crest, we asked if the expression of *FoxC1a*, a neural crest–derived periocular mesenchyme (POM) marker, was abnormal in Cdon morphants. The expression appeared normal in Cdon morphants (Fig. 17I, J). This is in agreement with the result obtained with CdonMO injection in the *sox10*::GFP transgenic line. This suggests

that the neural crest is not responsible for the eye phenotype of Cdon morphants.

Cdon has been associated to HPE in mice and humans (Cole and Krauss, 2003; Bae et al., 2011). Eye coloboma is sometimes a consecuence of midline defects (Gongal et al., 2011). Because *Cdon* is expressed in both the eye and the axial midline at neural plate stage (See Fig.9 B´, O) lack of Cdon at the midline could interfere with Shh gradient formation, leading to an expansion of *Pax2* expression. Alternatively, *Cdon* expression in the optic vesicle itself could be necessary for correct proximo-distal patterning of the eye. We decided to test the latter possibility. For this purpose, we performed heterochronic transplants in zebrafish (Fig. 18). Cells from GFP-labeled donors at 50% epiboly were injected with CdonMO and then transplanted in the region fated to become the eye field in shield stage embryos (Fig. 18A) (Woo and Fraser, 1995). Transplants that were well localized in the eye field caused eye anomalies when compared to the non-transplanted eye (Fig. 18B-E). The defects were confirmed by ISH with the VSP marker, which is expanded in Cdon morphants (See Fig.

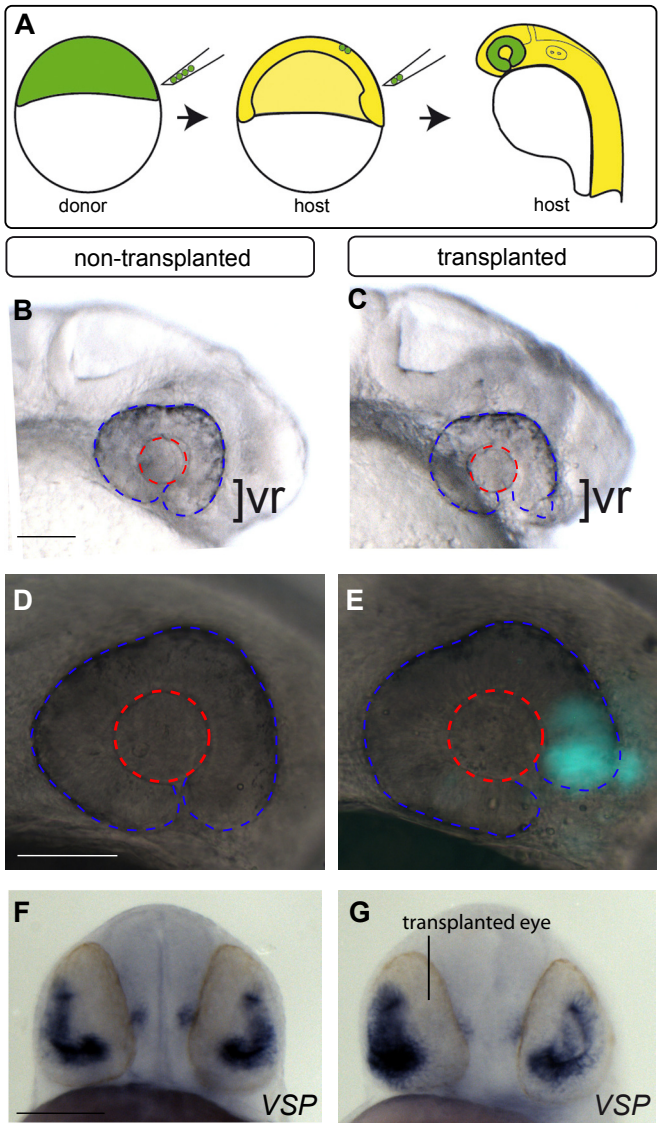

Fig. 18. Transplant experiments indicate that *Cdon* expression in the presumptive neural retina prevents optic stalk expansion. A) Embryos at mid-blastula stage co-injected with CdonMO and GFP were used as donors and cells were transplanted to early gastrula stage hosts (55%–65% epiboly) in the region fated to become the eye field. Manipulated embryos were let develop until 28 hpf and then either prepared for live imaging **(B, C)** or fixed and mounted for microscope imaging **(D, E)** and ISH **(F, G)**. The transplanted eye **(C)** show alteration of the ventro-nasal region in comparison to the non-transplanted eye (4 embryos) **(B)**. The transplant is visualized by GFP expression (D). The frontal view shows that the VSP marker is expanded in the transplanted right eye (6/7 embryos) **(G)** in comparison to controls **(F)**. Red dashed line marks the lens vesicle and the blue dashed line outline the retina. Scale bars: 100 µm.

17A, B). In wild type embryos the VSP marker was symmetrically expressed in both eyes (Fig.18F). When Cdon knocked-down cells were transplanted only in one eye, VSP signal was increased in that eye, but not in the contralateral one (Fig. 18G). For technical reasons this experiment could not be repeated in a large number of embryos, making statistical analysis difficult. Nonetheless these findings supported the idea that *Cdon* expression specifically in the eye could be responsible of ventral defects seen in Cdon morphants directly.

To test this hypothesis further, it was necessary to interfere with *Cdon* expression in a timely and spatially controlled manner. Therefore we turned to the chicken embryo, in which such a control can be achieved. We designed a specific MO to block chick *Cdon* expression. This MO (cCdonMO) and the control MO (cctlMO) were designed with a carboxyfluorescein tag, in order to directly visualize the distribution of the MO after electroporation (Voiculescu et al., 2008). We forced cCdonMO by electroporation in HH9 embryos when *Cdon* is not yet expressed in the eye primordium (Fig. 19A) and then fixed the embryos at the optic vesicle stage (HH14) when the entire retina expresses *Cdon* (Fig. 19B). We succeeded to perform focal electroporations in the optic vesicle (Fig. 19C). To test the translation blocking capability of cCdonMO, chicken embryonic eyes were electroporated with cCdonMO or cctlMO (Fig. 19D) collected 24h later and processed for Western blot analysis. Mouse α-Cdon antibody crossreacted with the chicken protein detecting a single band of around 110 Kda (Fig.

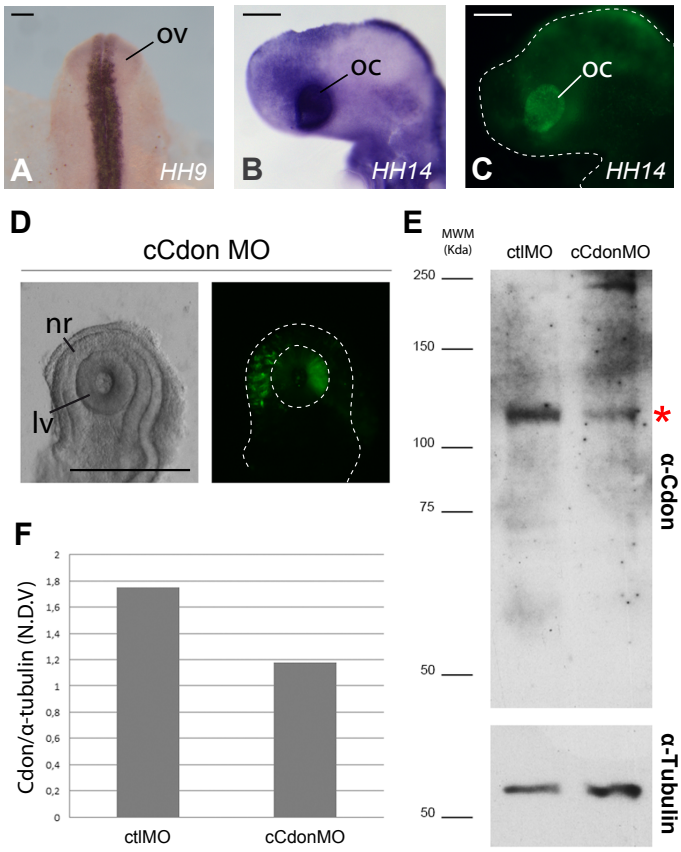

Fig. 19. cCdonMO efficiently interferes with chick *Cdon* expression. *Cdon* expression at HH9 and HH14 stages **(A, B)**. Carboxyfluorescein conjugated chicken *Cdon* MO (cCdonMO) and control MO, were electroporated in the chicken presumptive eye approximately at HH8-9 stages and analized at HH14 **(C, D)**. The interference efficiency of the MO was determined by Western blot with an antibody against mouse *Cdon* normalized using α-tubulin expression (N.D.V, normalized density values) **(E, F)**. Analysis of *Cdon* expression by ISH reveals that at HH9 *Cdon* is not expressed in the primitive optic vesicles (ov) **(A)** but it is expressed at HH14 in the early optic cup (oc) **(B)**. Chicken embryos at HH8-9 stage were electroporated with cCdonMO or control MO specifically in the eye **(C)**. At HH14 the electroporated eyes were dissected **(D)** and collected. The cCdonMO decreased the levels of Cdon relative to α-tubulin levels in the electroporated eyes. Scale bars: 200 µm. lv, lens vesicle; nr, neural retina.

19E). The intensity of the band was reduced in cCdonMO electroporated eyes in comparison to those electroporated with cctlMO (Fig. 19E). The protein levels were normalized using α-tubulin levels (Fig. 19E, F). This demonstrates that cCdonMO efficiently reduced the levels of Cdon protein in chicken embryos.

Because *Pax2* was the most informative molecular marker to follow the effect of *Cdon* abrogation in zebrafish, electroporated chicken embryos were also hybridized with a *Pax2* probe. cCdonMO electroporated embryos showed expansion and increased intensity of the *Pax2* signal in the retina (Fig. 20B) in comparison with cctlMO electroporated embryos (Fig. 20A). This effect was better appreciated when the cCdonMO was electroporated only in one of the eyes (Fig. 20C, D, E).

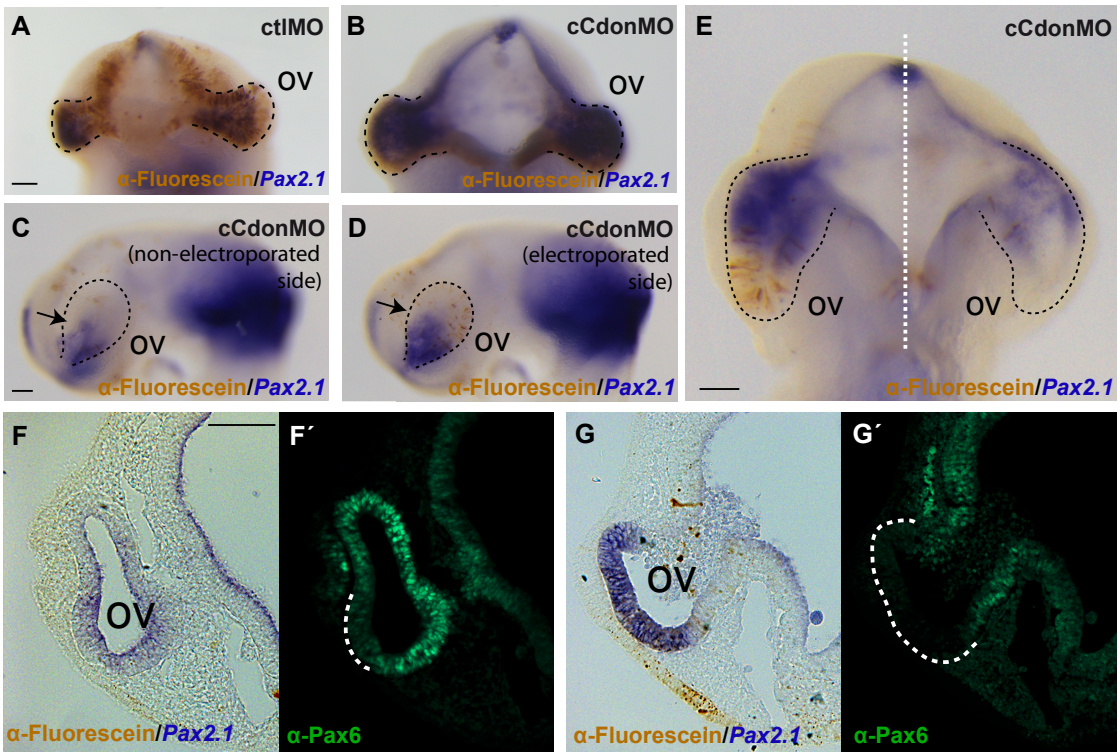

Fig. 20. Knock-down of *Cdon* in optic vesicles induces an expansion of the optic stalk at the expenses of the optic cup. Carboxyfluorescein conjugated chicken *Cdon* MO (cCdonMO) and control MO, were electroporated in one or both vesicles of chick embryos **(A, B,C-G´)** at HH8-9 stages. The embryos were fixed at HH14, analyzed by ISH with a *Pax2* probe (blue signal) and by immunohistochemistry with anti-fluorescein antibodies (brown signal) **(A-F, G)**. Pax6 immunohistochemistry was performed on cryostat sections of electroporated embryos **(F´, G´)**. Frontal **(A, B)** and lateral **(C, D)** views of embryos electroporated with control **(A)** or cCdonMO **(B-D)**. In electroporated eyes, *Pax2* expression is expanded in the entire optic vesicle of cCdonMO treated embryos (7 embryos) **(B)** in comparison with control MO (6 embryos) **(A)**. Ventral **(E)** and lateral **(C,D)** views of chicken electroporated embryos with cCdonMO in one eye (brown signal). *Pax2* expression is clearly expanded in the electroporated optic vesicle (6/9 embryos) **(D,E)** in comparison with the non-electroporated eye **(C,E)**. Frontal cryostat sections of a cCdonMO electroporated eye **(G, G´)** and a control eye **(F, F´)**. The electroporated eye shows *Pax2* expansion and *Pax6* reduction in the retina **(G, G´)** in contrast to a normal condition **(F, F´)**. The optic vesicles (ov) are outlined with a black dashed line. Black arrows in C and D indicate *Pax2* expression in the optic vesicle. Scale bar: 50 µm. ov, optic vesicle.

The closure of the optic fissure occurs fairly late in chick embryos since it begins around E6-E8 (Adler and Belecky-Adams, 2002). Although we let develop some embryos up to this stage we failed to observe coloboma in the embryos. Likely, this is a consequence of MO dilution. Indeed, at this stage we were unable to detect the fluorescent signal in the electroporated embryos. The knockdown analysis both in zebrafish and chicken suggest that Cdon function in the eye is conserved and that the eye phenotype of Cdon morphants is not produced by midline defects.

There is convincing evidence that the two paired box transcription factors Pax2 and Pax6 regulate each other's activity, establishing the boundary between the optic stalk and the optic cup (Schwarz et al., 2000). Consistent with this notion, *Pax2* overexpression in the cCdonMO electroporated eye (Fig. 20F, G) was associated with a reduction of Pax6 expression (Fig. 20F´, G´). This distribution is consistent with the phenotype described for the gain of Hh signaling function from the midline (Macdonald et al., 1995; Sanek et al., 2009). This suggests that *Cdon* expression in the retina may prevent the expansion of Shh signaling from the midline.

Cdon function in the retina is linked to Shh signaling.

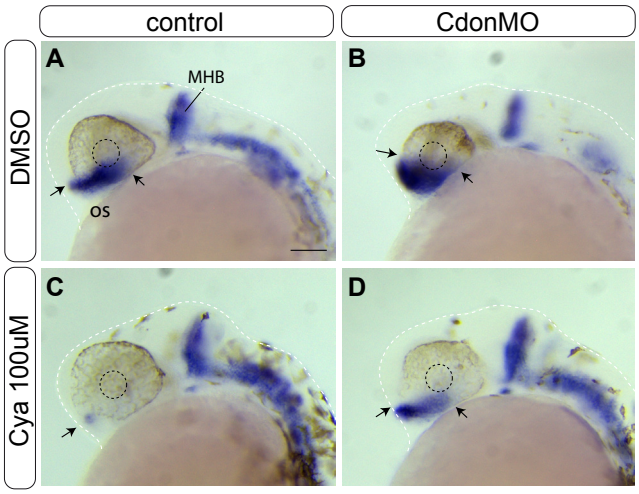

If *Cdon* expression in the retina may prevent the expansion of Shh signaling from the midline, inactivation of Hh signaling should rescue *Cdon* loss of function phenotype. To test this hypothesis we interfered with Hh signaling in Cdon morphants by incubating the embryos with cyclopamine (Cya), a drug that binds Smo and therefore blocks Hh signaling transduction. CdonMO

Fig. 21. Gain of Hh function is responsible of the optic stalk expansion observed in Cdon morphants. Analysis by ISH of the expression pattern of *Pax2.1* at 28 hpf in control or CdonMO injected embryos threated from 90% epiboly with Cyclopamine (Cya). Lateral views of embryos threated with Cya (100uM) **(B, D)** or DMSO **(A, C)**. Injection of CdonMO induces an expansion of the optic stalk region **(B)** in comparison with control **(A)**. Cya at 100uM abolished *Pax2.1* expression in the optic stalk in wild type embryos **(C)**. In CdonMO injected embryos, Cya treatment reduced the *Pax2.1* overexpression observed in CdonMO injected embryos to wild type levels (34/35 embryos) **(D)**. The lens is indicated by a black dashed line and the body perimeter of the embryo by a white dashed line. Arrows indicate the extension of the *Pax2.1* expression in the optic stalk. Scale bar: 100 µm. MHB, midbrain hindbrain boundary; os, optic stalk.

was injected in zebrafish embryos, which were let develop from epiboly stage until 28 hpf in medium (E3) containing Cya. Embryos were fixed and *Pax2.1* expression was analyzed (Fig. 21). As expected, in wild type embryos, Cya treatment at 100µM, strongly reduced *Pax2.1* expression in the optic stalk (Fig. 21A, C). In contrast, Cya administration counteracted *Pax2.1* expansion normally observed after Cdon knock-down (Fig. 21B), generating embryos with a nearly normal *Pax2.1* expression in the optic stalk (Fig. 21D). In contrast, the injection of CdonMO in the Shh mutant line *syu*^{tbx392} could not rescue the Cdon phenotype (data not shown). However, the proximo-distal specification of the eye in these mutant embryos is not affected suggesting that the lack of Shh is compensated by the Shh homolog, Twhh as already proposed in Schauerte et al., 1998.

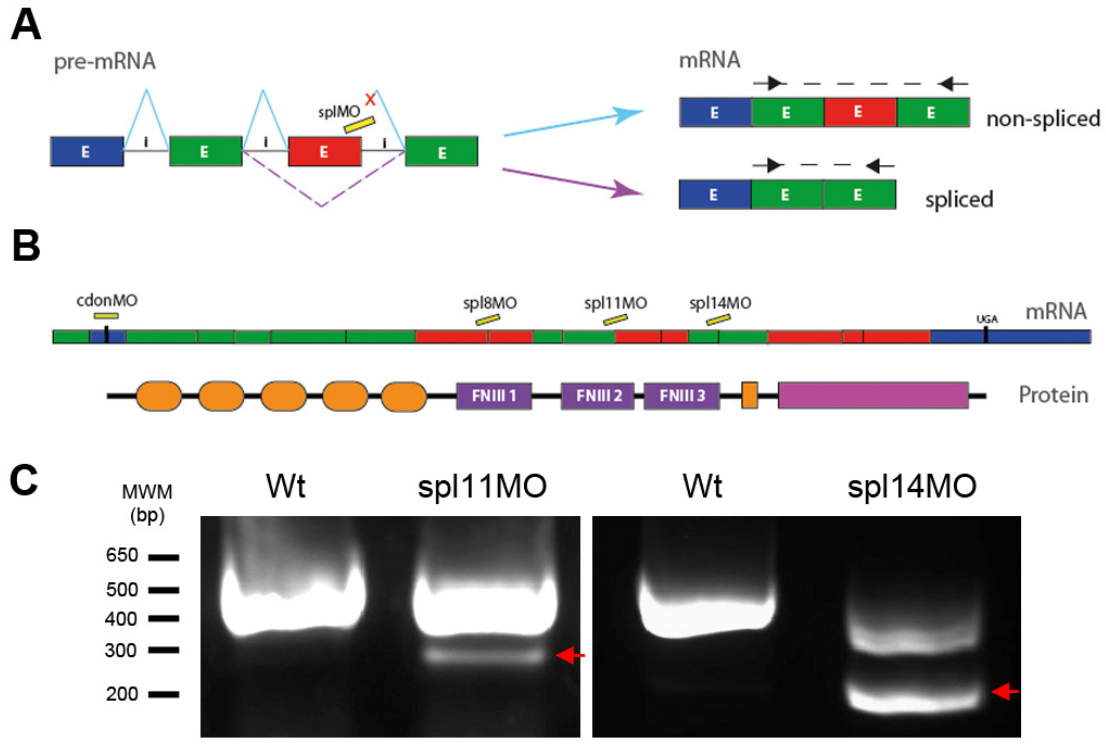

Fig. 22. MOs designed against splice sites efficiently remove the exons coding the *Ptc1* and *Shh* binding domains of Cdon. A) The cartoon depicts the mechanism of exon removal by splice blocking morpholinos. The color boxes represent exons and the black line the introns. The lightblue line depicts normal splicing and the violet dashed line the exon skipping induced by the morpholino (yellow box). Right panel shows the outcome of the MO activity; the non-spliced mRNA and the spliced mRNA. The MO activity can be assessed by RT-PCR with two primers complementary to the flanking exons (black arrows). A successful splice-modification appears as a change in the RT-PCR product. **B)** Graphic representation of cdon exon distribution and of the Cdon protein with its domain composition. **C)** RT-PCR of embryos injected with spl11MO and spl14MO. Splice Blocking MOs block pre-mRNA splicing inducing exon removal by targeting the exon-intron boundary. **(C)**. The position of the morpholinos used in this study is depicted in B, the boxes represent *Cdon* exons. Exons can be removed with (red boxes) or without (green box) frameshift changes. The Cdon domains are aligned with the respective coding exons. Removal of exon 11 or 14 produce a deletion in fibronectin III (FnIII) 2 (Ptch binding site) or FnIII 3 (Shh binding site) respectively without frameshift modifications.

These experients support the idea that the phenotype of Cdon morphants is a consequence of gain of Hh signaling function. As Cdon can interfere with Hh signaling by binding to Shh or Ptch (Yao et al., 2006; Izzi et al., 2011) we asked whether both interactions were relevant to Cdon function in the eye. According to the published data Cdon binds Shh through its Fn3 domain (Yao et al., 2006; McLellan et al., 2008) and Ptch through its Fn1-2 domains (Izzi et al., 2011). By aligning of the protein sequence of the zebrafish and human Cdon, we verified that the residues involved in Ptch and Shh binding are conserved among vertebrates (see supplementary material). In fact, the protein sequence of Fn2 and Fn3 domains are well conserved from Humans to Xenopus (data not shown). By analysis of the *Cdon* genomic (NC_007129.5) and protein (Q1L8D0) sequences we established that skipping of exon 11 or exon 14, which encode the Fn2 and Fn3 domains, respectively, would not alter the reading frame. Removal of exons can be achieved *in vivo* by MOs that can block nuclear processing events like pre-mRNA splicing. Targeting exon-intron boundaries is a method to generate an exon skipping (Fig. 22A) (Draper et al., 2001). In order to generate truncated forms of Cdon lacking the Ptch or Shh binding domains *in vivo,* splicing MO (spl11MO and spl14MO respectively) were designed (Fig. 22B) and injected in zebrafish embryos at 1 cell stage. The efficiency of the spl11MO and spl14MO was determined by RT-PCR of MO injected embryos using primers complementary to regions in the adjacent exons. Amplifications detected a band of molecular weight lower than that observed in controls (Fig. 22C). Thus in both cases, MOs modified the splicing of the respec-

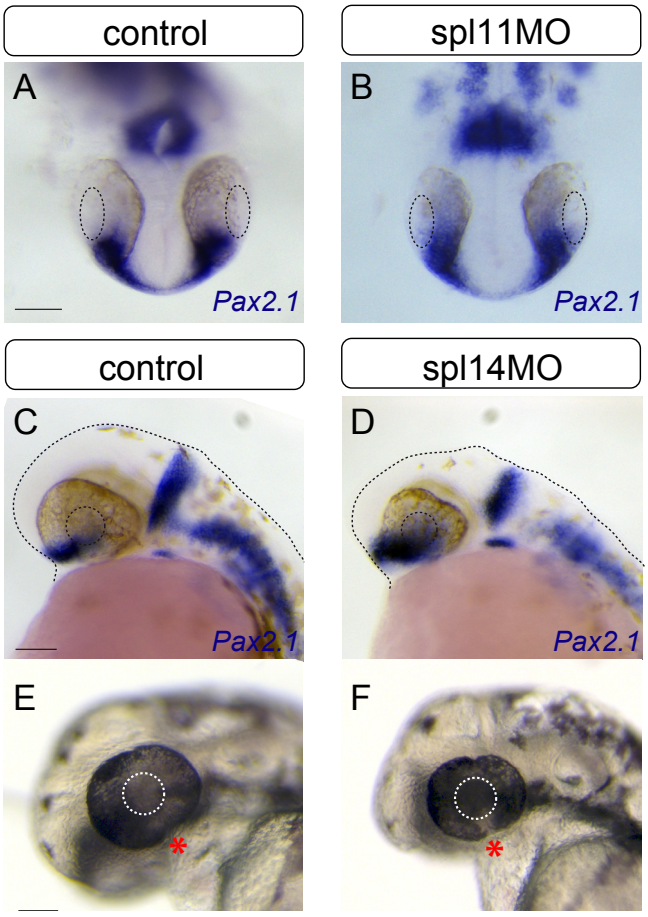

Fig. 23. Removal of the Shh binding domain of Cdon, but not that of Ptc1 phenocopies the effects of CdonMO. ISH analysis of the expression pattern of *Pax2.1* in controls **(A, C)**, spl11MO **(B)** and spl14MO **(D)** injected embryos at 28 hpf. Bright field lateral views of control **(E)** and spl14MO **(F)** injected embryo at 48 hpf. In spl11MO morphant embryos, the expression of *Pax2.1* appears normal (130/130 embryos) **(A, B)**. Spl14 morphants show an expansion of *Pax2.1* expression (58/86 embryos) **(D).** Some embryos show ventral defects in the eye at 48 hpf **(F)** not observed in controls **(C, E)**. Red asterisks indicate the position of the optic fissure. Dashed lines indicate the lens and the body perimeter of the embryos. Scale bars: 100 µm.

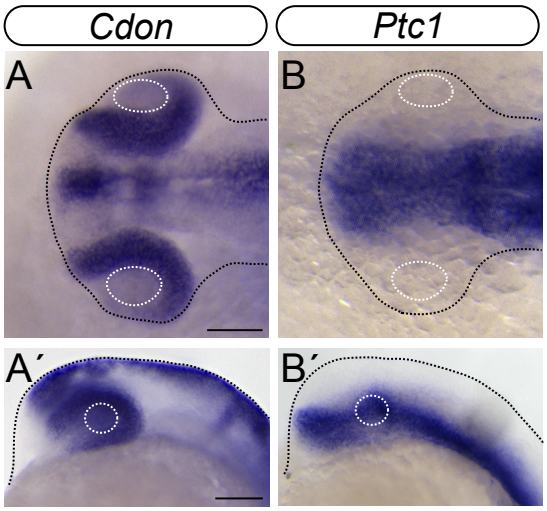

Fig. 24. *Cdon* and *Ptc1* expression pattern in zebrafish embryos. Dorsal **(A, B)** and lateral **(A´-B´)** views of zebrafish embryos hybridized *in toto* with specific probes for *Cdon* **(A, A´)** and for *Ptc1* **(B, B´)** at 20 somites. The expression patterns of both molecules are complementary and donot overlap. Dashed lines outline the lens and the embryo body. Scale bar: 100 µm.

tive targeted exons.

Spl11 morphants did not show evident changes in *Pax2.1* expression at 28 hpf (Fig. 23A, B), at least when embryos were injected in a 100uM to 600uM range of MO concentration. In contrast, spl14MO injected embryos exhibited an expansion of *Pax2.1* expression in the optic stalk region comparable to the *Pax2.1* overexpression obtained in Cdon morphants (Fig. 23C, D). At 48 hpf, some of the embryos failed to close the optic fissure (Fig. 23E, F). These results suggest that Cdon interaction with Shh, but not with Ptch, is critical for Cdon function in the optic cup. This is in agreement with the observation that Cdon and Ptch (referred as Patched1 (Ptc1) in zebrafish) are expressed in a complementary and non-overlapping distribution in the eye (Fig. 24).

Nevertheless we cannot completely rule out the possibility that skipping of exon 14

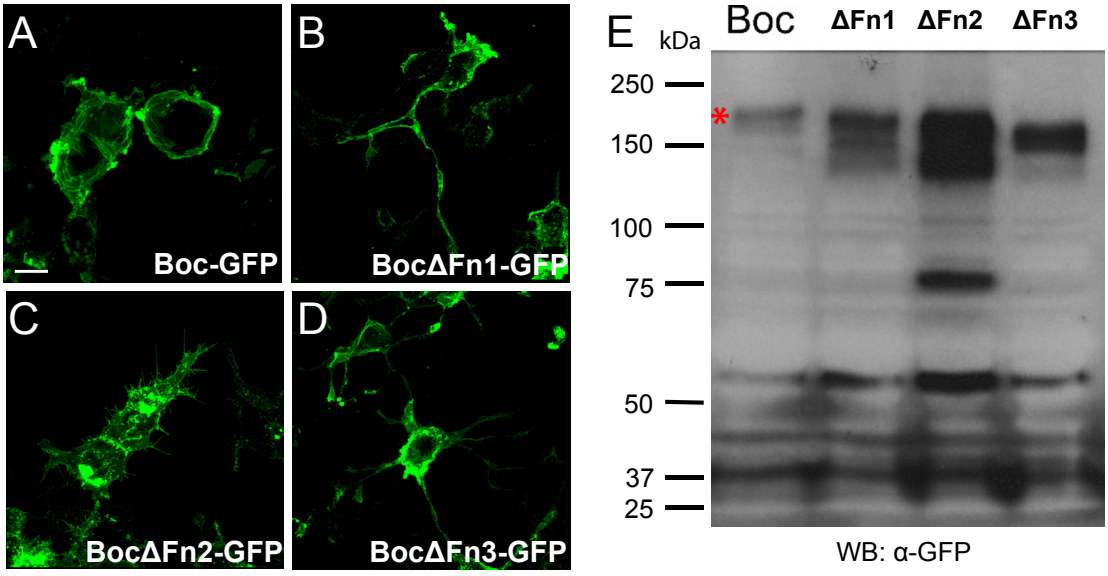

Fig. 25. Deletion of fibronectin domains of Boc does not affect protein stability or localization in transfected cell culture. A) HEK cells transfected with Boc-GFP or deleted versions of the fusion protein as indicated in the panels. Note that GFP signal is always detected at the cell membrane. **E)** Western Blot analysis of lysates from cells transfected with Boc-GFP or its derivatives. The asterisk indicates the position of the band corresponding to Boc-GFP. Scale bar: 2 µm.

may give rise to an unstable Cdon form affecting its turnover. Due to the lack of cross-reactivity of the Cdon antibody in zebrafish, we could not test this possibility directly. However, individual deletions of the fibronectin domains of the Cdon homolog Boc did not appear to affect the stability of the protein. Indeed, we deleted the fibronectin domains from a fusion construct of Boc-GFP (Boc-GFP). Transfection of the Boc-GFP plasmid or of its mutant variants (BocΔFn1-3) in Human Embryonic Kidney (HEK293) cells, revealed that all constructs were localized at the plasma membrane (Fig. 25A-D). Furthermore the translation and integrity of the different truncated peptides appeared normal by Western Blot analysis (Fig. 25E).

Studies in vertebrates have suggested that Cdon forms with Ptch an heterodimeric receptor (Bae et al., 2011). The normal phenotype of Spl11 morphants and the lack of overlapping expression of the two molecules suggest that Cdon in the eye acts with a Ptch independent mechanism.

Cdon binds all mammalian Hh proteins (Kavran et al., 2010). The phenotype of Cdon morphants is similar to the phenotype produced by Shh overexpression at the midline (Macdonald et al., 1995). We thus hypothesized that *Cdon* may act by controlling the diffusion of Shh secreted from the axial midline. To address this question *Cdon* was overexpressed in the neural tube close to the floor plate, an endogenous source of Shh. A complete mouse *Cdon* coding sequence cloned into the pCAG expression vector (pCAG-*Cdon*). HEK293 cells were transfected with the pCAG-Cdon DNA and 48h later the cells were collected and the proteins

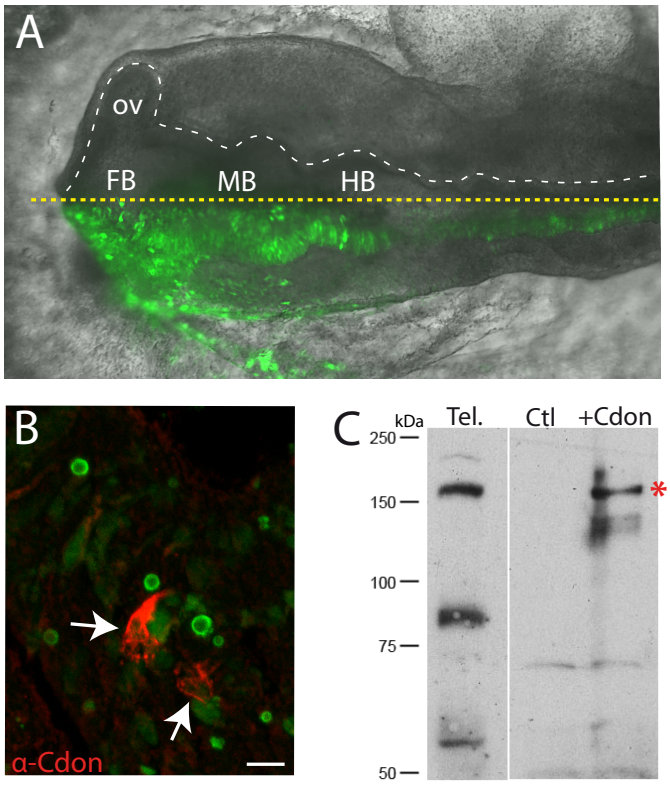

Fig. 26. Mouse Cdon is efficiently expressed in chicken neural tube. A) Chicken embryos were electroporated with a construct carrying mouse *Cdon* cDNA in half of the neural plate at HH5 and the embryos were selected by GFP expression at HH11. **B)** Cdon expression in the electroporated neural tube (green cells) was verified by IHC with a Cdon antibody (red cells, arrows) **C)** The plasmid carrying Cdon cDNA was transfected in HEK cells and the cell lysate was analyzed by WB with a Cdon antibody. Mouse telencephalon was used as a positive control. The lysate of Cdon transfected cells shows the expected band corresponding to the mouse Cdon. Yellow dashed line indicates the midline and white dashed line outlines the CNS. Scale bar: 5 µm. FB, forebrain; HB, hindbrain; MB, midbrain; ov, optic vesicles.

extracted in lysis buffer to perform a WB analysis using Cdon antibodies, to verify that the construct was well translated. The WB showed that Cdon was expressed correctly compared to mouse telencephalon lysate, which served as a positive control (Fig. 26C). Embryos were then electroporated at HH5 in a half of the neural plate and were let develop until HH11, when they showed an electroporated hemitube (Fig. 26A). Embryos were immunostained with Cdon antibodies to determine if the construct was well expressed and the protein well localized. A specific signal was localized at the plasma membrane of the cells (Fig. 26B). The chicken embryos were co-electroporated with the pCAG-Cdon construct and a GFP as a tracer or a GFP alone. Only GFP positive embryos were selected, sectioned, inmunostained with antibodies against Shh (Fig. 27A-F). The images of the sections were captured with a confocal microscope. In the non-electroporated half of the neural tubes or in control embryos electroporated with GFP alone, Shh signal was detected only in floor plate cells (Fig. 27A, B, D, E). Interestingly, in the Cdon electroporated half of the neural tube, Shh signal was detected away from the endogenous source of Shh, in cells with high levels of ectopic Cdon expression (Fig. 27D, E). This indicates that Cdon binds Shh secreted from the midline, suggesting that Cdon could modify Shh diffusion and therefore its signaling capability.

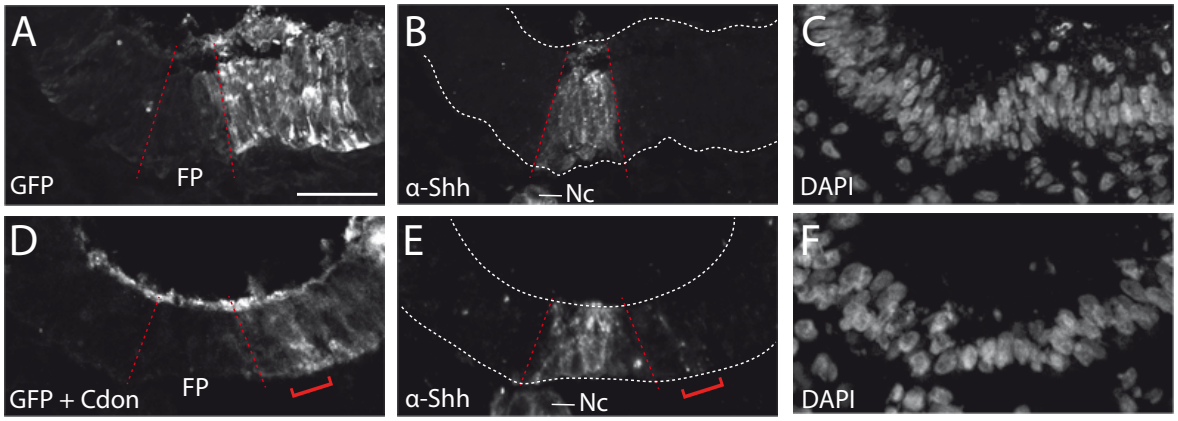

Fig. 27. Cdon enhances Shh diffusion *in vivo*. Chicken embryos were electroporated with a construct carrying mouse *Cdon* cDNA and GFP **(D-F)** or GFP alone **(A-C)**. The embryos were sectioned and Shh localization was determined by IHC **(B, E)**. Sections were counterstained with DAPI **(C, F)**. The electroporated half of the neural tube is showed in **A)** and **D).** Shh localizes to the floor plate (indicated by red dotted lines) **(B, E)**. In the presence of Cdon Shh seems to accumulate **(E,** red bracket**)** in cells with high Cdon expression **(D,** red bracket**)**. Scale bar: 50 µm. FP, floor plate; Nc, notochord.

FGF signaling acts downstream of Cdon.

In Xenopus embryos FGF signaling ventralizes the eye, expanding the optic stalk and the ventral retina (Lupo et al., 2005). In the MHB Fgf8 maintains, but does not initiate, the expression of *Pax2.1* (Reifers et al., 1998) . In Cdon morphants *Fgf8* was expanded in the optic stalk and telencephalon domains as shown in Fig.7 A-B´´.

We thus hypothesize that Fgf8 could at least in part mediate the expansion of the optic stalk caused by Cdon knock down. If this is the case inactivation of FGF signaling should rescue the *Cdon*-loss-of-function phenotype. To test this hypothesis we interfered with FGF signaling in *Cdon* morphants incubating the embryos with SU5402, a drug that interferes with the tyrosine kinase activity of the FGF receptors and thus inhibits the signal (Mohammadi et al., 1997). Zebrafish embryos injected with CdonMO were let develop in medium containing SU5402 from epiboly stage until 28 hpf. Embryos were fixed and *Pax2.1* expression was analyzed (Fig. 28). In wild type embryos, FGF treatment at 1µM slightly reduced *Pax2.1* expression in the optic stalk region (Fig. 20A, C). Instead SU5402 counteracted the expansion of *Pax2.1* expression observed in Cdon morphants (Fig. 28B), giving rise to embryos with a basically normal phenotype (Fig. 28D). This result suggests that FGF signaling acts downstream of Cdon mediating the optic stalk phenotype of Cdon morphants.

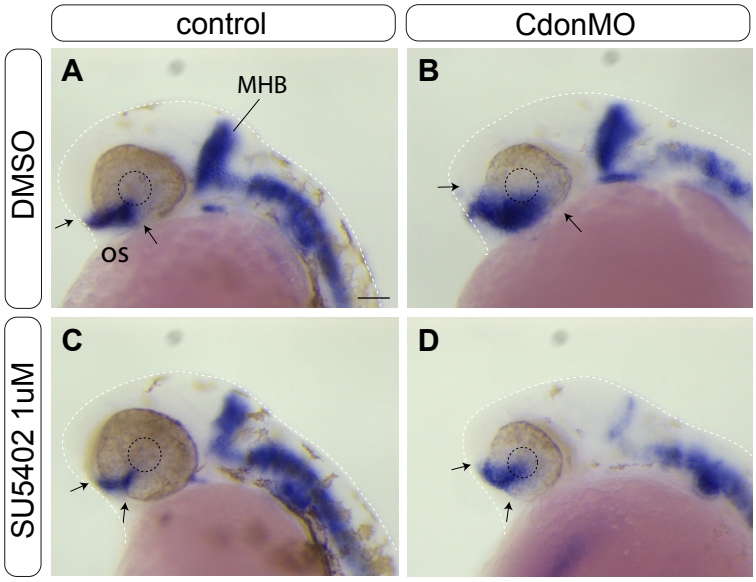

Fig. 28. FGF signaling acts downstream of Cdon to control proximo-distalization of the eye. Analysis by ISH of the expression pattern of *Pax2.1* at 28 hpf in control or CdonMO injected embryos threated from 90% epiboly with SU5402 inhibitor. Lateral views of embryos treated with SU5402 at 1uM **(B, D)** or DMSO **(A, C)**. Injection of CdonMO induces *Pax2.1* expansion in the optic stalk region **(B)** in comparison with control **(A)**. SU5402 administration at 1uM slightly reduces *Pax2.1* expression in the optic stalk of wild type embryos **(C)**. In CdonMO injected embryos, SU5402 treatment reduces the *Pax2.1* overexpression otherwise observed in CdonMO morphants (38/41 embryos) **(D)**. MHB, midbrain hindbrain boundary; os, optic stalk. The lens is indicated by a black dashed line and the body embryo is outlined with a white dashed line. Arrows indicate the extension of the *Pax2.1* expression in the optic stalk. Scale bar: 100 µM.

The developing retina is highly sensitive to FGF signal. Previous studies have showed that Fgf8, 3 and 24 cooperate to control naso-temporal patterning of the neural retina. Increased Fgf8 expression is associated with an expansion of the ventral and nasal retina (Picker and

Brand, 2005; Picker et al., 2009). We therefore tested whether the observed *Fgf8* expansion in Cdon morphants was also followed by defects in the naso-temporal patterning of the retina.

The CdonMO was injected in the transgenic line *Claudin*::GFP (*cldnb*::GFP) which expresses GFP in the nasal portion of the retina (Fig. 29A). In *Cdon* morphants, GFP expression driven by the *Claudin* enhancer was detected in both the nasal and the ventral-temporal quadrant of the retina (Fig. 29B). ISH with an *Efn5a* probe, which normally marks the nasal retina (Fig. 29C) was also expressed abnormally in the ventral-temporal region of the eye (Fig. 29D). In line with an expansion of the nasal region of the retina, the expression of the temporal marker *FoxD1* was absent from the ventral-temporal retina of Cdon morphants (Fig. 29F), as compared to control embryos (Fig. 29E). The gain of *Efn5a*-positive nasal fate

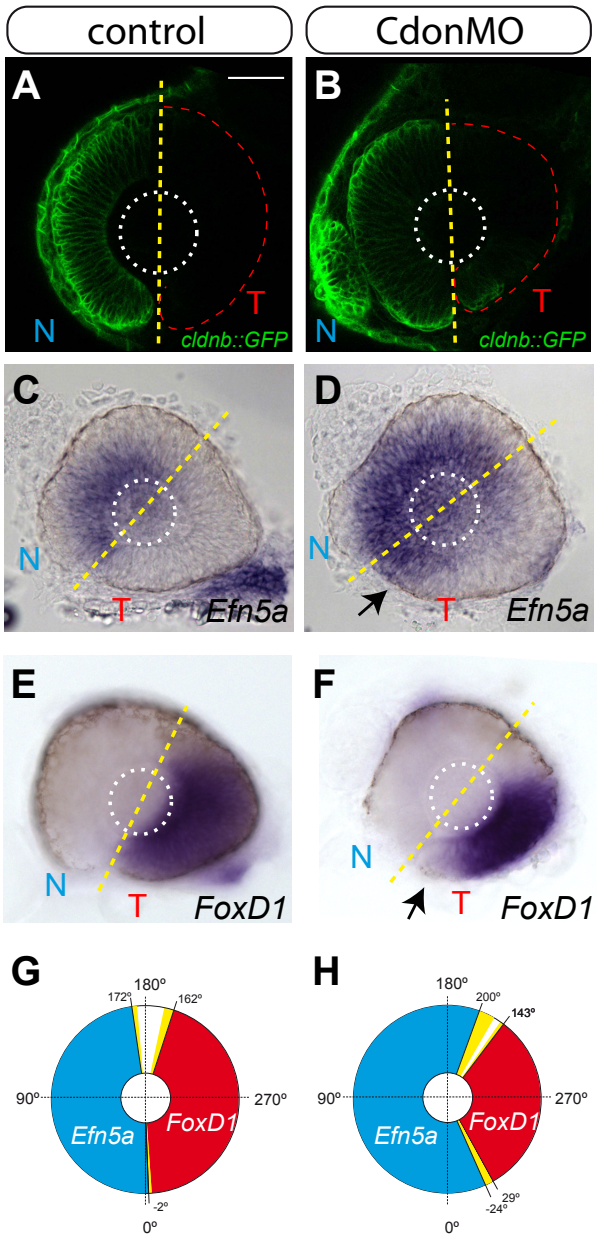

Fig. 29. Cdon is required for the naso-temporal patterning of the retina. The transgenic line *cldnb*::GFP, which express GFP in the nasal region of the retina, was injected with CdonMO **(A, B)**. Analysis by *in situ* hybridization of nasal (N) (*Efn5a*) and temporal (T) (*Foxd1*) markers of the retina **(C-F)**. Transgenic embryos injected with CdonMO show ectopic GFP expression in the temporal region of the retina **(B)** (16/30 embryos) in comparison with control embryos **(A)**. The same defect is observed with the nasal marker *Efn5a* **(C, D** arrow**)**. The temporal marker *Foxd1* is absent in the ventral-temporal quadrant of the retina in *Cdon* morphants **(F** arrow**)** in comparison to control **(E)**. Quantification of the changes in *Efna5a* (wt=14 embryos, MO=11 embryos, blue) and *FoxD1* (wt=8 embryos, MO=15 embryos, red) expression, determined by measuring the extent of the staining in degrees. The optic fissure was considered 0º. The standard deviation is in yellow. The nasal retina is expanded at the expenses of the temporal retina in Cdon morphants **(H, G)**. The yellow dotted line depicts the division between the nasal and temporal half of the retina. The lens is outlined in white and the retina in red. Scale bar: 50 µM.

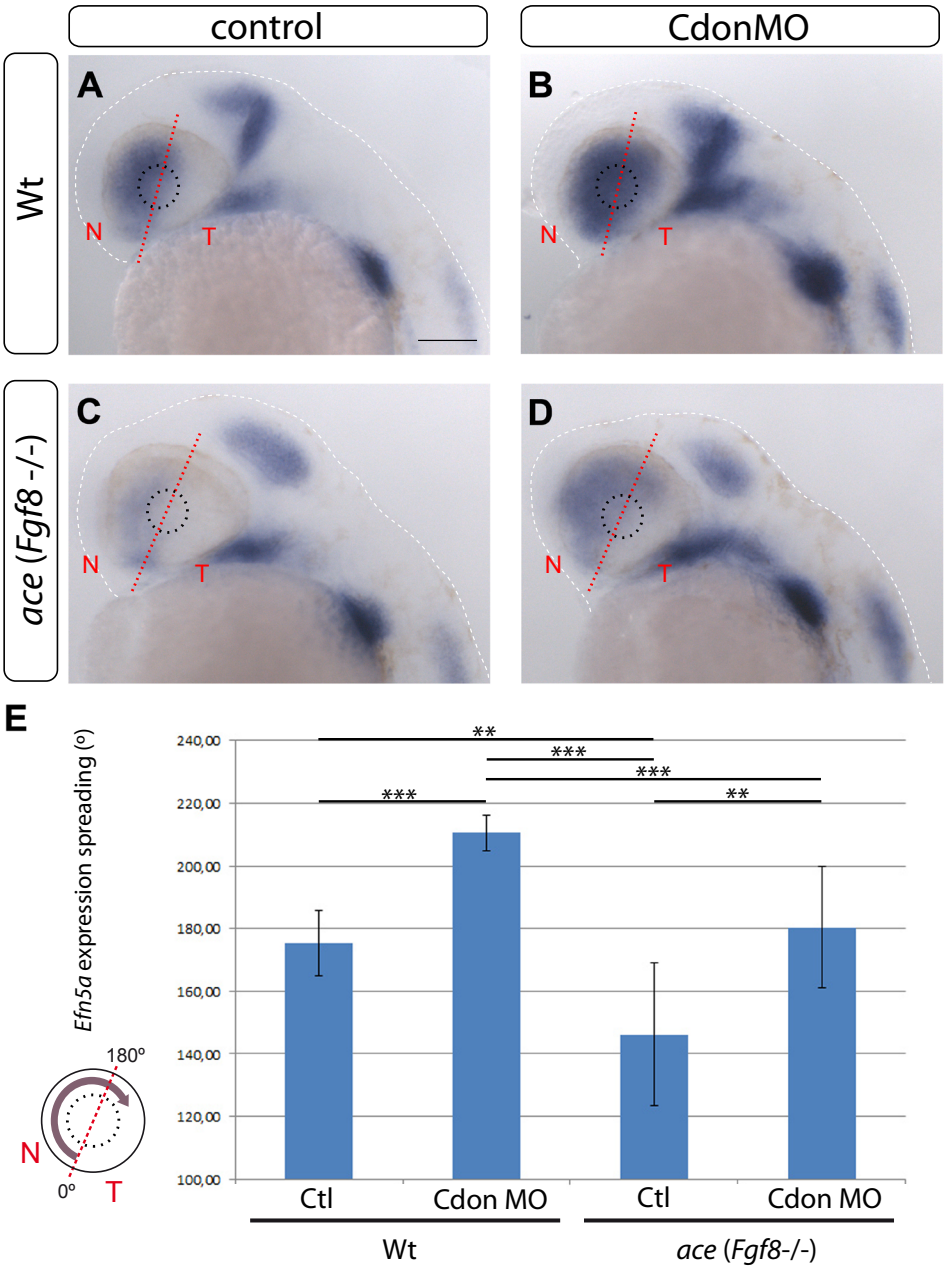

Fig. 30. *Fgf8* acts downstream of *Cdon* in naso-temporal patterning of the retina. ISH analysis of a nasal retina marker (*Efn5a*) **(A-D)** in wild type and *Fgf8a*$^{-/-}$ mutants (ace) injected with or without CdonMO. CdonMO injected embryos show expanded *Efn5a* expression in the retina **(B)** in comparison to control **(A)** and *ace* mutants show a reduction of *Efn5a* **(C)**. Note the reduction of *Efna5a* in *ace* mutants injected with CdonMO (14 embryos) **(D)** in comparison to wild type injected embryos **(B)**. Quantification of *Efn5a* expression in the eye, shows that in *ace* mutants the extent of *Efn5a* expression domain produced by Cdon knock-down is smaller than that of non-mutant CdonMO injected embryos (n=14 for each condition) **(E).** ** $p < 0.01$, *** $p < 0.001$ according to one-way ANOVA. The red dotted line depicts the division between the nasal **(N)** and temporal **(T)** half of the retina. The lens is indicated by a white dashed line. Scale bar: 100 µM.

at the expenses of the temporal marker *FoxD1* is plotted in figure 21G, H. Notably, the expression of the nasal marker *Foxg1* and of the temporal marker *Epha4b* did not seem to be affected (data not shown).

To corroborate that the increase of the nasal domain of the retina observed in Cdon morphants is a specific consequence of *Fgf8* overexpression (see Fig. 15), CdonMO was injected in the *Fgf8* mutant embryos (*ace*) (Reifers et al., 1998) at 1 cell stage. At 28 hpf the embryos were fixed and hybridized for the nasal marker *Efn5a*. In *ace* mutants *Efn5a* expression domain is reduced (Fig. 30A, C and (McMahon et al., 2009; Picker et al., 2009)) whereas in CdonMO it is expanded (Fig. 30B). Notably, *ace* mutants injected with CdonMO showed a wild type phenotype (Fig. 30D, E) indicating that *Fgf8* mediates, at least in part, the naso-temporal alterations observed in Cdon morphants. From these experiments, we conclude that *Fgf8* acts downstream of Cdon during the process of naso-temporal patterning of the retina.

Analysis of the regulatory elements that control *Cdon* expression.

Cdon expression pattern during development is very dynamic and complex but there is little information regarding the regulatory regions that control its expression. *Cdon* expression seems to be negatively regulated by Hh signaling in early mammalian embryos (Tenzen et al., 2006; Bergeron et al., 2011) supported by the abnormal levels of Cdon expression found in the limb buds of *Gli3* mutant embryos (McGlinn et al., 2005).

Recently, a medaka fish *Cdon* GFP reporter line was generated using the sequence localized at chr13:4420609-4421119 of the medaka genome. This line expresses GFP only in the proliferative regions of the CNS (Ramialison et al., 2012). The lack of GFP expression in the axial midline, the retina or the dorsal neural tube indicates that other elements regulate *Cdon* expression in these regions. In order to identify and characterize these elements we aligned the Cdon *locus* of different vertebrate species including the sequences ~200kb up and downstream of the *Cdon* coding sequence. We found little conservation outside the *Cdon* coding region between zebrafish and the other vertebrates (data not shown). Because this alignment was not informative, we aligned ~500kb of the zebrafish genome (chr18:42,238,809-42,745,581), containing the *Cdon* gene, with the corresponding sequences of *Tetraodon nigroviridis, Takifugu rubripes, Oryzias latipes* and *Gasterosteus aculeatus*. The alignment was performed with the Mulan software using the default settings (Ovcharenko et al., 2005) and with the "MultiZ Alignment & Conservation" track, available in the genome.ucsc.edu website. The alignment indicated the existence of several high conserved non-coding elements (Fig. 31A and data not shown). We selected nine sequences that com-

plied with the following criteria: more than 50% of sequence conservation among species and low degree of repeated sequences. These nine sequences were named A-I (Fig. 31A). The A and B sequences are localized downstream of *Cdon* coding region. The C, D and E sequences are instead found within the *Cdon* introns whereas the sequences F, G, H and I are upstream of *Cdon* coding region (Fig. 31A).

The sequences A-I were amplified by PCR from zebrafish DNA and were cloned by Gateway technology in the Zebrafish Enhancer Detection (ZED) vector (Bessa et al., 2009) which harbors the GFP gene as reporter of the cloned putative regulatory elements. The nine constructs (A-I) were co-injected with a transposase RNA in 1-cell stage embryos. The developing embryos were followed with a fluorescent stereo microscope to detect the onset of GFP expression. Sequences A, D, H and I drove GFP expression in the eye, telencephalon and dorsal neural tube at 24 hpf respectively in a proportion of the injected embryos. The most reproducible enhancer activity was observed in fishes injected with the D sequence, which drove GFP expression in the telencephalon of F0 injected embryos. The F1 progeny showed expression in the telencephalon (Fig. 31C) and in some cases in the retina and lens (Fig. 31B). The F2 generation will be fully analyzed to establish in detail the activity of this

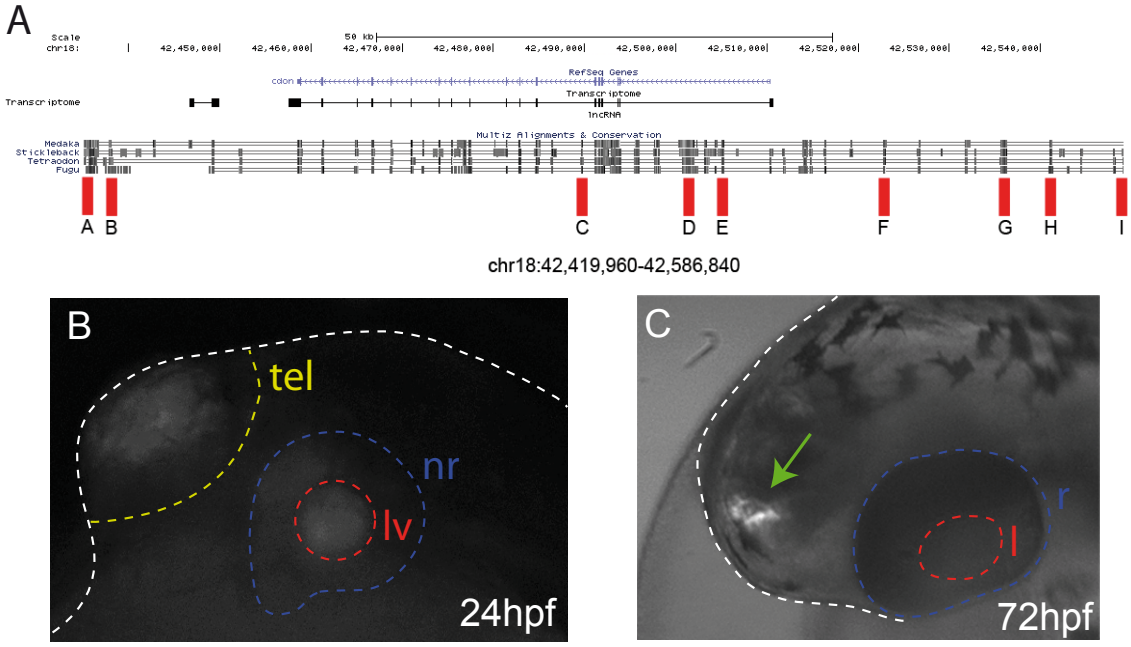

Fig. 31. Analysis of the Cdon regulatory regions. A) Organization of exons (blue boxes), introns and non-coding regions of the *Cdon* gene. Nine conserved sequences were selected as putative regulatory elements; the graphic shows their position relative to *Cdon* (red boxes, A-I). Each one of the sequences was cloned in ZED (Zebrafish Enhancer Detection), a vector designed for transgenic enhancer assay. The alignment of zebrafish, medaka, fugu, tetraodon and three-spined stickleback *Cdon* regions shows the conservation of the nine selected elements in fishes (gray boxes). **B)** The enhancer D F1 embryos drove GFP expression in the telencephalon (n=19, 3 independent lines and n=271 in transient lines). **C)** An F1 line drove GFP expression in the retina, lens and telencephalon (n=2). l, lens; lv, lens vesicle; nr, neural retina; r, retina; tel, telencephalon.

element.

To further localize regulatory regions that are not highlighted by the criteria of conservation among vertebrates, we analyzed histones marks in the human *CDON* gene through the ENCODE database available at www.genome.ucsc.edu. Histone H3 acetyl Lys27 antibody (H3K27AC), which marks active regulatory elements may distinguish active enhancers and promoters from their inactive counterparts. Human *CDON* gene displays a region that is marked by the H3K27AC, upstream of the promoter region, localized in the first intron (Fig. 32A). This data suggests that the first intron of *CDON* harbors regulatory elements.

The histone H3K27AC profile determined at various stages of zebrafish development (kindly provided by Prof. J. L. Gómez-Skarmeta) confirmed that the sequences D and E are

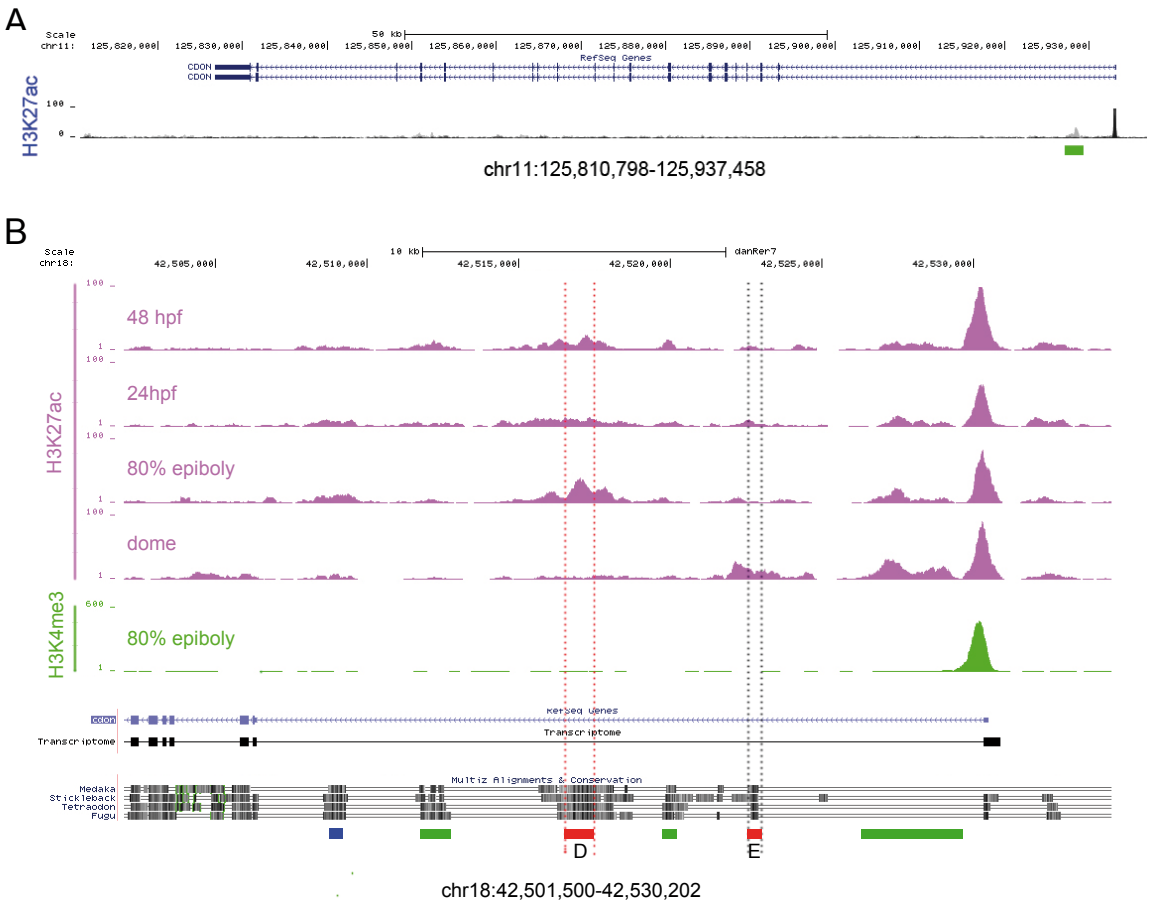

Fig. 32. *Cdon* first intron contains putative regulatory regions. A) Organization of exons and introns in *CDON* gene. H3K27ac signature marks active regulatory elements in the promotor region and the first intron of *CDON* (green box). **B)** The H3K27ac signature which marks active regulatory elements is depicted in purple, whereas the H3K4me3 signature which marks regulatory elements primarily associated with the promoters/transcription start sites, is depicted in green. The enhancers D and E are indicated with red boxes. A medaka homolog enhancer sequence is indicated with a blue box and three other putative regulatory elements are marked with green boxes. Multiple Alignment of zebrafish, medaka, fugu, tetraodon and three-spined stickleback *Cdon* regions shows the conservation among fishes of the selected and putative regulatory elements (gray boxes).

strong candidates to be regulatory elements. The D sequence appears to be active from 80% epiboly at least until 48 hpf (Fig. 32B). The E sequence appears to be active at dome stage and later on appears to be inactive (Fig. 32B). In addition to the D and E sequences, four other sequences within the first intron of *Cdon* are marked by H3K27ac and are thus putative regulatory elements (Fig. 32B, green and blue boxes). One of these sequences (chr18:42,508,500-42,509,000) (Fig. 32B, blue box) is in fact homologous to the *Cdon* enhancer isolated in medaka embryos (Ramialison et al., 2012). Together these data points to the presence of different regulatory elements that could control *Cdon* expression. Future studies will confirm their relevance and spatial-temporal activity in the regulation of *Cdon* expression.

DISCUSSION

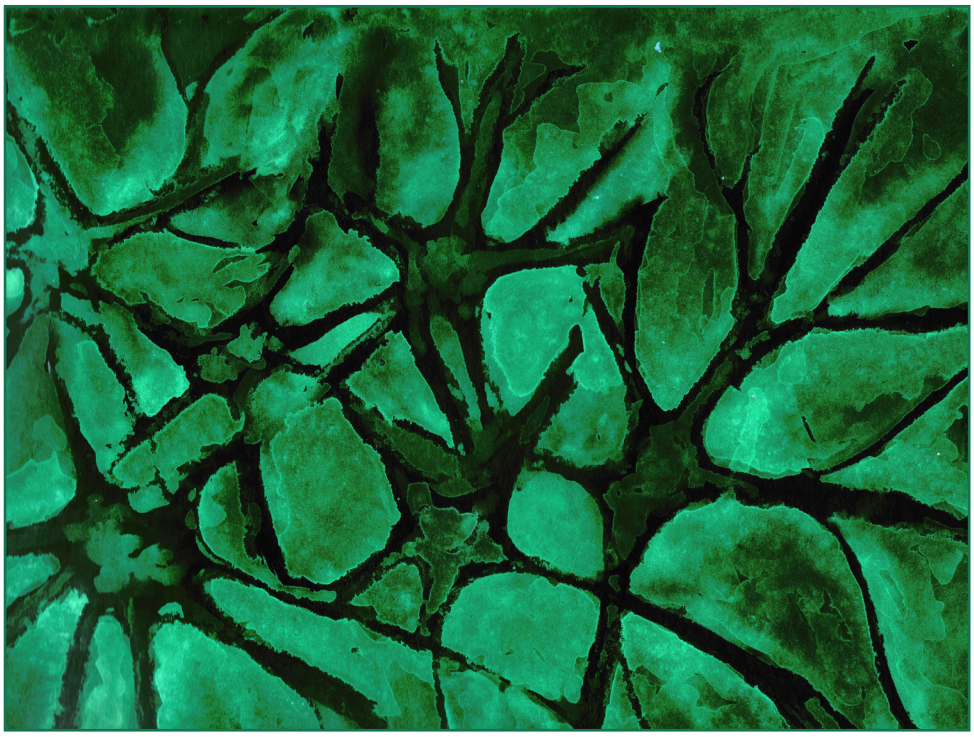

The CNS is highly regionalized along the antero-posterior and dorso-ventral axes. Hh signaling plays a key role in specifying ventral cell types throughout the neuroectoderm. Other molecular pathways, including nodal, retinoic acid and FGF signaling, have been also identified as important cues for the ventral patterning of the spinal cord, the telencephalon and the eye (Lupo et al., 2006). The organogenesis of the vertebrate eye is a multistep process that requires Hh signaling at different time points (Amato et al., 2004). Shh secreted from the midline is critical to establish and maintain the proximo-distal patterning of the eye, by controlling the balanced expression of *Pax2/Pax6* in the optic stalk and retina domains, respectively (Macdonald et al., 1995; Take-uchi et al., 2003). Shh is also necessary to confer ventral identity to the retina (Huh et al., 1999; Zhang and Yang, 2001; Sasagawa et al., 2002). We thus propose that the Shh binding molecule, Cdon, can act as a negative modulator of Hh signaling in vertebrates. Cdon expressed in the retina acts to protect the optic cup from Shh activity by binding and preventing Shh diffusion. This function is needed to establish a correct proximo-distal patterning of the eye. In the absence of Cdon, the Shh gradient becomes expanded to more distal regions enlarging the optic stalk domain at expense of the retina promoting ventral eye defects (Fig. 33).

This model adds a novel function to Cdon, opposite from what has been so far proposed in vertebrates. In fact, in vertebrates, Cdon acts as a positive modulator of Hh signaling during development. *Cdon* KO mice present a microform of HPE, which partially resemble the phenotype of *Shh*$^{-/-}$ mice (Cole and Krauss, 2003; Zhang et al., 2006a; Allen et al., 2007; Hong and Krauss, 2012). Human patients with mutations in *CDON* display HPE (Bae et al., 2011). Shh expression and its target genes are downregulated in *Cdon* mutants (Tenzen et al., 2006; Zhang et al., 2006a; Allen et al., 2011; Zhang et al., 2011). *In vitro* experiments demonstrated that in Cdon absence, Hh signaling is impaired (Zhang et al., 2006a; Bae et al., 2011) and ectopic expression of Cdon promotes Shh-dependent cell fate specification in the neural tube (Tenzen et al., 2006). In *Drosophila* the Cdon homologs Boi/Ihog are necessary for Hh signaling activation (Lum et al., 2003; Yao et al., 2006; Camp et al., 2010). However, Boi/Ihog can also act as negative modulators of Hh signaling in some contexts, participating in the secretion and titration of Hh ligand limiting long-range signaling (Hartman et al., 2010; Yan et al., 2010; Callejo et al., 2011; Bilioni et al., 2012).

In *Drosophila*, these functions were revealed thanks to the distinct advantages of this model organism that includes an efficient control of time and tissue specific transgene expression or amenable techniques to generate knockout and gene replacement. In mice instead a conditional Cdon knock-out is not yet available. Therefore to avoid possible masking effects of an earlier phenotype, we addressed the study of *Cdon* function using zebrafish and chicken embryos, in which it is possible to interfere with gene expression in a controlled manner.

In our knock-down model in zebrafish, the levels of *Cdon* expression are reduced rather than being completely depleted. Nevertheless, we expected to observe an eye phenotype consistent with the loss of Hh signaling: that is to say a reduction of the proximal structures, the optic stalk, and a cyclopic phenotype produced by the fusion of the retinas at

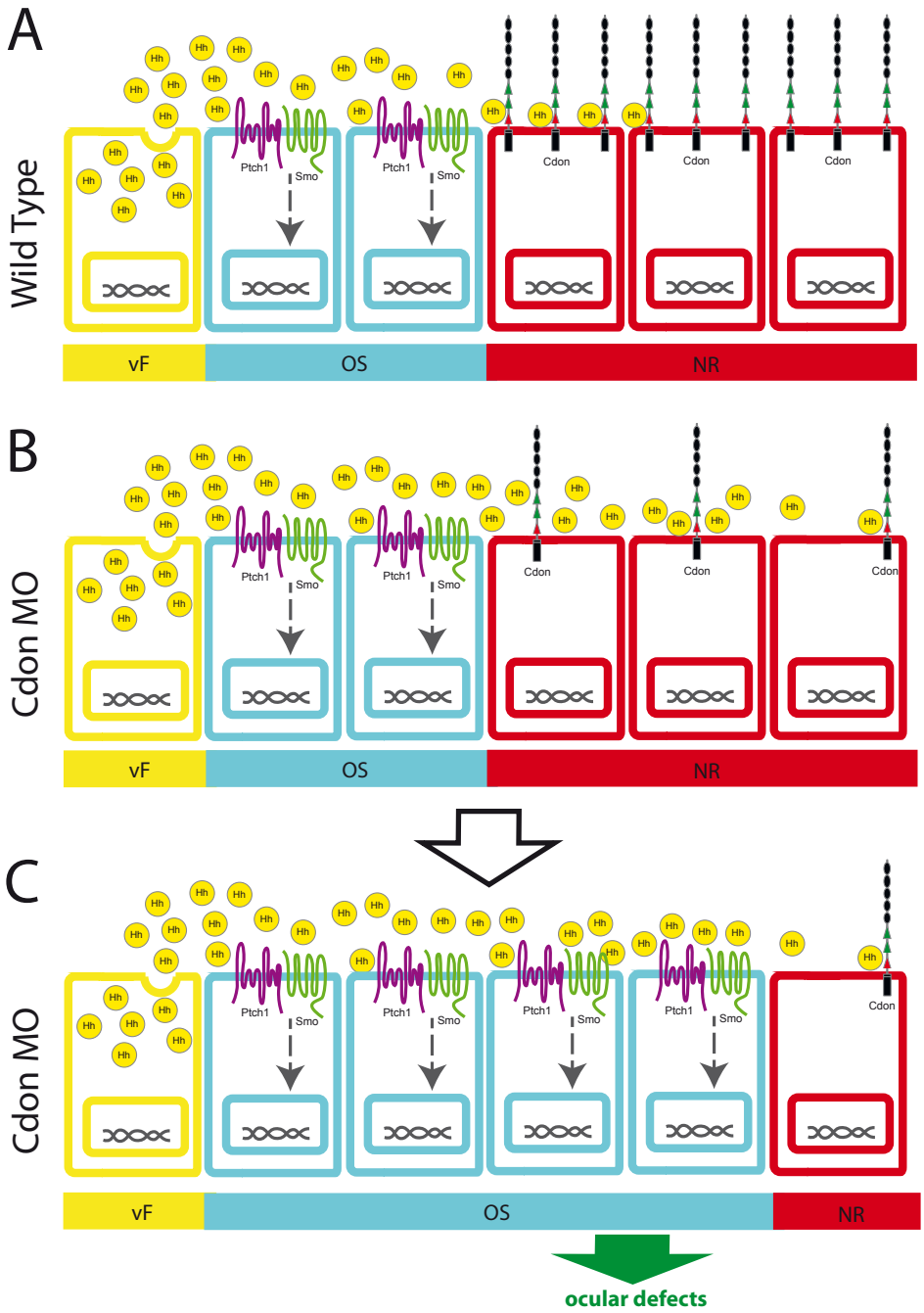

Fig. 33. Model of the proposed function of Cdon in early eye development. The cells of the ventral forebrain are represented in yellow (vF), those of the optic stalk (OS) in light blue and those of the neural retina (NR) in red. **A)** Cdon expressed in the retina binds Shh secreted from the midline thus restraining its diffusion and protecting the retina from signaling activation during the establishment of the proximo-distal patterning of the eye. **B)** In absence of Cdon, the ligand spreads to more distal region. **C)** Consequently, the optic stalk domain is expanded giving rise to ocular defects.

the midline. Unexpectedly, the eye phenotype of *Cdon* knock-down was compatible with an opposite scenario: a gain of Hh signaling. Indeed in both, zebrafish and chick embryos we always observed an expansion of the optic stalk and ventral retina domain visualized by an expanded *Pax2* expression. These results contrast with the proposed function of Cdon as a positive modulator of Hh signaling (Tenzen et al., 2006; Zhang et al., 2006a).

Several lines of evidence indicate that the transcription factor Pax2 is a direct Shh target. *Pax2* expression in the optic stalk and choroid fissure is dependent on Shh (Chiang et al., 1996; Varga et al., 2001; Zhang and Yang, 2001; Perron et al., 2003) and Shh overexpression is sufficient to induce the expression of *Pax2* in more distal optic vesicle territories, from which it is normally absent (Ekker et al., 1995; Macdonald et al., 1995; Zhang and Yang, 2001; Perron et al., 2003). *Pax2* in turn is required to establish the proximo-distal patterning of the eye.

The development of the eye in the teleost fish *Astyanax mexicanus* is the clearest example of the consequence of an expansion of Hh signaling from the midline. In their natural environment, these fishes exist in two forms: a surface dwelling river morph and a cave-living blind morph (cavefish). One of the most surprising characteristic of the cavefish is that the anterior expression domain of Shh (and that of Twhh) at the embryonic ventral midline is expanded throughout forebrain development (Yamamoto et al., 2004; Menuet et al., 2007). This expansion of Hh signaling results in hyper activation of downstream genes like *Pax2* during optic vesicle and optic cup stages and also in the lack of the ventral quadrant of the retina that leads to eye degeneration (Yamamoto et al., 2004). Our observations are in line with this scenario and strongly suggest that Hh signaling is expanded in Cdon morphants. The evidence described above and the experiments in which the optic stalk phenotype was counteracted by blocking Hh signaling further support the critical role of Hh signaling in the observed Cdon phenotype.

In Cdon morphants the repositioning of the boundary between the optic stalk and the neural retina is associated with ventral eye defects and the presence of coloboma due to a failure in optic fissure closure. Other studies in fishes are consistent with the idea that Hh signaling overactivation is responsible of similar defects. In fact, *blowout* mutants (*Ptc1*$^{-/-}$) (Lee et al., 2008), *uta1* mutants (*Ptc2*$^{-/-}$) (Lee et al., 2012), *Zic2a* morphants (Sanek et al., 2009), the uncharacterized *aussicht (aus)* mutant (Heisenberg et al., 1999) and Shh overexpression (Ekker et al., 1995; Macdonald et al., 1995) are all characterized by an expansion of Hh signaling that leads to *Pax2* overactivation in the optic stalk and by optic coloboma formation. The consequence of Shh overexpression in chicken is similar. Optic cups infected with a virus that leads to Shh ectopic expression, display microphthalmia at E6. This is accompanied by a loss of ventral retina, abnormal folding of the retina and/or pigmented epithelium, ab-

normal ciliary margins, and a widened optic fissure (Zhang and Yang, 2001). Notably i*n ovo* electroporation of Pax2 in the ventral optic cup results in the formation of coloboma (Sehgal et al., 2008). By contrast loss of *Pax2* function leads to optic nerve hypoplasia and coloboma in humans and in a number of animal models (Sanyanusin et al., 1995; Torres et al., 1995; Macdonald et al., 1997; Otteson et al., 1998). Interestingly, the presence of coloboma have been described in patients with a deletion in the human *SHH* gene (Schimmenti et al., 2003). In summary, an unbalanced expression of the signals responsible for the proximo-distal patterning of the optic vesicle, modifies the position of the boundary between the optic stalk and the retina, thus affecting the closure of the optic fissure.

In the zebrafish mutant strain *syu* (*Shh*$^{-/-}$), there are no obvious abnormalities of *Pax2* or *Pax6* expression in the developing eye. This indicates that the lack of *Shh* alone does not affect proximo-distal fates in the developing eye of the zebrafish (Schauerte et al., 1998), possibly because *Twhh* may compensate Shh activity. In fact, in zebrafish Twhh expression and function are similar to those of Shh in proximo distal patterning of the eye (Ekker et al., 1995). This suggests that Cdon may bind other Hh ligands in zebrafish. In line with this idea and the fact that Hh signaling mediates the phenotype of Cdon morphants, the downregulation of Cdon in *syu* mutants did not rescue the optic stalk expansion.

If Hh signaling is altered in Cdon morphants, targets of the pathway should be modified, either in its expression level or distribution. However, we could not detect any evident change in the expression of different readouts of the Hh pathway in Cdon morphants. The expression pattern of *Ptc1*, *Shh*, *Nkx2.1*, *Nkx2.2*, *Gli2*, *Gli2b*, *Gli3*, *Boc* and *Cdon* itself appeared normal in Cdon knock-down embryos (data not shown). However, ISH is a poorly sensitive technique and subtle changes might have gone unappreciated. Other studies reporting similar phenotypic consequences associated to a gain of Hh function have not described evident alterations in the expression of Hh pathway components. One example is the zebrafish *aus* mutant, carrying a mutation in a regulator of *Fgf8* expression (Heisenberg et al., 1999). Its phenotype includes the overexpression of *Fgf8* and *Pax2.1*, the incomplete closure of the optic fissure and nasal retina expansion, with little if any *Shh* ectopic expression (Heisenberg et al., 1999). Zic2a morphants present a phenotype similar to that of *aus* mutants. The phenotype could be rescued in a *Smo*$^{-/-}$ background or by blocking Hh signaling with *Hhip* mRNA injection, although the expression of Hh signaling targets was not analyzed (Sanek et al., 2009). We thus believe that the changes of Hh signaling in these and our studies might be very subtle and possibly restricted in space and time so that variations might be buffered by the regulation of the pathway itself. We propose that in absence of Cdon the Shh gradient becomes modified. Verifying this modification requires the visualization of Shh protein in fishes. Unfortunately and despite the many attempts, we did not succeeded in performing

this experiment. Therefore to address if *Cdon* knock down affects the Hh pathway, we plan to perform MO injections in the Hh signaling reporter zebrafish line *ptc1*::KAEDE (Huang et al., 2012), in the hope to have a better resolution.

Aberrant Shh signaling is one of the leading causes of HPE. Individuals suffering from mild forms of HPE are also affected by coloboma. Given the overlap in mutational etiology, HPE and coloboma are likely to represent in some cases severe and mild manifestations of the same phenotypic spectrum. To avoid the effect that the abrogation of *Cdon* expression in the midline could generate, we blocked the expression of *Cdon* specifically in the retina of chicken embryos by the electroporation of a specific MO. When Cdon was down regulated in the retina, *Pax2* was overexpressed in the optic stalk and retina domains suggesting that these phenotypes are independent of midline defects.

In mice and in zebrafish, Cdon is expressed transiently in the prechordal plate mesendoderm and notochord and in the ventral structures that produce and respond to Shh. In this structure *Cdon* functions as a positive regulator of the Shh pathway, necessary for proper patterning of the ventral telencephalon and floor plate of the neural tube (Tenzen et al., 2006; Kang et al., 2008; Oh et al., 2009). Cdon deficiency in mice results in HPE with strain-specific severity due to defective Shh signaling in and/or from the prechordal plate (Cole and Krauss, 2003; Zhang et al., 2006a). Additionally, *Cdon* mutant mice display multiple anomalies of eye development, including the disruption of ventral patterning, coloboma and defective lens (Zhang et al., 2009). Notably, eye anomalies displayed by Cdon morphants are similar to those described for *Cdon* mutant mice, however the expression pattern of some molecular markers are affected in a distinct manner. *Cdon*$^{-/-}$ embryos present a downregulation of ventral (*Pax2.1, Vax2*) and dorsal (*Tbx5* and *Bmp4*) patterning genes (Zhang et al., 2009). This difference may be explained by the primary cause of the *Cdon*$^{-/-}$ mouse phenotype likely linked to Cdon function in axial midline. In Cdon morphants instead we did not observed midline defects. It is possible that a possible overlap of *Cdon* with either *Boc*, *Gas1* or *LRP2* expression could compensate *Cdon* knock down. Alternatively, the remaining *Cdon* levels in zebrafish morphants are sufficient to allow correct embryo development at early stages. By contrast eye development may require high Cdon levels. In absence of these levels Shh signaling becomes expanded, promoting *Pax2* upregulation.

Although it has been suggested that Cdon and Ptch act in concert in Shh signaling (Bae et al., 2011), we have shown by ISH that there are many contexts during development in which the expression patterns of both molecules do not overlap. *Cdon* expression in the retina or in the dorsal neural tube does not overlap with that of *Ptc1*, suggesting that Cdon has Ptch independent functions. Our experiments using splicing blocking MO´s demonstrated that removal of the Shh binding domain (FNIII 3) domain of Cdon (Okada et al., 2006; Tenzen

et al., 2006; McLellan et al., 2008) induced a phenotype similar to that of CdonMO injected embryos. However removal of the Ptch binding domain (FNIII 2) of *Cdon*, resulted in embryos with a wild type phenotype. These observations are consistent with a mechanism in which Cdon acts on Hh signaling independently of its interaction with Ptch. Notably, all the mutations in the *CDON* gene that cause HPE in humans falls outside the Shh binding domain and the resulting CDON variants still present effective Shh binding. In contrast, wild-type CDON associates with PTCH1 but the mutated variants are less efficient (Bae et al., 2011). This indicates that normally Cdon plays an important role in the axial midline likely by binding to both Shh and Ptch and thus acting as a positive modulator of Hh signaling. By contrast, Cdon interaction with Shh but not with Ptch could be important for the development of a normal eye. These results support the idea that Cdon could have multiple, independent functions in Hh signaling during development depending on the biological context.

Besides its role in Hh signaling, Cdon can also interact with N-cadherin, activating p38α/β MAPK signaling (Kang et al., 2003; Lu and Krauss, 2010). We cannot totally exclude that this Cdon interaction might be also relevant to eye development, because N-cadherin zebrafish mutants present eye defects (Yamaguchi et al., 2010). Furthermore, Cadherin-mediated cell adhesion is critical for the closure of the mouse optic fissure (Chen et al., 2012). N-cadherin restricts cell proliferation in the dorsal region of the zebrafish neural tube, regulating cell-cycle length. Enhanced proliferation in N-cadherin mutants is mediated by ligand-independent activation of Hh signaling (Chalasani and Brewster, 2011). Considering that *Cdon*$^{-/-}$ mice also display dorsal CNS phenotypes, including defects in proliferation and differentiation of cortical neural precursors (Zhang et al., 2006b), it might be interesting to investigate if Cdon and cadherins could act together during CNS development.

Our experiment showing ectopic expression of Cdon in the chick neural tube suggests that Cdon binds Shh with high efficiency. In this assay, we detected an accumulation of Shh in the cells that expressed high levels of Cdon close to the floor plate, a source of Shh, but not in cells with similar Cdon expression levels located more dorsally. Similar results were obtained by the electroporation of Boc in the neural tube (unpublished data of the laboratory). A possible explanation for this observation is that Cdon (and Boc), could act as Shh "sinks" (for instance, by endocytosis and degradation of the ligand). This mechanism is similar to that described for Glypican-3 (Capurro et al., 2008), Patched (Chen and Struhl, 1996; Lee et al., 2008) or Hhip (Chuang and McMahon, 1999) which bind Shh and restrict its diffusion and thus the activation of the pathway.

Besides Hh ligands, glypicans and Xhip can regulate the activity of Wnt and FGF ligands (Song et al., 1997; Tsuda et al., 1999; Grisaru et al., 2001; Cornesse et al., 2005). How the context-specific interplay among different signaling pathways produces distinct temporal

and spatial outcomes is an open question in the field of developmental biology. Whether Cdon interferes with the activity of other secreted signaling molecules is unknown. It is also unexplored whether Cdon has additional binding partners. These are open questions that might be important to address in the future.

FGF and Hh signaling act in positive feedback loop in different developmental contexts (Brewster et al., 2000), including forebrain development (Bertrand and Dahmane, 2006). In line with this observation, in Cdon morphants, the FGF pathway appears upregulated. Cdon depletion could affect Shh signaling as a consequence of the expression of *Fgf8*.

The participation of *Fgf8* in the molecular cascade of eye development was demonstrated in cavefish. *Fgf8*, expressed in the rostral forebrain is activated 2 hours earlier in cavefish embryos than in their surface counterparts. This occurs in response to the higher Shh signaling levels present in the cavefish. It has been proposed that this crucial heterochrony is responsible for morphogenesis defects of the eye in the cavefish (Pottin et al., 2011). Although we have not tested it, it is possible that a similar heterochrony could be present in Cdon morphants. This issue could be addressed with a detailed analysis of the onset of *Fgf8* expression and/or with a time course of the inhibition of FGF signaling with pharmacological treatment. It will be also interesting to test whether *Cdon* expression is modified in cavefish embryos.

Fgf8 is expanded not only in the optic stalk but also in the telencephalon of Cdon morphants. Results obtained in chick, mouse and zebrafish highlight the role of the Hh and FGF pathways and a cross-regulation between the two pathways at distinct and precise times during telencephalon ventralization (Bertrand and Dahmane, 2006; Rash and Grove, 2011). Notably, *Cdon* is expressed in the dorsal telencephalon, opening the possibility that *Cdon* might has a similar role here.

Knock-down of *Cdon* in *ace* (*Fgf8*-/-) mutant embryos did not lead to mayor alterations in patterning of the nasal retina, as instead observed in wild type embryos, supporting that *Fgf8* acts downstream of Cdon. In contrast, other aspects of retinal patterning were not affected in CdonMO injected *ace* mutants suggesting that Cdon function is mediated by additional proteins. For example, other FGF might mediate Cdon function, since there are several examples in in which multiple Fgf ligands seems to control tissue development including several examples in sensory organs (Picker 2009; Martinez-Morales 2005; Zelarayan et al., 2007). Therefore, the analysis of the expression pattern of other FGF family members in Cdon morphants is an important issue for future research.

In this study, we did not analyze whether Wnt signaling components are altered in Cdon morphants. Ablation of canonical Wnt signaling during early eye development causes

coloboma and microphthalmia (Pinson et al., 2000; Stump et al., 2003). It has been proposed that the Wnt and Hedgehog pathways exhibit reciprocal inhibition in the Xenopus retina (Borday et al., 2012). As in fishes, adult amphibians produce retinal neurons from a pool of neural stem cells localized in the CMZ. The Wnt pathway restrains Hh activity in the CMZ by regulating the expression of transcriptional repressor Gli3. In turn, Hh signaling negatively regulates Wnt activity in the CMZ by transcriptional activation of Secreted Frizzled Related Protein 1 (*Sfrp1)*, an antagonist of Wnt signaling (Borday et al., 2012). *Cdon* expression localize to the CMZ at later stages of in zebrafish development. Furthermore, *Cdon* can be regulated in a positive manner by Gli3 (McGlinn et al., 2005). It is thus possible that *Cdon* could be an important factor in the proposed crosstalk between Hh and Wnt pathways. Recently, in *Drosophila* the secreted protein Shifted (Shf), a member of Wnt inhibitory factor 1 (WIF1) family and its vertebrate ortholog WIF1 have been shown to interact with the Hh co-receptor Ihog (Avanesov and Blair, 2012; Bilioni et al., 2012). Whereas vertebrate WIF1 blocks Wnt signaling (Hsieh et al., 1999; Hunter et al., 2004), *Drosophila* WIF1 (Shifted (Shf)) regulates only Hh distribution and spreading through the extracellular matrix (Glise et al., 2005; Gorfinkiel et al., 2005). This specificity is conferred by the WIF domain of those proteins (Sanchez-Hernandez et al., 2012). Notably, Ihog can increase the Wnt-inhibitory activity of vertebrate WIF1; this result raises the possibility of the existence of an interaction between WIF1 and Cdon or Boc (Avanesov and Blair, 2012), which would support our hypothesis.

At the moment there is little information about the precise regulation of *Cdon* or is homolog *Boc*. *Cdon* and *Boc* seem to be negatively regulated by Hh signaling in early vertebrate embryos (Tenzen et al., 2006; Bergeron et al., 2011) as also supported by the abnormal levels of *Cdon* expression found in the limb buds of *Gli3* mutant embryos (McGlinn et al., 2005). We have isolated a number of non-coding conserved sequences on the *Cdon* locus that could have enhancer activity. Only one sequence (D) showed a clear enhancer activity. To establish if the other sequences have enhancer activity we need to analyze the F1 stable transgenic embryos of the different isolated elements. However these conserved sequences could have other regulatory functions, e.g. silencers. Another possibility is that these sequences require to act in coordination with other genetic elements and therefore they need to be tested in more details to establish their possible function in *Cdon* regulation.

We isolated possible regulatory sequences based on their conservation among different species. However, there is additional information obtained with the analysis of histone marks in the zebrafish genome at four developmental stages (Gómez-Skarmeta lab, unpublished data). The integration of the different histone modification information can be used systematically to assign functional attributes to genomic regions (Hon et al., 2009). This

information points with more precision to the sequences that are potential regulatory elements at different stages of development. Using this information, we have detected that the first intron of zebrafish *Cdon* seems to harbor a cluster of conserved non-coding sequences, which are likely regulatory elements. Further studies of the elements inside the first intron of *Cdon* will be important to understand *Cdon* regulation.

The analysis of these elements may also give hints on the possible trans-acting factors. The transgenic lines carrying the different elements, can be analyzed through pharmacological treatments with inhibitors, injection of RNAs or MOs to dissect the regulatory control of *Cdon*.

Conclusion

We propose here that Cdon is able to act as a negative modulator of Hh signaling in vertebrates at least in the context of eye development. This proposed mechanism improves our understanding of the dynamic Hh signaling network and may have implications in other cellular and pathological contexts, included for instance in cancer (Stecca and Ruiz, 2010). If Cdon plays a similar role in other developmental contexts is still an open question.

CONCLUSIONS

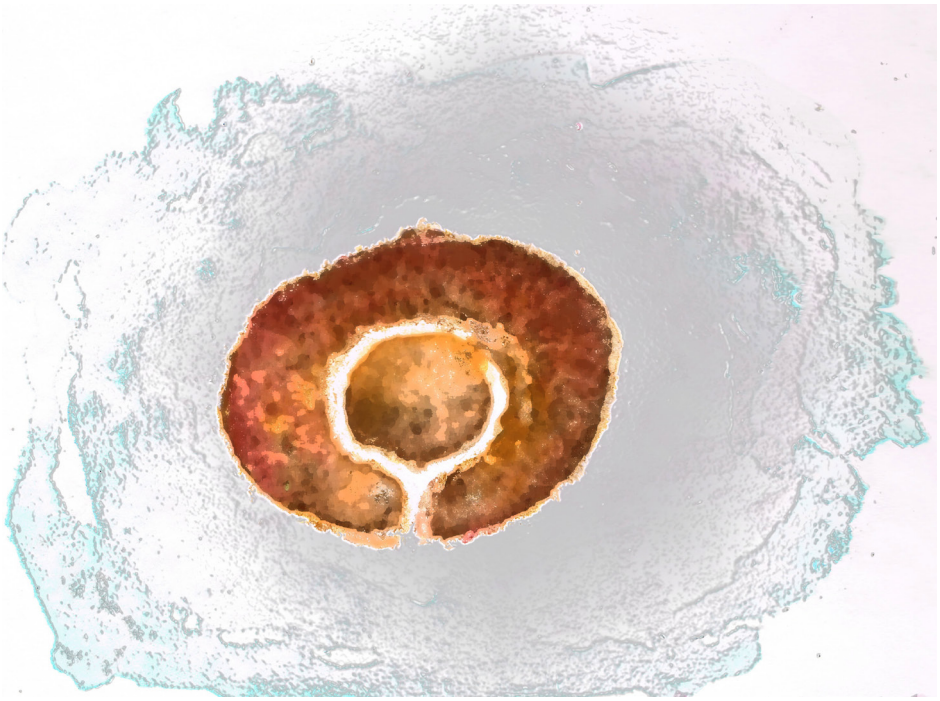

1. *Cdon* mRNA expression pattern in the developing eye is conserved from teleost to mammals.

2. Downregulation of *Cdon* causes ventral eye defects and expansion of the optic stalk domain in zebrafish.

3. *Cdon* expression in the presumptive retina prevents optic stalk expansion.

4. Hh signaling mediates the enlargement of the optic stalk observed in Cdon morphants.

5. Cdon interaction with Shh (but not with Ptc) is critical for the proper positioning of the boundary between the optic stalk and the neural retina.

6. Neuroepithelial cells that ectopically express Cdon accumulate Shh protein secreted from the floor plate.

7. Cdon acts as a negative modulator of Hh signaling in vertebrate eye formation.

8. FGF signaling mediates the enlargement of the optic stalk in Cdon morphants.

9. Cdon is required for proper naso-temporal patterning of the retina.

10. Fgf8 acts downstream of Cdon during naso-temporal patterning of the retina.

SUPPLEMENTARY MATERIAL

Sequences.

The information about *Cdon* exon and intro regions was obtained from the National Center for Biotechnology Information (NCBI). Reference Sequence: Chromosome: 18; NC_007129.5 (chr18:42,454,187-42,530,202).

Cdon sequences from Mouse, Human and Zebrafish (Q32MD9**,** Q4KMG0 and Q1L8D0 respectively**)** were obtained from Uniprot (Consortium, 2012). The locations and sequences of the fibronectin type-III 2 and 3 domains were obtained from UniProt (Consortium, 2012)

Alignment among human, mouse and zebrafish Cdon sequences.

The Cdon Danio Rerio sequence is not annotated in UniProt database, therefore zebrafish Cdon sequence of Danio Rerio was aligned with the fibronectin type-III 2 (purple) and 3 (green) of *Mus musculus* and *Homo sapiens* using Clustal Omega (Goujon et al., 2010; Sievers et al., 2011).

Q4KMG0 (CDON_HUMAN)

```
>sp|Q4KMG0|CDON_HUMAN Cell adhesion molecule-related/down-regulated by
oncogenes OS=Homo sapiens GN=CDON PE=1 SV=2
```

MHPDLGPLCTLLYVTLTILCSSVSSDLAPYFTSEPLSAVQKLGGPVVLHCSAQPVTTRIS

WLHNGKTLDGNLEHVKIHQGTLTILSLNSSLLGYYQCLANNSIGAIVSGPATVSVAVLGD

FGSSTKHVITAEEKSAGFIGCRVPESNPKAEVRYKIRGKWLEHSTENYLILPSGNLQILN

VSLEDKGSYKCAAYNPVTHQLKVEPIGRKLLVSRPSSDDVHILHPTHSQALAVLSRSPVT

LECVVSGVPAPQVYWLKDGQDIAPGSNWRRLYSHLATDSVDPADSGNYSCMAGNKSGDVK

YVTYMVNVLEHASISKGLQDQIVSLGATVHFTCDVHGNPAPNCTWFHNAQPIHPSARHLT

AGNGLKISGVTVEDVGMYQCVADNGIGFMHSTGRLEIENDGGFKPVIITAPVSAKVADGD

FVTLSCNASGLPVPVIRWYDSHGLITSHPSQVLRSKSRKSQLSRPEGLNLEPVYFVLSQA

GASSLHIQAVTQEHAGKYICEAANEHGTTQAEASLMVVPFETNTKAETVTLPDAAQNDDR

SKRDGSETGLLSSFPVKVHPSAVESAPEKNASGISVPDAPIILSPPQTHTPDTYNLVWRA

GKDGGLPINAYFVKYRKLDDGVGMLGSWHTVRVPGSENELHLAELEPSSLYEVLMVARSA

AGEGQPAMLTFRTSKEKTASSKNTQASSPPVGIPKYPVVSEAANNNFGVVLTDSSRHSGV

PEAPDRPTISTASETSVYVTWIPRANGGSPITAFKVEYKRMRTSNWLVAAEDIPPSKLSV

EVRSLEPGSTYKFRVIAINHYGESFRSSASRPYQVVGFPNRFSSRPITGPHIAYTEAVSD

TQIMLKWTYIPSSNNNTPIQGFYIYYRPTDSDNDSDYKRDVVEGSKQWHMIGHLQPETSY

DIKMQCFNEGGESEFSNVMICETKVKRVPGASEYPVKDLSTPPNSLGSGGNVGPATSPAR

SSDMLYLIVGCVLGVMVLILMVFIAMCLWKNRQQNTIQKYDPPGYLYQGSDMNGQMVDYT

TLSGASQINGNVHGGFLTNGGLSSGYSHLHHKVPNAVNGIVNGSLNGGLYSGHSNSLTRT

HVDFEHPHHLVNGGGMYTAVPQIDPLECVNCRNCRNNNRCFTKTNSTFSSSPPPVVPVVA

PYPQDGLEMKPLSHVKVPVCLTSAVPDCGQLPEESVKDNVEPVPTQRTCCQDIVNDVSSD

GSEDPAEFSRGQEGMINLRIPDHLQLAKSCVWEGDSCAHSETEINIVSWNALILPPVPEG

CAEKTMWSPPGIPLDSPTEVLQQPRET

Q32MD9 (CDON_MOUSE)

>sp|Q32MD9|CDON_MOUSE Cell adhesion molecule-related/down-regulated by oncogenes OS=Mus musculus GN=Cdon PE=1 SV=2

MHPDLGPLWTLLYVLVILCSSVSSDLAPYFISEPLSAVQKLGRPVVLHCSAKPVTARISW

LHNGKRLDRNTEQIKIHRGTLTILSLNPSLSGCYQCVANNSVGAVVSGPATVSAAALGDF

DSSTMHVITAEEKNTGFIGCRVPESNPKAEVRYKIRGKWLKHSTGNYIILPSGNLQVLNV

SSKDKGSYKCAAYNPVTSELKVEPTGRKLLVSRPSSNGFHILHPALSQALAVLPHSPVTL

ECVVSGVPASQVYWLKDGQDAVAGSNWRRLYSHLATASIDPADSGNYSCVVGNKSGDVKH

VTYMVNVLEHASISKGLHDQKVSLGATVHFTCDVHGNPAPNRTWFHNAQPIHPSSRHLTE

GNVLKITRVVMEDSGLYQCVADNGIGFMQSTGRLQIEQDSGWKPVIVTAPANIEVMDGDF

VTLSCNATGVPVPVIHWYGRHGLITSHPSQVLRSKPRKSHLFRPGDLDLEPVYLIMSQAG

SSSLSIQAVTLEHAGKYTCEATNKHGSTQSEAFLTVVPFETNTKAESVTPSEASQNDERD

PQDGSESSLLNLFPVKVHPSGVELPAERNASVPDAPNILSPPQTHMPDTYNLVWRAGRDG

GMPINAYFVKYRKLDDGSGAVGSWHTVRVPGSENELHLTELEPSSLYEVLMVARSAVGEG

QPAMLTFRTSKEKMASSKNTQASFPPVGVPKRPVTAEASNSNFGVVLTDSSRHSGVPEAP

DRPTISMASETSVYVTWIPRANGGSPITAFKVEYKRMRTSDWLVAAEDIPPSKLSVEVRS

LEPGSIYKFRVIAINHYGESFRSSASRPYQVAGFPNRFSNRPITGPHIAYTEAVSDTQIM

LKWTYVPSSNNNTPIQGFYIYYRPTDSDNDSDYKRDVVEGSKQWHTIGHLQPETSYDIKM

QCFNEGGESEFSNVMICETKVKRVPGASDYPVKELSTPPSSSGNAGNVGPATSPARSSDM

LYLIVGCVLGVMVLILMVFIALCLWKSRQQSTIQKYDPPGYLYQGSEINGQMVEYTTLSG

AARINGSVHGGFLSNGCSHLHHKGPSGVNGTLSGNINGGLYSAHTNSLTRACVEFEHPHH

LVNSGGVYTAVPQMDPLECINCRNCRNNNRCFTKTNSPLPVVPVVASYPQGGLEMKPLNA

MKVPVCPASTVPDHGQLPDDCVKDSVAPIPTQHTCCQDNISDINSDSTEDTAEFSRGDSS

GHSEAEDKVFSWNPLILSPVLEDCGEKTARSPPGPPLDGLSVVLQQAQET

Alignment among mouse and human Cdon FNIII 2 sequences with Cdon zebrafish sequence.

```
Cdon_Danio_rerio          MEDGGLRLLSAVLCVCHTLLLNCPTVLSFSFRAEPLSAILKQGSSVHLHCTTHPATARIS
FnIII_2_Mus_musculus      ------------------------------------------------------------
FnIII_2_Homo_sapiens      ------------------------------------------------------------

Cdon_Danio_rerio          WLFQGQPLDPSHHSGVELSQDSLSLSNLQPALTGSYQCSARSETGSIISRHARVTIADIE
FnIII_2_Mus_musculus      ------------------------------------------------------------
FnIII_2_Homo_sapiens      ------------------------------------------------------------

Cdon_Danio_rerio          EFAETHRRSFTVNKGDTAVIECPLPRSNPPALPRFRIRGKWLEQSTDEYLILPSGNLQIV
FnIII_2_Mus_musculus      ------------------------------------------------------------
FnIII_2_Homo_sapiens      ------------------------------------------------------------

Cdon_Danio_rerio          SVSSEHQGMYKCGAYNPLTRETRVEAHGTKLLVKDSESSSPVRIVYPITPRSLTVDQSGS
FnIII_2_Mus_musculus      ------------------------------------------------------------
FnIII_2_Homo_sapiens      ------------------------------------------------------------

Cdon_Danio_rerio          LTLECVVSGSLSSKVKWMKNGAELSLSSKRMLSHSNLVLNDIQPGDGGHYSCSVPTDRGA
FnIII_2_Mus_musculus      ------------------------------------------------------------
FnIII_2_Homo_sapiens      ------------------------------------------------------------

Cdon_Danio_rerio          VVSVNYTVNVLAHVSILRGLSDQAAVAGSSVRFTCAASGNPTPNITWLLNAAPLSSSPRL
FnIII_2_Mus_musculus      ------------------------------------------------------------
FnIII_2_Homo_sapiens      ------------------------------------------------------------
```

```
Cdon_Danio_rerio          KISGTSLLISSTTLQDQGIYQCMFDNGISSAQSTGRLSIQSEPQSSSISAVPVKTQPSVH
FnIII_2_Mus_musculus      ------------------------------------------------------------
FnIII_2_Homo_sapiens      ------------------------------------------------------------

Cdon_Danio_rerio          PIQSDEGDELFLSMGEAALGETVGPPTERIGDRPTPEAPIIISPPQTHKPNMYDLEWRAG
FnIII_2_Mus_musculus      ------------------------------------------------------------
FnIII_2_Homo_sapiens      ------------------------------------------------------------

Cdon_Danio_rerio          RDWGIAIIAYFVKYRKVDDMGNVVGSWHTVRVPGSEKSLPLSELEPSSLYEVLMVARSAA
FnIII_2_Mus_musculus      ------------------------------------------------------------
FnIII_2_Homo_sapiens      ------------------------------------------------------------

Cdon_Danio_rerio          GEGQPAMLTFRTGKERASPNKNPSKAPIVSLPEKTPEDKTTNTYYGVVIHDRVPEAPDRP
FnIII_2_Mus_musculus      ----------------------------------------------------PEAPDRP
FnIII_2_Homo_sapiens      ----------------------------------------------------PEAPDRP
                                                                     *******

Cdon_Danio_rerio          TISMATESSVYVTWIPRANGGSPITAFRVEYRKQGRNGDWIIAADNISPLKLSVEVRNLE
FnIII_2_Mus_musculus      TISMASETSVYVTWIPRANGGSPITAFKVEYKRM-RTSDWLVAAEDIPPSKLSVEVRSLE
FnIII_2_Homo_sapiens      TISMASETSVYVTWIPRANGGSPITAFKVEYKRM-RTSDWLVAAEDIPPSKLSVEVRSLE
                          *****:*:*********************:***::  *..**::**::* * *******.**

Cdon_Danio_rerio          PGSTYRFRVIAMNNYGESPASATSRPYQVSMSSSPVSNRPVTGPHISSTDAVSDTQILLR
FnIII_2_Mus_musculus      PGSIYKFRVIAINHYGESFRSSASRPY---------------------------------
FnIII_2_Homo_sapiens      PGSIYKFRVIAINHYGESFRSSASRPY---------------------------------
                          *** *:*****:*.****  *::****

Cdon_Danio_rerio          WTYTPSSNNNTPIQGFYIYYRPTDSDNDSDYKKDVVEGFKFWHMIGELQPETSYDIKMQC
FnIII_2_Mus_musculus      ------------------------------------------------------------
FnIII_2_Homo_sapiens      ------------------------------------------------------------
```

```
Cdon_Danio_rerio          YNDGGESEYSNVMICETKARQPPGVPSLRPITPPGFYPADTPSQPGGLLYLIVGCVLGVM
FnIII_2_Mus_musculus      ------------------------------------------------------------
FnIII_2_Homo_sapiens      ------------------------------------------------------------

Cdon_Danio_rerio          VLILLVFIVMCLWRNRQQNSMHKYDPPNYIYQSAEMNGHVLDYSALPGSSHVNGSVHTGC
FnIII_2_Mus_musculus      ------------------------------------------------------------
FnIII_2_Homo_sapiens      ------------------------------------------------------------

Cdon_Danio_rerio          GHTAPMMPQTCHHLHHKLPNGLALLNGSGGLYPAGHPHAHDTSLHQNNMEYEHPSPHHLH
FnIII_2_Mus_musculus      ------------------------------------------------------------
FnIII_2_Homo_sapiens      ------------------------------------------------------------

Cdon_Danio_rerio          NGGGIYTALPQNDSSDCMSCQNFCNNNRCYTKTNGTFSGGTLPLMHRVAARQPDGLEMMP
FnIII_2_Mus_musculus      ------------------------------------------------------------
FnIII_2_Homo_sapiens      ------------------------------------------------------------

Cdon_Danio_rerio          LNPILSRCHGRDSPQLNGCQDRDSVQQAEEGNVPPLSHNSPCLPVETKSSLEQQRGVQQV
FnIII_2_Mus_musculus      ------------------------------------------------------------
FnIII_2_Homo_sapiens      ------------------------------------------------------------

Cdon_Danio_rerio          QHEDSEGPVVCWERLGLDLDCKEKTAWISTGSLTGDLIQPTVQEI
FnIII_2_Mus_musculus      ---------------------------------------------
FnIII_2_Homo_sapiens      ---------------------------------------------
```

Alignment among mouse and human Cdon FNIII 3 sequences with Cdon zebrafish sequence.

```
Cdon_Danio_rerio          MEDGGLRLLSAVLCVCHTLLLNCPTVLSFSFRAEPLSAILKQGSSVHLHCTTHPATARIS
FnIII_3_Mus_musculus      ------------------------------------------------------------
FnIII_3_Homo_sapiens      ------------------------------------------------------------

Cdon_Danio_rerio          WLFQGQPLDPSHHSGVELSQDSLSLSNLQPALTGSYQCSARSETGSIISRHARVTIADIE
FnIII_3_Mus_musculus      ------------------------------------------------------------
FnIII_3_Homo_sapiens      ------------------------------------------------------------

Cdon_Danio_rerio          EFAETHRRSFTVNKGDTAVIECPLPRSNPPALPRFRIRGKWLEQSTDEYLILPSGNLQIV
FnIII_3_Mus_musculus      ------------------------------------------------------------
FnIII_3_Homo_sapiens      ------------------------------------------------------------

Cdon_Danio_rerio          SVSSEHQGMYKCGAYNPLTRETRVEAHGTKLLVKDSESSSPVRIVYPITPRSLTVDQSGS
FnIII_3_Mus_musculus      ------------------------------------------------------------
FnIII_3_Homo_sapiens      ------------------------------------------------------------

Cdon_Danio_rerio          LTLECVVSGSLSSKVKWMKNGAELSLSSKRMLSHSNLVLNDIQPGDGGHYSCSVPTDRGA
FnIII_3_Mus_musculus      ------------------------------------------------------------
FnIII_3_Homo_sapiens      ------------------------------------------------------------

Cdon_Danio_rerio          VVSVNYTVNVLAHVSILRGLSDQAAVAGSSVRFTCAASGNPTPNITWLLNAAPLSSSPRL
FnIII_3_Mus_musculus      ------------------------------------------------------------
FnIII_3_Homo_sapiens      ------------------------------------------------------------
```

```
Cdon_Danio_rerio          KISGTSLLISSTTLQDQGIYQCMFDNGISSAQSTGRLSIQSEPQSSSISAVPVKTQPSVH
FnIII_3_Mus_musculus      ------------------------------------------------------------
FnIII_3_Homo_sapiens      ------------------------------------------------------------

Cdon_Danio_rerio          PIQSDEGDELFLSMGEAALGETVGPPTERIGDRPTPEAPIIISPPQTHKPNMYDLEWRAG
FnIII_3_Mus_musculus      ------------------------------------------------------------
FnIII_3_Homo_sapiens      ------------------------------------------------------------

Cdon_Danio_rerio          RDWGIAIIAYFVKYRKVDDMGNVVGSWHTVRVPGSEKSLPLSELEPSSLYEVLMVARSAA
FnIII_3_Mus_musculus      ------------------------------------------------------------
FnIII_3_Homo_sapiens      ------------------------------------------------------------

Cdon_Danio_rerio          GEGQPAMLTFRTGKERASPNKNPSKAPIVSLPEKTPEDKTTNTYYGVVIHDRVPEAPDRP
FnIII_3_Mus_musculus      ------------------------------------------------------------
FnIII_3_Homo_sapiens      ------------------------------------------------------------

Cdon_Danio_rerio          TISMATESSVYVTWIPRANGGSPITAFRVEYRKQGRNGDWIIAADNISPLKLSVEVRNLE
FnIII_3_Mus_musculus      ------------------------------------------------------------
FnIII_3_Homo_sapiens      ------------------------------------------------------------

Cdon_Danio_rerio          PGSTYRFRVIAMNNYGESPASATSRPYQVSMSSSPVSNRPVTGPHISSTDAVSDTQILLR
FnIII_3_Mus_musculus      ----------------------------------------PITGPHIAYTEAVSDTQIMLK
FnIII_3_Homo_sapiens      ----------------------------------------PITGPHIAYTEAVSDTQIMLK
                                                                  *:*****: *:*******:*:

Cdon_Danio_rerio          WTYTPSSNNNTPIQGFYIYYRPTDSDNDSDYKKDVVEGFKFWHMIGELQPETSYDIKMQC
FnIII_3_Mus_musculus      WTYVPSSNNNTPIQGFYIYYRPTDSDNDSDYKRDVVEGSKQWHTIGHLQPETSYDIKMQC
FnIII_3_Homo_sapiens      WTYIPSSNNNTPIQGFYIYYRPTDSDNDSDYKRDVVEGSKQWHMIGHLQPETSYDIKMQC
                          *** ****************************:***** * ** **.*************
```

```
Cdon_Danio_rerio          YNDGGESEYSNVMICETKARQPPGVPSLRPITPPGFYPADTPSQPGGLLYLIVGCVLGVM
FnIII_3_Mus_musculus      FNEGGESEFSNVMICET----------------------------------------
FnIII_3_Homo_sapiens      FNEGGESEFSNVMICET----------------------------------------
                          :*:*****:********

Cdon_Danio_rerio          VLILLVFIVMCLWRNRQQNSMHKYDPPNYIYQSAEMNGHVLDYSALPGSSHVNGSVHTGC
FnIII_3_Mus_musculus      ------------------------------------------------------------
FnIII_3_Homo_sapiens      ------------------------------------------------------------

Cdon_Danio_rerio          GHTAPMMPQTCHHLHHKLPNGLALLNGSGGLYPAGHPHAHDTSLHQNNMEYEHPSPHHLH
FnIII_3_Mus_musculus      ------------------------------------------------------------
FnIII_3_Homo_sapiens      ------------------------------------------------------------

Cdon_Danio_rerio          NGGGIYTALPQNDSSDCMSCQNFCNNNRCYTKTNGTFSGGTLPLMHRVAARQPDGLEMMP
FnIII_3_Mus_musculus      ------------------------------------------------------------
FnIII_3_Homo_sapiens      ------------------------------------------------------------

Cdon_Danio_rerio          LNPILSRCHGRDSPQLNGCQDRDSVQQAEEGNVPPLSHNSPCLPVETKSSLEQQRGVQQV
FnIII_3_Mus_musculus      ------------------------------------------------------------
FnIII_3_Homo_sapiens      ------------------------------------------------------------

Cdon_Danio_rerio          QHEDSEGPVVCWERLGLDLDCKEKTAWISTGSLTGDLIQPTVQEI
FnIII_3_Mus_musculus      ---------------------------------------------
FnIII_3_Homo_sapiens      ---------------------------------------------
```

Consensus symbols

***** (asterisk) indicates positions which have a single, fully conserved residue.

: (colon) indicates conservation between groups of strongly similar properties - scoring > 0.5 in the Gonnet PAM 250 matrix.

. (period) indicates conservation between groups of weakly similar properties - scoring =< 0.5 in the Gonnet PAM 250 matrix.

Zebrafish Cdon fibronectin type-III 2 and 3 sequences obtained from the alignment with mouse and human Cdon fibronectin type-III 2 and 3 sequences.

Q1L8D0 (Q1L8D0_DANRE)

>tr|Q1L8D0|Q1L8D0_DANRE Cell adhesion molecule-related/down-regulated by oncogenes OS=Danio rerio GN=cdon PE=2 SV=2

MEDGGLRLLSAVLCVCHTLLLNCPTVLSFSFRAEPLSAILKQGSSVHLHCTTHPATARIS

WLFQGQPLDPSHHSGVELSQDSLSLSNLQPALTGSYQCSARSETGSIISRHARVTIADIE

EFAETHRRSFTVNKGDTAVIECPLPRSNPPALPRFRIRGKWLEQSTDEYLILPSGNLQIV

SVSSEHQGMYKCGAYNPLTRETRVEAHGTKLLVKDSESSSPVRIVYPITPRSLTVDQSGS

LTLECVVSGSLSSKVKWMKNGAELSLSSKRMLSHSNLVLNDIQPGDGGHYSCSVPTDRGA

VVSVNYTVNVLAHVSILRGLSDQAAVAGSSVRFTCAASGNPTPNITWLLNAAPLSSSPRL

KISGTSLLISSTTLQDQGIYQCMFDNGISSAQSTGRLSIQSEPQSSSISAVPVKTQPSVH

PIQSDEGDELFLSMGEAALGETVGPPTERIGDRPTPEAPIIISPPQTHKPNMYDLEWRAG

RDWGIAIIAYFVKYRKVDDMGNVVGSWHTVRVPGSEKSLPLSELEPSSLYEVLMVARSAA

GEGQPAMLTFRTGKERASPNKNPSKAPIVSLPEKTPEDKTTNTYYGVVIHDRVPEAPDRP

TISMATESSVYVTWIPRANGGSPITAFRVEYRKQGRNGDWIIAADNISPLKLSVEVRNLE

PGSTYRFRVIAMNNYGESPASATSRPYQVSMSSSPVSNRPVTGPHISSTDAVSDTQILLR

WTYTPSSNNNTPIQGFYIYYRPTDSDNDSDYKKDVVEGFKFWHMIGELQPETSYDIKMQC

YNDGGESEYSNVMICETKARQPPGVPSLRPITPPGFYPADTPSQPGGLLYLIVGCVLGVM

VLILLVFIVMCLWRNRQQNSMHKYDPPNYIYQSAEMNGHVLDYSALPGSSHVNGSVHTGC

GHTAPMMPQTCHHLHHKLPNGLALLNGSGGLYPAGHPHAHDTSLHQNNMEYEHPSPHHLH

NGGGIYTALPQNDSSDCMSCQNFCNNNRCYTKTNGTFSGGTLPLMHRVAARQPDGLEMMP

LNPILSRCHGRDSPQLNGCQDRDSVQQAEEGNVPPLSHNSPCLPVETKSSLEQQRGVQQV

QHEDSEGPVVCWERLGLDLDCKEKTAWISTGSLTGDLIQPTVQEI

The homolog residues important for Cdon function in Hh signaling (in the Ptch binding domain) are highlighted in blue (Bae et al., 2011). The homolog residues important for Shh binding are highlighted in red (McLellan et al., 2008).

Enhancer Detection.

For the enhancer analysis alignments we used the following sequences obtained from UCSC Genome Browser website. The sequences A-I were amplified by PCR from zebrafish DNA using the primers listed in table IX.

Danio rerio, chr18:42,238,809-42,745,581

Tetraodon nigroviridis; chr16:5,282,323-5,169,430

Takifugu rubripes; chr11:8,230,678- 8,132,445

Oryzias latipes; chr13:4,271,233-4,579,683

Gasterosteus aculeatus; chr1:15,349,426-15,539,451

Table IX. List of primers to amplify the possible *Cdon* regulatory elements.

Enh	Primer F	Primer R	start	end
A	TAGAAAAACCAACTCTATAGA-CACC	GGAGTCAAAGACATTATAGCAT-TAC	42419960	42420318
B	GAGTCTTTTTCGCCGACTGGGG	CTTGTGTTTCGGTGGAGCAGCT	42424126	42424445
C	AGCCAACATTTGGAAAAGAC	TGAGAAGGCTGTGAGTGTGA	42499655	42500039
D	TCTACAGAGTGTAGGTGACCTT	GTGTAGCATGCATCGTAGATGT	42516402	42517273
E	TGGCCATGTATTGATTCAAA	CATCGGTTATCCAGTACAGA	42522330	42522663
F	GTCCTGGTAATAGGAAGTGC-GGGGC	ACGACCTGATTGAGGCCCGA	42548364	42548712
G	CACTTCTGGTTTAGTTTCAGTT	ATCTATCCTGCCTTGTATCAAC	42567249	42568543
H	TTTTAAAGTGTGTGAGAGAG-TATGC	CATTTTTCTGTCATGATCCG	42574828	42575312
I	AAGAGTAGAGACATATGGAACG	TTCTGTGCTATAAATTACCC	42586581	42586840

The histone profile data of H3K27AC of zebrafish *Cdon* was kindly provided by Dr. Jose Luis Gómez-Skarmeta (unpublished data).

REFERENCES

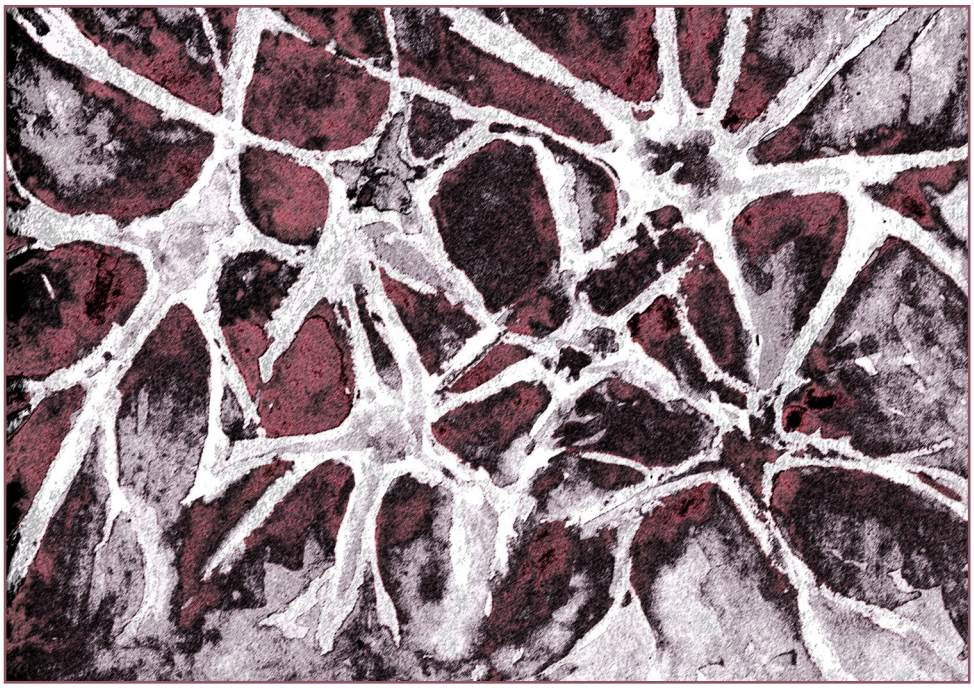

Adelmann, H. (1929) 'Experimental studies on the development of the eye. II. The eye-forming potencies of the median portions of the urodelan neural plate (Triton teniatus and Amblystoma punctatum) ', *Journal of Experimental Zoology* 54(2): 26.

Adler, R. and Belecky-Adams, T. L. (2002) 'The role of bone morphogenetic proteins in the differentiation of the ventral optic cup', *Development* 129(13): 3161-71.

Alcedo, J., Ayzenzon, M., Von Ohlen, T., Noll, M. and Hooper, J. E. (1996) 'The Drosophila smoothened gene encodes a seven-pass membrane protein, a putative receptor for the hedgehog signal', *Cell* 86(2): 221-32.

Allen, B. L., Song, J. Y., Izzi, L., Althaus, I. W., Kang, J. S., Charron, F., Krauss, R. S. and McMahon, A. P. (2011) 'Overlapping roles and collective requirement for the coreceptors GAS1, CDO, and BOC in SHH pathway function', *Dev Cell* 20(6): 775-87.

Allen, B. L., Tenzen, T. and McMahon, A. P. (2007) 'The Hedgehog-binding proteins Gas1 and Cdo cooperate to positively regulate Shh signaling during mouse development', *Genes Dev* 21(10): 1244-57.

Amato, M. A., Boy, S. and Perron, M. (2004) 'Hedgehog signaling in vertebrate eye development: a growing puzzle', *Cell Mol Life Sci* 61(7-8): 899-910.

Amores, A., Force, A., Yan, Y. L., Joly, L., Amemiya, C., Fritz, A., Ho, R. K., Langeland, J., Prince, V., Wang, Y. L. et al. (1998) 'Zebrafish hox clusters and vertebrate genome evolution', *Science* 282(5394): 1711-4.

Avanesov, A. and Blair, S. S. (2012) 'The Drosophila WIF1 homolog Shifted maintains glypican-independent Hedgehog signaling and interacts with the Hedgehog co-receptors Ihog and Boi', *Development*.

Ayers, K. L., Gallet, A., Staccini-Lavenant, L. and Therond, P. P. (2010) 'The long-range activity of Hedgehog is regulated in the apical extracellular space by the glypican Dally and the hydrolase Notum', *Dev Cell* 18(4): 605-20.

Ayers, K. L., Mteirek, R., Cervantes, A., Lavenant-Staccini, L., Therond, P. P. and Gallet, A. (2012) 'Dally and Notum regulate the switch between low and high level Hedgehog pathway signalling', *Development* 139(17): 3168-79.

Bae, G. U., Domene, S., Roessler, E., Schachter, K., Kang, J. S., Muenke, M. and Krauss, R. S. (2011) 'Mutations in CDON, Encoding a Hedgehog Receptor, Result in Holoprosencephaly and Defective Interactions with Other Hedgehog Receptors', *Am J Hum Genet*.

Beachy, P. A., Cooper, M. K., Young, K. E., von Kessler, D. P., Park, W. J., Hall, T. M., Leahy, D. J. and Porter, J. A. (1997) 'Multiple roles of cholesterol in hedgehog protein biogenesis and signaling', *Cold Spring Harb Symp Quant Biol* 62: 191-204.

Bergeron, S. A., Tyurina, O. V., Miller, E., Bagas, A. and Karlstrom, R. O. (2011) 'Brother of cdo (umleitung) is cell-autonomously required for Hedgehog-mediated ventral CNS patterning in the zebrafish', *Development* 138(1): 75-85.

Bertrand, N. and Dahmane, N. (2006) 'Sonic hedgehog signaling in forebrain development and its interactions with pathways that modify its effects', *Trends Cell Biol* 16(11): 597-605.

Bessa, J., Tena, J. J., de la Calle-Mustienes, E., Fernandez-Minan, A., Naranjo, S., Fernandez, A., Montoliu, L., Akalin, A., Lenhard, B., Casares, F. et al. (2009) 'Zebrafish enhancer detection (ZED) vector: a new tool to facilitate transgenesis and the functional analysis of cis-regulatory regions in zebrafish', *Dev Dyn* 238(9): 2409-17.

Bilioni, A., Sanchez-Hernandez, D., Callejo, A., Gradilla, A. C., Ibanez, C., Mollica, E., Carmen Rodriguez-Navas, M., Simon, E. and Guerrero, I. (2012) 'Balancing hedgehog, a retention and release equilibrium given by Dally, Ihog, Boi and shifted/dWif', Dev Biol.

Borday, C., Cabochette, P., Parain, K., Mazurier, N., Janssens, S., Tran, H. T., Sekkali, B., Bronchain, O., Vleminckx, K., Locker, M. et al. (2012) 'Antagonistic cross-regulation between Wnt and Hedgehog signalling pathways controls post-embryonic retinal proliferation', *Development* 139(19): 3499-509.

Bornemann, D. J., Duncan, J. E., Staatz, W., Selleck, S. and Warrior, R. (2004) 'Abrogation of heparan sulfate synthesis in Drosophila disrupts the Wingless, Hedgehog and Decapentaplegic signaling pathways', *Development* 131(9): 1927-38.

Brewster, R., Mullor, J. L. and Ruiz i Altaba, A. (2000) 'Gli2 functions in FGF signaling during antero-posterior patterning', *Development* 127(20): 4395-405.

Brown, J. D., Dutta, S., Bharti, K., Bonner, R. F., Munson, P. J., Dawid, I. B., Akhtar, A. L., Onojafe, I. F., Alur, R. P., Gross, J. M. et al. (2009) 'Expression profiling during ocular development identifies 2 Nlz genes with a critical role in optic fissure closure', *Proc Natl Acad Sci U S A* 106(5): 1462-7.

Burke, R., Nellen, D., Bellotto, M., Hafen, E., Senti, K. A., Dickson, B. J. and Basler, K. (1999) 'Dispatched, a novel sterol-sensing domain protein dedicated to the release of cholesterol-modified hedgehog from signaling cells', *Cell* 99(7): 803-15.

Cadigan, K. M. and Peifer, M. (2009) 'Wnt signaling from development to disease: insights from model systems', *Cold Spring Harb Perspect Biol* 1(2): a002881.

Callejo, A., Bilioni, A., Mollica, E., Gorfinkiel, N., Andres, G., Ibanez, C., Torroja, C., Doglio, L., Sierra, J. and Guerrero, I. (2011) 'Dispatched mediates Hedgehog basolateral release to form the long-range morphogenetic gradient in the Drosophila wing disk epithelium', *Proc Natl Acad Sci U S A* 108(31): 12591-8.

Camp, D., Currie, K., Labbe, A., van Meyel, D. J. and Charron, F. (2010) 'Ihog and Boi are essential for Hedgehog signaling in Drosophila', *Neural Dev* 5: 28.

Capurro, M. I., Xu, P., Shi, W., Li, F., Jia, A. and Filmus, J. (2008) 'Glypican-3 inhibits Hedgehog signaling during development by competing with patched for Hedgehog binding', *Dev Cell* 14(5): 700-11.

Cavodeassi, F., Carreira-Barbosa, F., Young, R. M., Concha, M. L., Allende, M. L., Houart, C., Tada, M. and Wilson, S. W. (2005) 'Early stages of zebrafish eye formation require the coordinated activity of Wnt11, Fz5, and the Wnt/beta-catenin pathway', *Neuron* 47(1): 43-56.

Cohen, M. M., Jr. (2010) 'Hedgehog signaling update', *Am J Med Genet A* 152A(8): 1875-914.

Cole, F. and Krauss, R. S. (2003) 'Microform holoprosencephaly in mice that lack the Ig superfamily member Cdon', *Curr Biol* 13(5): 411-5.

Consortium, T. U. (2012) 'Reorganizing the protein space at the Universal Protein Resource (UniProt)', *Nucleic Acids Res* 40(Database issue): D71-5.

Cooper, M. S., Szeto, D. P., Sommers-Herivel, G., Topczewski, J., Solnica-Krezel, L., Kang, H. C., Johnson, I. and Kimelman, D. (2005) 'Visualizing morphogenesis in transgenic zebrafish embryos using BODIPY TR methyl ester dye as a vital counterstain for GFP', *Dev Dyn* 232(2): 359-68.

Cornesse, Y., Pieler, T. and Hollemann, T. (2005) 'Olfactory and lens placode formation is controlled by the hedgehog-interacting protein (Xhip) in Xenopus', *Dev Biol* 277(2): 296-315.

Creanga, A., Glenn, T. D., Mann, R. K., Saunders, A. M., Talbot, W. S. and Beachy, P. A. (2012) 'Scube/You activity mediates release of dually lipid-modified Hedgehog signal in soluble form', *Genes Dev* 26(12): 1312-25.

Chalasani, K. and Brewster, R. M. (2011) 'N-cadherin-mediated cell adhesion restricts cell proliferation in the dorsal neural tube', *Mol Biol Cell* 22(9): 1505-15.

Chang, D. T., Lopez, A., von Kessler, D. P., Chiang, C., Simandl, B. K., Zhao, R., Seldin, M. F., Fallon, J. F. and Beachy, P. A. (1994) 'Products, genetic linkage and limb patterning activity of a murine hedgehog gene', *Development* 120(11): 3339-53.

Chang, L., Blain, D., Bertuzzi, S. and Brooks, B. P. (2006) 'Uveal coloboma: clinical and basic science update', *Curr Opin Ophthalmol* 17(5): 447-70.

Charron, F., Stein, E., Jeong, J., McMahon, A. P. and Tessier-Lavigne, M. (2003) 'The morphogen sonic hedgehog is an axonal chemoattractant that collaborates with netrin-1 in midline axon guidance', *Cell* 113(1): 11-23.

Chen, S., Lewis, B., Moran, A. and Xie, T. (2012a) 'Cadherin-mediated cell adhesion is critical for the closing of the mouse optic fissure', *PLoS One* 7(12): e51705.

Chen, S., Li, H., Zueckert-Gaudenz, K., Paulson, A., Guo, F., Trimble, R., Peak, A., Seidel, C., Deng, C., Furuta, Y. et al. (2012b) 'Defective FGF signaling causes coloboma formation and disrupts retinal neurogenesis', *Cell Res*.

Chen, Y. and Struhl, G. (1996) 'Dual roles for patched in sequestering and transducing Hedgehog', *Cell* 87(3): 553-63.

Chiang, C., Litingtung, Y., Lee, E., Young, K. E., Corden, J. L., Westphal, H. and Beachy, P. A. (1996) 'Cyclopia and defec-

tive axial patterning in mice lacking Sonic hedgehog gene function', *Nature* 383(6599): 407-13.

Christ, A., Christa, A., Kur, E., Lioubinski, O., Bachmann, S., Willnow, T. E. and Hammes, A. (2012) 'LRP2 is an auxiliary SHH receptor required to condition the forebrain ventral midline for inductive signals', *Dev Cell* 22(2): 268-78.

Chuang, J. C. and Raymond, P. A. (2002) 'Embryonic origin of the eyes in teleost fish', *Bioessays* 24(6): 519-29.

Chuang, P. T. and McMahon, A. P. (1999) 'Vertebrate Hedgehog signalling modulated by induction of a Hedgehog-binding protein', *Nature* 397(6720): 617-21.

Dailey, L., Ambrosetti, D., Mansukhani, A. and Basilico, C. (2005) 'Mechanisms underlying differential responses to FGF signaling', *Cytokine Growth Factor Rev* 16(2): 233-47.

Dakubo, G. D., Wang, Y. P., Mazerolle, C., Campsall, K., McMahon, A. P. and Wallace, V. A. (2003) 'Retinal ganglion cell-derived sonic hedgehog signaling is required for optic disc and stalk neuroepithelial cell development', *Development* 130(13): 2967-80.

Denef, N., Neubuser, D., Perez, L. and Cohen, S. M. (2000) 'Hedgehog induces opposite changes in turnover and subcellular localization of patched and smoothened', *Cell* 102(4): 521-31.

Dessaud, E., Yang, L. L., Hill, K., Cox, B., Ulloa, F., Ribeiro, A., Mynett, A., Novitch, B. G. and Briscoe, J. (2007) 'Interpretation of the sonic hedgehog morphogen gradient by a temporal adaptation mechanism', *Nature* 450(7170): 717-20.

Dierker, T., Dreier, R., Petersen, A., Bordych, C. and Grobe, K. (2009) 'Heparan sulfate-modulated, metalloprotease-mediated sonic hedgehog release from producing cells', *J Biol Chem* 284(12): 8013-22.

Draper, B. W., Morcos, P. A. and Kimmel, C. B. (2001) 'Inhibition of zebrafish fgf8 pre-mRNA splicing with morpholino oligos: a quantifiable method for gene knockdown', *Genesis* 30(3): 154-6.

Echelard, Y., Epstein, D. J., St-Jacques, B., Shen, L., Mohler, J., McMahon, J. A. and McMahon, A. P. (1993) 'Sonic hedgehog, a member of a family of putative signaling molecules, is implicated in the regulation of CNS polarity', *Cell* 75(7): 1417-30.

Eiraku, M., Takata, N., Ishibashi, H., Kawada, M., Sakakura, E., Okuda, S., Sekiguchi, K., Adachi, T. and Sasai, Y. (2011) 'Self-organizing optic-cup morphogenesis in three-dimensional culture', *Nature* 472(7341): 51-6.

Ekker, S. C., Ungar, A. R., Greenstein, P., von Kessler, D. P., Porter, J. A., Moon, R. T. and Beachy, P. A. (1995) 'Patterning activities of vertebrate hedgehog proteins in the developing eye and brain', *Curr Biol* 5(8): 944-55.

Erskine, L. and Herrera, E. (2007) 'The retinal ganglion cell axon's journey: insights into molecular mechanisms of axon guidance', *Dev Biol* 308(1): 1-14.

Fabre, P. J., Shimogori, T. and Charron, F. (2010) 'Segregation of ipsilateral retinal ganglion cell axons at the optic chiasm requires the Shh receptor Boc', *J Neurosci* 30(1): 266-75.

Fietz, M. J., Concordet, J. P., Barbosa, R., Johnson, R., Krauss, S., McMahon, A. P., Tabin, C. and Ingham, P. W. (1994) 'The hedgehog gene family in Drosophila and vertebrate development', *Dev Suppl*: 43-51.

Fuse, N., Maiti, T., Wang, B., Porter, J. A., Hall, T. M., Leahy, D. J. and Beachy, P. A. (1999) 'Sonic hedgehog protein signals not as a hydrolytic enzyme but as an apparent ligand for patched', *Proc Natl Acad Sci U S A* 96(20): 10992-9.

Glise, B., Miller, C. A., Crozatier, M., Halbisen, M. A., Wise, S., Olson, D. J., Vincent, A. and Blair, S. S. (2005) 'Shifted, the Drosophila ortholog of Wnt inhibitory factor-1, controls the distribution and movement of Hedgehog', Dev Cell 8(2): 255-66.

Goetz, S. C. and Anderson, K. V. (2010) 'The primary cilium: a signalling centre during vertebrate development', *Nat Rev Genet* 11(5): 331-44.

Gongal, P. A., French, C. R. and Waskiewicz, A. J. (2011) 'Aberrant forebrain signaling during early development underlies the generation of holoprosencephaly and coloboma', *Biochim Biophys Acta* 1812(3): 390-401.

Goodrich, L. V., Johnson, R. L., Milenkovic, L., McMahon, J. A. and Scott, M. P. (1996) 'Conservation of the hedgehog/patched signaling pathway from flies to mice: induction of a mouse patched gene by Hedgehog', *Genes Dev* 10(3): 301-12.

Gorfinkiel, N., Sierra, J., Callejo, A., Ibanez, C. and Guerrero, I. (2005) 'The Drosophila ortholog of the human Wnt inhibitor factor Shifted controls the diffusion of lipid-modified Hedgehog', Dev Cell 8(2): 241-53.

Goujon, M., McWilliam, H., Li, W., Valentin, F., Squizzato, S., Paern, J. and Lopez, R. (2010) 'A new bioinformatics analysis tools framework at EMBL-EBI', *Nucleic Acids Res* 38(Web Server issue): W695-9.

Graw, J. (2010) 'Eye development', *Curr Top Dev Biol* 90: 343-86.

Grisaru, S., Cano-Gauci, D., Tee, J., Filmus, J. and Rosenblum, N. D. (2001) 'Glypican-3 modulates BMP- and FGF-mediated effects during renal branching morphogenesis', *Dev Biol* 231(1): 31-46.

Guillemot, F. and Cepko, C. L. (1992) 'Retinal fate and ganglion cell differentiation are potentiated by acidic FGF in an in vitro assay of early retinal development', *Development* 114(3): 743-54.

Haas, P. and Gilmour, D. (2006) 'Chemokine signaling mediates self-organizing tissue migration in the zebrafish lateral line', *Dev Cell* 10(5): 673-80.

Hamburger, V. and Hamilton, H. L. (1992) 'A series of normal stages in the development of the chick embryo. 1951', *Dev Dyn* 195(4): 231-72.

Hartman, T. R., Zinshteyn, D., Schofield, H. K., Nicolas, E., Okada, A. and O'Reilly, A. M. (2010) 'Drosophila Boi limits Hedgehog levels to suppress follicle stem cell proliferation', *J Cell Biol* 191(5): 943-52.

Heisenberg, C. P., Brennan, C. and Wilson, S. W. (1999) 'Zebrafish aussicht mutant embryos exhibit widespread overexpression of ace (fgf8) and coincident defects in CNS development', *Development* 126(10): 2129-40.

Hoffman, T. L., Javier, A. L., Campeau, S. A., Knight, R. D. and Schilling, T. F. (2007) 'Tfap2 transcription factors in zebrafish neural crest development and ectodermal evolution', *J Exp Zool B Mol Dev Evol* 308(5): 679-91.

Hollway, G. E., Maule, J., Gautier, P., Evans, T. M., Keenan, D. G., Lohs, C., Fischer, D., Wicking, C. and Currie, P. D. (2006) 'Scube2 mediates Hedgehog signalling in the zebrafish embryo', *Dev Biol* 294(1): 104-18.

Hon, G., Wang, W. and Ren, B. (2009) 'Discovery and annotation of functional chromatin signatures in the human genome', *PLoS Comput Biol* 5(11): e1000566.

Hong, M. and Krauss, R. S. (2012) 'Cdon mutation and fetal ethanol exposure synergize to produce midline signaling defects and holoprosencephaly spectrum disorders in mice', *PLoS Genet* 8(10): e1002999.

Hooper, J. E. and Scott, M. P. (1989) 'The Drosophila patched gene encodes a putative membrane protein required for segmental patterning', *Cell* 59(4): 751-65.

Hsieh, J. C., Kodjabachian, L., Rebbert, M. L., Rattner, A., Smallwood, P. M., Samos, C. H., Nusse, R., Dawid, I. B. and Nathans, J. (1999) 'A new secreted protein that binds to Wnt proteins and inhibits their activities', Nature 398(6726): 431-6.

Huang, P., Xiong, F., Megason, S. G. and Schier, A. F. (2012) 'Attenuation of Notch and Hedgehog signaling is required for fate specification in the spinal cord', *PLoS Genet* 8(6): e1002762.

Huh, S., Hatini, V., Marcus, R. C., Li, S. C. and Lai, E. (1999) 'Dorsal-ventral patterning defects in the eye of BF-1-deficient mice associated with a restricted loss of shh expression', *Dev Biol* 211(1): 53-63.

Hunter, D. D., Zhang, M., Ferguson, J. W., Koch, M. and Brunken, W. J. (2004) 'The extracellular matrix component WIF-1 is expressed during, and can modulate, retinal development', Mol Cell Neurosci 27(4): 477-88.

Hyer, J., Mima, T. and Mikawa, T. (1998) 'FGF1 patterns the optic vesicle by directing the placement of the neural retina domain', *Development* 125(5): 869-77.

Ingham, P. W. (2012) 'Hedgehog signaling', Cold Spring Harb Perspect Biol 4(6).

Ingham, P. W. and McMahon, A. P. (2001) 'Hedgehog signaling in animal development: paradigms and principles', *Genes Dev* 15(23): 3059-87.

Ingham, P. W., Nakano, Y. and Seger, C. (2011) 'Mechanisms and functions of Hedgehog signalling across the metazoa', *Nat Rev Genet* 12(6): 393-406.

Ingham, P. W., Taylor, A. M. and Nakano, Y. (1991) 'Role of the Drosophila patched gene in positional signalling', *Nature* 353(6340): 184-7.

Izzi, L., Levesque, M., Morin, S., Laniel, D., Wilkes, B. C., Mille, F., Krauss, R. S., McMahon, A. P., Allen, B. L. and Charron, F. (2011) 'Boc and Gas1 each form distinct Shh receptor complexes with Ptch1 and are required for Shh-mediated cell proliferation', *Dev Cell* 20(6): 788-801.

Jaillon, O., Aury, J. M., Brunet, F., Petit, J. L., Stange-Thomann, N., Mauceli, E., Bouneau, L., Fischer, C., Ozouf-Costaz, C., Bernot, A. et al. (2004) 'Genome duplication in the teleost fish Tetraodon nigroviridis reveals the early vertebrate protokaryotype', *Nature* 431(7011): 946-57.

Kamiguchi, H. and Lemmon, V. (2000) 'IgCAMs: bidirectional signals underlying neurite growth', *Curr Opin Cell Biol* 12(5): 598-605.

Kang, J. S., Bae, G. U., Yi, M. J., Yang, Y. J., Oh, J. E., Takaesu, G., Zhou, Y. T., Low, B. C. and Krauss, R. S. (2008) 'A Cdo-Bnip-2-Cdc42 signaling pathway regulates p38alpha/beta MAPK activity and myogenic differentiation', *J Cell Biol* 182(3): 497-507.

Kang, J. S., Feinleib, J. L., Knox, S., Ketteringham, M. A. and Krauss, R. S. (2003) 'Promyogenic members of the Ig and cadherin families associate to positively regulate differentiation', *Proc Natl Acad Sci U S A* 100(7): 3989-94.

Kang, J. S., Gao, M., Feinleib, J. L., Cotter, P. D., Guadagno, S. N. and Krauss, R. S. (1997) 'CDO: an oncogene-, serum-, and anchorage-regulated member of the Ig/fibronectin type III repeat family', *J Cell Biol* 138(1): 203-13.

Kang, J. S., Mulieri, P. J., Hu, Y., Taliana, L. and Krauss, R. S. (2002) 'BOC, an Ig superfamily member, associates with CDO to positively regulate myogenic differentiation', *EMBO J* 21(1-2): 114-24.

Kang, J. S., Yi, M. J., Zhang, W., Feinleib, J. L., Cole, F. and Krauss, R. S. (2004) 'Netrins and neogenin promote myotube formation', *J Cell Biol* 167(3): 493-504.

Kavran, J. M., Ward, M. D., Oladosu, O. O., Mulepati, S. and Leahy, D. J. (2010) 'All mammalian Hedgehog proteins interact with cell adhesion molecule, down-regulated by oncogenes (CDO) and brother of CDO (BOC) in a conserved manner', *J Biol Chem* 285(32): 24584-90.

Kawakami, T., Kawcak, T., Li, Y. J., Zhang, W., Hu, Y. and Chuang, P. T. (2002) 'Mouse dispatched mutants fail to distribute hedgehog proteins and are defective in hedgehog signaling', *Development* 129(24): 5753-65.

Kimmel, C. B., Ballard, W. W., Kimmel, S. R., Ullmann, B. and Schilling, T. F. (1995) 'Stages of embryonic development of the zebrafish', *Dev Dyn* 203(3): 253-310.

Krauss, S., Concordet, J. P. and Ingham, P. W. (1993) 'A functionally conserved homolog of the Drosophila segment polarity gene hh is expressed in tissues with polarizing activity in zebrafish embryos', *Cell* 75(7): 1431-44.

Langenberg, T., Kahana, A., Wszalek, J. A. and Halloran, M. C. (2008) 'The eye organizes neural crest cell migration', *Dev Dyn* 237(6): 1645-52.

Lawson, N. D. and Weinstein, B. M. (2002) 'In vivo imaging of embryonic vascular development using transgenic zebrafish', *Dev Biol* 248(2): 307-18.

Lee, C. S., May, N. R. and Fan, C. M. (2001) 'Transdifferentiation of the ventral retinal pigmented epithelium to neural retina in the growth arrest specific gene 1 mutant', *Dev Biol* 236(1): 17-29.

Lee, J., Cox, B. D., Daly, C. M., Lee, C., Nuckels, R. J., Tittle, R. K., Uribe, R. A. and Gross, J. M. (2012) 'An ENU mutagenesis screen in zebrafish for visual system mutants identifies a novel splice-acceptor site mutation in patched2 that results in Colobomas', Invest Ophthalmol Vis Sci 53(13): 8214-21.

Lee, J., Willer, J. R., Willer, G. B., Smith, K., Gregg, R. G. and Gross, J. M. (2008) 'Zebrafish blowout provides genetic evidence for Patched1-mediated negative regulation of Hedgehog signaling within the proximal optic vesicle of the vertebrate eye', *Dev Biol* 319(1): 10-22.

Li, Z., Joseph, N. M. and Easter, S. S., Jr. (2000) 'The morphogenesis of the zebrafish eye, including a fate map of the optic vesicle', *Dev Dyn* 218(1): 175-88.

Lu, M. and Krauss, R. S. (2010) 'N-cadherin ligation, but not Sonic hedgehog binding, initiates Cdo-dependent p38alpha/

beta MAPK signaling in skeletal myoblasts', *Proc Natl Acad Sci U S A* 107(9): 4212-7.

Lum, L., Yao, S., Mozer, B., Rovescalli, A., Von Kessler, D., Nirenberg, M. and Beachy, P. A. (2003) 'Identification of Hedgehog pathway components by RNAi in Drosophila cultured cells', *Science* 299(5615): 2039-45.

Lupo, G., Gestri, G., O'Brien, M., Denton, R. M., Chandraratna, R. A., Ley, S. V., Harris, W. A. and Wilson, S. W. (2011) 'Retinoic acid receptor signaling regulates choroid fissure closure through independent mechanisms in the ventral optic cup and periocular mesenchyme', *Proc Natl Acad Sci U S A* 108(21): 8698-703.

Lupo, G., Harris, W. A. and Lewis, K. E. (2006) 'Mechanisms of ventral patterning in the vertebrate nervous system', *Nat Rev Neurosci* 7(2): 103-14.

Lupo, G., Liu, Y., Qiu, R., Chandraratna, R. A., Barsacchi, G., He, R. Q. and Harris, W. A. (2005) 'Dorsoventral patterning of the Xenopus eye: a collaboration of Retinoid, Hedgehog and FGF receptor signaling', *Development* 132(7): 1737-48.

Ma, Y., Erkner, A., Gong, R., Yao, S., Taipale, J., Basler, K. and Beachy, P. A. (2002) 'Hedgehog-mediated patterning of the mammalian embryo requires transporter-like function of dispatched', *Cell* 111(1): 63-75.

Macdonald, R., Barth, K. A., Xu, Q., Holder, N., Mikkola, I. and Wilson, S. W. (1995) 'Midline signalling is required for Pax gene regulation and patterning of the eyes', *Development* 121(10): 3267-78.

Macdonald, R., Scholes, J., Strahle, U., Brennan, C., Holder, N., Brand, M. and Wilson, S. W. (1997) 'The Pax protein Noi is required for commissural axon pathway formation in the rostral forebrain', *Development* 124(12): 2397-408.

Marigo, V., Davey, R. A., Zuo, Y., Cunningham, J. M. and Tabin, C. J. (1996) 'Biochemical evidence that patched is the Hedgehog receptor', *Nature* 384(6605): 176-9.

Martinelli, D. C. and Fan, C. M. (2007) 'Gas1 extends the range of Hedgehog action by facilitating its signaling', *Genes Dev* 21(10): 1231-43.

Martinez-Morales, J. R., Del Bene, F., Nica, G., Hammerschmidt, M., Bovolenta, P. and Wittbrodt, J. (2005) 'Differentiation of the vertebrate retina is coordinated by an FGF signaling center', *Dev Cell* 8(4): 565-74.

Masai, I., Stemple, D. L., Okamoto, H. and Wilson, S. W. (2000) 'Midline signals regulate retinal neurogenesis in zebrafish', *Neuron* 27(2): 251-63.

McCarthy, R. A., Barth, J. L., Chintalapudi, M. R., Knaak, C. and Argraves, W. S. (2002) 'Megalin functions as an endocytic sonic hedgehog receptor', *J Biol Chem* 277(28): 25660-7.

McGlinn, E., van Bueren, K. L., Fiorenza, S., Mo, R., Poh, A. M., Forrest, A., Soares, M. B., Bonaldo Mde, F., Grimmond, S., Hui, C. C. et al. (2005) 'Pax9 and Jagged1 act downstream of Gli3 in vertebrate limb development', *Mech Dev* 122(11): 1218-33.

McLellan, J. S., Zheng, X., Hauk, G., Ghirlando, R., Beachy, P. A. and Leahy, D. J. (2008) 'The mode of Hedgehog binding to Ihog homologues is not conserved across different phyla', *Nature* 455(7215): 979-83.

McMahon, C., Gestri, G., Wilson, S. W. and Link, B. A. (2009) 'Lmx1b is essential for survival of periocular mesenchymal cells and influences Fgf-mediated retinal patterning in zebrafish', *Dev Biol* 332(2): 287-98.

Menuet, A., Alunni, A., Joly, J. S., Jeffery, W. R. and Retaux, S. (2007) 'Expanded expression of Sonic Hedgehog in Astyanax cavefish: multiple consequences on forebrain development and evolution', *Development* 134(5): 845-55.

Mohammadi, M., McMahon, G., Sun, L., Tang, C., Hirth, P., Yeh, B. K., Hubbard, S. R. and Schlessinger, J. (1997) 'Structures of the tyrosine kinase domain of fibroblast growth factor receptor in complex with inhibitors', *Science* 276(5314): 955-60.

Mohammadi, M., Olsen, S. K. and Ibrahimi, O. A. (2005) 'Structural basis for fibroblast growth factor receptor activation', *Cytokine Growth Factor Rev* 16(2): 107-37.

Moore, K. B., Mood, K., Daar, I. O. and Moody, S. A. (2004) 'Morphogenetic movements underlying eye field formation require interactions between the FGF and ephrinB1 signaling pathways', *Dev Cell* 6(1): 55-67.

Morcillo, J., Martinez-Morales, J. R., Trousse, F., Fermin, Y., Sowden, J. C. and Bovolenta, P. (2006) 'Proper patterning of the optic fissure requires the sequential activity of BMP7 and SHH', *Development* 133(16): 3179-90.

Mulieri, P. J., Kang, J. S., Sassoon, D. A. and Krauss, R. S. (2002) 'Expression of the boc gene during murine embryogenesis', *Dev Dyn* 223(3): 379-88.

Nakano, T., Ando, S., Takata, N., Kawada, M., Muguruma, K., Sekiguchi, K., Saito, K., Yonemura, S., Eiraku, M. and Sasai, Y. (2012) 'Self-formation of optic cups and storable stratified neural retina from human ESCs', *Cell Stem Cell* 10(6): 771-85.

Nakano, Y., Guerrero, I., Hidalgo, A., Taylor, A., Whittle, J. R. and Ingham, P. W. (1989) 'A protein with several possible membrane-spanning domains encoded by the Drosophila segment polarity gene patched', *Nature* 341(6242): 508-13.

Neumann, C. J. and Nuesslein-Volhard, C. (2000) 'Patterning of the zebrafish retina by a wave of sonic hedgehog activity', *Science* 289(5487): 2137-9.

Newman, S. and Müller, G. (2006) Genes and Form: Inherency in the Evolution of Developmental Mechanisms. in E. M. N.-H. C. Rehmann-Sutter (ed.) *Genes in Development Re-Reading the Molecular Paradigm*

Durham: Duke University Press.

Nuesslein-Volhard, C. and Dahm, R. (2002) *Zebrafish*: Oxford University Press.

Nusslein-Volhard, C. and Wieschaus, E. (1980) 'Mutations affecting segment number and polarity in Drosophila', *Nature* 287(5785): 795-801.

Oh, J. E., Bae, G. U., Yang, Y. J., Yi, M. J., Lee, H. J., Kim, B. G., Krauss, R. S. and Kang, J. S. (2009) 'Cdo promotes neuronal differentiation via activation of the p38 mitogen-activated protein kinase pathway', *FASEB J* 23(7): 2088-99.

Ohlig, S., Farshi, P., Pickhinke, U., van den Boom, J., Hoing, S., Jakuschev, S., Hoffmann, D., Dreier, R., Scholer, H. R., Dierker, T. et al. (2011) 'Sonic hedgehog shedding results in functional activation of the solubilized protein', *Dev Cell* 20(6): 764-74.

Okada, A., Charron, F., Morin, S., Shin, D. S., Wong, K., Fabre, P. J., Tessier-Lavigne, M. and McConnell, S. K. (2006) 'Boc is a receptor for sonic hedgehog in the guidance of commissural axons', *Nature* 444(7117): 369-73.

Otteson, D. C., Shelden, E., Jones, J. M., Kameoka, J. and Hitchcock, P. F. (1998) 'Pax2 expression and retinal morphogenesis in the normal and Krd mouse', *Dev Biol* 193(2): 209-24.

Ovcharenko, I., Loots, G. G., Giardine, B. M., Hou, M., Ma, J., Hardison, R. C., Stubbs, L. and Miller, W. (2005) 'Mulan: multiple-sequence local alignment and visualization for studying function and evolution', *Genome Res* 15(1): 184-94.

Ozeki, H., Shirai, S., Nozaki, M., Ikeda, K. and Ogura, Y. (1999) 'Maldevelopment of neural crest cells in patients with typical uveal coloboma', *J Pediatr Ophthalmol Strabismus* 36(6): 337-41.

Pages, F. and Kerridge, S. (2000) 'Morphogen gradients. A question of time or concentration?', *Trends Genet* 16(1): 40-4.

Perron, M., Boy, S., Amato, M. A., Viczian, A., Koebernick, K., Pieler, T. and Harris, W. A. (2003) 'A novel function for Hedgehog signalling in retinal pigment epithelium differentiation', *Development* 130(8): 1565-77.

Picker, A. and Brand, M. (2005) 'Fgf signals from a novel signaling center determine axial patterning of the prospective neural retina', *Development* 132(22): 4951-62.

Picker, A., Cavodeassi, F., Machate, A., Bernauer, S., Hans, S., Abe, G., Kawakami, K., Wilson, S. W. and Brand, M. (2009) 'Dynamic coupling of pattern formation and morphogenesis in the developing vertebrate retina', *PLoS Biol* 7(10): e1000214.

Pittack, C., Grunwald, G. B. and Reh, T. A. (1997) 'Fibroblast growth factors are necessary for neural retina but not pigmented epithelium differentiation in chick embryos', *Development* 124(4): 805-16.

Pottin, K., Hinaux, H. and Retaux, S. (2011) 'Restoring eye size in Astyanax mexicanus blind cavefish embryos through modulation of the Shh and Fgf8 forebrain organising centres', *Development* 138(12): 2467-76.

Ramialison, M., Reinhardt, R., Henrich, T., Wittbrodt, B., Kellner, T., Lowy, C. M. and Wittbrodt, J. (2012) 'Cis-regulatory properties of medaka synexpression groups', *Development* 139(5): 917-28.

Rash, B. G. and Grove, E. A. (2011) 'Shh and Gli3 regulate formation of the telencephalic-diencephalic junction and suppress an isthmus-like signaling source in the forebrain', *Dev Biol* 359(2): 242-50.

Reifers, F., Bohli, H., Walsh, E. C., Crossley, P. H., Stainier, D. Y. and Brand, M. (1998) 'Fgf8 is mutated in zebrafish acerebellar (ace) mutants and is required for maintenance of midbrain-hindbrain boundary development and somitogenesis', *Development* 125(13): 2381-95.

Riddle, R. D., Johnson, R. L., Laufer, E. and Tabin, C. (1993) 'Sonic hedgehog mediates the polarizing activity of the ZPA', *Cell* 75(7): 1401-16.

Robu, M. E., Larson, J. D., Nasevicius, A., Beiraghi, S., Brenner, C., Farber, S. A. and Ekker, S. C. (2007) 'p53 activation by knockdown technologies', *PLoS Genet* 3(5): e78.

Roelink, H., Augsburger, A., Heemskerk, J., Korzh, V., Norlin, S., Ruiz i Altaba, A., Tanabe, Y., Placzek, M., Edlund, T., Jessell, T. M. et al. (1994) 'Floor plate and motor neuron induction by vhh-1, a vertebrate homolog of hedgehog expressed by the notochord', *Cell* 76(4): 761-75.

Rojas-Rios, P., Guerrero, I. and Gonzalez-Reyes, A. (2012) 'Cytoneme-mediated delivery of hedgehog regulates the expression of bone morphogenetic proteins to maintain germline stem cells in Drosophila', *PLoS Biol* 10(4): e1001298.

Ryan, K. E. and Chiang, C. (2012) 'Hedgehog secretion and signal transduction in vertebrates', *J Biol Chem* 287(22): 17905-13.

Sanchez-Camacho, C. and Bovolenta, P. (2008) 'Autonomous and non-autonomous Shh signalling mediate the in vivo growth and guidance of mouse retinal ganglion cell axons', *Development* 135(21): 3531-41.

Sanchez-Hernandez, D., Sierra, J., Ortigao-Farias, J. R. and Guerrero, I. (2012) 'The WIF domain of the human and Drosophila Wif-1 secreted factors confers specificity for Wnt or Hedgehog', *Development* 139(20): 3849-58.

Sanek, N. A., Taylor, A. A., Nyholm, M. K. and Grinblat, Y. (2009) 'Zebrafish zic2a patterns the forebrain through modulation of Hedgehog-activated gene expression', *Development* 136(22): 3791-800.

Sanyanusin, P., Schimmenti, L. A., McNoe, L. A., Ward, T. A., Pierpont, M. E., Sullivan, M. J., Dobyns, W. B. and Eccles, M. R. (1995) 'Mutation of the PAX2 gene in a family with optic nerve colobomas, renal anomalies and vesicoureteral reflux', *Nat Genet* 9(4): 358-64.

Sasagawa, S., Takabatake, T., Takabatake, Y., Muramatsu, T. and Takeshima, K. (2002) 'Axes establishment during eye morphogenesis in Xenopus by coordinate and antagonistic actions of BMP4, Shh, and RA', *Genesis* 33(2): 86-96.

Schauerte, H. E., van Eeden, F. J., Fricke, C., Odenthal, J., Strahle, U. and Haffter, P. (1998) 'Sonic hedgehog is not required for the induction of medial floor plate cells in the zebrafish', *Development* 125(15): 2983-93.

Schimmenti, L. A., de la Cruz, J., Lewis, R. A., Karkera, J. D., Manligas, G. S., Roessler, E. and Muenke, M. (2003) 'Novel mutation in sonic hedgehog in non-syndromic colobomatous microphthalmia', *Am J Med Genet A* 116A(3): 215-21.

Schlessinger, J. (2000) 'Cell signaling by receptor tyrosine kinases', *Cell* 103(2): 211-25.

Schmitt, E. A. and Dowling, J. E. (1994) 'Early eye morphogenesis in the zebrafish, Brachydanio rerio', *J Comp Neurol* 344(4): 532-42.

Schmitt, E. A. and Dowling, J. E. (1996) 'Comparison of topographical patterns of ganglion and photoreceptor cell differentiation in the retina of the zebrafish, Danio rerio', *J Comp Neurol* 371(2): 222-34.

Schwarz, M., Cecconi, F., Bernier, G., Andrejewski, N., Kammandel, B., Wagner, M. and Gruss, P. (2000) 'Spatial specification of mammalian eye territories by reciprocal transcriptional repression of Pax2 and Pax6', *Development* 127(20): 4325-34.

Sehgal, R., Karcavich, R., Carlson, S. and Belecky-Adams, T. L. (2008) 'Ectopic Pax2 expression in chick ventral optic cup phenocopies loss of Pax2 expression', *Dev Biol* 319(1): 23-33.

Shi, Y. and Massague, J. (2003) 'Mechanisms of TGF-beta signaling from cell membrane to the nucleus', *Cell* 113(6): 685-700.

Sievers, F., Wilm, A., Dineen, D., Gibson, T. J., Karplus, K., Li, W., Lopez, R., McWilliam, H., Remmert, M., Soding, J. et al. (2011) 'Fast, scalable generation of high-quality protein multiple sequence alignments using Clustal Omega', *Mol Syst Biol* 7: 539.

Song, H. H., Shi, W. and Filmus, J. (1997) 'OCI-5/rat glypican-3 binds to fibroblast growth factor-2 but not to insulin-like growth factor-2', *J Biol Chem* 272(12): 7574-7.

Soules, K. A. and Link, B. A. (2005) 'Morphogenesis of the anterior segment in the zebrafish eye', *BMC Dev Biol* 5: 12.

Srivastava, M., Simakov, O., Chapman, J., Fahey, B., Gauthier, M. E., Mitros, T., Richards, G. S., Conaco, C., Dacre, M., Hellsten, U. et al. (2010) 'The Amphimedon queenslandica genome and the evolution of animal complexity', *Nature* 466(7307): 720-6.

Stecca, B. and Ruiz, I. A. A. (2010) 'Context-dependent regulation of the GLI code in cancer by HEDGEHOG and non-HEDGEHOG signals', J Mol Cell Biol 2(2): 84-95.

Stone, D. M., Hynes, M., Armanini, M., Swanson, T. A., Gu, Q., Johnson, R. L., Scott, M. P., Pennica, D., Goddard, A., Phillips, H. et al. (1996) 'The tumour-suppressor gene patched encodes a candidate receptor for Sonic hedgehog', *Nature* 384(6605): 129-34.

Taipale, J., Cooper, M. K., Maiti, T. and Beachy, P. A. (2002) 'Patched acts catalytically to suppress the activity of Smoothened', *Nature* 418(6900): 892-7.

Takaesu, G., Kang, J. S., Bae, G. U., Yi, M. J., Lee, C. M., Reddy, E. P. and Krauss, R. S. (2006) 'Activation of p38alpha/beta MAPK in myogenesis via binding of the scaffold protein JLP to the cell surface protein Cdo', *J Cell Biol* 175(3): 383-8.

Take-uchi, M., Clarke, J. D. and Wilson, S. W. (2003) 'Hedgehog signalling maintains the optic stalk-retinal interface through the regulation of Vax gene activity', *Development* 130(5): 955-68.

Tenzen, T., Allen, B. L., Cole, F., Kang, J. S., Krauss, R. S. and McMahon, A. P. (2006) 'The cell surface membrane proteins Cdo and Boc are components and targets of the Hedgehog signaling pathway and feedback network in mice', *Dev Cell* 10(5): 647-56.

The, I., Bellaiche, Y. and Perrimon, N. (1999) 'Hedgehog movement is regulated through tout velu-dependent synthesis of a heparan sulfate proteoglycan', *Mol Cell* 4(4): 633-9.

Thisse, B., Pflumio, S., Fürthauer, M., Loppin, B., Heyer, V., Degrave, A., Woehl, R., Lux, A., Steffan, T., Charbonnier, X.Q. and Thisse, C. (2001) 'Expression of the zebrafish genome during embryogenesis (NIH R01 RR15402)', *ZFIN Direct Data Submission (http://zfin.org)*.

Thisse, B., Thisse, C. (2004) 'Fast Release Clones: A High Throughput Expression Analysis', *ZFIN Direct Data Submission (http://zfin.org)*.

Torres, M., Gomez-Pardo, E., Dressler, G. R. and Gruss, P. (1995) 'Pax-2 controls multiple steps of urogenital development', *Development* 121(12): 4057-65.

Trousse, F., Marti, E., Gruss, P., Torres, M. and Bovolenta, P. (2001) 'Control of retinal ganglion cell axon growth: a new role for Sonic hedgehog', *Development* 128(20): 3927-36.

Tsuda, M., Kamimura, K., Nakato, H., Archer, M., Staatz, W., Fox, B., Humphrey, M., Olson, S., Futch, T., Kaluza, V. et al. (1999) 'The cell-surface proteoglycan Dally regulates Wingless signalling in Drosophila', *Nature* 400(6741): 276-80.

Tukachinsky, H., Kuzmickas, R. P., Jao, C. Y., Liu, J. and Salic, A. (2012) 'Dispatched and scube mediate the efficient secretion of the cholesterol-modified hedgehog ligand', *Cell Rep* 2(2): 308-20.

Tukachinsky, H., Lopez, L. V. and Salic, A. (2010) 'A mechanism for vertebrate Hedgehog signaling: recruitment to cilia and dissociation of SuFu-Gli protein complexes', *J Cell Biol* 191(2): 415-28.

van Amerongen, R. and Nusse, R. (2009) 'Towards an integrated view of Wnt signaling in development', *Development* 136(19): 3205-14.

van den Heuvel, M. and Ingham, P. W. (1996) 'smoothened encodes a receptor-like serpentine protein required for hedgehog signalling', *Nature* 382(6591): 547-51.

Varga, Z. M., Amores, A., Lewis, K. E., Yan, Y. L., Postlethwait, J. H., Eisen, J. S. and Westerfield, M. (2001) 'Zebrafish smoothened functions in ventral neural tube specification and axon tract formation', *Development* 128(18): 3497-509.

Veeman, M. T., Axelrod, J. D. and Moon, R. T. (2003) 'A second canon. Functions and mechanisms of beta-catenin-inde-

pendent Wnt signaling', *Dev Cell* 5(3): 367-77.

Voiculescu, O., Papanayotou, C. and Stern, C. D. (2008) 'Spatially and temporally controlled electroporation of early chick embryos', *Nat Protoc* 3(3): 419-26.

Wang, Y. P., Dakubo, G., Howley, P., Campsall, K. D., Mazarolle, C. J., Shiga, S. A., Lewis, P. M., McMahon, A. P. and Wallace, V. A. (2002) 'Development of normal retinal organization depends on Sonic hedgehog signaling from ganglion cells', *Nat Neurosci* 5(9): 831-2.

Wilson, S. W. and Houart, C. (2004) 'Early steps in the development of the forebrain', *Dev Cell* 6(2): 167-81.

Willnow, T. E., Hilpert, J., Armstrong, S. A., Rohlmann, A., Hammer, R. E., Burns, D. K. and Herz, J. (1996) 'Defective forebrain development in mice lacking gp330/megalin', *Proc Natl Acad Sci U S A* 93(16): 8460-4.

Woo, K. and Fraser, S. E. (1995) 'Order and coherence in the fate map of the zebrafish nervous system', *Development* 121(8): 2595-609.

Xavier, G. M. and Cobourne, M. T. (2011) 'Scube2 expression extends beyond the central nervous system during mouse development', *J Mol Histol* 42(5): 383-91.

Yamaguchi, M., Imai, F., Tonou-Fujimori, N. and Masai, I. (2010) 'Mutations in N-cadherin and a Stardust homolog, Nagie oko, affect cell-cycle exit in zebrafish retina', *Mech Dev* 127(5-6): 247-64.

Yamamoto, Y., Stock, D. W. and Jeffery, W. R. (2004) 'Hedgehog signalling controls eye degeneration in blind cavefish', *Nature* 431(7010): 844-7.

Yan, D., Wu, Y., Yang, Y., Belenkaya, T. Y., Tang, X. and Lin, X. (2010) 'The cell-surface proteins Dally-like and Ihog differentially regulate Hedgehog signaling strength and range during development', *Development* 137(12): 2033-44.

Yao, S., Lum, L. and Beachy, P. (2006) 'The ihog cell-surface proteins bind Hedgehog and mediate pathway activation', *Cell* 125(2): 343-57.

Zelarayan, L. C., Vendrell, V., Alvarez, Y., Dominguez-Frutos, E., Theil, T., Alonso, M. T., Maconochie, M. and Schimmang, T. (2007) 'Differential requirements for FGF3, FGF8 and FGF10 during inner ear development', Dev Biol 308(2): 379-91.

Zhang, W., Hong, M., Bae, G. U., Kang, J. S. and Krauss, R. S. (2011) 'Boc modifies the holoprosencephaly spectrum of Cdo mutant mice', *Dis Model Mech* 4(3): 368-80.

Zhang, W., Kang, J. S., Cole, F., Yi, M. J. and Krauss, R. S. (2006a) 'Cdo functions at multiple points in the Sonic Hedgehog pathway, and Cdo-deficient mice accurately model human holoprosencephaly', *Dev Cell* 10(5): 657-65.

Zhang, W., Mulieri, P. J., Gaio, U., Bae, G. U., Krauss, R. S. and Kang, J. S. (2009) 'Ocular abnormalities in mice lacking the immunoglobulin superfamily member Cdo', *FEBS J* 276(20): 5998-6010.

Zhang, W., Yi, M. J., Chen, X., Cole, F., Krauss, R. S. and Kang, J. S. (2006b) 'Cortical thinning and hydrocephalus in mice lacking the immunoglobulin superfamily member CDO', *Mol Cell Biol* 26(10): 3764-72.

Zhang, X. M. and Yang, X. J. (2001) 'Temporal and spatial effects of Sonic hedgehog signaling in chick eye morphogenesis', *Dev Biol* 233(2): 271-90.

Zheng, X., Mann, R. K., Sever, N. and Beachy, P. A. (2010) 'Genetic and biochemical definition of the Hedgehog receptor', *Genes Dev* 24(1): 57-71.

Zolessi, F. R., Poggi, L., Wilkinson, C. J., Chien, C. B. and Harris, W. A. (2006) 'Polarization and orientation of retinal ganglion cells in vivo', *Neural Dev* 1: 2.

APPENDIX

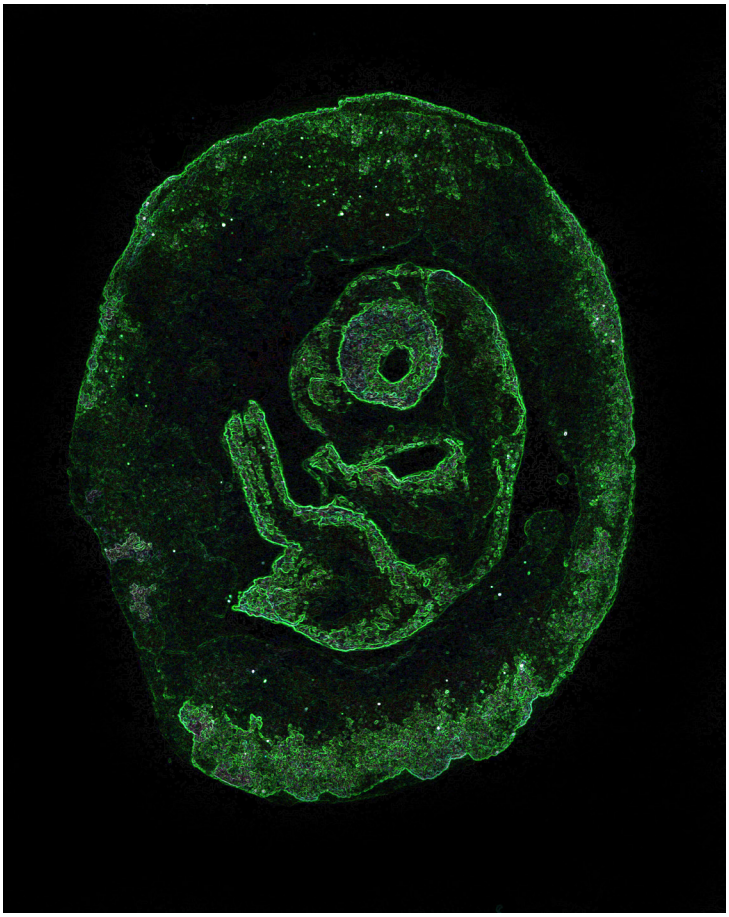

The International Journal of Biochemistry & Cell Biology 44 (2012) 698–702

Contents lists available at SciVerse ScienceDirect

The International Journal of Biochemistry & Cell Biology

journal homepage: www.elsevier.com/locate/biocel

Molecules in focus

Cdon and Boc: Two transmembrane proteins implicated in cell–cell communication

Luisa Sanchez-Arrones [1], Marcos Cardozo [1], Francisco Nieto-Lopez, Paola Bovolenta *

Centro de Biología Molecular "Severo Ochoa", CSIC-UAM and CIBER de Enfermedades Raras (CIBERER), c/ Nicolas Cabrera, 1, Madrid 28049, Spain

ARTICLE INFO

Article history:
Received 9 December 2011
Received in revised form 20 January 2012
Accepted 27 January 2012
Available online 3 February 2012

Keywords:
Cell adhesion
IgG superfamily of CAMs
Hh signaling
Myoblast

ABSTRACT

Cdon and Boc, and their *Drosophila* homologues Ihog and Boi, are evolutionary conserved transmembrane glycoproteins belonging to a subgroup of the Immunoglobulin superfamily of cell adhesion molecules (CAMs). Initially isolated in vertebrates as CAMs that link cadherin function with MAPK signaling in myoblast differentiation, they have thereafter been shown to act as essential receptors for the Hedgehog (Hh) family of secreted proteins. They associate with both ligand and other Hh receptor components, including Ptch and Gas1, thus forming homo- and heteromeric complexes. In *Drosophila*, they are also involved in ligand processing and release from Hh producing cells. Cdon/Boc and Ihog/Boi can substitute one another and play redundant functions is some contexts. In addition, Boc, but not Cdon, mediates axon guidance information provided by Hh in specific neuronal populations, whereas mutations in the CDON cause holoprosencephaly, a human congenital anomaly defined by forebrain midline defects prominently associated with diminished Hh pathway activity.

1. Introduction

Cell to cell communication is at the basis of coherent organ development and tissue homeostasis. There are several different ways in which cells interact with one another but cell adhesion and activation of signaling cascades by extracellular molecules are two prominent mechanisms. Cdon (cell adhesion molecule-related, down-regulated by oncogenes, also noted as Cdo) and Boc (Brother of Cdon), the two molecules here on focus, are emerging as important mediators of both functions.

The *Cdon* gene was isolated out of a screening designed to identify novel transformation suppressor genes using a cDNA library derived from a rat fibroblast cell line, resistant to oncogene-induced anchorage-independent growth (Kang et al., 1997). The corresponding gene product was characterized as a cell surface glycoprotein of the Immunoglobulin (Ig)/fibronectin type III-like (FNIII) family and soon after implicated in myogenic differentiation (Kang et al., 1998). Low stringency screening of a human fetal brain cDNA library with a rat *Cdon* probe lead to the identification of a related gene named *Boc*, which encoded a protein with similar effects on myoblast differentiation (Kang et al., 1998, 2002). Both genes are highly conserved among vertebrates whereas, in the *Drosophila* counterparts, a high degree of conservation is found only in the region predicted to encode the extracellular domain (Kang et al., 2002). The *Drosophila* homologues were thereafter independently identified in a RNA interference screening in tissue culture cells for new components of the Hh signaling pathway and received the name of *ihog* (*interference hedge*hog) and *boi* (b*rother of ihog*) (Lum et al., 2003). Both vertebrate and invertebrate proteins were shown to bind the N-terminal and biologically active Hh (HhN) or Shh (ShhN) peptides (Yao et al., 2006), prompting the investigation on *Cdo*/*Boc* and *ihog*/*boi* function in different directions.

2. Structure and interactions

The human *CDON* gene maps to the minus strand of a gene rich genomic region on chromosome 11q24.2 and is composed of 20 exons. Although data base predictions identify different alternative transcription start sites, only two transcripts have been so far described encoding isoforms of 1287 and 1264 aa. The shorter isoform has received the most attention. *BOC* similarly localizes to a gene-rich region but to the plus strand of chromosome 3q13.2. Its 20 exons encode an 1114 aa protein that shares 34% identity with CDON (Kang et al., 2002).

Cdon and Boc proteins have been characterized as cell surface glycoproteins belonging to a subgroup of the Immunoglobulin (Ig) superfamily of cell adhesion molecules (CAMs), that also includes the Robo axon-guidance receptors. Their ectodomain respectively contains five and four Ig-like domains, followed by three FNIII

* Corresponding author at: Centro de Biología Molecular Severo Ochoa, CSIC-UAM, Universidad Autónoma de Madrid, c/ Nicolás Cabrera, 1, 28049 Cantoblanco, Madrid, Spain. Tel.: +34 91 196 4718 (office); +34 91 196 4720 (lab); fax: +34 91 196 4420.
E-mail address: pbovolenta@cbm.uam.es (P. Bovolenta).
[1] These authors contributed equally to this work.

1357-2725/$ – see front matter © 2012 Elsevier Ltd. All rights reserved.
doi:10.1016/j.biocel.2012.01.019

repeats (Fn1-3), a single trans-membrane domain and a divergent intracellular region of variable length (Fig. 1A), which may account for some of their functional differences (Kang et al., 2002; Mulieri et al., 2002). The presence of four Ig domains and only two FNIII repeats (Fn1, 2) distinguished the *Drosophila* Ihog and Boi from their vertebrate homologues (Fig. 1A) (Kang et al., 2002; Yao et al., 2006). Sequence analysis reveals that Cdon/Boc Fn2 and Fn3 are respectively homologous to the Fn1 and Fn2 of Ihog/Boi (Kang et al., 2002).

Boc and Cdon form homophilic and heterophilic complexes in *cis* by interaction of the ecto- and intracellular domains (Kang et al., 2002) (Fig. 1B–D). Cdon has also been shown to interact with Neogenin (Kang et al., 2004), an Ig/FnIII CAM family member that acts as receptor for the axon guidance cue Netrin. Furthermore, during myoblast and neuronal differentiation, *cis*-interaction of N-Cadherin with Fn1 (Kang et al., 2003; Lu and Krauss, 2010) promotes binding of the Cdon intracellular domain to Bnip-2 and JLP, two proteins that function as scaffolds for small GTPases and p38 pathway components, respectively (Kang et al., 2008; Takaesu et al., 2006; Oh et al., 2009). The Cdon–Bnip-2 complex furthers interacts with Cdc42 and stimulates its activity, which, in turn, is required for p38-dependent differentiation (Fig. 1B). Activation of the same pathway has been also observed after Cdon association with the non-receptor tyrosine kinase Abl (Bae et al., 2009) (Fig. 1B).

Cdon/Boc and Ihog/Boi bind members of the Hh family with high-affinity, but, notably, with different and evolutionary non-conserved modes (Okada et al., 2006; Tenzen et al., 2006; Yao et al., 2006; McLellan et al., 2008). Biochemical, biophysical, and X-ray structural studies demonstrated that Shh-Cdon interaction is calcium dependent and involves a previously unappreciated binuclear calcium-binding site on ShhN (McLellan et al., 2008) and the Cdon/Boc Fn3 (Tenzen et al., 2006; Yao et al., 2006; McLellan et al., 2008). This interaction mode is conserved for all vertebrate Hh proteins (Kavran et al., 2010). Instead, and despite the general extensive homology between invertebrate and vertebrate Hh proteins, the HhN surface that binds Ihog is different (a single common residue) from that implicated Shh/Cdon interaction (McLellan et al., 2008). Furthermore, HhN-Ihog binding is heparin-dependent and involves the Ihog/Boi Fn1, which is not homologous to the Cdon/Boc Fn3 (Yao et al., 2006) (Fig. 1A, B). The Cdon-like binding mode is conserved in vertebrates and the Ihog-like mode in arthropods, but how interaction occurs in other species remains to be determined (McLellan et al., 2008).

Besides ligand binding, Ihog/Boi can form a complex with the Hh receptor Patched (Ptch) and this heteromeric interaction is required for both high-affinity ligand binding and presentation of Ptch at the cell surface, providing initial indications that Ihog or Boi are obligate co-receptors for efficient Hh reception (Zheng et al., 2010). This requirement is conserved in vertebrates (Fig. 1B, C), where an additional Hh binding protein, Gas1, can substitute Cdon or Boc function in specific contexts as demonstrated by genetic inactivation studies in mice (Bae et al., 2011; Izzi et al., 2011; Allen et al., 2011). Notably, Cdon has also been shown to associate with Gas1 (Fig. 1D).

The relevance of simultaneous interaction of Cdon/Boc with both ligand and other Hh receptor proteins is supported by mutation analysis. A mutation in Cdon that does not interfere with Shh binding, but weakens interaction with Ptch and Gas1, is associated with low Shh signaling activation (Bae et al., 2011). Conversely, a point mutation in the Hh protein that interferes with Boc, Cdon and Gas1 but not with Ptch binding prevents Shh signaling activation (Izzi et al., 2011).

3. Expression, activation and turnover

Boc and Cdon mRNAs were initially localized to cells of the myogenic lineages (Kang et al., 1998, 2002; Mulieri et al., 2002) but their distribution has been thereafter detected from gastrulation stages in many tissues of different vertebrate species. In general, their expression is mostly associated to domains of proliferating and undifferentiated cells where both genes are co-expressed, indicating cooperative activities (Mulieri et al., 2002). Both genes have also unique sites of expression that may explain the so far specific function of Boc (Connor et al., 2005; Fabre et al., 2010; Okada et al., 2006) and Cdon (Ming et al., 1998; Cole and Krauss, 2003) as we will detail later. In *Drosophila*, *ihog* and *boi* are widely distributed at embryonic and larva L3 stages (http://flybase.org).

At early stages of vertebrate embryonic development, Boc and Cdon are abundantly expressed in the head folds, somites, the developing lungs, primitive gut and tracheal mesenchyme, the

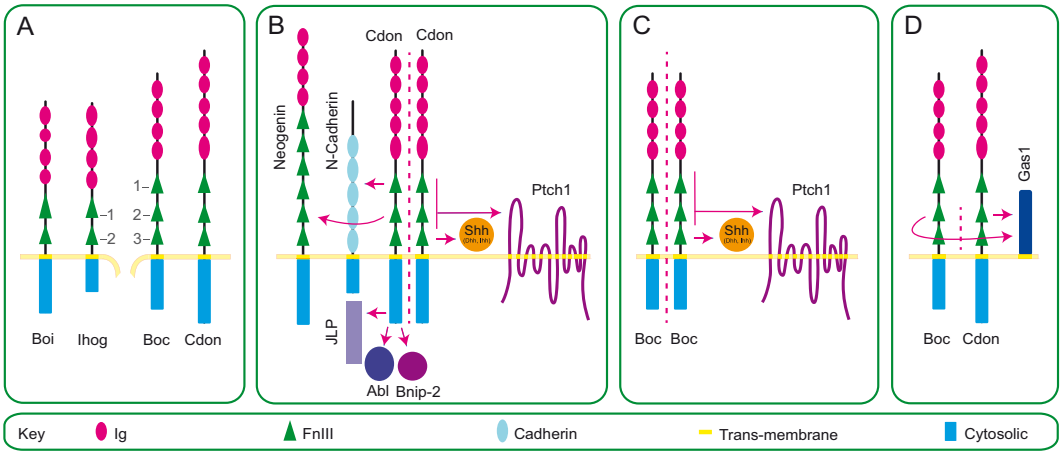

Fig. 1. Schematic diagram representing the structure and protein interactions of Boc and Cdon. (A) Comparison of the domain organization of Boc and Cdon with that of their *Drosophila* homologs, Boi and Ihog. Numbers indicate the position of each Fibronectin type III (FnIII) domain. (B) Cdon forms homo- and heteromeric complexes binding to Neogenin and N-cadherin and interacts with the cytosolic proteins JLP, Abl, Bnip-2. Within the Shh signaling pathways Cdon (B) and Boc (C) associate with Shh, Dhh, Ihh and Ptch1. (D) Boc and Cdon can interact in *cis* and bind Gas1. Arrows and dotted lines depict protein interactions. Ig, Immunoglobulin domain. FnIII, Fibronectin type III domain.

digestive tract and urogenital system, the limb buds, the dorsal aspect of the entire neural tube and sensory organs, including the inner ear, the olfactory apparatus and the developing eye (Kang et al., 2002; Mulieri et al., 2000, 2002; Connor et al., 2005; McGlinn et al., 2005; Bergeron et al., 2011). Later on, Boc and Cdon have been also detected in the cortical progenitors of the telencephalon, the prospective hippocampus, the dorsal thalamus and epithalamus and the dorsal superior and inferior coliculi (Aglyamova and Agarwala, 2007).

In mice *Cdon* mRNA is also transiently expressed at low levels in the notochord (Tenzen et al., 2006), whereas *Boc* has been transiently detected in the zebrafish ventral spinal cord prior to expression in the dorsal neural tube, in the branchial arches and in the hypothalamus and hindbrain (Bergeron et al., 2011). As the central nervous system develops, Boc, but not Cdon, localizes to the differentiated commissural neurons of the spinal cord (Okada et al., 2006; Tenzen et al., 2006) and to the ipsilaterally projecting retinal ganglion cells (RGCs) (Fabre et al., 2010; Sanchez-Camacho and Bovolenta, 2008), influencing the axon outgrowth of both types of neurons.

At the moment there is little information regarding the precise regulation of *Cdon*/*Boc* and *ihog*/*boi* expression and the turnover of the respective encoded proteins. *Cdon* and *Boc* both seem to be negatively regulated by Hh signaling in early vertebrate embryos (Tenzen et al., 2006; Bergeron et al., 2011) as also supported by the abnormal levels of *Cdon* expression found in the limb buds of *Gli3* mutant embryos (McGlinn et al., 2005). However, there is also evidence for Shh-mediated *Boc* upregulation in cerebellar granule cell precursors (Lee et al., 2010). Nevertheless, the final levels of receptors at the membrane might be tightly regulated by a complex feed-back regulatory mechanism as in both vertebrates and invertebrates *Cdo*/*Boc* and *ihog*/*boi* participate in Hh pathway activation (Lum et al., 2003; Okada et al., 2006; Tenzen et al., 2006; Yao et al., 2006; Izzi et al., 2011; Allen et al., 2011) and regulate the extracellular Hh distribution, likely restricting its range of action (Yan et al., 2010; Hartman et al., 2010; Callejo et al., 2011) (Fig. 2A).

4. Biological functions

As already mentioned, Cdon/Boc and iHog/Boi are cell adhesion molecules and important regulators of Hh signaling in different contexts. As such, they have been shown to regulate different developmental and homeostatic events with Hh-independent and dependent mechanisms. The studies exploring the function of both proteins in different species are rapidly growing. Below we highlight a few prominent aspects of their activities.

Specification and differentiation of skeletal myocytes are tightly regulated and require the activity of transcription factors such as myogenic regulatory factors (MRF) and myocyte enhance factor-2 (MEF2). MRF and MEF2 are in turn controlled by the p38α/β mitogen-activated protein kinase (MAPK) signaling pathway and p38α deficiency impairs myoblast differentiation (Krauss, 2010). Cell adhesion mediated by cadherins, including N-, R- and M-cadherins, is also a key factor in skeletal muscle differentiation (Krauss, 2010). Cdon acts at the interface between these two events. As mentioned above, Cdon associates at the plasma membrane with N- and M-cadherins. Upon interaction, the intracellular region of Cdon undergoes a change and stably associates with Bnip-2/Cdc42 and JLP/p38α/β, leading to p38 activation and thus myogenic differentiation (Fig. 1B). These changes do not occur when Cdon binds Shh, thus Cdon acts as a non-ligand-binding signaling co-receptor for N-cadherin in this context (Lu and Krauss, 2010). Similarly, Cdon associates with Neogenin, and both molecules are required for Netrin-mediated activation of FAK and ERK signaling in myoblasts (Bae et al., 2009). In line with these multiple functions, *Cdon*$^{-/-}$ mice present delayed skeletal muscle development (Cole et al., 2004).

Cdon, Boc, Cadherins and Neogenin are co-expressed in different tissues, but whether their functional interaction is muscle specific or occurs in other tissues needs to be explored. Indeed, most of the currently known, additional functions of Cdon and Boc can be explained by their participation in the Hh signaling pathway, forming a functional receptor with Ptch in several tissues and/or

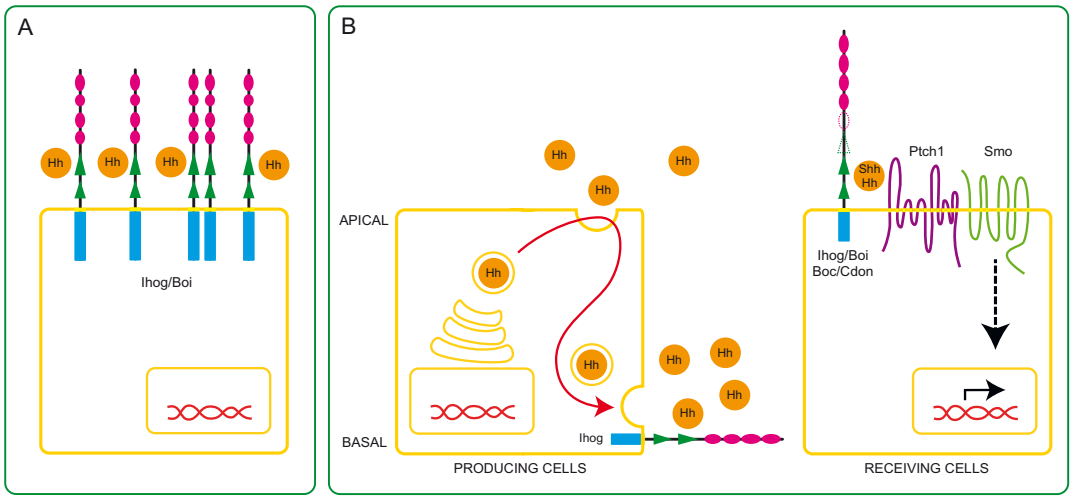

Fig. 2. Schematic diagram of the proposed functions for Cdon/Boc and Ihog/Boi in the Hh signaling. (A) Ihog and Boi can titrate Hh levels in the extracellular space, acting as molecular sinks. (B) In the Hh producing cell, Hh undergoes apico-basal recycling in the wing imaginal disc epithelium. Ihog in the latero-basal membrane contributes to processes of Hh release and membrane attachment. In the receiving cell, Ihog, Boi, Boc and Cdon associate with both Hh ligands and Patched (Ptch) receptor increasing the Hh signaling response. Pathways activation further involves release of Smoothened (Smo) inhibition and transcription activation of target genes.

cell types (Fig. 2B). Notably, their function appears redundant in different contexts. For example, Boc and Gas1 can substitute one another in the cerebellum and both of them can associate with the Ptch receptor to mediate Shh-dependent proliferation of cerebellar granule neuron progenitors. Consequently, only combined genetic inactivation of the two molecules impairs cerebellar development (Izzi et al., 2011). Similarly, Boc, Gas1 as well as Cdon play overlapping and essential roles during early Hh-dependent patterning of the mammalian ventral neural tube and further contribute the specification of different neural progenitors (Allen et al., 2011). Only embryos deficient in the three genes die before birth and are characterized by a phenotype similar to that in *Shh* null embryos, with severe holoprosencephaly (HPE) – a phenotype defined by forebrain midline defects – cyclopia, heart and limb malformations (Allen et al., 2011; Izzi et al., 2011). This overlapping activity does not seem to be conserved in zebrafish, where loss of Boc function, that characterizes the *umleitung* (*uml*) mutant, is sufficient to cause defects in patterning of the ventral neural tube, somites and upper jaw. Mechanistically, Boc seems required to maximize the response of cells exposed to high Hh concentrations; in its absence, cells no longer express genes that are normally activated by high Hh levels (Bergeron et al., 2011).

Boc, but not Cdon, has also been implicated in mediating axon guidance information provided by Shh. Both spinal cord commissural and RGC axons respond to Shh secreted by ventral midline cells, the floor plate and the pre- and post-optic areas, respectively. Their response is however different. Floor plate-derived Shh attracts Boc-positive commissural axons from the dorsal spinal cord toward the midline, whereas the growth of contralateral projecting RGC axons is suppressed by Shh, which, expressed at the chiasm borders, funnels the growth of axons to the contralateral side of the brain (rev. in Sanchez-Camacho and Bovolenta, 2009). Genetic inactivation of *Boc* prevents commissural axons to reach the floor plate (Okada et al., 2006), with a mechanism that seems to involve a Src-kinase dependent non-canonical pathway (Yam et al., 2009). In contrast to commissural neurons, contralaterally projecting RGCs do not express *Boc*, suggesting that Shh-mediated repulsion involves a different receptor complex. Notably however, *Boc* localizes to the small population of ipsilaterally projecting RGCs, the axons of which respond positively to Shh stimulation (Sanchez-Camacho and Bovolenta, 2008). In *Boc* null embryos, the number of ipsilateral projecting axons is reduced, leading to the hypothesis that Boc contributes to the segregation visual axons at the optic chiasm (Fabre et al., 2010). Further supporting that *Boc* has a relevant function in axon guidance, knock-down of *Boc* function in zebrafish causes defects in the trajectory of the dorso-ventrally projecting supraoptic and epiphyseal tracts, which aberrantly grow toward the anterior and postoptic commissure, respectively. In addition, axons of the posterior commissure were defasciculated and ectopically extended toward rostro-dorsal regions (Connor et al., 2005). Whether all these defects are Hh-dependent or may alternatively imply the cell adhesion properties of Boc needs to be investigated.

In contrast to $Boc^{-/-}$ mice that are characterized by axon guidance defects, *Cdon* deficient mice display different forms of HPE with strain-specific severity that goes from mild facial defects to brain and eye malformations (Cole and Krauss, 2003; Zhang et al., 2006, 2009), suggesting that Cdon has some spatio-temporal unique function during embryonic development. Underscoring a unique function during mammalian development, mutations in *CDON* have been found in patients affected by HPE (Bae et al., 2011). Nevertheless, defects of $Cdon^{-/-}$ embryos aggravate in absence of *Boc*. Indeed, $Cdo^{-/-}$;$Boc^{-/-}$ animals display severe brain defects and strong craniofacial anomalies, associated to reduced expression of *Shh* and its target genes (Zhang et al., 2011). The phenotype of double-mutant mice is however milder than that of *Shh*-null mice, likely owing to the compensating expression of Gas1 (Allen et al., 2011; Izzi et al., 2011).

In *Drosophila*, loss of either *boi* or *ihog* function has no consequences in the development of the imaginal discs that are normally strongly dependent on Hh signaling. Their combined inactivation however recapitulates *hh* loss of function, suggesting that Boi and Ihog play a redundant function in Hh pathway activation (Zheng et al., 2010; Camp et al., 2010). Notably, Ihog and Boi have been also related to the formation of the Hh gradient, as both proteins can sequester and titrate the amount of ligand available for Ptch binding, thus limiting long-range signaling (Yan et al., 2010; Zheng et al., 2010; Hartman et al., 2010).

As in vertebrates, specific independent functions for Ihog and Boi have been also described. Indeed, Boi, but not Ihog, is expressed in apical cells of the *Drosophila* ovary where it suppresses follicle stem cell proliferation by binding to and sequestering Hh on the apical cell surface, thereby controlling Hh long-range distribution (Hartman et al., 2010). Ihog instead together with Dally-like (Dlp), an additional protein previously implicated in Hh reception, has been shown to act as a key component of Hh secretion from the producing cells (Fig. 2B). Ihog and Dlp both interact with Ptc during Hh reception (Yao et al., 2006; Yan et al., 2010) and both interact with Dispatched during Hh release from the producing cells (Callejo et al., 2011). In the *Drosophila* wing imaginal disc epithelium, Hh undergoes apico-basal recycling in the producing cells to form a basolateral gradient. Ihog anchors Hh to the basolateral plasma membranes, where it binds to Ptch localized to the baso-lateral side of the responding cells and activates the downstream signaling cascade (Callejo et al., 2011). Whether Boi has a similar role and what makes Ihog acquire different functions in the producing and receiving cells are still unanswered questions that deserve attention.

5. Possible medical applications

Mutations in *CDON* have already been associated with human HPE and *BOC* may represent a silent HPE modifier gene (Zhang et al., 2011). However, besides HPE, alterations in Shh signaling cause other severe pathological conditions including Carpenter, Ellis-van Creveld, Smith-Lemli-Opitzl and Pallister-Hall Diseases, Greig Cephalopolysyndactyly or the Gorlin syndrome. Search for possible implications of Cdon and Boc in these conditions is thus a necessary step toward the understanding of the possible medical implication of these molecules. The important role of Cdon in eye formation and that of Boc in RGC axon guidance are also reasons to consider these genes as possible candidates for inborn ocular malformations. The fundamental role of Cdon and Boc in Hh signaling suggests also that they might be relevant targets for therapy in Hh dependent tumors.

Acknowledgments

We are in debt with Prof. Isabel Guerrero for helpful discussion and critical reading of the manuscript. Work in our laboratory is supported by grants from the Spanish MICINN (BFU2010-16031), Comunidad Autonoma de Madrid (CAM, P-SAL-0190-2006), Fundación ONCE, Fundaluce and CIBERER to P.B. and by an Institutional Grant from the Fundación Ramon Areces. LSA, MC and FN are supported by a postdoctoral contract from the CSIC (JAEDOC-012), and predoctoral contracts from the MICINN (BES-2008-005457) and (AP2009-0349), respectively.

References

Aglyamova GV, Agarwala S. Gene expression analysis of the hedgehog signaling cascade in the chick midbrain and spinal cord. Developmental Dynamics 2007;236:1363–73.

Allen BL, Song JY, Izzi L, Althaus IW, Kang JS, Charron F, et al. Overlapping roles and collective requirement for the coreceptors GAS1, CDO, and BOC in SHH pathway function. Developmental Cell 2011;20:775–87.
Bae GU, Domene S, Roessler E, Schachter K, Kang JS, Muenke M, et al. Mutations in CDON, encoding a hedgehog receptor, result in holoprosencephaly and defective interactions with other hedgehog receptors. American Journal of Human Genetics 2011;89:231–40.
Bae GU, Kim BG, Lee HJ, Oh JE, Lee SJ, Zhang W, et al. Cdo binds Abl to promote p38alpha/beta mitogen-activated protein kinase activity and myogenic differentiation. Molecular and Cellular Biology 2009;29:4130–43.
Bergeron SA, Tyurina OV, Miller E, Bagas A, Karlstrom RO. Brother of cdo (umleitung) is cell-autonomously required for Hedgehog-mediated ventral CNS patterning in the zebrafish. Development 2011;138:75–85.
Callejo A, Bilioni A, Mollica E, Gorfinkiel N, Andres G, Ibanez C, et al. Dispatched mediates Hedgehog basolateral release to form the long-range morphogenetic gradient in the Drosophila wing disk epithelium. Proceedings of the National Academy of Sciences of the United States of America 2011;108:12591–8.
Camp D, Currie K, Labbe A, van Meyel DJ, Charron F. Ihog and Boi are essential for Hedgehog signaling in Drosophila. Neural Development 2010;5:28.
Cole F, Krauss RS. Microform holoprosencephaly in mice that lack the Ig superfamily member Cdon. Current Biology 2003;13:411–5.
Cole F, Zhang W, Geyra A, Kang JS, Krauss RS. Positive regulation of myogenic bHLH factors and skeletal muscle development by the cell surface receptor CDO. Developmental Cell 2004;7:843–54.
Connor RM, Allen CL, Devine CA, Claxton C, Key B. BOC, brother of CDO, is a dorsoventral axon-guidance molecule in the embryonic vertebrate brain. Journal of Comparative Neurology 2005;485:32–42.
Fabre PJ, Shimogori T, Charron F. Segregation of ipsilateral retinal ganglion cell axons at the optic chiasm requires the Shh receptor Boc. Journal of Neuroscience 2010;30:266–75.
Hartman TR, Zinshteyn D, Schofield HK, Nicolas E, Okada A, O'Reilly AM. Drosophila Boi limits Hedgehog levels to suppress follicle stem cell proliferation. The Journal of Cell Biology 2010;191:943–52.
Izzi L, Levesque M, Morin S, Laniel D, Wilkes BC, Mille F, et al. Boc and Gas1 each form distinct Shh receptor complexes with Ptch1 and are required for Shh-mediated cell proliferation. Developmental Cell 2011;20:788–801.
Kang JS, Bae GU, Yi MJ, Yang YJ, Oh JE, Takaesu G, et al. A Cdo-Bnip-2-Cdc42 signaling pathway regulates p38alpha/beta MAPK activity and myogenic differentiation. The Journal of Cell Biology 2008;182:497–507.
Kang JS, Feinleib JL, Knox S, Ketteringham MA, Krauss RS. Promyogenic members of the Ig and cadherin families associate to positively regulate differentiation. Proceedings of the National Academy of Sciences of the United States of America 2003;100:3989–94.
Kang JS, Gao M, Feinleib JL, Cotter PD, Guadagno SN, Krauss RS. CDO: an oncogene-, serum-, and anchorage-regulated member of the Ig/fibronectin type III repeat family. The Journal of Cell Biology 1997;138:203–13.
Kang JS, Mulieri PJ, Hu Y, Taliana L, Krauss RS. BOC, an Ig superfamily member, associates with CDO to positively regulate myogenic differentiation. EMBO Journal 2002;21:114–24.
Kang JS, Mulieri PJ, Miller C, Sassoon DA, Krauss RS. CDO, a robo-related cell surface protein that mediates myogenic differentiation. The Journal of Cell Biology 1998;143:403–13.
Kang JS, Yi MJ, Zhang W, Feinleib JL, Cole F, Krauss RS. Netrins and neogenin promote myotube formation. The Journal of Cell Biology 2004;167:493–504.
Kavran JM, Ward MD, Oladosu OO, Mulepati S, Leahy DJ. All mammalian Hedgehog proteins interact with cell adhesion molecule, down-regulated by oncogenes (CDO) and brother of CDO (BOC) in a conserved manner. Journal of Biological Chemistry 2010;285:24584–90.
Krauss RS. Regulation of promyogenic signal transduction by cell–cell contact and adhesion. Experimental Cell Research 2010;316:3042–9.
Lee EY, Ji H, Ouyang Z, Zhou B, Ma W, Vokes SA, et al. Hedgehog pathway-regulated gene networks in cerebellum development and tumorigenesis. Proceedings of the National Academy of Sciences of the United States of America 2010;107:9736–41.
Lu M, Krauss RS. N-cadherin ligation, but not Sonic hedgehog binding, initiates Cdo-dependent p38alpha/beta MAPK signaling in skeletal myoblasts. Proceedings of the National Academy of Sciences of the United States of America 2010;107:4212–7.
Lum L, Yao S, Mozer B, Rovescalli A, Von Kessler D, Nirenberg M, et al. Identification of Hedgehog pathway components by RNAi in Drosophila cultured cells. Science 2003;299:2039–45.
McGlinn E, van Bueren KL, Fiorenza S, Mo R, Poh AM, Forrest A, et al. Pax9 and Jagged1 act downstream of Gli3 in vertebrate limb development. Mechanisms of Development 2005;122:1218–33.
McLellan JS, Zheng X, Hauk G, Ghirlando R, Beachy PA, Leahy DJ. The mode of Hedgehog binding to Ihog homologues is not conserved across different phyla. Nature 2008;455:979–83.
Ming JE, Roessler E, Muenke M. Human developmental disorders and the Sonic hedgehog pathway. Molecular Medicine Today 1998;4:343–9.
Mulieri PJ, Kang JS, Sassoon DA, Krauss RS. Expression of the boc gene during murine embryogenesis. Developmental Dynamics 2002;223:379–88.
Mulieri PJ, Okada A, Sassoon DA, McConnell SK, Krauss RS. Developmental expression pattern of the cdo gene. Developmental Dynamics 2000;219:40–9.
Oh JE, Bae GU, Yang YJ, Yi MJ, Lee HJ, Kim BG, et al. Cdo promotes neuronal differentiation via activation of the p38 mitogen-activated protein kinase pathway. The FASEB Journal: Official Publication of the Federation of American Societies for Experimental Biology 2009;23:2088–99.
Okada A, Charron F, Morin S, Shin DS, Wong K, Fabre PJ, et al. Boc is a receptor for sonic hedgehog in the guidance of commissural axons. Nature 2006;444:369–73.
Sanchez-Camacho C, Bovolenta P. Autonomous and non-autonomous Shh signalling mediate the in vivo growth and guidance of mouse retinal ganglion cell axons. Development 2008;135:3531–41.
Sanchez-Camacho C, Bovolenta P. Emerging mechanisms in morphogen-mediated axon guidance. BioEssays: News and Reviews in Molecular, Cellular and Developmental Biology 2009;31:1013–25.
Takaesu G, Kang JS, Bae GU, Yi MJ, Lee CM, Reddy EP, et al. Activation of p38alpha/beta MAPK in myogenesis via binding of the scaffold protein JLP to the cell surface protein Cdo. The Journal of Cell Biology 2006;175:383–8.
Tenzen T, Allen BL, Cole F, Kang JS, Krauss RS, McMahon AP. The cell surface membrane proteins Cdo and Boc are components and targets of the Hedgehog signaling pathway and feedback network in mice. Developmental Cell 2006;10:647–56.
Yam PT, Langlois SD, Morin S, Charron F. Sonic hedgehog guides axons through a noncanonical, Src-family-kinase-dependent signaling pathway. Neuron 2009;62:349–62.
Yan D, Wu Y, Yang Y, Belenkaya TY, Tang X, Lin X. The cell-surface proteins Dally-like and Ihog differentially regulate Hedgehog signaling strength and range during development. Development 2010;137:2033–44.
Yao S, Lum L, Beachy P. The ihog cell-surface proteins bind Hedgehog and mediate pathway activation. Cell 2006;125:343–57.
Zhang W, Hong M, Bae GU, Kang JS, Krauss RS. Boc modifies the holoprosencephaly spectrum of Cdo mutant mice. Disease Models & Mechanisms 2011;4:368–80.
Zhang W, Kang JS, Cole F, Yi MJ, Krauss RS. Cdo functions at multiple points in the Sonic Hedgehog pathway, and Cdo-deficient mice accurately model human holoprosencephaly. Developmental Cell 2006;10:657–65.
Zhang W, Mulieri PJ, Gaio U, Bae GU, Krauss RS, Kang JS. Ocular abnormalities in mice lacking the immunoglobulin superfamily member Cdo. The FEBS Journal 2009;276:5998–6010.
Zheng X, Mann RK, Sever N, Beachy PA. Genetic and biochemical definition of the Hedgehog receptor. Genes & Development 2010;24:57–71.

OPEN ACCESS Freely available online

PLoS one

Pαx6 Expression in Postmitotic Neurons Mediates the Growth of Axons in Response to SFRP1

Alvaro Sebastián-Serrano[1], Africa Sandonis[2], Marcos Cardozo[2], Fernanda M. Rodríguez-Tornos[1], Paola Bovolenta[2], Marta Nieto[1]*

1 Centro Nacional de Biotecnología, Consejo Superior de Investigaciones Científicas, Madrid, Spain, **2** Centro de Biologia Molecular Severo Ochoa, Consejo Superior de Investigaciones Científicas-UAM, and CIBER de Enfermedades Raras, Madrid, Spain

Abstract

During development, the mechanisms that specify neuronal subclasses are coupled to those that determine their axonal response to guidance cues. Pax6 is a homedomain transcription factor required for the specification of a variety of neural precursors. After cell cycle exit, *Pax6* expression is often shut down in the precursor progeny and most postmitotic neurons no longer express detectable levels of the protein. There are however exceptions and high Pax6 protein levels are found, for example, in postmitotic retinal ganglion cells (RGCs), dopaminergic neurons of the olfactory bulb and the limbic system in the telencephalon. The function of Pax6 in these differentiating neurons remains mostly elusive. Here, we demonstrate that Pax6 mediates the response of growing axons to SFRP1, a secreted molecule expressed in several Pax6-positive forebrain territories. Forced expression of *Pax6* in cultured postmitotic cortical neurons, which do not normally express *Pax6*, was sufficient to increment axonal length. Growth was blocked by the addition of anti-SFRP1 antibodies, whereas exogenously added SFRP1 increased axonal growth of Pax6-transfected neurons but not that of control or untransfected cortical neurons. In the reverse scenario, shRNA-mediated knock-down of *Pax6* in mouse retinal explants specifically abolished RGCs axonal growth induced by SFRP1, but had no effect on RGCs differentiation and it did not modify the effect of Shh or Netrin on axon growth. Taken together these results demonstrate that expression of Pax6 is necessary and sufficient to render postmitotic neurons competent to respond to SFRP1. These results reveal a novel and unexpected function of *Pax6* in postmitotic neurons and situate *Pax6* and SFRP1 as pair regulators of axonal connectivity.

Citation: Sebastián-Serrano A, Sandonis A, Cardozo M, Rodríguez-Tornos FM, Bovolenta P, et al. (2012) Pαx6 Expression in Postmitotic Neurons Mediates the Growth of Axons in Response to SFRP1. PLoS ONE 7(2): e31590. doi:10.1371/journal.pone.0031590

Editor: Amit Singh, University of Dayton, United States of America

Received June 15, 2011; **Accepted** January 16, 2012; **Published** February 16, 2012

Funding: This work was funded by the (MICINN) Ministerio de Ciencia e Innovación grants (SAF2008-00211; PIE-200820I166; BFU2007-61774), and a grant from the Spanish Comunidad de Madrid CCG08-CSIC/SAL-3464. ASS from the MICINN (BES-2006-13901). FMR holds a fellowship from La Caixa foundation. The funders had no role in study design, data collection and analysis, decision to publish, or preparation of the manuscript.

Competing Interests: The authors have declared that no competing interests exist.

* E-mail: mnlopez@cnb.csic.es

Introduction

The selective response of axons to elongation and guidance cues encountered along their paths enables the precise formation of neuronal circuits and the formation of topographic maps. During development, mechanisms that specify neuronal subclasses are coupled to those that specify their axonal response through the selective expression of transcription factors.

Pax6 is a homeodomain transcription factor expressed in several territories of the developing nervous system, mostly in the proliferative regions containing neural precursors [1]. The vast majority of the neural progeny of these precursors including neurons of the dorsal cortical plate or neural stem cell (NSCs) derived neurons, shut down *Pax6* expression upon exiting the cell cycle. Consequently, very few postmitotic populations express *Pax6*. Notable examples are the retinal ganglion cells (RGCs), the dopaminergic neurons of the olfactory bulb and certain neurons in the basal telencephalon and midbrain [2,3,4,5]. While the role of *Pax6* in neural precursors has been widely explored, revealing a central function in cell fate specification and cell cycle regulation [5,6,7,8,9], less attention has been paid to its functions in postmitotic neurons, with the major exception of a recent study demonstrating that Pax6 is needed for the survival of dopaminergic neurons in the olfactory bulb [10].

RGCs are one of the best-characterized postmitotic populations that express *Pax6* [11]. *Pax6* expression in both developing and mature RGCs is graded, with higher levels in the ventro-temporal distal cells and lower in the proximal domains [11]. These two differentially expressing *Pax6* populations project to distinct non-overlapping and complementary topographic regions of the superior culliculus and lateral geniculate nucleus (LGN), which suggests that *Pax6* may contribute to control axon targeting. Indeed, RGCs of mice overexpressing *Pax6* show disrupted axonal trajectories and abnormal bundle formation [12], whereas changes in Pax6 expression in the RGCs correlate with axonal regeneration in the optic nerve of lizards and zebrafish [13]. Still, there is no information on whether *Pax6* is directly involved in the control of axon growth and what guidance cues, if any, depend upon its activity.

Secreted Frizzled-Related Protein 1 (SFRP1) is one of the factors known to stimulate the directional growth of RGCs axons in *Xenopus* and chick retina. This activity is independent of Wnt signaling and modulated by extracellular matrix molecules [14,15]. Mouse *Sfrp1* is expressed in several structures of the

embryonic and adult eye and brain, including the pigmented retina, cornea, ciliary bodies, lens epithelium, the prospective thalamus and the proliferative regions of the telencephalon [14,16,17,18,19]. The SFRP1 distribution often coincides with that of Pax6 or decorates the axonal pathways of Pax6 expressing neurons [14,16,17,18,19], raising the possibility of a functional relationship between the two molecules.

Here we show that expression of *Pax6* in neuronal postmitotic populations is necessary and sufficient to confer neurons with a positive response to SFRP1. Over-expression of *Pax6* rendered cultured cortical neurons competent to respond to endogenous and exogenous SFRP1. Conversely, knock-down of *Pax6* in mouse retinal explants abolishes RGC axonal growth induced by SFRP1 without affecting RGC differentiation or their axonal response to a different guidance cue like sonic hedgehog (Shh) or Netrin. These results suggest that *Pax6* and SFRP1 are pair regulators of axonal connectivity in the retina and reveal a new function of *Pax6* in the postmitotic populations.

Results

1. *Pax6* induces axonal growth in postmitotic neurons

The majority of postmitotic neurons, including those derived from telencephalic *Pax6* positive precursors, such as cerebral cortical neurons or neurons derived from cortical neural stem cells (NSCs), do not express *Pax6* [2] (Fig. S1a). To test the consequences of *Pax6* expression in postmitotic populations, we forced its expression in neurons derived from mouse NSCs. NSCs grown as neurospheres were nucleofected with CAG-empty vector or CAG-*Pax6*, together with a CAG-*GFP* that allowed the visualization of transfected cells. GFP staining demonstrated efficient transfection by FACs cytometry (Fig. S1b) and immunostaining of plated cells confirmed that cells transfected with CAG-*Pax6*, but not those transfected with the empty vector, had nuclear Pax6 protein expression (Fig. S1a). Plated transfected cells were then allowed to differentiate for 9 days to analyze their differentiation and morphology. GFP neurons identified by β-tubulin III expression show an advance differentiated asymmetrical polarized morphology, both in control and Pax6 transfected cells (Fig. 1 c), and the longer neurite was identified as the axon by MAP1b staining (not shown), a selective marker of the distal part of the growing axon [24]. Overexpression of *Pax6* alone was sufficient to promote axonal extension compared to control neurons (Fig. 1a). Quantitative analysis of β-tubulin III positive-projections confirmed a significant increment of the axonal length from neurons transfected with CAG-*Pax6* both at 6 and 9 days of culture (Fig. S2 and Fig. 1a, respectively). Similar results were obtained upon quantification of MAP1b projecting axons (not shown). The total number and extension of the additional neurites was not affected (Figure S1c).

Several reports have shown that *Pax6* over-expression induces precursor cells to exit the cell cycle and differentiate [9,25]. To discard the possibility that increased axonal length was a consequence of a premature exit from cell cycle and, thus, of an extended time of differentiation, we restricted our study to those cells that were leaving the cell cycle at similar times. To visualize cohorts of nascent neurons, BrdU was added on the second day of culture and extensively washed after 12 h. Analysis of BrdU-positive neurons on the ninth day of culture confirmed that the axons of the *Pax6* expressing population were significantly longer than those of cells transfected with mock vector (Fig. 1b and c). Restricting to this cohort of BrdU neurons correlated with a higher increment in axonal length as expected from the analysis of a more homogenous population (compared Fig. 1a and b). This demonstrates that the effect in axonal growth is unrelated to an early exit from the cell cycle. To strengthen this conclusion, we over-expressed *Pax6* in non-proliferating primary cortical neurons and quantified the length of MAP1b projections, obtaining similar results (Fig. 1d and e), although the increment of outgrowth was less evident than that observed in NCSs, likely owing to the heterogeneity of primary differentiating neurons. Together, these experiments demonstrated that *Pax6* expression in differentiated neurons stimulates process elongation by a cell cycle independent mechanism.

2. *Pax6* mediates the axonal response to SFRP1

SFRP1 is expressed by the neural precursors of the ventricular zone (VZ) of the dorsal telencephalon, which give rise to both cortical neurons and NSCs [2]. We confirmed that neural precursor cells cultivated *in vitro* also express detectable levels of the SFRP1 protein (Fig. 2a). We therefore postulated that SFRP1 produced and secreted in the culture by undifferentiated cells was responsible for the selective axonal growth of *Pax6*-transfected neurons. Addition of antibodies against SFRP1 to the culture media two days after NSCs transfection completely blocked *Pax6*-induced axonal growth, leading to processes with a length undistinguishable from that of control cells (Fig. 2b). This result was specific since addition of control unrelated antibodies had no effect (Fig. 2b). This data indicated that *Pax6* stimulated the growth of NSCs derived neurons in response to endogenous SFRP1 produced in the *in vitro* culture.

To support this conclusion, we next assayed the effects of exogenously added SFRP1 upon forced expression of *Pax6* in primary cortical neurons or neurons derived from NSCs. Purified, recombinant SFRP1 was added to the neuronal culture after transfection and the early axonal response was evaluated after two or three days in cortical neurons and NSCs, respectively. Notably, addition of exogenous SFRP1 to control neurons had no effect on the length of their axons, but stimulated, in a dose dependent manner, the elongation of those belonging to Pax6-positive neurons (Fig. 2c, d and Fig. S3). Therefore, *Pax6* appears to be necessary and sufficient to confer cortical neurons with the competence to respond to SFRP1 of exogenous or endogenous origin.

Postmitotic RGCs express Pax6 [4] and their axons respond to SFRP1 [14]. We therefore asked whether this response was similarly dependent on Pax6. To this end we decided to knock-down *Pax6* using shRNA lentiviral constructs. Effective knock-down of the Pax6 protein by the shRNA lentiviral constructs was first evaluated in cultured mammalian CHO cells transfected with *Pax6* (See Methods and Fig. S1d). Selected constructs were thereafter targeted to the retina of E13.5 embryos by *in utero* electroporation. A CAG-GFP plasmid was co-electroporated to visualize targeted cells and their axons. The expression of Pax6 and the fate of the targeted cells were analyzed at E19.5 in histological sections. In retinas targeted with either control or *Pax6* shRNA, the majority of GFP-positive cells were located in the inner layers, corresponding with the normal location of RGCs (Fig. 3a and b). Double staining with anti-Pax6 and -GFP antibodies demonstrated strong expression of Pax6 in GFP-positive control cells but undetectable levels in the majority of cells electroporated with the *Pax6*-shRNA (Fig. 3a). Quantification of the number of GFP and Pax6 positive cells demonstrated that the selected shRNA resulted in efficient down-modulation of *Pax6* in the mouse retina cells (Fig. 3a, graph). No significant changes were observed in the number of apoptotic, Caspase3-positive cells [26] (Fig. 3a). Because *Pax6* is involved in cell fate decisions and cell cycle exit [4,9,27] we next analyzed the molecular identity of the

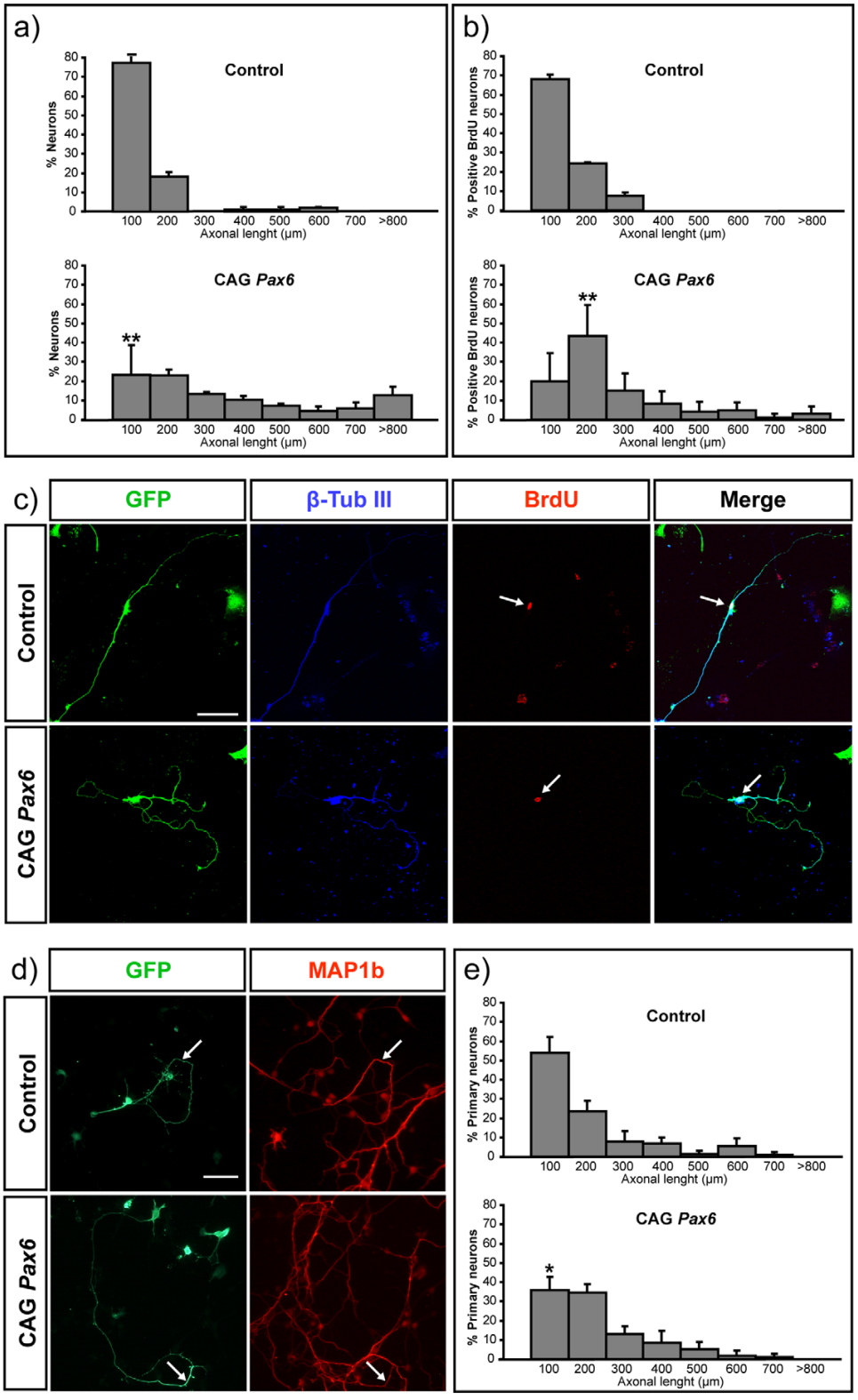
a)
Control
% Neurons
Axonal lenght (µm)
CAG Pax6
**
b)
Control
% Positive BrdU neurons
CAG Pax6
**
c)
GFP
β-Tub III
BrdU
Merge
Control
CAG Pax6
d)
GFP
MAP1b
e)
Control
% Primary neurons
CAG Pax6
*

Figure 1. Ectopic expression of *Pax6* stimulates axonal growth in cortical neurons. NSCs were nucleofected with CAG-empty vector or CAG-*Pax6* and co-electroporated with CAG-*GFP*. **a**) The graph shows the percentage of nucleofected neurons with respect to their axonal length after 9 days of differentiation. Over-expression of *Pax6* increments the axonal length compared with control neurons. **b**) The graph shows quantification of the axonal length of a cohort of BrdU positive neurons. **c**) Nucleofected neurons were identified by the specific expression of β-tubulin III and GFP. BrdU staining allowed us to compared neurons of similar birth dates. The effect in axonal growth is unrelated to an early exit from the cell cycle. Arrows point to BrdU stained nuclei. Bar indicates 50 μm. **d**) Cortical primary neurons were also transfected with CAG-empty vector or CAG-*Pax6*, and with CAG-*GFP*. Transfected primary axons were identified by GFP and MAP1b staining. Arrows indicate the distal part of the axon stained by MAP1b. Bar indicates 70 μm. **e**) The graph shows the percentage of primary neurons with respect to their axonal length. Data are expressed as the mean ± SD. (*) $p<0.05$; (**) $p<0.01$.
doi:10.1371/journal.pone.0031590.g001

GFP electroporated cells using two RGC specific markers: Islet-1/2, that marks most of RGCs [28], and Brn3, which labels only a subpopulation [29]. In control retinas, an important proportion of GFP positive cells showed expression of Islet-1/2 and Brn3, with the expected pattern. Down-regulation of *Pax6* did not block RGC generation but somehow favored the increase of the number of Islet-1/2 positive cells, which was less clearly correlated with that of *Brn3* positive cells (Fig. 3b). This moderated shift in the proportion of RGCs cells might be associated to the reported effects in cell cycle exit [4,9,27], rather than on selective cell death, which was invariant (Fig. 3a).

Given that shRNA-mediated knock-down of *Pax6* in E13.5 retinal precursors did not interfere with RGC generation and organization, we examined the response of *Pax6* deficient RGCs to SFRP1 [14]. Explants from E13.5 retinas electroporated *ex vivo* with control shRNA or shRNA constructs targeting *Pax6* were seeded on laminin-coated coverslips, stimulated with SFRP1 and fixed 24 h after. Staining with anti-β-tubulin III confirmed that, as in chick and *Xenopus* [14], SFRP1 stimulated axonal outgrowth and extension from control mouse retinas, increasing the proportion of axons longer than 900 μm (Fig. 4a). Similarly, addition of SFRP1 to control electroporated retinal explants doubled the proportion of GFP-positive electroporated RGCs with axons longer than 200 μm (Fig. 4b), although the average length was appreciably shorter than that of axons from non-electroporated retinas (compare Fig. 4a and 4b). Likely, this is because

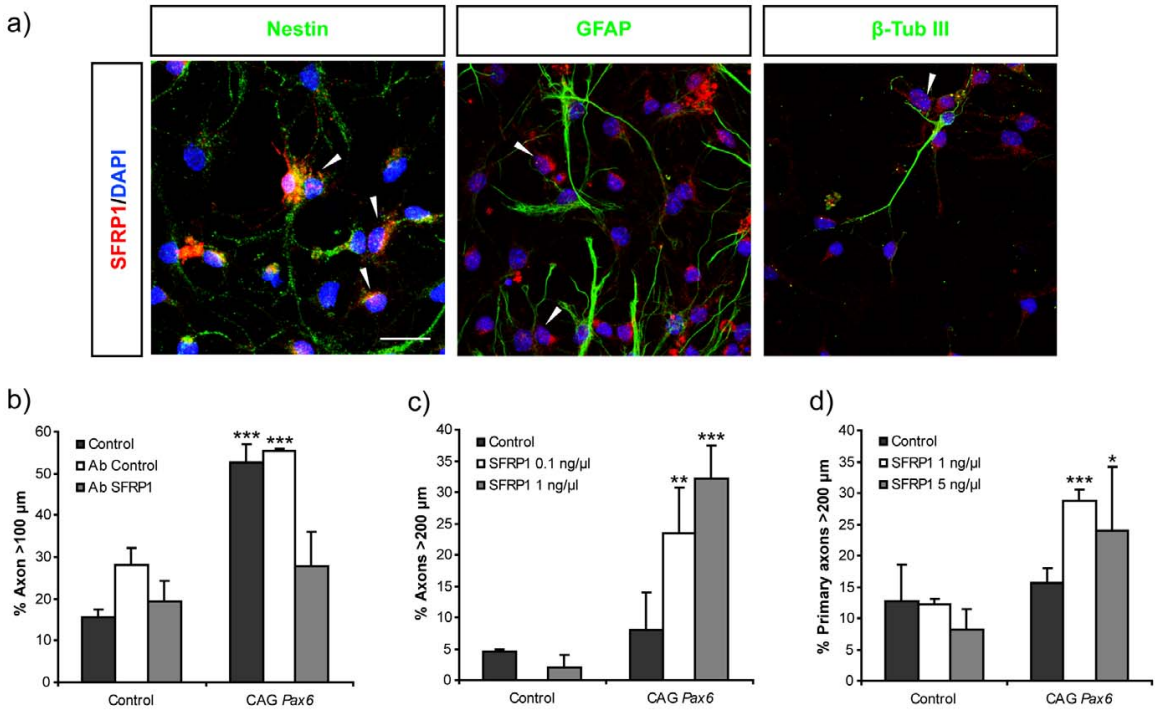

Figure 2. SFRP1 secreted by cortical cells *in vitro* is responsible for the axonal growth observed in *Pax6* over-expressing neurons. a) Immunofluorescence shows expression of SFRP1 (red) in differentiating, NSCs cultured for 5 days. Cells were double labeled with anti-nestin, GFAP and β-tubulin III. SFRP1 expression is found in the cytoplasma of Nestin-positive cells or in some with a low GFAP expression (arrowheads). No SFRP1 expression was found in cell with high GFAP levels or in β-tubulin III-positive cells. Bar represents 20 μm. **b**) The graphs show the percent of axons longer than 100 μm upon *Pax6* overexpression in NSCs when cultured in the presence or absence of control or anti-SFRP1 antibodies. Note that antibody against SFRP1 blocks axonal growth stimulated by the ectopic expression of *Pax6*. **c, d**) Response to increasing concentrations of purified recombinant SFRP1 in neurons derived from NSC c) or primary cortical neurons (d). NSCs (c) and primary neurons (d) were transfected with control empty CAG and CAG-*Pax6* vectors and stimulated with different concentrations of SFRP1.Addition of recombinant SFRP1 only stimulates the growth and elongation of axons of neurons ectopically expressing *Pax6*. Data are expressed as the mean ± SD. (*) $p<0.05$; (**) $p<0.01$; (***) $p<0.001$. Number of axons per condition >50 (n = 3).
doi:10.1371/journal.pone.0031590.g002

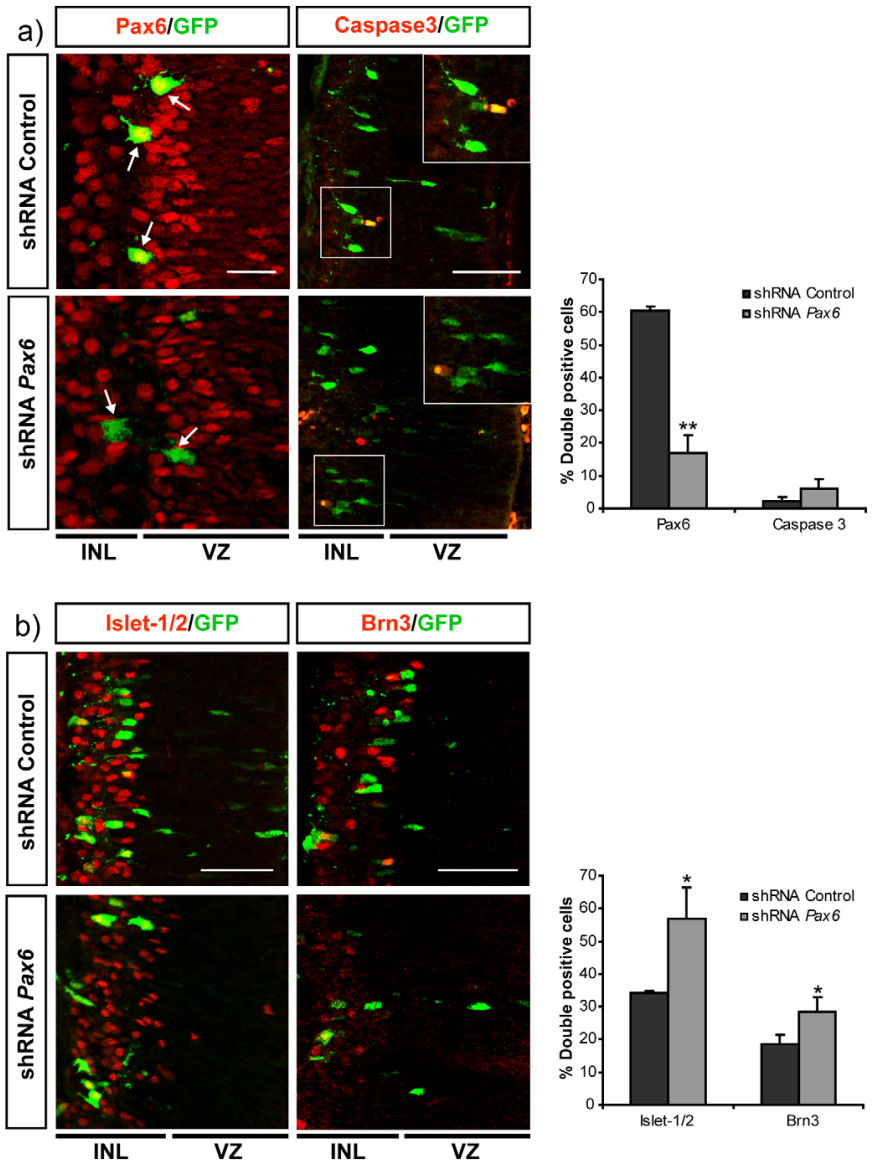

Figure 3. Knock-down of *Pax6* in the embryonic retina does not interfere with the generation of RGCs. Frontal cryostat sections of E19.5 retinas after electroporation at E13.5 with shRNAs constructs control and targeting *Pax6* and immunostained (red) for Pax6 and Caspase 3 (**a**) or Islet-1/2 and Brn3 (**b**) as indicated in the panels. Electroporated cells are visualized with GFP (green). The graphs show the quantification of the proportion of the double positive cells for the indicated marker. Note that shRNA efficiently target Pax6 without inducing cell death (a) or changes in expression of markers for postmitotic RGCs (b). Bar indicates 10 in (a) and 40 μm in (b). Data are expressed as the mean ± SD. (*) $p<0.05$; (**) $p<0.01$. Number of axons per condition >60 (n = 3). INL, inner layer; VZ, ventricular zone.
doi:10.1371/journal.pone.0031590.g003

targeted cells only account for newly generated RGCs [30]. Knock-down of *Pax6* in RGCs prevented their response to SFRP1 (Fig. 4b) but did not interfere with axonal initiation because the total number of axons per explants was not significantly different in control and *Pax6* shRNA electroporated retinas in the presence or absence of SFRP1 (not shown). Furthermore, in non-stimulated explants, the length of GFP positive axons was similar in both control and *Pax6* shRNA electroporated retinas (Fig. 4b). Notably, axonal growth was restored when knock-down was attempted in the presence of a silent mutant form of *Pax6* resistant to shRNA, excluding off-target effects of the shRNA constructs (not shown). Furthermore, *Pax6* knock-down had no effect on the response of dorsal retinal explants to exogenously added Shh (Fig. 5a and 5b) or Netrin1 (Fig. 5c), additional axon guidance cues known to modify RGC axon growth [23,31,32]. These results indicated that the expression of *Pax6* in mouse RGCs prompt axon extension

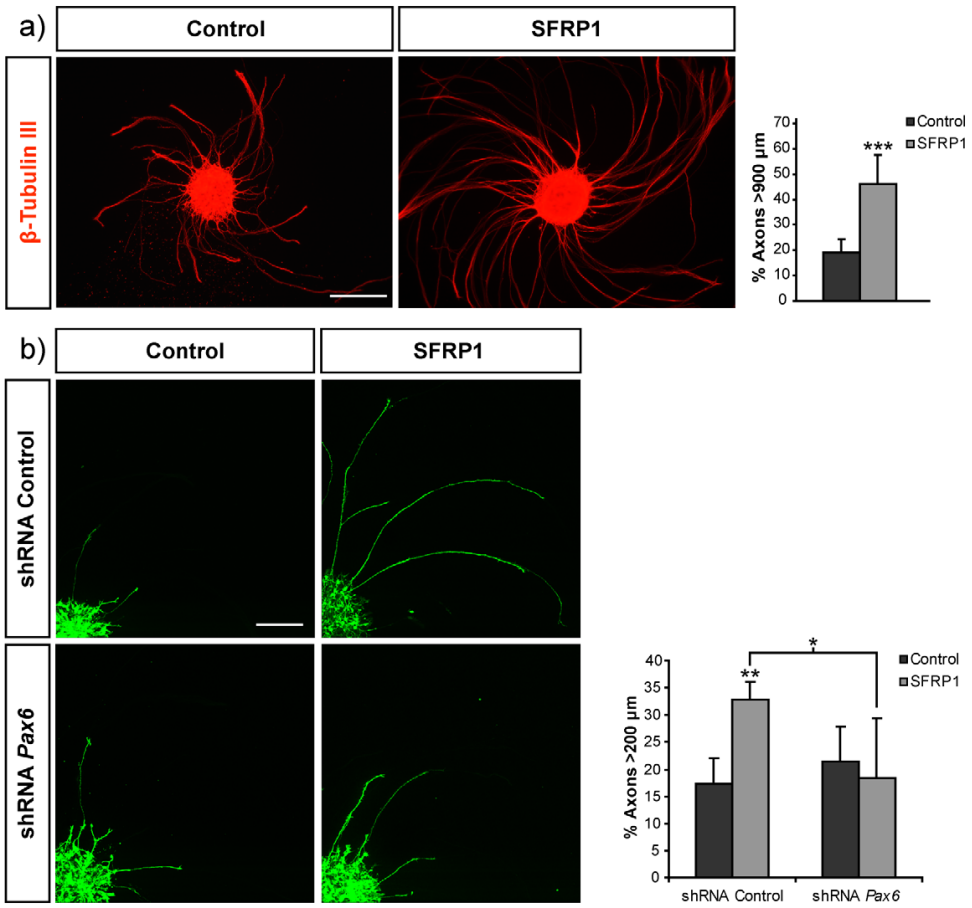

Figure 4. Knock-down of *Pax6* blocks SFRP1 stimulated growth of retinal axons. a) Low magnification images (a) and confocal micrographs (b) of explants from control (a) or electroporated retinal explants (b) seeded onto laminin coated coverslip and cultured in the absence or presence of recombinant SFRP1 as indicated in the panels. Explants in (a) were stained with β-tubulin III whereas those in (b) were co-electroporated with CAG-GFP and shRNA control or shRNA targeting *Pax6* and axons were visualized by GFP expression. Graph shows quantification of the proportion of total axon longer than 900 (a) or 200 (b) µm. Note that knocking-down *Pax6* inhibits the axonal response stimulated by SFRP1. Bar indicates 300 (a) and 150 µm (b). Data are expressed as the mean ± SD. (*) $p<0.05$ comparing stimulated populations; (**) $p<0.01$ and (***) $p<0.001$ compared with control.
doi:10.1371/journal.pone.0031590.g004

specifically in response to SFRP1, whereas it does not influence the response to Shh and Netrin1.

The Fz2 receptor appears to mediate the axonal response to SFRP1 in RGCs [14]. Thus, the selective induction of the expression of this receptor appeared as possible feasible mechanism of the action of Pax6. However, equal expression of Fz2 protein was detected in the axons of RGCs electroporated with either control or shRNAs targeting Pax6. Similarly quantitative PCR analysis did not reveal significant differences in the mRNA levels of *Fz2* from control and Pax6 overexpressing neurospheres or primary neurons (Fig. S4). Similarly, there were no significant changes in the expression of other members of the Frizzled receptor family expressed in the retina, [33], including Fz3, Fz5, Fz6 and Fz7 (Fig. S4). We therefore consider the possibility that Pax6 could regulate the expression of members of the family of Unc receptors, Unc5a, Unc5b, Unc5c and Unc5d, that contain SFRP1 binding domains [34] or that of other receptors implicated in axonal guidance like Neuropilin1 or PlexinD1 [35]. However, Pax6 overexpression in primary cortical cells did not induce significant changes in the expression of any of these genes (Fig. S4), suggesting that other factors might be involved.Hence, the regulation of the expression any of these receptors does not underlie the specific response to SFRP1 triggered by Pax6. Altogether, our results demonstrate that *Pax6* is necessary and sufficient to confer postmitotic differentiating neurons with the competence to respond to SFRP1, revealing a novel non neurogenic function of this pleiotropic transcription factor.

Discussion

Pax6 expression is crucial for dorsal-ventral and anterior-posterior patterning of the neural tube and controls neural precursor proliferation and fate decisions [13,36,37]. We herein demonstrated that expression of *Pax6* in postmitotic neurons is necessary and sufficient to provide axons with the competence to respond to SFRP1, a secreted molecule that can control growth

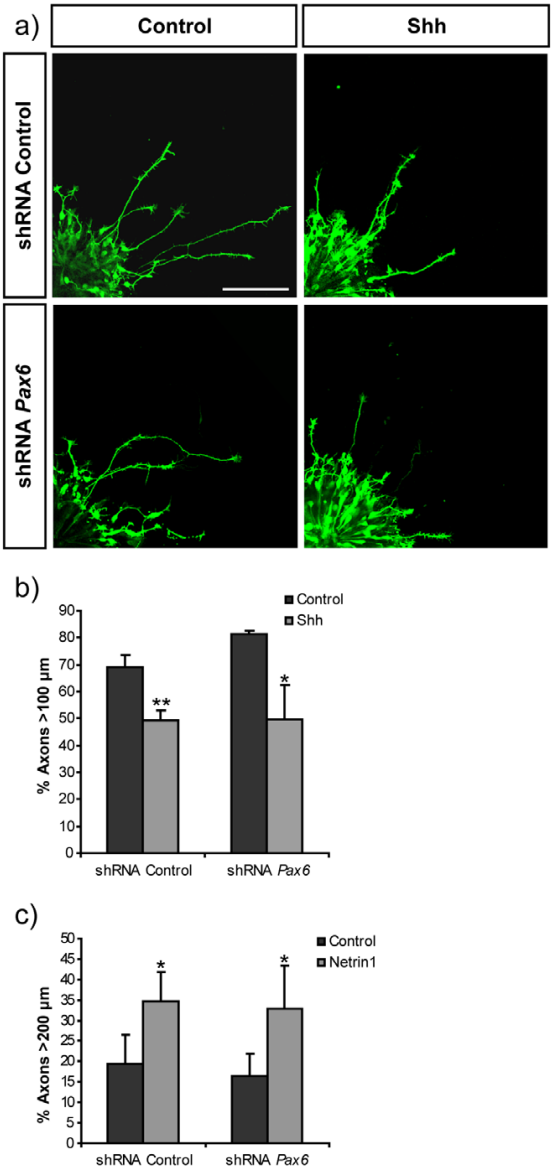

Figure 5. Knock-down of *Pax6* does not affect the response of retinal axons to Shh or Netrin 1. a) Micrographs show confocal images of GFP positive axons of retina explants co-electroporated with CAG-GFP and control shRNA or shRNA targeting Pax6. Explants were seeded onto laminin coated coverslip in the presence or absence of recombinant Shh. Bar indicates 100 µm. **b**) Graph shows quantification of the proportion of GFP positive axons longer than 100 µm in the presence or absence of recombinant Shh. **c**) Graph shows quantification of the proportion of GFP positive axons longer than 200 µm in the presence or absence of recombinant Netrin 1. Data are expressed as the mean ± SD. (*) $p<0.05$; (**) $p<0.01$.
doi:10.1371/journal.pone.0031590.g005

cone movements [14]. This conclusion is based on the observation that abrogation or activation of Pax6 expression in neuronsthat, respectively, normally do or do not express Pax6, correlates with the response of their axons to SFRP1. This novel activity adds up to the very limited examples of Pax6 functions in postmitotic neurons, namely the control of dopaminergic neuron survival via the regulation of Crystallin αA [10]. In progenitors, other recent studies have also pointed out non-neurogenic roles of Pax6, such as the downregulation of the neurotrophin receptor $p75^{NTR}$ [38]. Together, these studies consistently highlight alternative functions of this pleiotropic factor.

Although much progress has been made in defining the mechanisms directing the formation of brain circuitry, there is still much to learn about the precise coordination between axonal connectivity and the acquisition of neuronal identities, which, through the selective expression of certain specific transcription factors, specifies the interpretation of these signals. Indeed, the reported number of such transcription factors is still limited and needs to be expanded to obtain a truly comprehensive landscape of the determinants of neuronal connectivity. Moreover, the mechanisms that accurately synchronize acquisition of neuronal subtype identity with guidance molecule expression deserve further elucidation. Examples of this coordination are offered by the LIM homeodomain protein control of EphA receptor and ephrin-A ligand expression during motor neuron innervation of limb muscle [39]. Similarly, Lhx2/9 in the dorsal spinal cord directly regulates the expression of Rig-1 [40], a divergent member of the Robo family, required for midline crossing of commissural axons [41]. In the retina, expression of *Zic2* in the ventro-temporal retina determines ipsilateral identity of RGCs [42] and controls the behavior of their axons likely by regulating the expression of EphB1 [43], a specific guidance receptor implicated in ephrinB2-mediated repulsion of uncrossed axons at the optic chiasm midline [44]. However, genetic control of receptor expression is not always an evident explanation, and there are also multiple transcription factors shown to be critical in directing axonal trajectories by still unknown or alternative pathways. In the cerebral cortex for example, *Ctip2*, and *Satb2*, determine the final targets of corticospinal motor neurons and callosal projecting neurons, respectively [45,46,47,48,49] and recent studies report that these two cell populations differentially respond to Sema3A, a potent repellant of cortical axons [50]. Surprisingly, similar levels of Sema3A receptors are found in cells expressing Satb2 or Ctip2, and the selective response is proposed to be dependent on the control of the receptor's endocytic and signaling pathway [51].

In this scenario, our data provide an additional example of a transcription factor that selectively controls the response to axon guidance cues. Although we clearly demonstrated a relationship between Pax6 expression and response to SFRP1 in different neurons, we did not found an obvious mechanism to explain this relationship. In chick and *Xenopus*, SFRP1 binds to Fz2 to mediate axonal response [14]. Our experiments indicate the unlikely involvement of the Fz2 receptor and suggest other unknown mechanisms that we have been so far unable to decipher. There are several possible scenarios. Other yet undefined SFRP1 receptors or co-receptors might be involved. Pax6 might also control the expression of other molecules involved in the pathway downstream of SFRP1 response. Alternative Pax6 may regulate the expression of ECM molecules known to be needed to control SFRP1 response, such as laminin and fibronectin [14]. Previous microarray analysis of Pax6 mutants and cells over-expressing Pax6 makes way to these possibilities and have shown regulation of guidance molecules receptors such as the Netrin receptor Unc5h, PlexinA2 and EphA5, signal transduction molecules of the Wnt pathway such as Gpc3, or cell adhesion molecules such as tenascin C or cadherin 11 [52,53]. Notably, the screening of a phage display peptide library revealed that SFRP1 binds with high affinity to the peptide motif L/V-VDGRW-L/V, which is present

in Unc5H3 [34], although, whether the two proteins actually interact is still unknown.

Understanding the role of Pax6 and SFRP1 in the selective connectivity of neuronal subclasses may contribute to untangle a piece of the puzzle of brain circuits. In particular, in the retina, developing RGCs express different levels of Pax6 protein [11] and their axons travel in the vicinity of several anatomical domains of expression of SFRP1 that may serve as cue to establish their connectivity [15,18,54,55]. In regard to other *Pax6* positive postmitotic populations in the brain, as the ones referred above, *Sfrp1* expression patterns would be consistent with a possible role of the Pax6-SFRP1 pair in circuit formation [16,19]. However, although *Sfrp1* knock out mice have been generated and are viable, defects in axonal connectivity have not yet been investigated [16] and will require attention in the future, especially in relation to *Pax6*, as our results indicate.

Besides axon guidance, an additional interesting implication of our study is raised by the blocking experiments using anti-SFRP1 antibodies. Our data evidenced the secretion of endogenous SFRP1 by NSCs and differentiating primary cortical cells, which is consistent with the reported *Sfrp1* expression patterns in the developing and adult brain [19,56]. NCS express Pax6 both *in vivo* and *in vitro*, which suggests possible roles for the coordinated functions of both molecules in the physiology of NSCs and neural niches.

Methods

Animals

All animal procedures were approved by the National Center for Biotechnology Animal Care and Use Committee, in compliance with National and European Legislation (ID 080016). C57BL6 mice were obtained from Harlan Laboratories, Inc. (Indianapolis, US). Morning of the day of the appearance of the vaginal plug was defined as embryonic day (E) 0.5.

Antibodies, immunohistochemistry, histology

Mouse embryos were fixed with 4% paraformaldehyde (PFA) in 0.1 M phosphate-buffered saline (PBS; pH 7.4) and cryoprotected in 30% sucrose in PBS. 10–20 μm horizontal sections were produced and mounted on Superfrost plus microscope slides (Fisher Scientific, Pittsburgh, PA). Inmunostaining of tissue sections and explants, or cell cultures was performed as described [20] using the following antibodies: rabbit anti-GFP (Molecular probes, Eugene, OR, 1:500), mouse anti-β-tubulin III (Sigma-Aldrich, ST Louis, MO, 1:1000), rat anti-Bromodeoxiuridine (BrdU) (BD Biosciences, San Jose, CA, 1:250), mouse anti-Islet-1/2 (39.4D5 1:10) developed by T. Jessell and the monoclonal antibody anti-Nestin (Rat 401, 1:100) developed by S. Hockfield, were obtained from the Development Studies Hybridoma Bank developed under the auspices of the NICHD and maintained by The University of Iowa, Department of Biological Sciences, Iowa City, IA 52242, rabbit anti-SFRP1 (Abcam, Cambridge UK, 1:500), goat anti-Brn3 (C-13) (Santa Cruz Biotechnology, Inc., Santa Cruz, CA, 1:250), rabbit anti-Caspase3 (Cell Signaling Tech Inc, Danuers, MA, 1:500), rabbit anti-Pax6 (Covance, Princeton, NJ, 1:500), mouse anti-MAP1b (Covance, Princeton, NJ, 1:500), rabbit anti-Fz2 (Abcam, Cambridge, UK, 1:200), mouse anti-GFAP (Sigma-Aldrich, ST Louis, MO, 1:400), and Alexa Fluor 488-, 594- or 647-conjugated fluorescent secondary antibodies (Molecular probes, Eugene, OR, 1:500).

Epifluorescece and confocal microscopy

Confocal microscopy was performed with a TCS-SP5 (Leica Microsystems GmbH, Welzlar, Germany) Laser Scanning System. Tissue sections of 50 and 20 μm were analyzed by taking 0.2 μm serial optical sections with the LASAF v2.2.1 software (Leica Microsystems GmbH, Welzlar, Germany). Fluorescence microscopy was performed with a Leica DMRXA and images were captured with Leica CW4000 FISH Version V1.2 software.

DNA constructs and recombinant proteins

The hairpin sequences targeting *Pax6* were: TRCN0000075377:ICCGGCCTGAAGCAAGAATACAGGTACTCGAGTACCTGTATTCTTGCTTCAGGTTTTTG; ITRCN0000075376:ICCGGCATGGCAAACAACCTGCCTATCTCGAGATAGGCAGGTTGTTTGCCATGTTTTTG;ITRCN0000075375:ICCGGGACGGCATGTATGATAAACTACTCGAGTAGTTTATCATACATGCCGTCTTTTTG;ITRCN0000075374:ICCGGCCACTTCAACAGGACTCATTTCTCGAGAAATGAGTCCTGTTGAAGTGGTTTTTG.

Pax6 and green fluorescence protein (GFP) cDNAs were under the cytomegalovirus enhancer, chicken *β-actin* promoter, and rabbit *β-globin* poly (A) signal (CAG) (cytomegalovirus [CMV] and beta-actin) promoter. For knock-down experiments, a mixture of the selected shRNA lentiviral constructs (1 μg/μl) and pCAG-GFP (1 μg/μl) was used. For testing off-target effects, we co-electroporated a construct driving expression of a silent resistant form of *Pax6* (1 μg/μl; CAG-mut*Pax6*; see Text S1) and shRNA targeting *Pax6* (1 μg/μl) plasmids. *Pax6* lentiviral shRNA constructs were obtained from Sigma-Aldrich Inc. (St. Louis, MO). Purified recombinant SFRP1 protein was generated as previously described [21] and recombinant purified N-Shh (2.5 μg/ml) was a kind gift from Dr. Sebastian Pons [22].

In utero and *ex vivo* electroporation

In utero and *ex vivo* electroporations were performed as described previously [23]. E13.5 pregnant C57BL6 female mice were anesthetized by continuous inhalation of Isoflurane (Baxter. Deerfield, US). The abdomen was opened and the uterine horns exposed. The DNA solution containing 0.03% fast green in PBS was injected into one eye of each embryo using a pulled glass micropipette. The head of each embryo was placed between tweezer type electrodes (CUY 650 P5 Nepa GENE, Chiba, Japan) and five square electric pulses (38V, 50 ms) were passed at 1 sec intervals using an Electro Square Porator ECM 830 (BTX, Harvard Apparatus, Holliston, MA, USA). The wall and skin of the abdominal cavity were sutured and the embryos were allowed to develop normally until E16-P0. For the *ex vivo* electroporation the head of the E13.5 embryos were transfer to a dissecting dish where they were electroporated with the above conditions. Then, electroporated retinas were dissected and incubated in DMEM-F12 (Gibco, Invitrogen, Carlsbad, CA) supplemented with N2 (Gibco, Invitrogen, Carlsbad, CA) medium at 37°C, 5% CO_2 for 24 hours.

Retinal explants and analysis of axonal growth

Dorsal retinal microexplants were plated on glass coverslips coated with poly-D-Lys (50 μg/ml; Sigma-Aldrich, Co. St. Louis, MO) and laminin (10 μg/ml; Invitrogen, Carlsbad, CA) and grown for 24 hours in DMEM-F12 medium supplemented with N2 in the presence or absence of SFRP1 (2 ng/μl) or N-Shh (1 ng/μl). After 24 hours, explants were fixed in 4% PFA at RT for 30 minutes and immunostained with anti-β-tubulin III and anti-GFP antibodies. Axonal length was determined in confocal images employing LaserPix v.4 image software (Bio-Rad). In non-electroporated explants, axonal length was estimated by counting the number of β-tubulin III positive axons crossing 600 and 900 μm radius circumferences of a minimum of 100 axons in each

of three independent experiments (n = 3). For electroporated explants, we measured the length of each individual GFP positive axon from the edge of the explant up to the distal tip of the growth cone. Knock-down of *Pax6* in RGCs did not interfere with axonal initiation because the number of total axons per explants was not significantly different in control and *Pax6* shRNA electroporated retinas (not shown). It was also not affected by treatment with SFRP1, Netrin1 or Shh. For SFRP1 experiments at least 50 axons per condition in each independent experiments (n = 6) or 60 neurons per condition (n = 4) in Shh and Netrin1 experiments. We chose to specifically study SFRP1 response in dorsal explants because this population expresses high levels of Pax6 and is homogeneously composed of contra-laterally projecting axons facilitating the analysis of SFRP1 response.

Neurosphere culture and nucleofection

Dorsal telencephalons of E13.5 WT embryos were dissected and cells were dissociated employing trypsin and a flamed-tip, glass Pasteur pipette. Dissociated cells were cultured in DMEM-F12 supplemented with N2 (Gibco, Invitrogen, Carlsbad, CA), heparin, recombinant human basic fibroblast growth factor (FGF-2) (10 ng/ml; R&D Systems, Minneapolis, MN), and epidermal growth factor (EGF; 10 ng/ml; Gibco, Invitrogen, Carlsbad, CA). Neurosphere cultures were passage every 3 days by mechanical dissociation. Dissociated cells were transfected using the nucleofector (Amaxa Biosystems, Gaithersburg, MD) with 5 μg of a 1:1 mixture of CAG-GFP and CAG-Pax6 or CAG- empty vector. Nucleofection efficiency and GFP positive cells were analyzed by flow cytometer (Coulter Epix XL) and data were analyzed with the Win MIDI software. Nucleofected neurospheres were seeded on glass coverslips coated with poly-D-Lys and cultured in DMEM-F12 supplemented with N2, heparin and 1% fetal calf serum (FCS). Cells were fixed in 4% PFA at RT for 30 minutes, then immunostained with anti-β-tubulin III and anti-GFP antibodies. Axonal length was determined with the LaserPix v.4 image software (Bio-Rad, Richmond, CA) over images taken with a fluorescence microscopy Leica DMRXA. For analysis of the effects of *Pax6*, cells were fixed after 6 or 9 days in culture. To compare neurons that exit at the same time from the cell cycle, postmitotic neurons were labeled with a 12 h pulse of Bromo-deoxiuridine (BrdU, Sigma-Aldrich, ST Louis, MO) (0.5 ng/ml) in the media and subsequently extensively washed. For blocking the endogenous SFRP1 activity a mix of anti-SFRP1 antibodies (4 μg/ml dialyzed in PBS): rabbit anti-SFRP-1 and goat anti-SFRP-1 (H-90 and C-19; Santa Cruz Biotechnology, Inc., Santa Cruz, CA) or a control IgG (4 μg/ml, dialyzed in PBS; rabbit anti-p-αPAK Ser 199/204; Santa Cruz Biotechnology, Inc., Santa Cruz, CA) were added to the culture media after nucleofection. For stimulation experiments, SFRP1 was added to the media 24 h after the nucleofection and the early axonal growth measured 3 days after the addition of SFRP1.

Primary neurons culture and transfection

Dissociated cells from the dorsal telencephalon of E13.5 embryos were seeded onto 24 well Poly-D-Lys coated plates in Neurobasal media supplemented with B27 complement (Gibco, Invitrogen, Carlsbad, CA) and BrdU (0.5 ng/ml) to test proliferation. 24 h after seeding, cells where co-transfected with CAG-*Pax6* or the empty CAG- vector and CAG-GFP using lipofectamine 2000 (Invitrogen, Carlsbad, CA) and following manufacture procedure. Three days after transfection, cells were fixed with PFA 4%, and immunostained with anti-β-tubulin III and anti-GFP antibodies to measure their axonal length as describe next. GFP positive neurons did not incorporate BrdU demonstrating an effect on posmitotic neurons independent of cell cycle exit. As mentioned, SFRP1 was added to the media 24 h after transfection and the axons measured 2 days after the addition of the protein.

Quantification of axonal length

In neurons differentiated from NSC or primary neurons, we identified the axon by morphological criteria and the specific staining of MAP1b, selectively localized to the distal part of axonal projections [24], but not in neurites. As illustrated in Fig. 1d, staining with MAP1b allowed us to identify the axon in primary neurons, while GFP staining reveals transfected cells. In neurons derived from NSCs after 6 and 9 days of differentiation, a long projection neurite was always clearly observed (Fig. 1c) and quantified as an axon. Specific staining with MAP1b demonstrated that the axon was always the longest neurite projection (99% Map1b positive projections were the longest neurite in the cell (>100 cells counted). Accordingly, experiments in which we measure MAP1b or the morphological identified neurite gave equivalent results (compared results shown in Fig. 1e and Fig. 2). We measured the axonal length from the nucleus of the neurons to the distal end of the axon where the growth cone is localized. We analyzed a minimum of 50 axons per condition in four independent experiments (n = 4).

Statistical analysis

Quantitative results are expressed as the mean ± SD. Axonal length distributions of each population were compared using a Chi-square test. Differences in gene expression was analyzed were compared with Student's two-sample t test. P values are indicated in figure legends.

Supporting Information

Figure S1 Efficiency of *Pax6* overexpression and inhibition. a) Transfection of pCAG-*Pax6* in NSCs results in efficient overexpression of Pax6 proteins in NSC derived neurons. Pax6 proteins are not expressed normally in GFP positive CAG-control targeted neurons, but are ectopically expressed (yellow) in cells transfected with CAG-*Pax6* plasmid. Bar indicates 20 μm. **b**) Fluorescent-activating cell sorting (FACs) analysis demonstrates more than 20% transfection efficiency. **c**) Ectopic Pax6 expression in NSCs does not alter the total number of secondary and primary neurites per cell. The number of neurites, excluding the axon, was quantified 9 days after transfection. **d**) Transfection of shRNA lentiviral constructs efficiently suppresses the ectopic expression of Pax6 in CHO cells. CHO cells co-trasfected with CAG-Pax6; control shRNA and CAG-GFP show expression of Pax6 protein (red). Pax6 is down-modulated in cells transfected with CAG-*Pax6* and shRNAs targeting *Pax6*. Number of cells >100 (n = 3). Bar indicates 30 μm. Graph represents the proportion of GFP positive cells expressing Pax6 protein. Data are expressed as the mean ± SD. (***) $p<0.001$.
(TIF)

Figure S2 Ectopic expression of *Pax6* stimulates axonal growth in cortical neurons. NSCs were nucleofected with CAG-empty vector or CAG-*Pax6* and co-electroporated with CAG-*GFP*. Graph shows the percentage of nucleofected neurons with respect to their axonal length after 6 days of differentiation. Results are equivalent to those obtained at 9 days. Over-expression of *Pax6* increments the axonal length compare with control neurons. Data are expressed as the mean ± SD. (**) $p<0.01$.
(TIF)

Figure S3 SFRP1 stimulated axonal response in *Pax6* over-expressing neurons but not in the control population. Graph represents the population distribution of neurons with axons longer than 100 μm or more. Data are expressed as the mean ± SD. (**) $p<0.01$; (***) $p<0.001$.
(TIF)

Figure S4 Knock-down of *Pax6* did not affect the expression of Fz2 receptor. a) Micrographs show confocal images of GFP positives axons in retina explants that were electroporated with shRNA control or shRNA targeting *Pax6*, and with CAG-GFP. Both populations present low levels of Fz2 expression and a positive dotted pattern of Fz2 staining. GFP negative mature axons presented a stronger signal. Bar indicates 3 μm. **b**) Q-PCR detection of the relative expression of the mRNA of Fz1, Fz3, Fz5, Fz6, Unc5a, Unc5b, Unc5c, Unc5d, Neuropilin1 and PlexinD1 from primary cultured neurons. Expression levels are relative to GAPDH transcript and normalized to one control sample (see Text S2). There are no differences in the relative mRNA expression of these receptors in control and Pax6 transfected cells.
(TIF)

Text S1 cDNA sequence for the silent mutant form of *Pax6* resistant.
(DOCX)

Text S2 Methods for real-time quantitative RT-PCR (Q-PCR).
(DOCX)

Acknowledgments

We are grateful to S. Gutierrez-Erlandsson, R. Gutierrez, A. Morales and T. Poderoso for technical assistance.

Author Contributions

Conceived and designed the experiments: PB ASS MN. Performed the experiments: ASS MC AS FMR. Analyzed the data: ASS MC FMR. Contributed reagents/materials/analysis tools: AS. Wrote the paper: MN.

References

1. Georgala PA, Carr CB, Price DJ (2011) The role of Pax6 in forebrain development. Dev Neurobiol.
2. Stoykova A, Gruss P (1994) Roles of Pax-genes in developing and adult brain as suggested by expression patterns. J Neurosci 14: 1395–1412.
3. Marquardt T, Ashery-Padan R, Andrejewski N, Scardigli R, Guillemot F, et al. (2001) Pax6 is required for the multipotent state of retinal progenitor cells. Cell 105: 43–55.
4. Marquardt T, Gruss P (2002) Generating neuronal diversity in the retina: one for nearly all. Trends Neurosci 25: 32–38.
5. Hsieh YW, Yang XJ (2009) Dynamic Pax6 expression during the neurogenic cell cycle influences proliferation and cell fate choices of retinal progenitors. Neural Dev 4: 32.
6. Heins N, Malatesta P, Cecconi F, Nakafuku M, Tucker KL, et al. (2002) Glial cells generate neurons: the role of the transcription factor Pax6. Nat Neurosci 5: 308–315.
7. Hack MA, Sugimori M, Lundberg C, Nakafuku M, Gotz M (2004) Regionalization and fate specification in neurospheres: the role of Olig2 and Pax6. Mol Cell Neurosci 25: 664–678.
8. Ericson J, Rashbass P, Schedl A, Brenner-Morton S, Kawakami A, et al. (1997) Pax6 controls progenitor cell identity and neuronal fate in response to graded Shh signaling. Cell 90: 169–180.
9. Estivill-Torrus G, Pearson H, van Heyningen V, Price DJ, Rashbass P (2002) Pax6 is required to regulate the cell cycle and the rate of progression from symmetrical to asymmetrical division in mammalian cortical progenitors. Development 129: 455–466.
10. Ninkovic J, Pinto L, Petricca S, Lepier A, Sun J, et al. (2011) The transcription factor Pax6 regulates survival of dopaminergic olfactory bulb neurons via crystallin alphaA. Neuron 68: 682–694.
11. Baumer N, Marquardt T, Stoykova A, Ashery-Padan R, Chowdhury K, et al. (2002) Pax6 is required for establishing naso-temporal and dorsal characteristics of the optic vesicle. Development 129: 4535–4545.
12. Manuel M, Pratt T, Liu M, Jeffery G, Price DJ (2008) Overexpression of Pax6 results in microphthalmia, retinal dysplasia and defective retinal ganglion cell axon guidance. BMC Dev Biol 8: 59.
13. Rodger J, King CE, Lukehurst S, Chen PB, Dunlop SA, et al. (2006) Changing Pax6 expression correlates with axon outgrowth and restoration of topography during optic nerve regeneration. Neuroscience 142: 1043–1054.
14. Rodriguez J, Esteve P, Weinl C, Ruiz JM, Fermin Y, et al. (2005) SFRP1 regulates the growth of retinal ganglion cell axons through the Fz2 receptor. Nat Neurosci 8: 1301–1309.
15. Bovolenta P, Esteve P, Ruiz JM, Cisneros E, Lopez-Rios J (2008) Beyond Wnt inhibition: new functions of secreted Frizzled-related proteins in development and disease. J Cell Sci 121: 737–746.
16. Trevant B, Gaur T, Hussain S, Symons J, Komm BS, et al. (2008) Expression of secreted frizzled related protein 1, a Wnt antagonist, in brain, kidney, and skeleton is dispensable for normal embryonic development. J Cell Physiol 217: 113–126.
17. de Iongh RU, Abud HE, Hime GR (2006) WNT/Frizzled signaling in eye development and disease. Front Biosci 11: 2442–2464.
18. Leimeister C, Bach A, Gessler M (1998) Developmental expression patterns of mouse sFRP genes encoding members of the secreted frizzled related protein family. Mech Dev 75: 29–42.
19. Kim AS, Lowenstein DH, Pleasure SJ (2001) Wnt receptors and Wnt inhibitors are expressed in gradients in the developing telencephalon. Mech Dev 103: 167–172.
20. Cubelos B, Sebastian-Serrano A, Beccari L, Calcagnotto ME, Cisneros E, et al. (2010) Cux1 and Cux2 regulate dendritic branching, spine morphology, and synapses of the upper layer neurons of the cortex. Neuron 66: 523–535.
21. Esteve P, Trousse F, Rodriguez J, Bovolenta P (2003) SFRP1 modulates retina cell differentiation through a beta-catenin-independent mechanism. J Cell Sci 116: 2471–2481.
22. Alvarez-Rodriguez R, Barzi M, Berenguer J, Pons S (2007) Bone morphogenetic protein 2 opposes Shh-mediated proliferation in cerebellar granule cells through a TIEG-1-based regulation of Nmyc. J Biol Chem 282: 37170–37180.
23. Sanchez-Camacho C, Bovolenta P (2008) Autonomous and non-autonomous Shh signalling mediate the in vivo growth and guidance of mouse retinal ganglion cell axons. Development 135: 3531–3541.
24. Black MM, Slaughter T, Fischer I (1994) Microtubule-associated protein 1b (MAP1b) is concentrated in the distal region of growing axons. J Neurosci 14: 857–870.
25. Haubst N, Berger J, Radjendirane V, Graw J, Favor J, et al. (2004) Molecular dissection of Pax6 function: the specific roles of the paired domain and homeodomain in brain development. Development 131: 6131–6140.
26. Bahr M (2000) Live or let die - retinal ganglion cell death and survival during development and in the lesioned adult CNS. Trends Neurosci 23: 483–490.
27. Ouyang J, Shen YC, Yeh LK, Li W, Coyle BM, et al. (2006) Pax6 overexpression suppresses cell proliferation and retards the cell cycle in corneal epithelial cells. Invest Ophthalmol Vis Sci 47: 2397–2407.
28. Pak W, Hindges R, Lim YS, Pfaff SL, O'Leary DD (2004) Magnitude of binocular vision controlled by islet-2 repression of a genetic program that specifies laterality of retinal axon pathfinding. Cell 119: 567–578.
29. Erkman L, Yates PA, McLaughlin T, McEvilly RJ, Whisenhunt T, et al. (2000) A POU domain transcription factor-dependent program regulates axon pathfinding in the vertebrate visual system. Neuron 28: 779–792.
30. Garcia-Frigola C, Carreres MI, Vegar C, Herrera E (2007) Gene delivery into mouse retinal ganglion cells by in utero electroporation. BMC Dev Biol 7: 103.
31. de la Torre JR, Hopker VH, Ming GL, Poo MM, Tessier-Lavigne M, et al. (1997) Turning of retinal growth cones in a netrin-1 gradient mediated by the netrin receptor DCC. Neuron 19: 1211–1224.
32. Deiner MS, Kennedy TE, Fazeli A, Serafini T, Tessier-Lavigne M, et al. (1997) Netrin-1 and DCC mediate axon guidance locally at the optic disc: loss of function leads to optic nerve hypoplasia. Neuron 19: 575–589.
33. Van Raay TJ, Vetter ML (2004) Wnt/frizzled signaling during vertebrate retinal development. Dev Neurosci 26: 352–358.
34. Chuman Y, Uren A, Cahill J, Regan C, Wolf V, et al. (2004) Identification of a peptide binding motif for secreted frizzled-related protein-1. Peptides 25: 1831–1838.
35. Bovolenta P (2005) Morphogen signaling at the vertebrate growth cone: a few cases or a general strategy? J Neurobiol 64: 405–416.
36. Nural HF, Mastick GS (2004) Pax6 guides a relay of pioneer longitudinal axons in the embryonic mouse forebrain. J Comp Neurol 479: 399–409.
37. Jones L, Lopez-Bendito G, Gruss P, Stoykova A, Molnar Z (2002) Pax6 is required for the normal development of the forebrain axonal connections. Development 129: 5041–5052.

38. Nikoletopoulou V, Plachta N, Allen ND, Pinto L, Gotz M, et al. (2007) Neurotrophin receptor-mediated death of misspecified neurons generated from embryonic stem cells lacking Pax6. Cell Stem Cell 1: 529–540.
39. Kania A, Jessell TM (2003) Topographic motor projections in the limb imposed by LIM homeodomain protein regulation of ephrin-A:EphA interactions. Neuron 38: 581–596.
40. Wilson SI, Shafer B, Lee KJ, Dodd J (2008) A molecular program for contralateral trajectory: Rig-1 control by LIM homeodomain transcription factors. Neuron 59: 413–424.
41. Sabatier C, Plump AS, Le M, Brose K, Tamada A, et al. (2004) The divergent Robo family protein rig-1/Robo3 is a negative regulator of slit responsiveness required for midline crossing by commissural axons. Cell 117: 157–169.
42. Herrera E, Brown L, Aruga J, Rachel RA, Dolen G, et al. (2003) Zic2 patterns binocular vision by specifying the uncrossed retinal projection. Cell 114: 545–557.
43. Lee R, Petros TJ, Mason CA (2008) Zic2 regulates retinal ganglion cell axon avoidance of ephrinB2 through inducing expression of the guidance receptor EphB1. J Neurosci 28: 5910–5919.
44. Williams SE, Mann F, Erskine L, Sakurai T, Wei S, et al. (2003) Ephrin-B2 and EphB1 mediate retinal axon divergence at the optic chiasm. Neuron 39: 919–935.
45. Molyneaux BJ, Arlotta P, Hirata T, Hibi M, Macklis JD (2005) Fezl is required for the birth and specification of corticospinal motor neurons. Neuron 47: 817–831.
46. Chen B, Schaevitz LR, McConnell SK (2005) Fezl regulates the differentiation and axon targeting of layer 5 subcortical projection neurons in cerebral cortex. Proc Natl Acad Sci U S A 102: 17184–17189.
47. Britanova O, de Juan Romero C, Cheung A, Kwan KY, Schwark M, et al. (2008) Satb2 is a postmitotic determinant for upper-layer neuron specification in the neocortex. Neuron 57: 378–392.
48. Alcamo EA, Chirivella L, Dautzenberg M, Dobreva G, Farinas I, et al. (2008) Satb2 regulates callosal projection neuron identity in the developing cerebral cortex. Neuron 57: 364–377.
49. Arlotta P, Molyneaux BJ, Chen J, Inoue J, Kominami R, et al. (2005) Neuronal subtype-specific genes that control corticospinal motor neuron development in vivo. Neuron 45: 207–221.
50. Castellani V, Chedotal A, Schachner M, Faivre-Sarrailh C, Rougon G (2000) Analysis of the L1-deficient mouse phenotype reveals cross-talk between Sema3A and L1 signaling pathways in axonal guidance. Neuron 27: 237–249.
51. Carcea I, Ma'ayan A, Mesias R, Sepulveda B, Salton SR, et al. (2011) Flotillin-mediated endocytic events dictate cell type-specific responses to semaphorin 3A. J Neurosci 30: 15317–15329.
52. Holm PC, Mader MT, Haubst N, Wizenmann A, Sigvardsson M, et al. (2007) Loss- and gain-of-function analyses reveal targets of Pax6 in the developing mouse telencephalon. Mol Cell Neurosci 34: 99–119.
53. Osumi N, Hirota A, Ohuchi H, Nakafuku M, Iimura T, et al. (1997) Pax-6 is involved in the specification of hindbrain motor neuron subtype. Development 124: 2961–2972.
54. Frowein J, Campbell K, Gotz M (2002) Expression of Ngn1, Ngn2, Cash1, Gsh2 and Sfrp1 in the developing chick telencephalon. Mech Dev 110: 249–252.
55. Mao W, Wordinger RJ, Clark AF (2010) Focus on molecules: SFRP1. Exp Eye Res 91: 552–553.
56. Augustine C, Gunnersen J, Spirkoska V, Tan SS (2001) Place- and time-dependent expression of mouse sFRP-1 during development of the cerebral neocortex. Mech Dev 109: 395–397.

ARTICLES

nature neuroscience

SFRPs act as negative modulators of ADAM10 to regulate retinal neurogenesis

Pilar Esteve[1–3], Africa Sandonìs[1–3], Marcos Cardozo[1–3], Jordi Malapeira[4–6], Carmen Ibañez[1], Inmaculada Crespo[1–3], Severine Marcos[1–3], Sara Gonzalez-Garcia[1], Maria Luisa Toribio[1], Joaquin Arribas[4–6], Akihiko Shimono[7], Isabel Guerrero[1] & Paola Bovolenta[1–3]

It is well established that retinal neurogenesis in mouse embryos requires the activation of Notch signaling, but is independent of the Wnt signaling pathway. We found that genetic inactivation of Sfrp1 and Sfrp2, two postulated Wnt antagonists, perturbs retinal neurogenesis. In retinas from *Sfrp1*$^{-/-}$; *Sfrp2*$^{-/-}$ embryos, Notch signaling was transiently upregulated because Sfrps bind ADAM10 metalloprotease and downregulate its activity, an important step in Notch activation. The proteolysis of other ADAM10 substrates, including APP, was consistently altered in Sfrp mutants, whereas pharmacological inhibition of ADAM10 partially rescued the *Sfrp1*$^{-/-}$; *Sfrp2*$^{-/-}$ retinal phenotype. Conversely, ectopic Sfrp1 expression in the *Drosophila* wing imaginal disc prevented the expression of Notch targets, and this was restored by the coexpression of Kuzbanian, the *Drosophila* ADAM10 homolog. Together, these data indicate that Sfrps inhibit the ADAM10 metalloprotease, which might have important implications in pathological events, including cancer and Alzheimer's disease.

During embryonic development, Notch and Wnt signaling orchestrate cell proliferation and cell fate decisions in a wide variety of tissues. The functional relationship between the two signaling pathways is intricate, and complementary or mutually exclusive activation has been reported during processes such as myogenesis, hematopoiesis and neurogenesis of the telencephalon or neural tube[1].

Notch and Wnt signaling are also required for the development of the vertebrate neural retina. This structure develops from a neuroepithelium composed of multipotent progenitors, which go through a series of competence states to give rise to six neuronal and one glial cell types[2]. As progenitor cells produce the various cell types, Notch through lateral inhibition maintains neighboring cells in a multipotent, proliferative state, ensuring that sufficient numbers of progenitors are retained for consecutive waves of neurogenesis. Thus, downregulation of Notch is a prerequisite for retinal neuronal differentiation[2].

Wnt–β-catenin signaling has also been implicated in the proliferation of vertebrate retinal precursors. However, in the mouse embryonic neural retina this function is limited to progenitor cells located in the periphery[3,4]. Wnt–β-catenin signaling is not active in the central retina, and cell proliferation and differentiation proceed normally in mice with conditional deletion of β-catenin in the neural retina, although retinal lamination is altered[5]. Similarly, retina-specific inactivation of Fzd5, a noncanonical Wnt receptor, mostly influences retinal vasculature formation but has no effect on neurogenesis[6]. Although these results do not strongly implicate Wnt signaling in retinal differentiation, *Sfrp1* and *Sfrp2*, two members of a family of postulated Wnt antagonists, are strongly expressed in the neural retina throughout neurogenesis[7]—raising the question of whether their function is related to Wnt signaling.

Sfrps (1–5 in mammals) are a family of secreted factors that fold in two independent domains. The cysteine-rich domain (CRD) at the N terminus shares similarities with the extracellular domain of the Wnt receptors Frizzled (Fzd) and ROR[8]. The C-terminal domain contains instead a netrin-related motif (NTR), which characterizes a number of unrelated proteins including Netrin-1, tissue inhibitors of metalloproteinases (TIMPs), complement proteins and type I procollagen C–proteinase enhancer proteins (PCOLCEs)[8]. Owing to their homology to the extracellular portion of Fzd receptors, Sfrps were first described and generally accepted as Wnt antagonists that bind and sequester Wnt ligands, thereby preventing signal activation. Gain of Sfrp1 or Sfrp2 function has supported this idea, as excess Sfrp function antagonizes Wnt signaling in a variety of contexts[8]. Loss of Sfrp function instead points to two additional important features. First, Sfrp function might be redundant, because genetic inactivation of individual family members in mice seems to have little effect on embryonic development[9,10]. Double inactivation of *Sfrp1* and *Sfrp2*, by contrast, causes a variety of alterations[9,11,12], some of which are worsened by the additional inactivation of *Sfrp5* (refs. 9,11). Second, Sfrps have Wnt-independent functions[9,12], as Sfrp-null phenotypes are only partially explained by overactivation of Wnt–β-catenin signaling[11] or alterations in the noncanonical Wnt-PCP (planar cell

[1]Centro de Biología Molecular "Severo Ochoa", Consejo Superior de Investigaciones Científicas (CSIC)–Universidad Autónoma de Madrid, Madrid, Spain. [2]Centro de Investigación Biomédica en Red de Enfermedades Raras, Madrid, Spain. [3]Instituto Cajal, CSIC, Madrid, Spain. [4]Vall d'Hebron Institute of Oncology, Barcelona, Spain. [5]Department of Biochemistry and Molecular Biology, Universitat Autònoma de Barcelona, Bellaterra, Spain. [6]Institució Catalana de Recerca i Estudis Avançats, Barcelona, Spain. [7]Cancer Science Institute of Singapore, National University of Singapore, Singapore. Correspondence should be addressed to P.E. (pesteve@cbm.uam.es) or P.B. (pbovolenta@cbm.uam.es).

Received 22 December 2010; accepted 2 March 2011; published online 10 April 2011; doi:10.1038/nn.2794

polarity) pathway. Consistent with this notion, several studies have implicated individual Sfrps in the Wnt-independent regulation of other cell signaling mechanisms. For example, Sfrp1 can interact with and inhibit the activity of RANKL, a member of the tumor necrosis factor (TNF) family that is involved in osteoclast formation[8]. Sfrp2 specifically binds to tolloid metalloproteinases and thereby regulates procollagen processing during myocardium infarction[13,14]. Sfrp2 also interacts with an integrin–fibronectin complex that modulates apoptosis[8]. Furthermore, Sizzled (a member of the family that is not present in mammals) acts as a negative feedback regulator of bone morphogenetic protein (BMP) signaling by binding to BMP1-Tolloid, a metalloprotease that normally degrades the BMP antagonist chordin[15,16].

By analyzing the functional consequences of compound inactivation of *Sfrp1* and *Sfrp2* during mouse retinal neurogenesis, we found that Sfrps have a Wnt-independent role in the regulation of Notch signaling. We explain this finding by demonstrating that Sfrps can bind to and downregulate the activity of ADAM10, a metalloprotease with multiple substrates, including Notch, N-cadherin and amyloid precursor protein (APP).

RESULTS

Sfrp1 and Sfrp2 are essential for proper eye development

Sfrp1 and *Sfrp2* are expressed during murine eye development with a complementary pattern that includes all eye structures[7]. *Sfrp1* transcripts are localized to the optic cup periphery and the retina pigmented epithelium from embryonic day 10.5 (E10.5), whereas *Sfrp2* is predominant in the neural retina (**Supplementary Fig. 1**).

Despite restricted mRNA expression, Sfrp proteins efficiently diffuse in the extracellular space[17] and Sfrp1 was also immunodetected, albeit at low levels, in the neural retina (**Supplementary Fig. 1**), supporting the proposed functional redundancy of Sfrps[9,11,12]. Accordingly, the eyes of *Sfrp1* or *Sfrp2* single-null embryos appeared histologically normal. By contrast at E16.5, the latest viable stage, the eyes of *Sfrp1*$^{-/-}$; *Sfrp2*$^{-/-}$ compound mutants (n = 20) were smaller than those of control littermates (n = 30) with visible morphological alterations, including dorsal peripheral defects, reduction in lens size, abnormal cornea and eye lid formation, increased thickness of the neural retina and abnormal vitreal accumulation of mesenchyme-derived angioblasts that normally form the hyaloid artery, the major vascular structure of the embryonic eye (**Supplementary Fig. 2**).

Inactivation of *Sfrp1* and *Sfrp2* alters retinal neurogenesis

Multipotent progenitors in the neural retina generate neurons and one type of glia with an established temporal order. The first cells to be generated are retinal ganglion cells (RGCs), followed by amacrine and cone photoreceptors, and bipolar neurons and Müller glial cells are the last[2]. Although Wnt signaling does not seem to participate in retinal neurogenesis[4,5], the neural retina of *Sfrp1*$^{-/-}$; *Sfrp2*$^{-/-}$ embryos was abnormally thick and had vascular defects, as shown by immunohistochemistry with endothelial and pericyte-specific markers (**Supplementary Fig. 2**). At E16.5, the number of Islet1$^+$, Pax6$^+$ RGCs, Islet1$^+$ and Pax6$^+$ amacrine cells and Otx2$^+$ early-born photoreceptors (74 ± 5.72 versus 52 ± 3.70 in controls) was greater in the neural retina of *Sfrp1*$^{-/-}$; *Sfrp2*$^{-/-}$ embryos than in wild-type embryos, whereas PKCα$^+$ bipolar progenitors were virtually absent (2.33 ± 0.408 versus 29 ± 3.417 in controls) (**Fig. 1a–h**).

This increased differentiation of *Sfrp1*$^{-/-}$; *Sfrp2*$^{-/-}$ retinas was not due to a premature onset of cell differentiation because we found no Tuj1$^+$ differentiating neurons in either control or mutant retinas at E10.5 (data not shown). However, half a day later Tuj$^+$ and Islet1/2$^+$ RGCs in mutant retinas clearly outnumbered those in control retinas (**Fig. 1i–l**). This difference was associated with a marked increase in

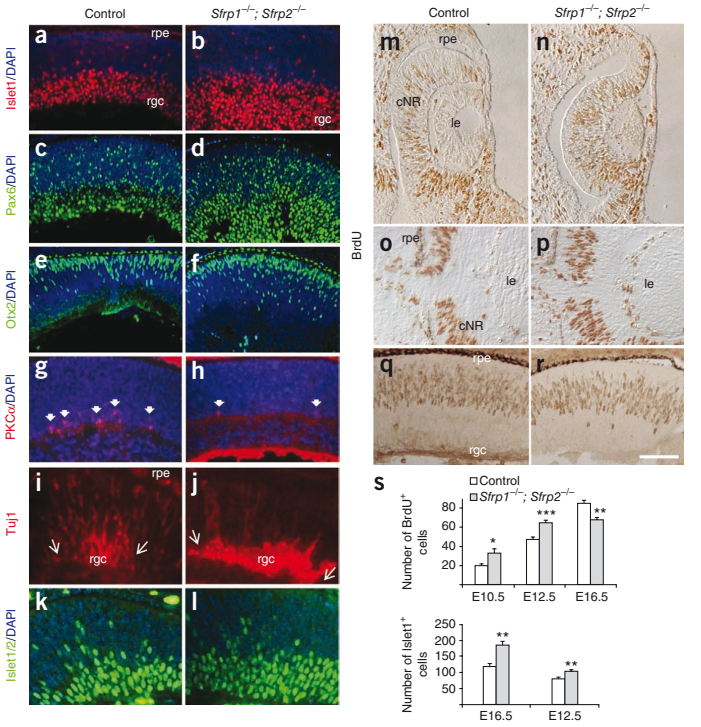

Figure 1 Neurogenesis is impaired in the central retina of *Sfrp1*$^{-/-}$; *Sfrp2*$^{-/-}$ embryos. (**a**–**r**) Frontal cryostat sections of E16.5 (**a**–**h**,**q**,**r**), E12.5 (**o**,**p**), E11.5 (**i**–**l**) and E10.5 (**m**,**n**) control and *Sfrp1*$^{-/-}$; *Sfrp2*$^{-/-}$ retinas immunostained with antibodies against Tuj1 (differentiated cells), Islet1 (RGCs and amacrine cells), Pax6 (RGCs and amacrine cells), Otx2 (bipolar cells and photoreceptors), PKC (bipolar cells) and BrdU (proliferating precursors) and counterstained with DAPI (blue; **a**–**h** and **k**,**l**). RGCs and amacrine cells are increased, whereas bipolar cells are decreased in the mutant retinas. Proliferation in the mutant retinas is increased at early stages but is reduced at E16.5 as compared to controls (compare **r** to **q**). (**s**) Quantification of BrdU$^+$, Islet1$^+$, Otx2$^+$ and PKC$^+$ cells. Positive cells were counted in equivalent areas of the central retina. Error bars are s.e.m. of at least three sections from four different embryos (n = 4). cNR, central neural retina; le, lens; RPE, retina pigmented epithelium. *P < 0.05; **P < 0.01; ***P < 0.001. Scale bar, 30 μm (**a**–**l**,**q**,**r**); 60 μm (**o**,**p**); 100 μm (**m**,**n**).

BrdU$^+$ proliferating cells, which was already evident in the neural retinas of E10.5 *Sfrp1*$^{-/-}$; *Sfrp2*$^{-/-}$ embryos when compared to control littermates (**Fig. 1m**,**n**). Furthermore, analysis of the distribution of E10.5 *Sfrp1*$^{-/-}$; *Sfrp2*$^{-/-}$ retinal cells during the cell cycle using flow cytometry–based DNA content analysis revealed an increased distribution in the G2/M phase (G_1, 55%; S, 29.3%; G_2, 6.58%) when compared to that of control littermates (G_1, 51.8%; S, 30.4%; G_2, 3.08%). This increase was only transient because at E16.5 the number of BrdU-positive cells was significantly reduced in the *Sfrp1*$^{-/-}$; *Sfrp2*$^{-/-}$ retinas as compared with controls ($P = 0.006$; **Fig. 1q**–**s**). Thus, inactivation of Sfrp1 and 2 seemed to force the generation of progenitor cells and their differentiation into early born neurons, possibly depleting the proliferating progenitor pool and consequently reducing late-born cell types.

Sfrp1 and Sfrp2 inhibit Notch signaling

The number of progenitor cells available for neural differentiation at any given time is controlled by Notch signaling[2]. To search for a Wnt-independent mechanism that could explain the neural retina phenotype of Sfrp mutants, we tested whether the Notch pathway was normally activated. Upon ligand binding, the Notch receptor becomes susceptible to two sequential proteolytic cleavages that enable the release of an active intracellular form of Notch (NICD). NICD translocates to the nucleus where it interacts with the CSL transcription factor and recruits coactivators to turn on the expression of Notch target genes, such as *Hes5* (ref. 18). Nuclear localization of NICD is then a reliable determinant of Notch signaling activation[18].

In E12.5 control retinas, the number of NICD$^+$ progenitor cells that were available for neural differentiation occupied only a reduced central region[19] (**Fig. 2a**) whereas in the Sfrp1 and 2 mutants a substantially larger number of NICD$^+$ cells were distributed in most of the neural retina (**Fig. 2b**). With time, this difference became progressively inverted: at E13.5 the number of NICD$^+$ cells was similar in control and mutant retinas but by E16.5 mutant retinas tended to contain fewer NICD$^+$ cells than control retinas (**Fig. 2c**–**f**,**k**). Consistent with broad activation of the Notch pathway, the distribution of *Hes5* was similarly expanded in the *Sfrp1*$^{-/-}$; *Sfrp2*$^{-/-}$retinas (**Fig. 2g**,**h**), whereas that of the Notch ligand Delta-like1 (*Dll-1*), which is repressed upon activation of Notch signaling[18] were abnormally low in the mutant neural retina (**Fig. 2i**,**j**). Quantitative RT-PCR analysis of *Hes5* (0.90 ± 0.11 in mutants versus 0.41 ± 0.007 in controls; $n = 3$, $P < 0.05$) and *Dll-1* (0.602 ± 0.052 in mutants versus 0.81 ± 0.048 in controls; $n = 3$, $P < 0.05$) mRNA levels from E12.5 and E13.5 control and Sfrp knockout retinas confirmed these variations. Together these data indicated that, in the absence of Sfrp1 and 2, Notch signaling was abnormally active in a larger number of retinal progenitors; this explains the early increase in cell proliferation. In turn, this simultaneous activation suppressed ligand expression, prematurely terminated proliferation of retinal progenitors and favored their differentiation, explaining the accumulation of early-differentiating neurons in *Sfrp*-null retinas.

We reasoned that if Sfrps directly or indirectly downregulate Notch activity, similar alterations should occur in other brain regions where Notch and Sfrp1 and 2 are coexpressed, such as the telencephalon[20,21]. Indeed, western blot analysis of E12.5 *Sfrp1*$^{-/-}$; *Sfrp2*$^{-/-}$ and control cortex revealed that Notch was expressed at similar levels in both extracts but that NICD expression was fourfold higher in the mutants (**Fig. 2l**). This increase was paralleled by defects in telencephalic neurogenesis similar to those observed in the retina (I.C., P.B. and P.E., unpublished observations).

ADAM10 inhibition rescues the Sfrp mutant retinal phenotype

The disintegrin and metalloprotease transmembrane protein ADAM10 is responsible for the first proteolytic cleavage of the Notch receptor on ligand binding[22,23]. ADAM10-mediated shedding of the Notch ectodomain is a limiting step for the subsequent proteolysis by the γ-secretase–presenilin complex, which releases the NICD. ADAM10 is inhibited by TIMPs[24] through the activity of their NTR modules[24,25]. Because Sfrp1 and 2 contain NTR modules[8], we postulated that they might normally downregulate the activity of ADAM10. If this were the case, inhibition of ADAM10 activity should counteract the impaired neurogenesis observed in the *Sfrp1*$^{-/-}$; *Sfrp2*$^{-/-}$ neural retina.

G1254023X is a synthetic compound that inhibits ADAM10 with high affinity[26]. We investigated its effect on retinal neurogenesis using organotypic optic cup cultures from E11.5 control and *Sfrp1*$^{-/-}$;

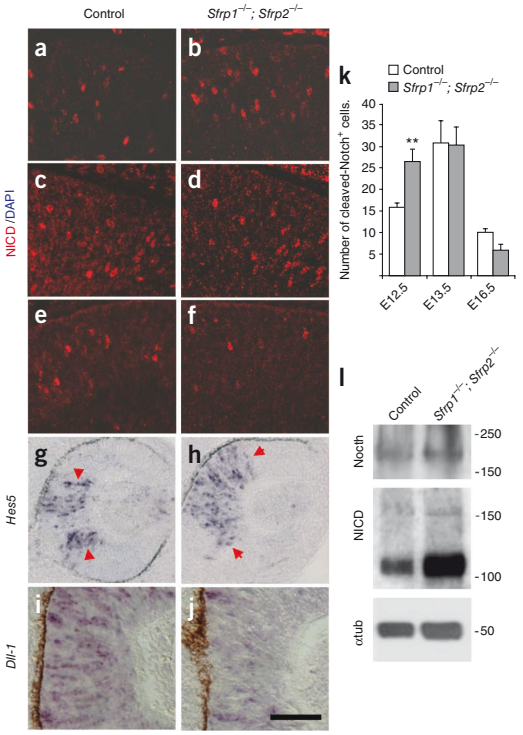

Figure 2 Notch signaling is transiently upregulated in *Sfrp1*$^{-/-}$; *Sfrp2*$^{-/-}$ retinas. (**a**–**j**) Frontal cryostat sections of E12.5 (**a**,**b**,**g**,**h**), E13.5 (**c**,**d**,**i**,**j**) and E16.5 (**e**,**f**) control and mutant embryos immunostained with antibodies against NICD (**a**–**f**) or hybridized with probes specific for *Hes5* (**g**,**h**) or *Dll-1* (**i**,**j**). Note the initial expansion of NICD and *Hes5* expression in the mutants (arrowheads in **g**,**h**). The expression of *Dll-1* is instead downregulated. (**k**) Quantification of the number of NICD$^+$ cells in the neural retina. Positive cells were counted in equivalent areas. Error bars are s.e.m. of at least three sections. Four embryos were analyzed in each case ($n = 4$). (**l**) Western blot analysis of the levels of Notch processing in lysates of E12.5 cortex from mutant and control embryos. The cleaved Notch fragment (NICD) is increased in the mutants as determined by band intensity quantification normalized with α-tubulin (3.5 versus 1.2 in controls), although Notch is expressed at similar levels in both tissues (1.482 versus 1.46 in controls). The data represent a typical experiment, which was repeated four times with similar results. Scale bar: 30 μm (**a**–**f**); 50 μm (**i**,**j**); 100 μm (**g**,**h**).

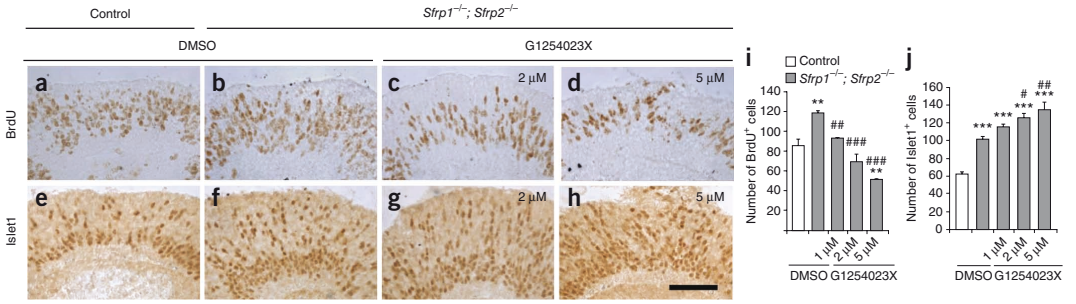

Figure 3 Inhibition of ADAM10 partially rescues the retinal phenotype of *Sfrp1*$^{-/-}$; *Sfrp2*$^{-/-}$ embryos. (**a**–**j**) Cryostat sections of organotypic optic cup cultures from E11.5 controls (**a**,**e**,**i**,**j**) or *Sfrp1*$^{-/-}$; *Sfrp2*$^{-/-}$ (**b**–**d**,**f**–**h**,**i**,**j**) embryos cultured for 24 h in the presence of DMSO (**a**,**b**,**e**,**f**,**i**,**j**) or 1–5 μM of the ADAM10 inhibitor G1254023X (**c**,**d**,**g**,**h**,**i**,**j**). Sections were immunostained with antibodies against BrdU (**a**–**d**) or Islet1 (**e**–**h**). (**i**,**j**) Quantification of BrdU$^+$ and Islet1$^+$ cells. Positive cells were counted in equivalent areas of the central retina. Note that cultured retinas from *Sfrp1*$^{-/-}$; *Sfrp2*$^{-/-}$ embryos show an increase in cell proliferation and differentiation similar to that observed *in vivo*. Addition of 1–2 μM G1254023X is sufficient to decrease proliferation but not differentiation to that of controls. Error bars are s.e.m. of at least three sections from five cultures ($n = 5$). *,$^{\#}P < 0.05$. **, $^{\#\#}P < 0.01$. ***, $^{\#\#\#}P < 0.001$. Asterisks indicate comparison between controls and GX-treated mutant cultures; hash marks between DMSO- and G1254023X-treated mutant cultures. Scale bar: 30 μm. α-tubulin (αtub) was used as a loading control.

Sfrp2$^{-/-}$ embryos (**Fig. 3**). After 24 h, culture conditions and treatment with vehicle (DMSO) alone did not significantly modify the difference in the rate of proliferation (measured by the number of BrdU$^+$ cells, $P = 0.377$) or differentiation (number of Islet1$^+$ cells, $P = 0.461$) observed *in vivo* between control and *Sfrp1*$^{-/-}$; *Sfrp2*$^{-/-}$ embryonic retinas (**Figs. 1s** and **3i**,**j** and **Supplementary Fig. 3**). Addition of G1254023X to the culture medium of control retinas reduced the rate of cell proliferation when compared to vehicle treatment (**Supplementary Fig. 3**). Exposure of *Sfrp1*$^{-/-}$;*Sfrp2*$^{-/-}$ optic cups to low concentrations of G1254023X was sufficient to reduce the number of BrdU$^+$ cells to values statistically undistinguishable from those of controls (**Fig. 3a**,**c**,**i**). However, increasing G1254023X concentrations (5 μM) further reduced the number of BrdU$^+$ cells in *Sfrp1*$^{-/-}$; *Sfrp2*$^{-/-}$ retinas to values below those of control retinas, supporting the idea that normally Sfrp1 and Sfrp2 negatively modulate, but do not completely block, Notch processing. Notably, G1254023X did not significantly change the number of Islet1$^+$ cells in the *Sfrp1*$^{-/-}$ *Sfrp2*$^{-/-}$ optic cup cultures at low doses ($P = 0.279$), but at higher concentrations favored cell differentiation (**Fig. 3e**–**h**,**j**). Probably, downregulation of ADAM10 at a time when a substantial amount of early-born neurons has been already generated (**Fig. 1l**,**s**) is not sufficient to restrain cell cycle exit in the mutants. Rather, further inhibition of Notch activation promotes neuronal differentiation, as reported in the retina[2].

Sfrps interfere with the proteolysis of ADAM10 substrates

Together, the above findings supported the possibility that the *Sfrp1*$^{-/-}$; *Sfrp2*$^{-/-}$ retinal phenotype could be at least in part explained by uncontrolled activity of ADAM10. We next postulated that, if this was the case, the processing of physiological ADAM10 substrates other than Notch should be equally altered in Sfrp null retinas.

ADAM10 sheds the extracellular domain of N-cadherin and L1-CAM, two cell adhesion molecules that are abundantly expressed in embryonic retinas. This proteolytic cleavage produces fragments of 40 kDa and 32 kDa, respectively, and is a prerequisite for further proteolysis by a γ-secretase, which generates intracellular peptides of 35 kDa for N-cadherin[27] and 28 kDa for L1-CAM[28]. Western blot analysis of extracts from E13 and E16.5 *Sfrp1*$^{-/-}$; *Sfrp2*$^{-/-}$ and control retinas showed that the amount of L1-CAM 32 kDa and N-cadherin 35 kDa peptides were almost doubled in the mutants (70% and 68% of control values, respectively), although both proteins were expressed at similar levels in both genotypes (**Fig. 4a**,**b**). Consistent with the latter observation, membrane-bound active β-catenin, which requires intact N-cadherin to tether the membrane[27], was almost undetectable in the mutant retinas (**Fig. 4c**,**d**).

In addition to neural development, ADAM10 is crucial for tissue homeostasis. Most notably, ADAM10 is responsible for the nonamyloidogenic processing of APP, a key protein in the onset of Alzheimer's

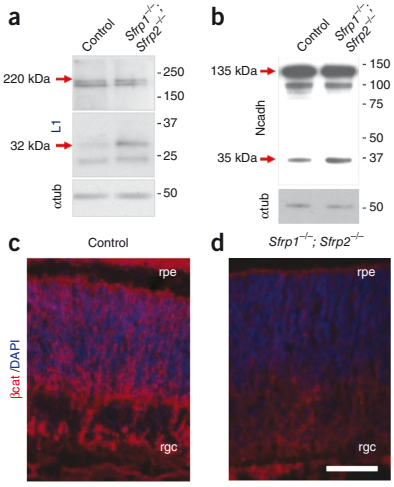

Figure 4 Sfrps interfere with ADAM10-mediated processing of N-cadherin and L1. (**a**,**b**) Western blot analysis of L1 (**a**) and N-cadherin (**b**) processing in lysates of retinas from E13.5 and E16.5 mutant and control embryos. The 32-kDa L1 and 35-kDa N-cadherin fragments (CTFs) are increased in *Sfrp1*$^{-/-}$; *Sfrp2*$^{-/-}$ mutants as determined by band intensity quantification normalized to α-tubulin (4.4 versus 2.58 in controls for L1, and 6.51 versus 3.86 in controls for N-cadherin). The data represent a typical experiment, which was repeated three times with similar results. (**c**,**d**) Increased N-cadherin processing is paralleled by loss of membrane-bound active β-catenin in the mutant retinas as compared to controls. Scale bar: 30 μm.

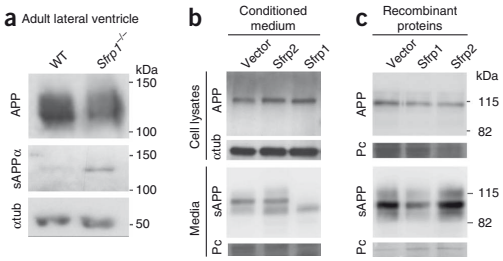

Figure 5 Sfrps interferes with ADAM10-mediated processing of APP. (**a**) Western blot analysis of total (APP) and soluble (sAPPα) present in lysates from the subventricular zone of the lateral ventricles from wild-type (WT) and *Sfrp1*$^{-/-}$ adult brains. The amount of sAPPα fragment is increased in mutants (normalized density values to α-tubulin: 11.1 versus 1.32 in controls). The data represent a typical experiment, which was repeated three times with similar results. (**b**,**c**) Western blot analysis of total APP and soluble sAPPα, respectively, in the cell lysate and conditioned medium of CHO cells stably transfected with *Sfrp2* or *Sfrp1* constructs (**b**, left column; densitometric analysis of sAPPα in the medium normalized to Ponceau-stained vector: 10.9 ± 2.2; Sfrp2: 13.3 ± 0.7; Sfrp1: 5.2 ± 1.7) or of CHO cells incubated with purified Sfrp1 or Sfrp2 proteins (**c**; densitometric analysis of sAPPα in the medium normalized to Ponceau-stained vector: 10.0 ± 1.6; Sfrp2: 11.8 ± 0.7; Sfrp1: 4.1 ± 2.2). In both cases Sfrp1, but not Sfrp2, decreases the amount of secreted APP without changing the levels of APP in the cell lysates.

disease. ADAM10-mediated processing of APP cleaves the protein within the βamyloid peptide, preventing its toxic generation and promoting the shedding of a large soluble APP ectodomain[29] (sAPPα). APP is poorly expressed in the developing retina (not shown) but its intact and sAPP forms are abundant in the subventricular zone of the lateral ventricle in adult mice[30]. If Sfrp1 normally antagonizes the α-secretase activity of ADAM10, sAPPα should be enriched in the lateral ventricle of adult *Sfrp1*$^{-/-}$ mice. Comparative western blot analysis of isolated lateral ventricle regions from *Sfrp1*$^{-/-}$ and wild-type brains confirmed an eightfold increase in sAPP in the mutants (**Fig. 5a**).

sAPPα is constitutively released from the surface of most cultured cells. Consistently, the amount of sAPPα recovered from CHO cells stably transfected with *Sfrp1*, but not *Sfrp2*, was substantially reduced (47%) compared to control, mock-transfected CHO cells, although APP was expressed at similar levels in all the cell lines (**Fig. 5b**). Similarly, the addition of soluble recombinant Sfrp1, but not Sfrp2, substantially reduced (35%) the levels of sAPPα recovered from the medium of CHO cells (**Fig. 5c**), further demonstrating that Sfrp1 is a specific inhibitor of ADAM10-mediated APP processing. The difference between Sfrp1 and Sfrp2 on APP processing raises the possibility that the inhibitory specificity of Sfrps may be influenced by the nature of the substrate, as shown for other TIMPs[31].

Together, these data indicate that Sfrp1, and probably Sfrp2, act as ADAM10-specific TIMPS.

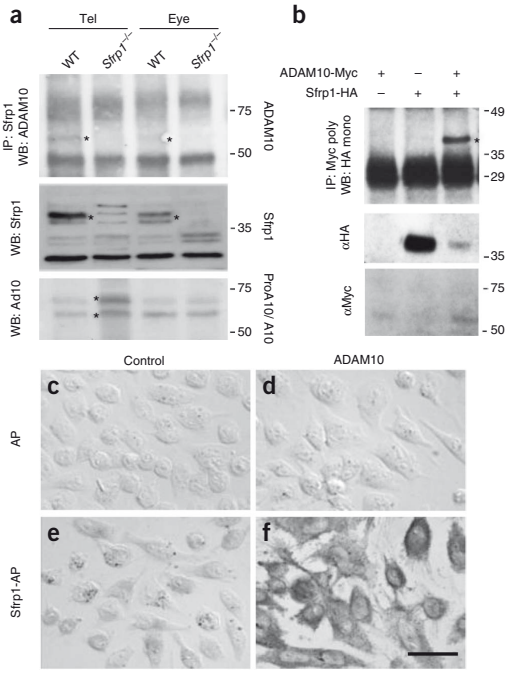

Sfrp1 and ADAM10 physically interact

TIMPs usually exert their action by binding to their target metalloproteases[31]. To test whether Sfrps acted with a similar mechanism, we investigated whether Sfrp1 and ADAM10 physically interact. To this end we attempted to coimmunoprecipitate Sfrp1 and ADAM10 from embryonic retinal tissue and cortical tissue, in which Sfrp1 is more abundantly expressed.

Sfrp1-specific antibodies immunoprecipitated ADAM10 from wild-type but not from *Sfrp1*$^{-/-}$; *Sfrp2*$^{-/-}$ tissues (**Fig. 6a**). Unfortunately, we found that ADAM10 antibodies were not efficient in reverse immunoprecipitation experiments. To circumvent this problem, we cotransfected Sfrp1-HA and ADAM10-myc constructs in 293T cells and analyzed the derived cell lysates to demonstrate that antibodies to myc specifically coimmunoprecipitated Sfrp1-HA with ADAM10 (**Fig. 6b**). Furthermore, secreted AP-tagged Sfrp1 seemed to bind more abundantly on ADAM10-overexpressing CHO cells than on mock-transfected cells, which constitutively express low ADAM10 levels[31] (**Fig. 6c–f**).

Sfrp1 targets ADAM10 function independently of Wnt

The above findings support the idea that Sfrps can bind ADAM10 and directly modulate its function. However, the partial rescue of the

Figure 6 Sfrps interacts with ADAM10. (**a**) Embryonic telencephalic and ocular tissue from wild-type and Sfrp mutants were immunoprecipitated with antibodies to Sfrp1 and analyzed by western blot with antibodies to ADAM10. Asterisks in the upper panel indicate the coimmunoprecipitation of ADAM10 in wild-type tissue. Asterisks in the middle panel indicate Sfrp1 in wild-type tissue. Asterisks in the bottom panel indicate ProADAM10 and ADAM10 bands. The data represent a typical experiment, which was repeated five times with similar results. (**b**) HEK 293T cells were transiently transfected with expression plasmids of ADAM-myc, Sfrp1-HA or a combination of both. After 48 h cell lysates were precipitated with anti-myc and analyzed by western blot with antibodies to HA. Note that ADAM10 can immunoprecipitate Sfrp1 (asterisk). The data represent a typical experiment, which was repeated five times with similar results. (**c–f**) CHO cells were transfected with an ADAM10 expression plasmid or with the empty vector. Cells were thereafter incubated with conditioned medium containing AP-Sfrp1 or AP alone. Increased binding of AP-Sfrp1 is observed in the ADAM10-overexpressing cell line. Scale bar, 25 μm.

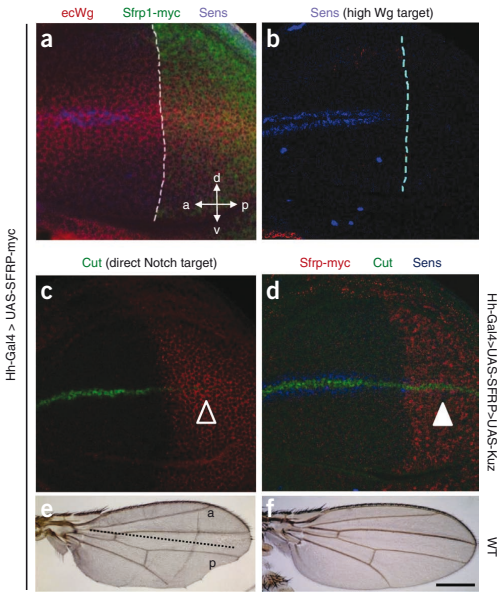

Figure 7 Sfrp1 interacts with Kuz in *Drosophila* wing imaginal discs. (**a**,**b**) Sens (blue) and extracellular wingless (ecWg) expressions (red) in a UAS-myc-Sfrp1>Hh-Gal4 wing imaginal disc. The wingless (Wg) target Sens is repressed in the posterior compartment where Sfrp1 is expressed (Myc in green) but not in the anterior compartment that serves as a control. (**c**) Cut (green) and Hh (red) expressions in Hh-Gal4>UAS-myc-Sfrp1 wing discs. Note the repression of the Notch target Cut (open arrowhead) in the area where Sfrp1 is expressed (Hh in red). (**d**) Sens (blue) and Cut (green) expression in a UAS-myc-Sfrp1/UAS-Kuz>Hh-Gal4 wing disc (Myc in red). The ectopic expression of both Sfrp1 and Kuz rescues the expression of the Notch target Cut (arrowhead) but has no effect on that of the Wg target Sens. (**e**) Adult UAS-myc-Sfrp1>Hh-Gal4 wing phenotype showing notches in the posterior wing margin, a phenotype characteristic of wingless and Notch signaling alterations. (**f**) Wild-type wing. Scale bar, 40 μm (**a–d**); 200 μm (**e**,**f**).

Sfrp phenotype by an ADAM10 inhibitor together with the notion that, in different contexts, Wnt and Notch activities are tightly linked prompted us to test whether Sfrps downregulate ADAM10 independently of Wnt signaling.

To this end we turned to the *Drosophila* wing imaginal disc, the development of which is regulated by both Wnt and Notch signaling. In contrast to the vertebrate retina, the interactions between these two pathways and their direct and specific downstream targets have been unequivocally identified in *Drosophila*[32]. *Drosophila* offers also a natural Sfrp-null background because no apparent Sfrp homolog has been identified in its genome[8]. Nevertheless, wingless efficiently binds to Sfrp1 (ref. 33) mimicking the vertebrate Wnt1 or Wnt8 interaction[34].

Taking advantage of this interaction, we have shown that HhGal4>UAS–Sfrp1 ectopic expression of Sfrp1 in the posterior compartment of the *Drosophila* wing imaginal disc interferes with the symmetrical gradient of wingless at the dorsoventral boundary of the wing imaginal disc (**Fig. 7**). It thereby prevents, in the posterior but not in the anterior compartment that serves as control, the expression of Senseless (Sens), a canonical target normally activated by high wingless levels in two discrete and symmetrical stripes at the dorsoventral compartment boundary[35] (P.E., A. Sandonis, C.I., A. Shimono, I.G. and P.B., unpublished observations) (**Fig. 7a**,**b**). We thus tested whether Sfrp1 could similarly interfere with the expression of genes that are directly activated by Notch signaling. Cut, one such target, is symmetrically expressed in the stripes of Sens at the dorsoventral compartment boundary[32]. In the HhGal4>UAS–Sfrp1 wing discs, Cut expression was totally abolished in the posterior but not the anterior compartment (**Fig. 7c**), supporting the idea that Sfrp1 interferes with Notch signaling. Consistently, the wings of adult UAS-myc-Sfrp1>Hh–Gal4 flies had notches in the posterior wing margin, a phenotype characteristic of alterations in the wingless and Notch pathways (**Fig. 7e**,**f**). Most notably, forced expression of Kuzbanian (Kuz; the *Drosophila* ADAM10 homolog) together with Sfrp1 in the posterior compartment completely rescued Cut expression, whereas it had no effect on expression of the wingless target Sens (**Fig. 7d**). Together these results strongly support the idea that Sfrp1 targets ADAM10 (Kuz) function, thereby interfering with Notch signaling independently of Wnt.

DISCUSSION

The onset and progression of neurogenesis in the vertebrate retina is regulated by interactions among the fibroblast growth factor, sonic hedgehog (Shh), Wnt and Notch signaling pathways. Comparison of the mechanisms that operate in different species offers two key observations. First, there are species-specific differences in the precise composition and onset of each pathway, which reflect individual retinal characteristics[36]. Second, individual elements of one pathway respond or are used in other signaling cascades or cellular activities. For example, in the eye, Hes1, an established Notch target, is also independently regulated by Shh and Wnt signaling[37,38], and β-catenin, a key element of Wnt signaling, has a well characterized function in cell-cell adhesion[5]. We have shown that Sfrps, which modulate Wnt signaling, act as negative regulators of Notch. This Sfrp function provides an additional example of how individual molecules are shared by different signaling cascades. Mechanistically, Sfrps bind and, independently of Wnt, downregulate the α-secretase activity of ADAM10, which is responsible for the proteolytic cleavage of the Notch receptor and thus for subsequent pathway activation[23]. Furthermore, by targeting ADAM10, Sfrps regulate the proteolysis of other specific substrates, including N-cadherin, L1-CAM and APP.

These conclusions stem from the initial observation that in *Sfrp1*$^{-/-}$; *Sfrp2*$^{-/-}$ embryos the periphery of the optic cup is not specified and the neural retina is abnormally thick. Specification of the optic cup periphery depends on Wnt signaling activation[3,4]. Sfrp1 and 2 are required to activate canonical signaling in the periphery of the optic cup, probably by promoting the diffusion of Wnt ligands (P.E., A. Sandonis, C.I., A. Shimono, I.G. and P.B., unpublished observations). However, this mechanism could not explain the transient increase in proliferation and enhanced generation of early born neurons in the *Sfrp1*$^{-/-}$; *Sfrp2*$^{-/-}$ neural retina, because previous studies had shown that Wnt signaling is not important for retinal neurogenesis in mice[5,6]. We also considered it unlikely that the retinal phenotype could be secondary to the vascular defects observed in Sfrp1- and 2-null mice, because neurogenesis proceeds normally in embryos in which the hyaloid artery does not form[39]. Instead, we showed that abnormal retinal neurogenesis could be explained by a transient increase in Notch signaling, probably caused by enhanced ADAM10 activity. In support of this interpretation, pharmacological inhibition of ADAM10 rescued the enhanced cell proliferation of *Sfrp1*$^{-/-}$; *Sfrp2*$^{-/-}$ neural retinas. Furthermore, conditional inactivation of *Adam10* in neural progenitor cells causes depletion of early

progenitors and a reduction in α-secretase–mediated processing of APP[22], a phenotype opposite to that observed in *Sfrp1*$^{-/-}$; *Sfrp2*$^{-/-}$ retinas or in the cortex of *Sfrp1*$^{-/-}$ embryos (I.C., P.B. and P.E., unpublished observations), where Notch and APP processing are upregulated. Similar defects also characterize the cortex of embryos that lack RECK (reversion-inducing cysteine-rich protein with Kazal motifs), a membrane protein that is localized to cortical precursor cells and is thought to inhibit ADAM10 sheddase activity but using Notch ligands as substrates[40].

Our analysis of the Sfrp-null ocular phenotype together with overexpression studies in the *Drosophila* wing disc support the idea that Sfrps independently modulate Wnt and Notch. Sfrp1 in the posterior compartment of the *Drosophila* wing imaginal disc interferes with the expression of Wnt and Notch target genes but coexpression of Sfrp1 and ADAM10 (Kuz) completely rescue the expression of Notch targets but not of wingless targets. Therefore, when coactivated, these pathways may compete for Sfrp-mediated regulation, providing an additional frame in which to interpret the reported functional interaction between Wnt-canonical and Notch signaling in several contexts[41].

The ADAM family of metalloproteases is large. Phylogenetic and functional analysis of the human members indicates that ADAM10 is closely related to ADAM17 but that they are separated by other family members. The distributions of *Adam10* and *Adam17* largely overlap and initial studies suggested that both metalloproteases participated in Notch and APP cleavage[29,42]. Therefore, we cannot exclude the possibility that abnormal activity of ADAM17 might contribute to the ocular phenotype of *Sfrp1*$^{-/-}$; *Sfrp2*$^{-/-}$ mice. The existence of Sfrp-mediated regulation of ADAM17 might, for example, help to explain why specific pharmacological inhibition of ADAM10 only partially rescued the retinal phenotype of *Sfrp1*$^{-/-}$; *Sfrp2*$^{-/-}$embryos. However, we favor the hypothesis that, at least in the CNS, Sfrp1 and 2 largely target ADAM10 function. Indeed, genetic inactivation in mice indicates that *Adam10* has a preponderant function in the developing CNS and cardiovascular system, whereas *Adam17* regulates epithelial maturation of multiple organs[42]. Furthermore, recent studies have shown that at least in the CNS Notch, APP and N-cadherin are ADAM10-specific substrates[22,43]. In line with these findings, we have shown that the proteolytic processing of these three substrates, as well as that of L1-CAM, was altered in *Sfrp1*$^{-/-}$; *Sfrp2*$^{-/-}$ mice. Nevertheless, future studies in other tissues, where ADAM17 appears to be preponderant, should help to resolve the specificity of Sfrps on ADAM regulation.

Sfrp2 and Sizzled, a nonmammalian Sfrp family member, have been shown to regulate Tolloid metalloproteinases (also known as procollagen C-proteinases), but with different functions. In vertebrates, BMP activity is in part controlled by the BMP antagonist Chordin which, in turn, is inactivated through cleavage by Tolloid. Sizzled, but apparently not Sfrp2 (ref. 13), binds to Tolloid and behaves as a TIMP to competitively inhibit its enzymatic activity, thereby preventing Chordin cleavage[15,16]. Sfrp2 instead interacts through its CRD with the nonprotease domain of Tolloid proteases and enhances or inhibits their procollagen-C proteinase activity[13] depending on its concentration[14]. The way in which Sfrp1, and possibly Sfrp2, inhibits ADAM10 is unclear but might be similar to the above mechanisms.

Sfrps, TIMPs and PCOLCEs share similarities in the NTR domain; in TIMPs and POLCEs, this domain is thought to interfere with protease activity[44]. The structure of ADAM10 comprises, adjacent to the catalytic and disintegrin domains, a cysteine-rich motif that is thought to mediate interactions with other molecules[42]. In a plausible model (**Supplementary Fig. 4**), binding of the respective cysteine-rich motifs may be responsible for Sfrp-ADAM interactions, which would bring the Sfrp NTR domain close to the ADAM10 catalytic site. Thus, Sfrp1 or 2 would interfere with the enzymatic activity of ADAM10 by competing for substrate binding. Given the molecular diversity of metalloprotease substrates, it is possible that the inhibitory specificity may be in part linked to the nature of the substrates, as suggested by the specific effect of Sfrp1 but not Sfrp2 on APP processing. This possibility is supported by tissue distribution. In fact, APP and Sfrp1, but not Sfrp2, are particularly abundant in the telencephalon. By contrast, ADAM10-mediated processing of Notch in the retina seems to involve both Sfrp1 and Sfrp2.

Independently of the precise mechanism of action, the dual role of Sfrps in the regulation of Wnt signaling and ADAM10 activity might be relevant in different pathological situations, especially in neurodegenerative diseases or metastatic events, where both Wnt signaling components and metalloproteases have key roles[41]. For example, ADAM10 confers metastatic capacity on colorectal cancer[45]. Loss of *SFRP1* and *SFRP2* expression due to promoter hypermethylation occurs frequently in proliferating and invasive tumors[8]. Conversely, ectopic Sfrp1 expression inhibits tumor growth and lung metastasis induced by inoculation of an invasive tumorigenic cell line[46], notably associated with changes in both Wnt–β-catenin and extracellular matrix components[46]. Thus, potentiation of Sfrp1 activity might control both Wnt-mediated tumor proliferation and ADAM-mediated invasion.

On the contrary, our results point to the inhibition of Sfrp1 as a potential mechanism for preventing the toxic accumulation of Aβ peptides, one of the landmarks of Alzheimer disease. Indeed, in the absence of Sfrp1 function, APP processing should shift toward the production of sAPPα, thus preventing the generation of Aβ, as recently shown for SIRT1, a deacetylase that directly activates the transcription of ADAM10 (ref. 47). Whether this would be beneficial in patients with Alzheimer's disease is worth testing, although it is becoming apparent that the contribution of APP proteolytic derivatives to the pathology of Alzheimer's disease is more complex than was originally envisaged.

METHODS

Methods and any associated references are available in the online version of the paper at http://www.nature.com/natureneuroscience/.

Note: Supplementary information is available on the Nature Neuroscience website.

ACKNOWLEDGMENTS

We thank J.M. Ruiz for help with initial experiments and I. Dompablo for technical assistance, H. Bellen (Jan and Dan Duncan Neurological Research Institute), T. Tabata (University of Tokyo), S. Campuzano (CSIC–Universidad Autónoma de Madrid) and the Developmental Studies Hybridoma Bank for *Drosophila* antibodies and stocks, and A. Ludwig (RWTH Aachen University) for the G1254023X compound. This work was supported by grants from the Spanish MICINN (BFU2007-61774), Fundación Mutual Madrileña (2006-0916), Comunidad Autonoma de Madrid (P-SAL-0190-2006), Programa Intramural Especial–CSIC and CIBERER intramural funds to P.B.; CSIC intramural funds to P.E.; grants BFU2008-03320/BMC and CSD2007-00008 from the Spanish Ministerio de Ciencia e Innovación to I.G. and an institutional grant from Fundación Areces given to the Centro de Biología Molecular "Severo Ochoa" to I.G. and M.L.T.

AUTHOR CONTRIBUTIONS

P.E. and A. Sandonis performed most of the immunohistochemical, *in situ* hybridization and western blot analysis. A. Shimono generated the Sfrp knockout mice. M.C. and I.C. performed immunoprecipitation and binding assays. J.M. and J.A. designed and performed APP shedding experiments in CHO cells. I.G. designed and performed (with C.I.) the assays in *Drosophila*. S.M. contributed Sfrp1 and Sfrp2 *in situ* hybridization localization. S.G.-G. and M.L.T. contributed expertise in Notch signaling and flow cytometry. P.B. and P.E. conceived and supervised the study and wrote the manuscript.

COMPETING FINANCIAL INTERESTS
The authors declare no competing financial interests.

Published online at http://www.nature.com/natureneuroscience/.
Reprints and permissions information is available online at http://www.nature.com/reprints/index.html.

1. Hayward, P., Kalmar, T. & Arias, A.M. Wnt/Notch signalling and information processing during development. *Development* **135**, 411–424 (2008).
2. Livesey, F.J. & Cepko, C.L. Vertebrate neural cell-fate determination: lessons from the retina. *Nat. Rev. Neurosci.* **2**, 109–118 (2001).
3. Cho, S.H. & Cepko, C.L. Wnt2b/beta-catenin-mediated canonical Wnt signaling determines the peripheral fates of the chick eye. *Development* **133**, 3167–3177 (2006).
4. Liu, H. *et al.* Ciliary margin transdifferentiation from neural retina is controlled by canonical Wnt signaling. *Dev. Biol.* **308**, 54–67 (2007).
5. Fu, X., Sun, H., Klein, W.H. & Mu, X. Beta-catenin is essential for lamination but not neurogenesis in mouse retinal development. *Dev. Biol.* **299**, 424–437 (2006).
6. Liu, C. & Nathans, J. An essential role for frizzled 5 in mammalian ocular development. *Development* **135**, 3567–3576 (2008).
7. Liu, H., Mohamed, O., Dufort, D. & Wallace, V.A. Characterization of Wnt signaling components and activation of the Wnt canonical pathway in the murine retina. *Dev. Dyn.* **227**, 323–334 (2003).
8. Bovolenta, P., Esteve, P., Ruiz, J.M., Cisneros, E. & Lopez-Rios, J. Beyond Wnt inhibition: new functions of secreted Frizzled-related proteins in development and disease. *J. Cell Sci.* **121**, 737–746 (2008).
9. Satoh, W., Gotoh, T., Tsunematsu, Y., Aizawa, S. & Shimono, A. Sfrp1 and Sfrp2 regulate anteroposterior axis elongation and somite segmentation during mouse embryogenesis. *Development* **133**, 989–999 (2006).
10. Trevant, B. *et al.* Expression of secreted frizzled related protein 1, a Wnt antagonist, in brain, kidney, and skeleton is dispensable for normal embryonic development. *J. Cell. Physiol.* **217**, 113–126 (2008).
11. Satoh, W., Matsuyama, M., Takemura, H., Aizawa, S. & Shimono, A. Sfrp1, Sfrp2, and Sfrp5 regulate the Wnt/beta-catenin and the planar cell polarity pathways during early trunk formation in mouse. *Genesis* **46**, 92–103 (2008).
12. Misra, K. & Matise, M.P. A critical role for sFRP proteins in maintaining caudal neural tube closure in mice via inhibition of BMP signaling. *Dev. Biol.* **337**, 74–83 (2010).
13. Kobayashi, K. *et al.* Secreted Frizzled-related protein 2 is a procollagen C proteinase enhancer with a role in fibrosis associated with myocardial infarction. *Nat. Cell Biol.* **11**, 46–55 (2009).
14. He, W. *et al.* Exogenously administered secreted frizzled related protein 2 (Sfrp2) reduces fibrosis and improves cardiac function in a rat model of myocardial infarction. *Proc. Natl. Acad. Sci. USA* **107**, 21110–21115 (2010).
15. Lee, H.X., Ambrosio, A.L., Reversade, B. & De Robertis, E.M. Embryonic dorsal-ventral signaling: secreted frizzled-related proteins as inhibitors of tolloid proteinases. *Cell* **124**, 147–159 (2006).
16. Muraoka, O. *et al.* Sizzled controls dorso-ventral polarity by repressing cleavage of the Chordin protein. *Nat. Cell Biol.* **8**, 329–338 (2006).
17. Mii, Y. & Taira, M. Secreted Frizzled-related proteins enhance the diffusion of Wnt ligands and expand their signalling range. *Development* **136**, 4083–4088 (2009).
18. Kopan, R. & Ilagan, M.X. The canonical Notch signaling pathway: unfolding the activation mechanism. *Cell* **137**, 216–233 (2009).
19. Del Monte, G., Grego-Bessa, J., Gonzalez-Rajal, A., Bolos, V. & De La Pompa, J.L. Monitoring Notch1 activity in development: evidence for a feedback regulatory loop. *Dev. Dyn.* **236**, 2594–2614 (2007).
20. Tokunaga, A. *et al.* Mapping spatio-temporal activation of Notch signaling during neurogenesis and gliogenesis in the developing mouse brain. *J. Neurochem.* **90**, 142–154 (2004).
21. Kim, A.S., Lowenstein, D.H. & Pleasure, S.J. Wnt receptors and Wnt inhibitors are expressed in gradients in the developing telencephalon. *Mech. Dev.* **103**, 167–172 (2001).
22. Jorissen, E. *et al.* The disintegrin/metalloproteinase ADAM10 is essential for the establishment of the brain cortex. *J. Neurosci.* **30**, 4833–4844 (2010).
23. Hartmann, D. *et al.* The disintegrin/metalloprotease ADAM 10 is essential for Notch signaling but not for alpha-secretase activity in fibroblasts. *Hum. Mol. Genet.* **11**, 2615–2624 (2002).
24. Amour, A. *et al.* The *in vitro* activity of ADAM-10 is inhibited by TIMP-1 and TIMP-3. *FEBS Lett.* **473**, 275–279 (2000).
25. Langton, K.P., Barker, M.D. & McKie, N. Localization of the functional domains of human tissue inhibitor of metalloproteinases-3 and the effects of a Sorsby's fundus dystrophy mutation. *J. Biol. Chem.* **273**, 16778–16781 (1998).
26. Ludwig, A. *et al.* Metalloproteinase inhibitors for the disintegrin-like metalloproteinases ADAM10 and ADAM17 that differentially block constitutive and phorbol ester–inducible shedding of cell surface molecules. *Comb. Chem. High Throughput Screen.* **8**, 161–171 (2005).
27. Reiss, K. *et al.* ADAM10 cleavage of N-cadherin and regulation of cell-cell adhesion and beta-catenin nuclear signaling. *EMBO J.* **24**, 742–752 (2005).
28. Riedle, S. *et al.* Nuclear translocation and signaling of L1-CAM in human carcinoma cells requires ADAM10 and presenilin/gamma-secretase activity. *Biochem. J.* **420**, 391–402 (2009).
29. Lichtenthaler, S.F. Alpha-secretase in Alzheimer's disease: molecular identity, regulation and therapeutic potential. *J. Neurochem.* **116**, 10–21 (2011).
30. Caillé, I. *et al.* Soluble form of amyloid precursor protein regulates proliferation of progenitors in the adult subventricular zone. *Development* **131**, 2173–2181 (2004).
31. Stetler-Stevenson, W.G. Tissue inhibitors of metalloproteinases in cell signaling: metalloproteinase-independent biological activities. *Sci. Signal.* **1**, re6 (2008).
32. Micchelli, C.A., Rulifson, E.J. & Blair, S.S. The function and regulation of cut expression on the wing margin of *Drosophila*: Notch, Wingless and a dominant-negative role for Delta and Serrate. *Development* **124**, 1485–1495 (1997).
33. Uren, A. *et al.* Secreted frizzled-related protein-1 binds directly to Wingless and is a biphasic modulator of Wnt signaling. *J. Biol. Chem.* **275**, 4374–4382 (2000).
34. Lopez-Rios, J., Esteve, P., Ruiz, J.M. & Bovolenta, P. The Netrin-related domain of Sfrp1 interacts with Wnt ligands and antagonizes their activity in the anterior neural plate. *Neural Develop.* **3**, 19 (2008).
35. Nolo, R., Abbott, L.A. & Bellen, H.J. Senseless, a Zn finger transcription factor, is necessary and sufficient for sensory organ development in *Drosophila*. *Cell* **102**, 349–362 (2000).
36. Esteve, P. & Bovolenta, P. Secreted inducers in vertebrate eye development: more functions for old morphogens. *Curr. Opin. Neurobiol.* **16**, 13–19 (2006).
37. Wall, D.S. *et al.* Progenitor cell proliferation in the retina is dependent on Notch-independent Sonic hedgehog/Hes1 activity. *J. Cell Biol.* **184**, 101–112 (2009).
38. Kubo, F. & Nakagawa, S. Hairy1 acts as a node downstream of Wnt signaling to maintain retinal stem cell–like progenitor cells in the chick ciliary marginal zone. *Development* **136**, 1823–1833 (2009).
39. Morcillo, J. *et al.* Proper patterning of the optic fissure requires the sequential activity of BMP7 and SHH. *Development* **133**, 3179–3190 (2006).
40. Muraguchi, T. *et al.* RECK modulates Notch signaling during cortical neurogenesis by regulating ADAM10 activity. *Nat. Neurosci.* **10**, 838–845 (2007).
41. Campbell, C., Risueno, R.M., Salati, S., Guezguez, B. & Bhatia, M. Signal control of hematopoietic stem cell fate: Wnt, Notch, and Hedgehog as the usual suspects. *Curr. Opin. Hematol.* **15**, 319–325 (2008).
42. Edwards, D.R., Handsley, M.M. & Pennington, C.J. The ADAM metalloproteinases. *Mol. Aspects Med.* **29**, 258–289 (2008).
43. Kuhn, P.H. *et al.* ADAM10 is the physiologically relevant, constitutive alpha-secretase of the amyloid precursor protein in primary neurons. *EMBO J.* **29**, 3020–3032 (2010).
44. Mott, J.D. *et al.* Post-translational proteolytic processing of procollagen C-terminal proteinase enhancer releases a metalloproteinase inhibitor. *J. Biol. Chem.* **275**, 1384–1390 (2000).
45. Gavert, N. *et al.* Expression of L1-CAM and ADAM10 in human colon cancer cells induces metastasis. *Cancer Res.* **67**, 7703–7712 (2007).
46. Matsuda, Y., Schlange, T., Oakeley, E.J., Boulay, A. & Hynes, N.E. WNT signaling enhances breast cancer cell motility and blockade of the WNT pathway by sFRP1 suppresses MDA-MB-231 xenograft growth. *Breast Cancer Res.* **11**, R32 (2009).
47. Donmez, G., Wang, D., Cohen, D.E. & Guarente, L. SIRT1 suppresses beta-amyloid production by activating the alpha-secretase gene ADAM10. *Cell* **142**, 320–332 (2010).

ONLINE METHODS

Animals. *Sfrp1*$^{-/-}$; *Sfrp2*$^{+/-}$ mutant mice were generated as described[9] and crossed to generate *Sfrp1*$^{-/-}$; *Sfrp2*$^{-/-}$ double-mutant embryos. *Sfrp1*$^{-/-}$; *Sfrp2*$^{+/-}$ mice were mated with a 129 and C57BL/6 mixed background to obtain *Sfrp1*$^{+/-}$; *Sfrp2*$^{+/-}$ double-heterozygous strain and further used to generate single *Sfrp1* and *Sfrp2* mutants. The eyes of *Sfrp1*$^{-/-}$ and *Sfrp2*$^{-/-}$ single mutants were normal and undistinguishable from those of age-matched wild types and therefore littermates were often used as controls for the double mutant embryos.

Antibodies. We used the following primary antibodies: mouse monoclonal anti-BrdU (1:500, Boehringer Manheim), mouse monoclonal anti-Islet1 (1:500, Hybridoma Bank, 39.4D5); rabbit polyclonal anti-Otx2 (1:500, Abcam); rabbit polyclonal anti-Calbindin-28K (1:2,000, Swant); mouse monoclonal anti-active β-catenin (ABC) (1:200, Millipore), mouse monoclonal anti-Myc (1:2,000, clone 9E10); rabbit polyclonal anti-Pax6 (1:500, Covance); mouse monoclonal anti-PKC (1:400, Sigma-Aldrich); mouse monoclonal anti-βIII-tubulin (1:4,000, Promega), rabbit polyclonal anti-cleaved Notch1 Val1744 (1:200, Cell Signaling), goat polyclonal Notch 1 (Santa Cruz) rabbit polyclonal anti-HA (1:2,000, Sigma-Aldrich), mouse monoclonal anti-HA (1:2,000, Sigma-Aldrich), rabbit polyclonal anti-Myc (Sigma-Aldrich), mouse monoclonal anti-amyloid precursor protein A4 (1:5,000, Millipore, clone 22C11), rabbit polyclonal anti-soluble APPα (1:500, Covance) rabbit polyclonal anti-Sfrp1 (1:500, AbCam), rabbit polyclonal anti-NG2 (1:500, Chemicon), mouse monoclonal N-cadherin C-terminal domain (1:500, Zymed Laboratories, clone 3B9), rabbit polyclonal 74 5H7 to the cytoplasmic part of L1 (a gift from V.P. Lemmon), goat polyclonal anti-Adam10 (1:500, RD) guinea-pig anti-Sens[35] (1:1,000, a gift from H. Bellen), rabbit anti-Hh (1:800, a gift from T. Tabata); mouse anti-wingless (1:50) and anti-Cut (prepared from cells obtained from the DSHB) and Lectin from Tomato biotin-conjugated (1:150, Sigma-Aldrich). Secondary antibodies: rabbit Alexa 488, rabbit Alexa 594, mouse Alexa 488 (1:2,000, Molecular Probes).

***In situ* hybridization (ISH), immunohistochemistry (IHC) and histological analysis.** E9–13.5 embryos were immersion-fixed in 4% paraformaldehyde (PFA)-phosphate buffer (wt/vol) for 3 h. Older embryos were transcardially perfused with the same fixative and post-fixed for 2 h. Tissue was then washed in phosphate buffer saline (PBS), incubated in a 30% sucrose-PBS solution (wt/vol) and embedded and frozen in a 7.5% gelatin in 15% sucrose solution (wt/vol). Cryostat sections were processed for ISH and IHC. ISH was performed with standard protocols. The following digoxigenin-labeled antisense riboprobes were used: *Dll-1*, *Hes5*, *Sfrp1* and *Sfrp2*. For BrdU analysis, pregnant mice were injected intraperitoneally with BrdU (50 μg g^{-1}), put to death 1 h later and processed for BrdU ICH. ICH analysis was performed as described but sections processed for Otx2, Pax6, Islet-1, phospho-Smad-1,5,8 and NICD were boiled at 115 °C for 2 min in 10 mM citrate buffer using a decloaking chamber (Biocare Medical) for antigen retrieval. NICD IHC was performed as described[19] and amplified with TSA (PerkinElmer). Immunostaining of the *Drosophila* imaginal discs was performed according to standard protocols and that of extracellular wingless as described[48]. Fluorescence-stained imaginal discs were examined using a confocal laser-scanning microscope (LSM510 Vertical, Zeiss). We analyzed a minimum of five double mutant embryos for each experimental condition.

Organotypic optic cup cultures. Optic cups from E11.5 mice were dissected, embedded in collagen matrices and cultured for 24 h in DMEM-F12 medium supplemented with N2 (Gibco) and different doses of the ADAM10 inhibitor G1254023X resuspended in DMSO (a gift from A. Ludwig) or DMSO alone. Cultures were incubated with BrdU (10 μM) for ten minutes before fixation in 4% PFA for 2 h. Cultured optic cups were then processed for immunohistochemistry as described above. We analyzed a minimum of five optic cups for each experimental condition.

Overexpression of Sfrp1 and Kuzbanian in *Drosophila*. Sfrp1 cDNA was fused in frame to a C-terminal Myc tag and cloned into a pUAST vector to generate transgenic fly lines expressing SFRP1 under the UAS promoter. The UAS-Kuz was a gift from S. Campuzano. UAS-Sfrp1 and UAS-Kuz were expressed using the Hh-Gal4 driver[49].

Immunoprecipitations and western blot analysis. E13 telencephalic and E15 ocular tissue from wild-type or Sfrp1- and 2-null embryos was isolated and homogenized in lysis buffer (150 mM NaCl, 2% TritonX-100 (wt/vol), 50 mM Tris, pH 8) containing proteinase and metalloprotease inhibitors (phenanthroline, Sigma). The lysates were centrifuged for 20 min at 4 °C, the supernatants were precleared in protein G–agarose beads (Sigma-Aldrich), pre-blocked with 1% BSA (wt/vol) for 1 h at 4 °C and centrifuged at 2,000 r.p.m. The supernatants were incubated with anti-Sfrp1 (1 μg) overnight at 4 °C in a rotor shaker. Protein G–agarose beads were added for 1 h, collected by centrifugation at 400*g*. and washed five times with lysis buffer before adding sample buffer without 2-mercaptoethanol. Beads were boiled for 5 min, collected by centrifugation and the supernatants resolved in 10% SDS-PAGE. Subconfluent HEK 293T cells were transiently cotransfected with constructs encoding mouse Sfrp1-HA and mouse ADAM10-myc using the FuGENE HD Transfection Reagent (Roche). After 48 h, cells were scraped in lysis buffer and immunoprecipitations were performed as described[50]. To detect sAPP, we plated CHO cells in 10-mm dishes in DMEM-F12 10% FCS (wt/vol). After 24 h, cells were incubated with serum-free DMEM in the presence of purified Sfrp1 or Sfrp2. Thereafter cell-conditioned medium was collected and concentrated on concanavalin-A beads (GE Healthcare). After electrophoresis, proteins were transferred to PDVF membranes (Hybond-P, Amersham), checked by Ponceau red staining and probed with antibodies against APP (mouse monoclonal anti-Alzheimer precursor protein A4). Western blot analysis was performed with tissues or cell lines lysed as above. Primary antibodies were detected with peroxidase-conjugated secondary antibodies followed by ECL Advanced Western Blotting Detection Kit (Amersham). Immunoprecipitations and western blots were repeated at least three times and gave similar results.

RNA extraction and Q-PCR. mRNA from stage E12.5 and E13.5 embryonic retinas was extracted using the QuickPrep Micro mRNA Purification Kit (GE Healthcare) and treated with DNase I. cDNAs were obtained by random priming reverse transcription using the First-Strand cDNA Synthesis Kit (GE Healthcare). RT-PCR reactions were run in triplicate in 96-well plates with the SYBR Green PCR Master Mix (Applied Biosystems), using an ABI PRISM 7700 Sequence Detection System (Applied Biosystems). Q-RT-PCR reactions were performed with 3 μl of cDNA, which was used for β-actin mRNA amplification for normalization and Hes5 mRNA. Primers were the following: *Hes5* forward: 5′-TTCAGCAAGTGACTTCTGCGA-3′; *Hes5* reverse: 5′-TCATAGAACCC CCGGTGGT-3′; β-actin forward: 5′-AGGTGTGATGGTGGGAATGG-3′; *Dll* forward: 5′-TTGGGCTTCTTTAAC; Dll-1 reverse: 5′-TCCACACACTCG TTAG-3′; β-actin reverse: 5′-GCCTCGTCACCCACATAGGA-3′. Data acquisition and analysis of the real-time RT-PCR assays were performed using the 7500 System SDS Software (v2.0.1, Applied Biosystems). The SYBR Green–double-stranded DNA complex signal was normalized to the passive reference dye (ROX) to correct for non-PCR-related well-to-well fluorescent fluctuations. Experiments were independently replicated at least three times.

Binding of Sfrp1 to Adam-myc overexpressing CHO line. The PCDNA3.1–AP-3myc-Sfrp1 construct was engineered using the PCDNA3.1–AP-3myc plasmid provided by J. Nathans. HEK293 cells were transiently transfected with PCDNA–AP-3myc-Sfrp1 or PCDNA-AP (alkaline phosphatase) plasmids and conditioned media were recovered after 48 h. Control or stably transfected *Adam10* CHO cells were grown in polylysine-coated coverslips. Cells were incubated with conditioned medium containing the AP or AP-3myc-Sfrp1 fusion protein for 90 min and the detection of bound AP was performed using standard protocols.

Statistical analysis. Normality of the distribution was tested by Kolmogorov-Smirnov test. Statistical significance was determined by *t*-test. One-way ANOVA was used to compare statistical significance among more than two groups. *Post hoc* analysis was performed for assessing specific group comparisons (Tukey), when the *F* value was significant. Values are expressed as means ± s.e.m. Calculations were made using the SPSS statistical package version 17.0 using a significance level of 0.05.

48. Torroja, C., Gorfinkiel, N. & Guerrero, I. Patched controls the Hedgehog gradient by endocytosis in a dynamin-dependent manner, but this internalization does not play a major role in signal transduction. *Development* **131**, 2395–2408 (2004).
49. Tanimoto, H., Itoh, S., ten Dijke, P. & Tabata, T. Hedgehog creates a gradient of DPP activity in *Drosophila* wing imaginal discs. *Mol. Cell* **5**, 59–71 (2000).
50. Rodriguez, J. *et al.* SFRP1 regulates the growth of retinal ganglion cell axons through the Fz2 receptor. *Nat. Neurosci.* **8**, 1301–1309 (2005).

doi:10.1038/nn.2794